FINAL REPORT

HYDRAULIC DESIGN OF PERMEABLE INTERLOCKING CONCRETE PAVEMENT

Prepared for the Interlocking Concrete Pavement Institute

By
Dr. John T. Kevern (Principal Investigator)
Dr. Jerry Richardson (Co-Principal Investigator)
Amanda Leipard (Graduate Research Assistant)
Monica Stochl (Graduate Research Assistant.

University of Missouri-Kansas City, Kansas City, MO

January 2016

Technical Report Documentation Page

1. Report No. ICPI2016-01	**2. Government Accession No.**	**3. Recipient's Catalog No.**	
4. Title and Subtitle HYDRAULIC DESIGN OF PERMEABLE INTERLOCKING CONCRETE PAVEMENT		**5. Report Date** January 2016	
		6. Performing Organization Code	
7. Author(s) Kevern, J.T., Richardson, J., Leipard, A., and Stochl, M.		**8. Performing Organization Report No.**	
9. Performing Organization Name and Address University of Missouri-Kansas City 5100 Rockhill Rd. Kansas City, MO 64110		**10. Work Unit No. (TRAIS)**	
		11. Contract or Grant No.	
12. Sponsoring Organization Name and Address University of Missouri-Kansas City 5100 Rockhill Rd. Kansas City, MO 64110		**13. Type of Report and Period Covered**	
		14. Sponsoring Agency Code	
15. Supplementary Notes			
16. Abstract			
17. Key Words Permeable interlocking concrete pavement, permeable pavement, hydraulic design		**18. Distribution Statement** No restrictions.	
19. Security Classification (of this report) Unclassified.	**20. Security Classification (of this page)** Unclassified.	**21. No. of Pages** 184	**22. Price** NA

16. Abstract

Urbanization causes increased stormwater runoff volume through the construction of impervious surfaces. The increased stormwater runoff results in increased stream erosion and flooding all with higher levels of pollutants. Other negative impacts of increased imperviousness include contribution to the urban heat island and decreased groundwater recharge among others. Permeable pavements are one key technology to improving the urban climate. This report discusses research performed on Permeable Interlocking Concrete Pavements (ICPI). The current design methodology includes a structural component, required for performance as a load-carrying surface and a hydrologic component, required to ensure sufficient water volume is captured. However, currently there is no overt design for transmittal of the stormwater through the pavement surface. The research contained herein describes the development of a hydraulic design methodology and verification to allow proper section of impervious to pervious area and prediction of maintenance requirements. A two-layer hydraulic flume was developed at the University of Missouri-Kansas City (UMKC) which allows evaluation of permeable pavement sections, surface material and base, which accept horizontal flow at a variety of potential pavement slopes. The flow is split between that infiltrated through the test section and that which overflows. Sections were constructed with 6mm, 10mm, and 12.5mm joint widths and characterized across pavement slopes up to 10%. The vertical infiltration as tested per ASTM C1781 was then compared to the measured horizontal infiltration capacity. Sections were also exposed to NJCAT synthetic stormwater applications to evaluate clogging performance under realistic flow regimes and to gage potential recovery. The project results were then incorporated into a hydraulic design program to evaluate potential site designs and to predict the anticipated maintenance period. The theory, testing specifics, results, statistical analysis, and design program fundamental development are presented in the body of the report. The appendix contains the user handbook along with a series of examples.

EXECUTIVE SUMMARY

The environmental impacts of increasing surface runoff produced by urbanization are extensive. Increased impervious spaces decrease the available infiltrating greenspace resulting in an overall increase of stormwater quantity, urban heat island effects, and decreasing groundwater, among others. Likewise, an increased runoff volume leads to an increase in urban stream flow creating additional stream erosion and flooding events. The amount of increased surface runoff due to urbanization can be as much as 10% of the water cycle with natural ground cover to as much as 55% of the water cycle when ground cover becomes 75-100% impervious surface. Impervious pavements also increase contaminant loading while permeable surfaces combat such loading.

Permeable surfaces are high porous (gaped) surfaces that allow stormwater to be captured and stored allowing for infiltration. Permeable surfaces such as Permeable Interlocking Concrete Pavements, PICPs combat the effects of urbanization by explicitly infiltrating water, a new concept to engineering practice for pavements.

The most common permeable surfaces include porous asphalt, pervious concrete, and PICPs. Proficient design criteria of pavements require four areas:

1) Structural Load Capacity, strength
2) Material Selection, durability and cost
3) Hydrologic Design, retention, detention
4) Hydraulic Design, flow rates, and depths

Design for durability or detention sizing have a large amount of supportive research while the hydraulic behavior of these surfaces lacks research. The misconception that a permeable surface has an infinite capacity to receive run-off from adjacent area are

common and the field testing method currently does not account for such run-on flow. The test method for permeable pavement's hydraulic performance is the ASTM C1781. The C1781 method measures the vertical surface infiltration of a permeable surface and does not describe the horizontal sheet flow capacity of the pavement. Additionally, field experience display decreasing infiltration rates due to aging surfaces that have acquired sedimentation clogging. Horizontal sheet flow with sediment clogging research has also been limited.

From a design perspective, horizontal flow should be considered in permeable pavements. The following research concentrates upon the horizontal hydraulic behavior of PICPS. Multiple test sections at various patterns were evaluated in a two layer hydraulic flume. The research targeted the determination for allowable contributing run-off area for a variety of design storms. Horizontal hydraulic flow such as the capture discharges, infiltration rates, and overflow flow rates for various block spacing across a broad range of pavement cross slopes was examined and analyzed.

Additionally, synthetic stormwater was created and the system was analyzed for hydraulic behavior. Clogging analysis included before, during, and after clogging (recapture) hydraulic behavior. In addition to the clogging and unclogging experiments the research included a pervious platform section for comparison and for a suggested alternative sub-base material in place of some of the aggregate base. A pervious concrete section would increase the structural load capacity for a PICPs.

The research presented herein was originally developed as two linked thesis, defended during the spring and summer of 2015 at the University of Missouri-Kansas City. The first by Amanda Leipard addressed the design, construction, and calibration of the two-level hydraulic flume along with the initial unclogged test results (Leipard, 2015). The second by Monica Stochl discussed the development of the design software and included the calibration with field results and clogging performance (Stochl, 2015).

TABLE OF CONTENTS

LIST OF FIGURES **1**

LIST OF TABLES **4**

1. BACKGROUND AND LITERATURE REVIEW **6**
Introduction of Clean Water Act 6
Urbanization in the Hydrologic Cycle 8
Best Management Practices 11
Permeable Pavements Designed as Best Management Practice 13
PICP Benefits and Concerns 14
Permeable Interlocking Concrete Paver Design 17
Hydraulic Development of PICP 25

2. PICP TESTING **30**
Flume Design 30
Calibration and Discharge Calculations 37
Test Section Placement 40
Infiltration 44
Test Section Calibration 46

3. FLOW RATE PERFORMANCE CURVE DEVELOPMENT **52**
Incipient Overflow Rate 56
Rotated Pattern Investigation 59

4. STATISTICAL ANALYSIS OF PERFORMANCE CURVE TESTING **61**
Analyzed Data and Normality Test 61
One-Way ANOVA Results 62
T-Test Comparisons 64

5. HYDRAULIC PERFORMANCE DURING CLOGGING **70**
Synthetic Stormwater Properties 70
Infiltration Flowrate (Left V Notch Weir) vs. Application Results 73
Infiltration and Overflow Rate Results and Comparisons 77
Infiltration per Previous Field Research 85

6. HYDRAULIC DESIGN **88**
Analyzing Flume Results 88
Calibrated Values for Design Model 94
Incorporation of Clogging Into the Hydraulic Design 96

7. PERVIOUS CONCRETE AS A BASE MATERIAL **101**
Material Properties 101
Platform Infiltration 102
PICP and Platform System 104

8. Design tool for Specifying PICP **107**

9. Project Summary and Conclusions **109**

10. References **112**

APPENDIX A – TESTING RESULTS **115**
1. Results of Hydraulic testing-All Tests 116
2. Statistical Analysis of Hydraulic Testing 131

3. Hydraulic performance PICP with Pervious Platform 139

APPENDIX B- DESIGN TOOL 149

Owner's Manual 149
Inputs 149
Project ID 150
Storm Information 150
Site Area Information 152
Outputs 156
Site Analysis 157
Storm Analysis 157
Design Considerations 160
Clogging Considerations 164

APPENDIX C - DESIGN TOOL EXAMPLES 166

Example 1 166
Example 1A 168
Example 1B 170
Example 2 172

LIST OF FIGURES

FIGURE 1. SIX MINIMUM CONTROL MEASURES (CASS COUNTY GOVERNMENT, 2014.) 8
FIGURE 2. EFFECT OF IMPERVIOUS SURFACE ON HYDROLOGIC CYCLE (NEH-653, 1998) 9
FIGURE 3. EXAMPLES OF STRUCTURAL BMP – RAIN GARDEN (SUNY-ESF, 2015) 12
FIGURE 4. EXAMPLE OF STRUCTURAL BMP - RAIN BARREL (RUTGERS, 2014) 12
FIGURE 5. TYPES OF PERMEABLE PAVEMENT (ICPI, 2014). 14
FIGURE 6. PICP CROSS SECTION (ICPI, 2014) 18
FIGURE 7. DETAIL DRAWINGS OF FULL EXFILTRATION OF PICP (ICPI, 2014) 20
FIGURE 8. DETAILED DRAWINGS OF PARTIAL EXFILTRATION OF PICP (ICPI, 2014) 21
FIGURE 9. DETAILED DRAWINGS OF NO-EXFILTRATION OF PICP (ICPI, 2014) 22
FIGURE 10. PERMEABLE PAVEMENT DESIGN FLOW CHART (ICPI, 2015) 23
FIGURE 11. WATER INFLOW AND OUTFLOW ON PERMEABLE PAVEMENT (COLLINS ET. AL., 2008) 25
FIGURE 12. FLUME FOR PERVIOUS CONCRETE INFILTRATION RESEARCH, (GRAHL, 2012) 26
FIGURE 13. OVERLAND FLOW DIAGRAM (RICHARDSON, 1989). 27
FIGURE 14. FULL AND PARTIAL EQUILIBRIUM HYDROGRAPH (RICHARDSON, 1989) 28
FIGURE 15. PAVEMENT TOP VIEW AND CROSS SECTION FOR INSIPIENT OVERFLOW 29
FIGURE 16. BOTTOM SUPPORT FRAME ASSEMBLY DRAWING 30
FIGURE 17. HEADBOX 31
FIGURE 18. BASE LAYER PART 1 DRAWING 32
FIGURE 19. COMPLETE FLUME ASSEMBLY DRAWING 33
FIGURE 20. LABORATORY CIRCULATION SYSTEM SCHEMATIC 34
FIGURE 21. COMPLETED TWO LAYER HYDRAULIC FLUME. 34
FIGURE 22. EXPERIMENT TESTING SECTION 35
FIGURE 23. 8 FEET OF HORIZONTAL SHEET FLOW 35
FIGURE 24. FLUME WITH VARIABLE SLOPE AND JACKING SYSTEM 36
FIGURE 25. MERRIUM (SG=2.95) U-TUBE MANOMETER ATTACHED TO THE VENTURI METER FOR MEASUREMENT OF TOTAL FLOW RATE 37
FIGURE 26. 3IN.X1.5IN. VENTURI METER 38
FIGURE 27. V NOTCH WEIRS IN TAIL BOX 39
FIGURE 28. TWO LAYER HYDRAULIC FLUME 40
FIGURE 29. AGGREGATE GRADATION SET IN FLUME 41
FIGURE 30. NO. 8 GRADATION FOR BASE AND 10 MM/12.5 MM SPACING FILLER MATERIAL 42
FIGURE 31. NO. 9 GRADATION FOR 6 MM SPACING FILLER MATERIAL 42
FIGURE 32. STRAIGHT HERRINGBONE PATTERN WITH HORIZONTAL FLOW 43
FIGURE 33. 45 DEGREE HERRINGBONE PATTERN WITHOUT HORIZONTAL FLOW 43
FIGURE 34. TEST SECTION INFILTRATION AND OVERFLOW SCHEMATIC 44
FIGURE 35. VERTICAL INFILTRATION C 1781 TEST 46
FIGURE 36. VERTICAL INFILTRATION C 1781 VS. PAVEMENT SLOPE FOR EACH PICP SPACING 47
FIGURE 37. WATER SERVICES BASE INSTALLATION 49
FIGURE 38. FINAL GRADING OF THE BEDDING LAYER 49
FIGURE 39. SETTING THE STRAIGHT HERRINGBONE PATTERN BY HAND 50
FIGURE 40. THE FINISHED INSTALLATION AFTER COMPACTION AND PRIOR TO OPENING 50
FIGURE 41. WATER SERVICES VERTICAL TEST AND PAVEMENT 6 MM STRAIGHT HERRINGBONE 51
FIGURE 42. TYPICAL PERFORMANCE CURVE EXPLANATION 52
FIGURE 43. PERFORMANCE CURVE 6 MM SPACING 0 % SLOPE 53
FIGURE 44. PERFORMANCE CURVE 10 MM SPACING 0 % SLOPE 54
FIGURE 45. PERFORMANCE CURVE 12.5 MM SPACING 0 % SLOPE 54
FIGURE 46. AVERAGE MAX OVERFLOW RATES PER PAVEMENT SLOPE 55
FIGURE 47. AVERAGE INCIPIENT OVERFLOW RATES PER PAVEMENT SLOPE 56
FIGURE 48. VERTICAL INFILTRATION AND HORIZONTAL INFILTRATION ACROSS PAVEMENT SLOPES 58

FIGURE 49. (LEFT) STRAIGHT HERRINGBONE PATTERN 6 MM SPACING (RIGHT) 45 DEGREE HERRINGBONE PATTERN 6 MM SPACING....59
FIGURE 50. NORMAL PROBABILITY CHECK....62
FIGURE 51. INTERVAL PLOT OF ANOVA GROUPS....64
FIGURE 52. BOXPLOT INCIPIENT OVERFLOW RATE BETWEEN 6 MM AND 10 MM....65
FIGURE 53. BOXPLOT INCIPIENT OVERFLOW RATE BETWEEN 10 MM AND 12.5 MM....66
FIGURE 54. BOXPLOT AVERAGE 6 MM VS. HERRINGBONE PATTERN INFILTRATION PER SECTION AREA (CFS/FT^2)....68
FIGURE 55. LOCATION AND PICTURE OF SYNTHETIC STORMWATER SOIL LOCATION....70
FIGURE 56. SYNTHETIC STORMWATER DISPENSED UPSTREAM OF THE TEST SECTION....72
FIGURE 57. SYNTHETIC STORMWATER PASSING OVER THE TEST SECTION....73
FIGURE 58. 6 MM SPACING FLOW RATE VS. APPLICATION RESULT....74
FIGURE 59. 10 MM SPACING FLOW RATE VS. APPLICATION RESULT....74
FIGURE 60. 12.5 MM SPACING FLOW RATE VS. APPLICATION RESULT....75
FIGURE 61. 12.5 MM SPACING FLOW RATE VS. APPLICATION RESULT....76
FIGURE 62. 10 MM SPACING FLOW RATE VS. APPLICATION RESULT....76
FIGURE 63. 12.5 MM SPACING FLOW RATE VS. APPLICATION RESULT....77
FIGURE 64. 6 MM TOTAL DISCHARGE, OVERFLOW, INFILTRATION RATES....78
FIGURE 65. 10 MM TOTAL DISCHARGE, OVERFLOW, INFILTRATION RATE....79
FIGURE 66. 12.5 MM TOTAL DISCHARGE, OVERFLOW, AND INFILTRATION RATE....80
FIGURE 67. 6 MM AFTER CLOGGING RECAPTURE RATE VS. APPLICATION RESULT....81
FIGURE 68. 10 MM AFTER CLOGGING RECAPTURE RATE VS. APPLICATION RESULT....81
FIGURE 69. 12.5 MM AFTER CLOGGING RECAPTURE RATE VS. APPLICATION RESULT....82
FIGURE 70. 6 MM BEFORE AND AFTER CLOGGING PERFORMANCE CURVE....83
FIGURE 71. 10 MM BEFORE AND AFTER CLOGGING PERFORMANCE CURVE....84
FIGURE 72. 12.5 MM BEFORE AND AFTER CLOGGING PERFORMANCE CURVE....84
FIGURE 73. 6 MM CALIBRATED INFILTRATION RATE PER STORMWATER APPLICATION CURVE....86
FIGURE 74. 10 MM CALIBRATED INFILTRATION RATE PER STORMWATER APPLICATION CURVE....87
FIGURE 75. 12.5 MM CALIBRATED INFILTRATION RATE PER STORMWATER APPLICATION CURVE....87
FIGURE 76. PERFORMANCE CURVE....88
FIGURE 77. CASE I - PAVEMENT TOP VIEW AND CROSS SECTION FOR INSIPIENT OVERFLOW....90
FIGURE 78. CASE II - PAVEMENT TOP VIEW AND CROSS SECTION FOR 1/4IN HEAD....91
FIGURE 79. CASE III - PAVEMENT TOP VIEW AND CROSS SECTION FOR 1/2IN HEAD....91
FIGURE 80. 6 MM AVERAGE MAX OVERFLOW UNIT RATE PER PAVEMENT CROSS SLOPE....92
FIGURE 81. 10MM AVERAGE MAX OVERFLOW UNIT RATE PER PAVEMENT CROSS SLOPE....93
FIGURE 82. 12.5 AVERAGE MAX OVERFLOW UNIT RATE PER PAVEMENT CROSS SLOPE....93
FIGURE 83. INFILTRATION VS. APPLICATION FOR THE 6MM SPACING....97
FIGURE 84. INFILTRATION VS. APPLICATION FOR THE 10MM SPACING....98
FIGURE 85. INFILTRATION VS. APPLICATION FOR THE 12.5MM SPACING....99
FIGURE 86. PCPC LIGHTWEIGHT PLATFORM....102
FIGURE 87. PCPC PLATFORM PERFORMANCE CURVE....103
FIGURE 88. PICP AND PCPC PLATFORM SYSTEM PERFORMANCE CURVE....105
FIGURE 89. PICP, PCPC PLATFORM, AND 12.5 MM AVERAGES PER PAYMENT SLOPE....105
FIGURE 90. CAVITATION EXAMPLE 10 % SLOPE....106
FIGURE 91. INPUT INTERFACE....149
FIGURE 92. (USDA-NRCS, 1986) SCS TR-55 STORM MAP....151
FIGURE 93. TOTAL PROPOSED SITE AREA....152
FIGURE 94. CASE I PROFILE AND CROSS SECTION....155
FIGURE 95. CASE II PROFILE AND CROSS SECTION....155
FIGURE 96. CASE III PROFILE AND CROSS SECTION....156
FIGURE 97. OUTPUT INTERFACE....157
FIGURE 98. CLOGGING INTERFACE....164
FIGURE 99. TYPICAL POLLUTANT LOADINGS FROM RUNOFF BY URBAN LAND USE (LB. /ACRE-YR.) (EPA, 2006)....164
FIGURE 100. EXAMPLE 1 SCHEMATIC AND CROSS SECTION....166

FIGURE 101. EXAMPLE 1 INPUT INTERFACE 167
FIGURE 102. EXAMPLE 1 OUTPUT INTERFACE..168
FIGURE 103. EXAMPLE IA AND IB SCHEMATIC AND CROSS SECTION 169
FIGURE 104. EXAMPLE 1A INPUT INTERFACE 169
FIGURE 105. EXAMPLE 1A OUTPUT INTERFACE...170
FIGURE 106. EXAMPLE 1B INPUT INTERFACE...171
FIGURE 107. EXAMPLE 1B OUTPUT INTERFACE 171
FIGURE 108. PHOTO OF EXAMPLE 2 PICP PARKING LOT IN LA JOLLA, CA (ICPI, 2015) 172
FIGURE 109. EXAMPLE 2 SCHEMATIC AND CROSS SECTION..173
FIGURE 110. EXAMPLE 2 PLANS FOR CONSTRUCTION 174
FIGURE 111. EXAMPLE 2 INPUT INTERFACE 175
FIGURE 112. EXAMPLE 2 OUTPUT INTERFACE...175

LIST OF TABLES

Table 1. Calibrated Coefficients....40
Table 2. C 1781 Average Vertical Infiltration, in/hr., Before Horizontal Test....46
Table 3. ASTM C1781 Experimental and Calibrated Vertical Infiltration 51
Table 4. Average Max Overflow Rates per Pavement Cross Slope 55
Table 5. Calculated Maximum Overflow Rates per Pavement Cross Slope 57
Table 6. Infiltration Rate at Overflow per Section Area per Group, cfs/section area. 60
Table 7. Example of Raw Data Values Used in Statistical Analysis 60
Table 8. Incipient Overflow Rates per Group Spacing, Slope....61
Table 9. One Way ANOVA Summary....63
Table 10. Individual Factor Summary and Confidence Intervals 63
Table 11. t-test Summary Comparison between 6 mm and 10 mm 64
Table 12. t-test Summary Comparison between 10 mm and 12.5 mm....66
Table 13. t-t Summary All 6 mm data values and Pattern Comparison....67
Table 14. Correlation Summary between Pavement Slopes and Overflow Rate....69
Table 15. Synthetic Stormwater Soil Particle Size and Percent by Mass 71
Table 16. 6 mm Clogging Test Infiltration and Application Summary....77
Table 17. 10 mm Clogging Test Infiltration and Application Summary....77
Table 18. 12.5 mm Clogging Test Infiltration and Application Summary....78
Table 19. 6 mm Summary Incipient Overflow Rate, Infiltration Rate per Section Area 78
Table 20. 10 mm Summary of Infiltration discharge per Stormwater Applications....79
Table 21. 12.5 mm Summary of Infiltration discharge per Stormwater Applications....80
Table 22. Kim et. al. Infiltration Values per Aggregate Filler Spacing (Kim et. al., 2013) 85
Table 23. Linear Regressed Overflow Equations 89
Table 24. Average Max Overflow Unit Rates per Pavement Cross Slope (cfs/ft.) 92
Table 25. Average Horizontal Infiltration Rates (in/hr.) 94
Table 26. C 1781 Experimental and Calibrated ASTM C1781 Vertical Infiltration (in/hr.)....95
Table 27.Experimental and Calibrated Horizontal Infiltration Rates (in/hr.)....95
Table 28. Clogging Equation Parameters....100
Table 29. 6mm Clogging Test Summary....100
Table 30. Summary of Concrete Mixture....101
Table 31. Hardened Concrete Results 102
Table 32. Strength Testing Results....102
Table 33. Horizontal Infiltration Averages per Pavement Slope....104
Table 34. Horizontal Infiltration at Overflow Point per Pavement Slope....106
Table 35. Land Category and Sub-type Relation 153
Table 36. Case Level Characteristics 154
Table 37. Runoff Coefficients (American Public Works Association) 158
Table 38. 6mm Hydraulic Characteristics Summary. 161
Table 39. 7mm Hydraulic Characteristics Summary....161
Table 40. 8 mm Hydraulic Characteristics Summary 162
Table 41. 9 mm Hydraulic Characteristics Summary 162
Table 42. 10mm Hydraulic Characteristics Summary....163
Table 43. 12.5 mm Hydraulic Characteristics Summary 163

1. BACKGROUND AND LITERATURE REVIEW

Introduction of Clean Water Act

The concept of stormwater management has recently become of greater concern due to compliance with Phase II of the National Pollutant Discharge Elimination System (NPDES) Permit Program. The NPDES program was developed as part of the Environmental Protection Agency's (EPA) Clean Water Act (CWA) (White and Boswell, 2007). The foundations of the CWA can be found in the 1972 Federal Water Pollution Control Act (FWPCA) amendments. The amendments were the first to create pollutant discharge limitations on a national level, set requirements for water quality of the United States, and create the first permit program within the NPDES (McCall III, 2014). The first amendments were meant for prevention of point source pollution discharge into U.S. waters. The EPA defines point source pollution as "any discernible, confined, and discrete conveyance… from which pollutants may be discharged. This term does not include return flows from irrigated agriculture or agriculture stormwater runoff" (Environmental Protection Agency, 2011). In 1977, another set of amendments were made to the FWPCA. The first set of amendments were unable to reduce toxic water pollution. In the second set of amendments established "priority pollutants" were established and more stringent guidelines and standards for major industrial categories (McCall III, 2014).

After the determination of how and what types of pollution problems needed remediation, Congress passed another amendment to the CWA addressed under NPDES. Phase I of the NPDES, promulgated in 1990, focused on the stormwater runoff with three distinct characteristics (Barnard, 2002):

(1) ‘Medium’ and ‘large’ municipal separate storm sewer systems (MS4) generally serving populations of 100,000 or greater
(2) Construction activity disturbing 5 acres or greater
(3) five categories of industrial activity

In 1996, the results of the National Water Quality Inventory found that approximately 40% of the United States water bodies did not meet water quality standards. The results of the inventory showed that 13 percent of polluted acres, 21 percent of polluted lakes, and 45 percent of polluted estuaries were impaired by urban/suburban stormwater runoff. This inventory concluded that polluted runoff was a leading source of the impairment of US water bodies (Barnard, 2002).

In December 1999, the EPA promoted Phase II of the NPDES. Phase II included the areas of investigation to affect small MS4s in “urbanized areas”, which were defined by the Bureau of Census, construction areas from one to five acres, and non-point source pollution (McCall III, 2014). Phase II extended the amount of municipalities affected by NPDES from around 1,100 to nearly 5,000 (Barnard, 2002). The Maximum Extent Practicable (MEP) became standard for water quality and quantity improvement. Best management practices (BMPs) were implemented to reach the MEP. Six minimum control measures were defined to be the basis of a management plan for measurable goals of reducing the amount of water pollution. Figure 1 summarizes the six minimum control measures.

Figure 1. Six Minimum Control Measures (Cass County Government, 2014.)

The six minimum control measures are created for the operators of municipal stormwater sewer and sanitary systems. The measures seen in Figure 1 are expected to significant decrease the pollutants found in nearby water bodies (EPA, 2014). By introducing the public to stormwater management through public education and involvement, the public can better understand their impact on the environment and how they can counteract urbanization. Illicit discharges are a main source of introduction of pollution into nearby systems. Construction is also a large source of pollution (Barnard, 2002). By controlling discharge during and after development, the amount of sediment pollution being introduced into the system will decrease. Finally, maintenance of stormwater management systems will ensure that the systems continuing to be highly functioning in reducing stormwater.

Urbanization in the Hydrologic Cycle

The use of BMPs in urban landscape began as flood and drainage controls, because an increase in urbanization has caused a major increase in the amount of impervious area. In the hydrologic cycle, the impervious area results in surface runoff, as previously stated, the greatest cause of pollution to U.S. water bodies. Urbanization can increase the amount of surface runoff from 10% of the water cycle with natural ground cover to as much as 55% of the water cycle when ground cover becomes 75-100% impervious surface. The water that does not infiltrate the ground is classified in the water cycle as runoff. Figure 2 from the Alliance of Crop, Soil, and Environmental Science Societies depicts the effects of urbanization on the hydrologic cycle.

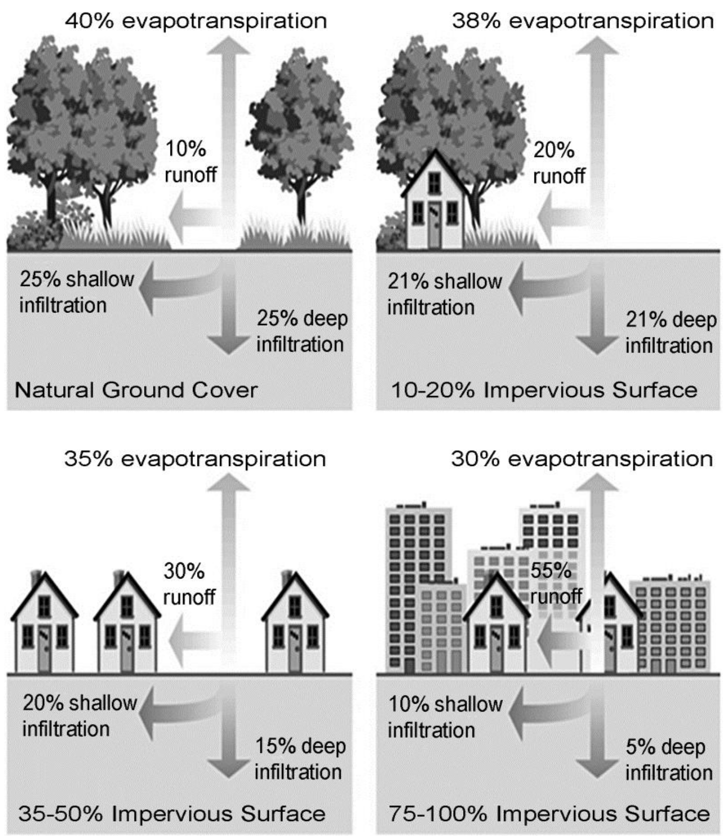

Figure 2. Effect of Impervious Surface on Hydrologic Cycle (NEH-653, 1998)

The removal of trees will decrease the amount of both shallow and deep infiltration and reduce evapotranspiration, which would have otherwise occurred through the plant leaves. Installation of impervious surfaces roofs and parking lots will decrease the chance of precipitation infiltrating the earth and divert it to nearby water bodies and stormwater sanitary and sewer systems (Mullaney and Lucke, 2013). The slight decrease of all the parts of the hydrologic cycle, evapotranspiration, shallow infiltration, and deep infiltration, will result in an increase in surface runoff.

Surface runoff, which leads to stormwater pollution, causes destruction to many habitats in nearby streams and water bodies (EPA, 2014). The two main components of stormwater pollution are: the increased volume and rate of runoff from impermeable surfaces and the actual amount of pollutant in runoff (EPA, 2014). Both should be taken into consideration because of their effects on surrounding ecosystems and environments.

Urbanization also results in greater amounts of a larger variety of pollutants entering the damaged water cycle. Sediments, pathogens, fertilizers/nutrients, hydrocarbons, metals, and more have been identified in large quantities in United States water bodies (EPA, 2005). The increase in velocity of runoff, because of reduced tree canopy, results in greater surface erosion of sediment and causes erosion of sediment into neighboring water bodies. The sediment is often carrying pesticides and herbicides from lawns and gardens, as well as viruses, bacteria, and nutrients from pet waste and failing septic systems. Fecal coliform is also a large contributing pollutant to water bodies neighboring large cities. In suburban and urban areas, the increase in population will also result in an increase in travel necessities and motor vehicles. The increase in transportation will introduce oil, grease, and toxic chemicals. During severe weather it is necessary to use methods, such as deicing, to make the roads travelable. Deicing road salts chemically change the runoff and carry this pollutant to nearby water bodies (EPA, 2014). Lastly, but commonly overlooked, is thermal pollution. Thermal pollution will cause a change in the dissolved oxygen levels of the small neighboring water bodies and destroy the current state of the habitats in the surrounding ecosystems. The EPA suggest the use of BMPs to reduce the damage these pollutants and many other the waters surrounding of urban and suburban areas.

Best Management Practices

The EPA has stated “the primary method to control stormwater discharges is the use of BMPs” (EPA, 2015). BMPs are used to mitigate the impacts on the environment from polluted runoff. A BMP can be a technique, measure, and/or a structural practice used as water pollution controls (EPA, 1999). BMPs were first created as a source of flood control. The implementation of the CWA made BMPs appropriate for pollutant removal. In the Stormwater Best Management Practice Design Guide, the EPA comments on the progression of BMPs saying, “In response to a growing national awareness and understanding of the wide range of environmental impacts associated with land use changes, particularly urbanization, BMPs have begun to be designed for stream channel protection and restoration, groundwater infiltration, and protection of riparian habitat and biota” (EPA, 1999).

BMPs are within two categories: structural and non-structural. Structural BMPs includes bioretention, bio swales, permeable pavement, rain gardens, and rain barrel. Non-structural BMPs include zoning and permitting regulations put in action to measure and audit of the amount of pollution and runoff being transported into the water cycle. Figure 3 and Figure 4 are examples of structural BMPs that can now be seen in everyday society, including a rain garden and rain barrel.

Figure 3. Examples of Structural BMP – Rain Garden (SUNY-ESF, 2015)

Figure 4. Example of Structural BMP - Rain Barrel (Rutgers, 2014)

Different BMPs should be used in different locations as appropriate. In a paper from the ASCE Low Impact Development of 2010, Fassman and Blackbourn states, "To mitigate or prevent the receiving water degradation, all aspects of the water cycle, including timing, rates, and volumes of stormwater runoff must be incorporated into the basis of the design" (Fassman and Blackbourn, 2010). The EPA has also recognized the need to account for variability between sites. Factors such as the watershed, terrain, physical site, community and environmental, and location and permitting, are considered in determining the most efficient BMP to implement at the site (EPA, 2004).

Permeable Pavements Designed as Best Management Practice

Permeable pavement is a BMP used to decrease the effects of impermeable area created by urbanization, while creating a surface adequate for constant foot or vehicle traffic. Pavement currently produce 25% of the impervious area in urban environments, and the runoff carries large amounts of heavy metals and hydrocarbons. The current design of pavement is created to prevent water from infiltrating into the underlying base course layer or sub-base; therefore, it is both sealed with an impermeable layer (Mullaney and Lucke, 2013). The idea of infiltrating through is pavements is a relatively new technique for stormwater control. Permeable pavement is a considerable alternative that has the ability to both reduce the pollution through infiltration through a pervious surface and capture and control runoff. Permeable pavements also have the ability to treat the pollution runoff through an interlaying filtration system in the design and provide detention for storage and groundwater recharge (Hunt III, 2010). There are four common types of permeable pavement currently in use: pervious concrete, porous asphalt, concrete grid pavers, and PICP, seen in Figure 5.

Pervious Concrete

Porous Asphalt

Concrete Grid Pavers

PICP

Figure 5. Types of Permeable Pavement (ICPI, 2014).

PICP Benefits and Concerns

There are many benefits to PICP that can be found in every stage of the design from construction and the ease of maintenance to the already discussed runoff improvements and pollution control. For example, PICP can be implemented at sites in need of quick construction because there is no need for curing time or delays due to cold weather during installation. PICP can promote foliage survival by providing air and water to the root system that would have been impeded by construction of impermeable pavements or other construction (ICPI, 2014).

The Interlocking Concrete Pavement Institute (ICPI) has recorded surface runoff reduction of 100% and, depending on subgrade soil, infiltration of 100% (ICPI, 2014). A study done by North Carolina (NC) State researched a combined system of impermeable pavement and grassed area compared to permeable pavement, referred to in the study as a grassed equivalent percentage. The SCS curve numbers (CN) were determined for events larger than 5.0 cm. The results showed that, "For the same rainfall depths based on SCS curve number method, a grassed sandy soil (CN: 61) would produce runoff. For the storms monitored, pavement reduced more runoff than a standard grass lawn. Therefore, the equivalent grass percentage was 100% for each event" (Hunt III, 2010).

The conclusions of the NC State study also found information on the surface infiltration rate of the permeable pavement in comparison to grass and impermeable surface results stating, "a permeable pavement with surface infiltration rate of 5.3 cm/hr. behaves as if it were 84% grass and 16% impermeable surface" (Hunt III, 2010).

Permeable pavements have also been shown to decrease harmful pollutants such as heavy metals, particulates such as suspended solids (sediment) and ammonia levels without the significant maintenance that is typically required for highway gullies (Roseen et. al., 2012; Schotlz and Grabowiecki, 2006). The increased water quality from PICP systems provides the desirable benefit for fulfillment of Phase II NPDES Storm Water Programs.

Ease of maintenance is considered a benefit because it only requires standard vacuum equipment to remove build up in the permeable joint on the surface. The high infiltration rates of the surface can be easily reestablished with the vacuuming (ICPI, 2014). This was proven in the NC State research, which also compared infiltration rates around stable and disturbed sediment landscapes. The results proved that removing clogging from the surface could greatly increase surface infiltration rates, up to nearly 99%. As seen, with the median surface infiltration rate of sites clogged with sediment to be 8.1 cm/hr., while the median surface infiltration rate of sites without sediment clogging was 2300 cm/hr. (Smith, 2010). This increase shows how extremely important maintenance is and how it can improve the capability of a site to control stormwater.

While these permeable pavement systems have been shown to provide adequate infiltration, life cycle, and maintenance has been shown to be a concern (Young, 2012). Life cycles of porous pavements have been related directly to hydraulic performance and the decrease of that performance (Young, 2012). Decrease of hydraulic performance can be caused by the clogging or collapsing of pavement pores. Clogging is a physical component or process of decreasing porosity from the accumulation of particulates (sediment) that occurs over time with permeable pavements (Young, 2008), thus pavement clogging would then adversely affect life cycle costs.

Permeable pavements have also been shown to mitigate urban island heat effects (Kevern et. al, 2012). Many pavements contribute to urban heat due to causing a decrease in evapotranspiration, heat absorption and bulk mass properties (Kevern, et. al., 2012) while permeable pavements have been shown to store less heat (Kevern, et. al., 2012). PICP systems alone have been shown to have lower surface temperatures however, cooling properties were related directly to available surface water (wetting) (Li, et. al., 2013). Regardless, PICP as a permeable pavement system can thus be used to mitigate urban island heat effects providing a much needed benefit.

Issues with permeable pavement systems include structural loading issues such as displacement due to wheel loading and decreased performance over the life of the system primarily due to clogging (Schotlz and Grabowiecki, 2006). Main causes of clogging are traffic sediment ground into pavement prior to being washed off, stormwater suspended sediment, and shear stress from vehicles (wheel loading issue) collapsing pores (Schotlz and Grabowiecki, 2006). However, several studies have found PICP and other permeable pavement systems to not suffer from significant clogging issues. According to Booth et al. (2003), after 6 years of permeable pavement use, which included a concrete block with lattice pattern, clogging issues were not found to be an issue. Similarly, Lucke (2011) found PICP system's infiltration was satisfactory after 8 years of continuous service with no maintenance performed on the pavers suggesting that clogging probably should not be as much of a concern.

Other non-hydrologic issues with permeable pavements include displacement due to tree roots. Trees lining such permeable pavements cause an increase in root structures in search of water (Lucke and Beecham, 2011) that is not found with impermeable pavements.

Since the EPA and the NPDES require infiltration and water quality improvement, systems such as PICP are becoming more widely used within urban environments. The benefits of PICP include groundwater recharge, increased over all stormwater quality such as peak flow mitigation and pollution reduction conceivably outweigh any issues such as possible clogging system issues.

Permeable Interlocking Concrete Paver Design

Permeable Interlocking Concrete Pavement (PICP) is a type of permeable pavement that uses filtration, infiltration, and detention while creating a surface that be applied for both vehicular and foot traffic. PICP are concrete pavers that are installed with voids that to promote infiltration through the pavers (Hunt, III, 2010). The voids will help surface runoff return to pre-development standards by improving the ability of the pavement system to transmit water to the soil. A typical cross section of PICP from the Interlocking Concrete Pavement Institute is depicted in Figure 6.

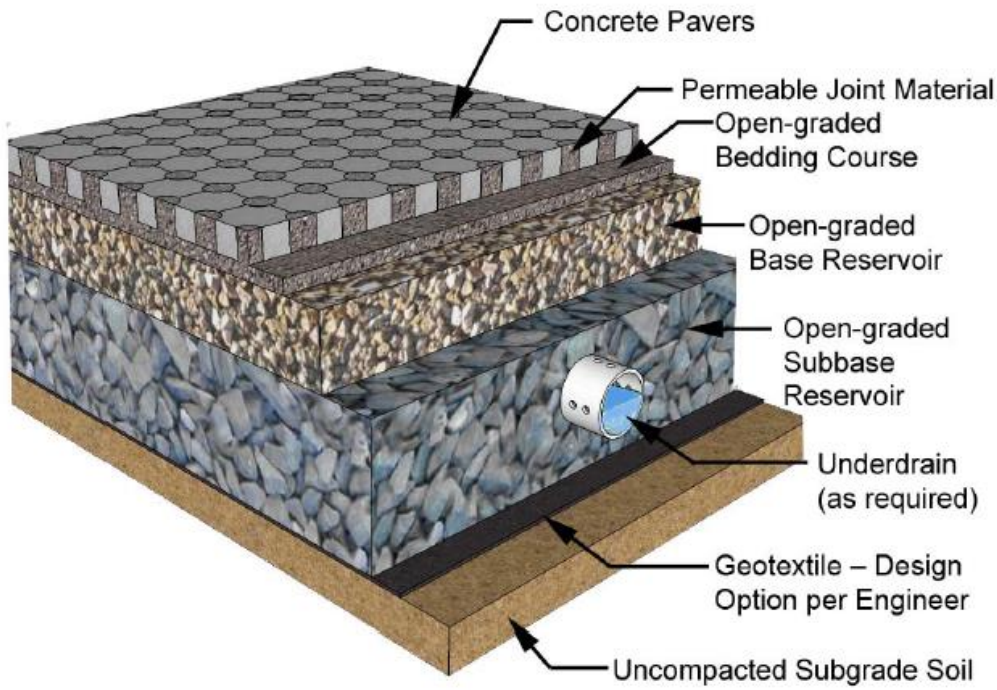

Figure 6. PICP Cross Section (ICPI, 2014)

The concrete pavers can be manufactured in a variety of shapes and size to meet design needs. Pavers along pedestrian areas are created at 2 ⅜ inch thickness. Pavers used for vehicular traffic are created at a minimum of 3 ⅛ inch thickness. The pavers are modeled with joints and opening at the corners and midpoints. Joints and openings with ASTM No. 8, 8/9, or 9 gradation stones promote infiltration. The open graded bedding course also consist of ASTM No. 8 or similar sized open-graded aggregate that provides a permeable bed about 2 inches thick for the pavers to set on. The open-graded base reservoir provides water storage, and acts as a choking layer between the open-graded bedding course and sub-base. The bedding course consist of ASMT No. 9 gradation. This layer is 6 in thick for vehicular use and 4 in thick for pedestrian use. The open-graded sub-base reservoir, also used for water storage between the large sized stones of ASTM No 2, 3, or 4. The size is site specific based on the amount of detention necessary, and this layer can be omitted in pedestrian use because of the increase in the of the base reservoir. (ICPI, 2014)

Both the underdrain and geotextile fabric are not necessary in every PICP installation. An underdrain is not needed for sites with high exfiltration soils, as the soil will not need extra help removing water from the base and sub-base. Sites with low infiltration soils have a perforated pipe connected to some type of outlet structure or other BMP, if the permeable pavement is part of a treatment train. Geotextile fabric is a separation between sub-base and subgrade to prevent mitigation of fines and clogging of effective pore space (ICPI, 2014).

The subgrade soil infiltration in classified based on the amount of percolation through the soil. For the purpose of this these, percolation will be referred to as exfiltration. There are three types of PICP systems based on the exfiltration into the open-graded stone base into the soil subgrade: full exfiltration, partial exfiltration, and no-exfiltration. In full exfiltration the water will exfiltrate through the base and sub-base directly to the soil subgrade. The amount of exfiltration in each application decreases as the infiltration rate of the soil decrease. For example, Full exfiltration is most commonly applied over soils such as sands and gravels with high infiltration rates (ICPI, 2014). Figure 7 shows a representative detailed installation schematic of full exfiltration to soil subgrade.

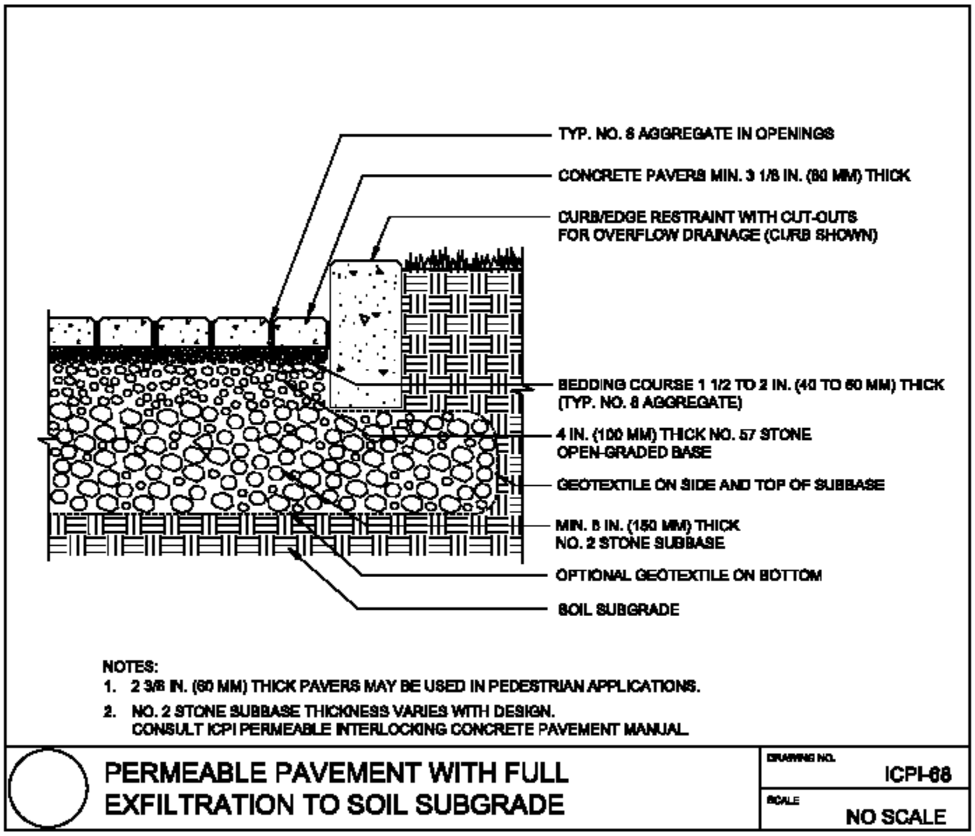

Figure 7. Detail Drawings of Full Exfiltration of PICP (ICPI, 2014)

While partial exfiltration is used over silts or clays and relies on the drainage of into the subgrade soil and drainage pipes to rid of excess water in the system. Figure 8 shows a representative installation schematic of partial exfiltration to soil subgrade. No-exfiltration is used when a low permeability is encountered at the site, such as loess soils or other fills soils. Water will degrade strength of the soil (ICPI, 2014). Figure 9 shows detailed drawings of no-exfiltration to soil subgrade.

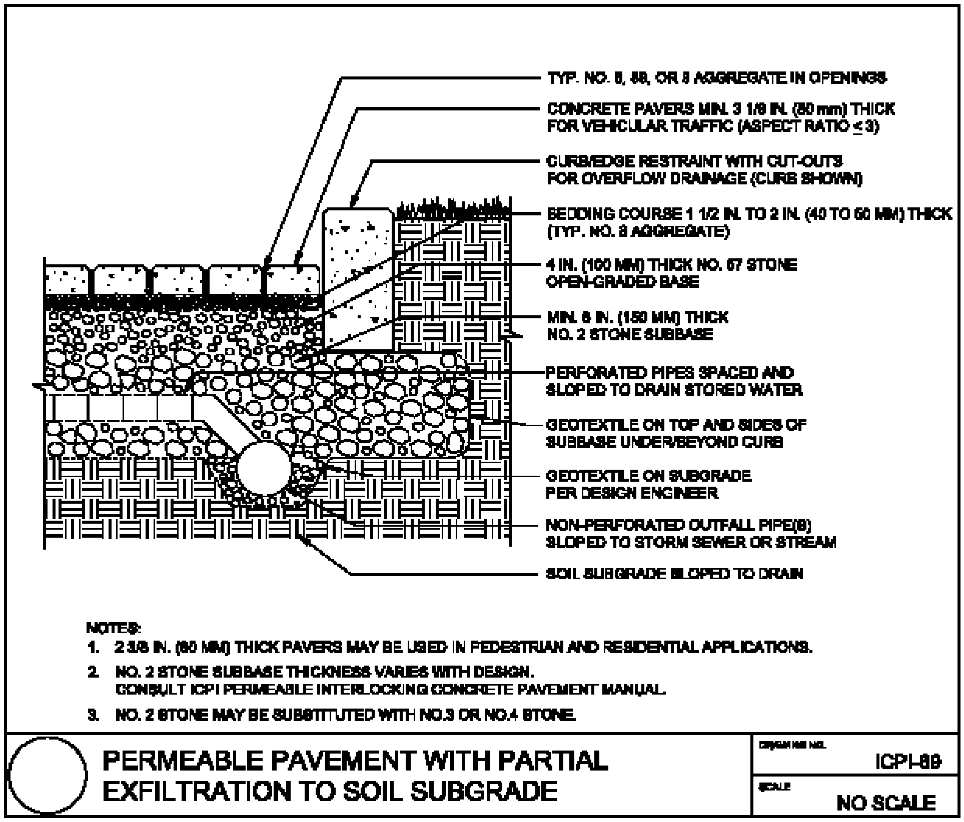

Figure 8. Detailed Drawings of Partial Exfiltration of PICP (ICPI, 2014)

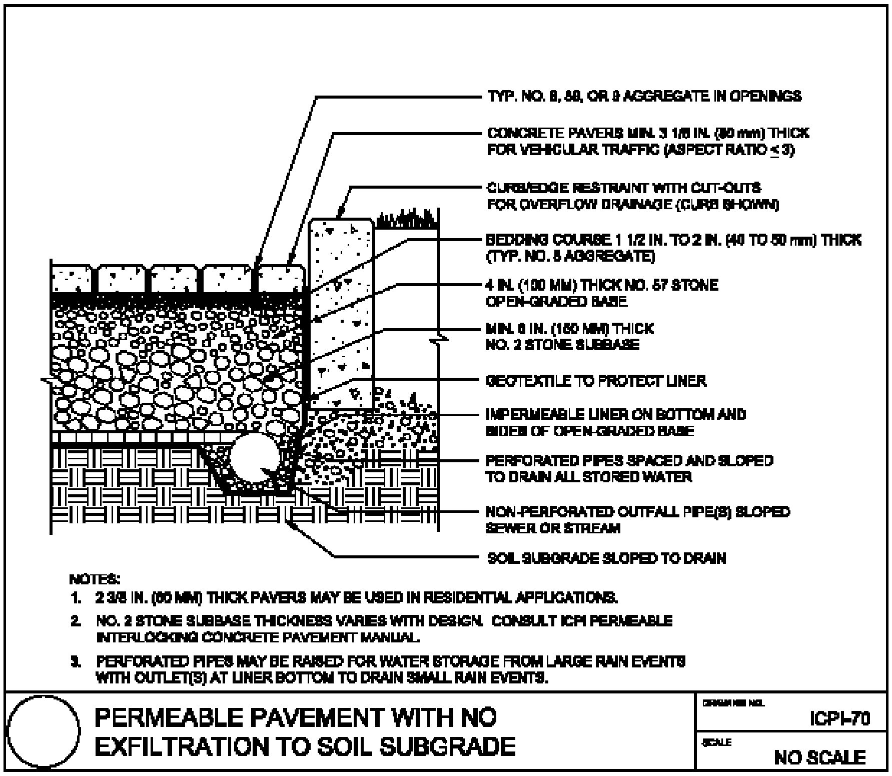

Figure 9. Detailed Drawings of No-Exfiltration of PICP (ICPI, 2014)

Overflows of each system are managed differently as well. Full exfiltration overflows are controlled "via perimeter drains to swales, bioretention areas, storm sewer outlets" (ICPI, 2014). Partial exfiltration daylights excess water into a sewer or stream. No-exfiltration systems are part of an assembly into a detention pond or can even be used for a reservoir for water harvesting or horizontal ground source heat pumps. (ICPI, 2014).

Common applications of PICP and other porous systems include parking lots, driveways, pedestrian access and bike lanes, as well as used for slope stabilization and erosion control (Schotlz and Grabowiecki, 2006). Design decisions of PICP include both structural and hydrological analysis just as in impermeable pavement design. Structural analyses for design include intended use of the PICP system, adequate strength and thickness of the base layer that accomplishes such use. Hydrologic factors that should be considered for design purposes include the volume of water that needs to be mitigated, the depth of the aggregate base and how much water via infiltration can be held. Figure 10 displays one example of a design flow chart for permeable pavement systems.

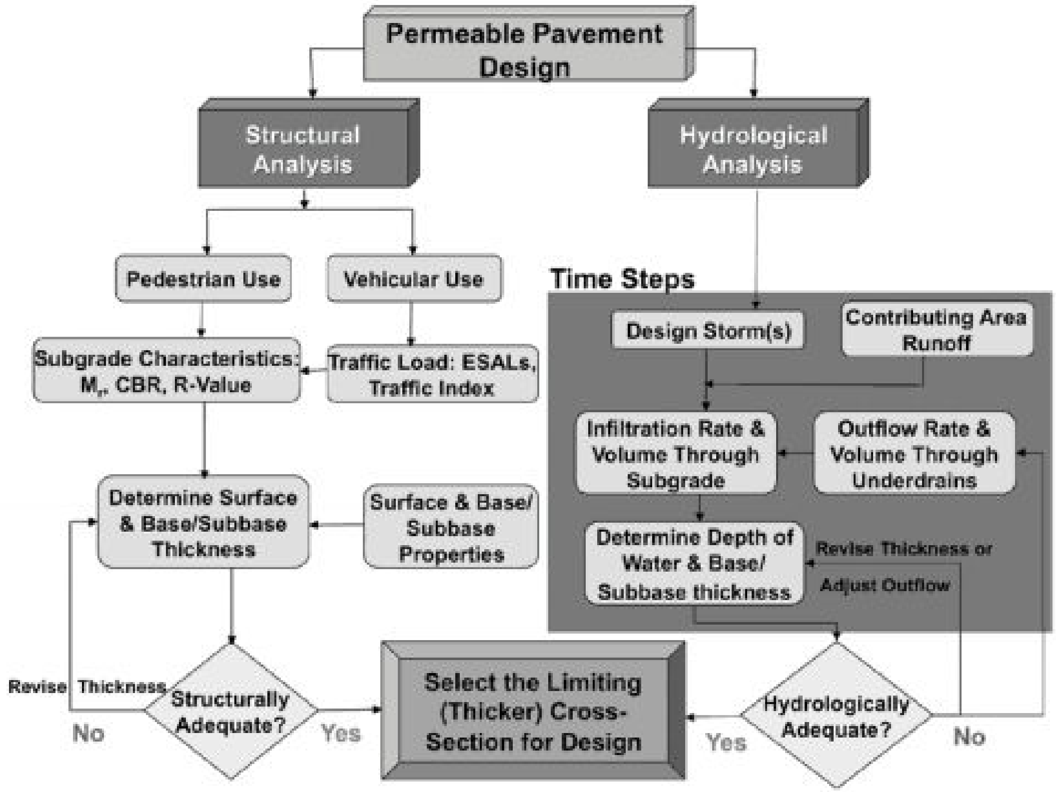

Figure 10. Permeable Pavement Design Flow Chart (ICPI, 2015)

Design of permeable pavements, such as PICP, for BMP's would include analysis of experimental testing for pollutant reduction, infiltration rates to predict the stormwater runoff reduction, and proper design including life cycle costs including installation and maintenance. Several studies have shown that porous pavements have been shown to adequately reduce pollutants from stormwater runoff (Roseen et. al., 2012). For the purpose of the following research, particular interest was placed upon infiltration and overflow flow rates. Infiltration rates from porous pavements have been shown to adequately infiltrate direct storm and runoff from adjacent areas for the most extreme storm events (Brown and Borst, 2014).

Previous research, such as the Brown and Borst, 2014 study, has concentrated on vertical infiltration hydraulic analysis of PICP field test sections. The hydraulic analysis has been conducted using the current test method for permeable pavement's hydraulic performance, the ASTM C1781 (ASTM, 2013). The ASTM C1781 method measures the vertical surface infiltration of a permeable surface and does not describe the horizontal sheet flow capacity of the pavement. Additionally, field sections display decreasing infiltration rates due to aging surfaces that have acquired sedimentation clogging. Horizontal sheet flow with sediment clogging research has not been conducted.

The structural design is based on traffic load. Impervious conventional highways are currently created using standard design methods created by American Association of State Highway and Transportation (AASHTO). When designing with pervious pavement, there has been a design shift to a new AASHTO 202 Mechanistic-Empirical Pavement Design Guide, which will consider highway loads, load testing, soil types, and climatic conditions (Smith and Hunt III, 2010).

In terms of the hydrologic design, it is necessary to consider the design storms, long term soil infiltration rate, and base/sub-base reservoir thickness and storage capacity (Smith and Hunt III, 2010). The inflow and outflow of water in PICP can be seen in Figure 11 created by the NC State Researchers using Permeable Pavement Design Pro to approximate how the water will act through the permeable pavement system and create a hydraulic profile for the system. Rainfall/snowmelt and runoff water from surrounding areas are the two contributing water sources in a standard PICP system. This contributing water source will take one of three paths after initial introduction to the PICP system; evaporation/transpiration, surface infiltration, or surface runoff. By increasing the permeable area with PICP, the amount of water that will become surface infiltration increases. Surface infiltration flow will then be directed to a subdrain through the base/sub-base layer or will become groundwater recharge (Collins et. al., 2008).

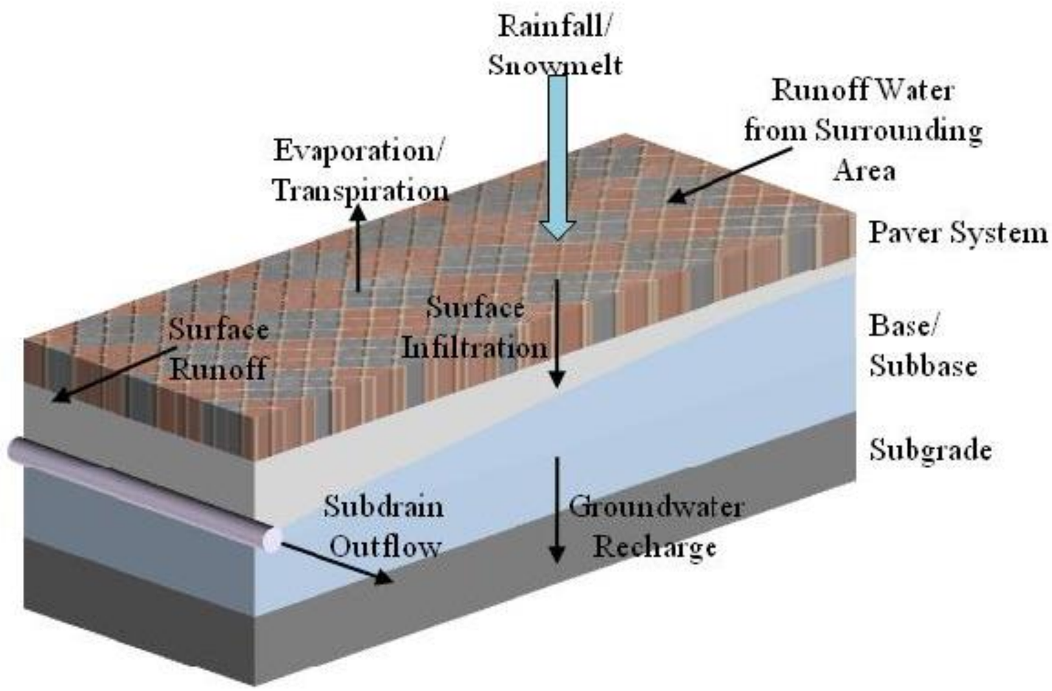

Figure 11. Water Inflow and Outflow on Permeable Pavement (Collins et. al., 2008)

Hydraulic Development of PICP

The initial laboratory deign was based on the thesis research performed by Grahl, (2012), "Hydraulic Design of Pervious Concrete Highway Shoulders." Grahl's research was similar as a flume was constructed to allow for infiltration and overflow discharge to be measured individually. Results indicated that vertical infiltration was greater than measured horizontal infiltration for Portland Cement Pervious Concrete (PCPC) test sections. The difference between the vertical and horizontal infiltration values led to the following research on PICP. Previous to this research PICP had been studied only via vertical infiltration and not for horizontal hydraulic sheet flow. As pavements receive discharge in the form of horizontal sheet flow, the hydraulic performance of PICP systems under such conditions may provide important information such as infiltration and overflow rates. Figure 12 shows the original flume which was refined for the following research.

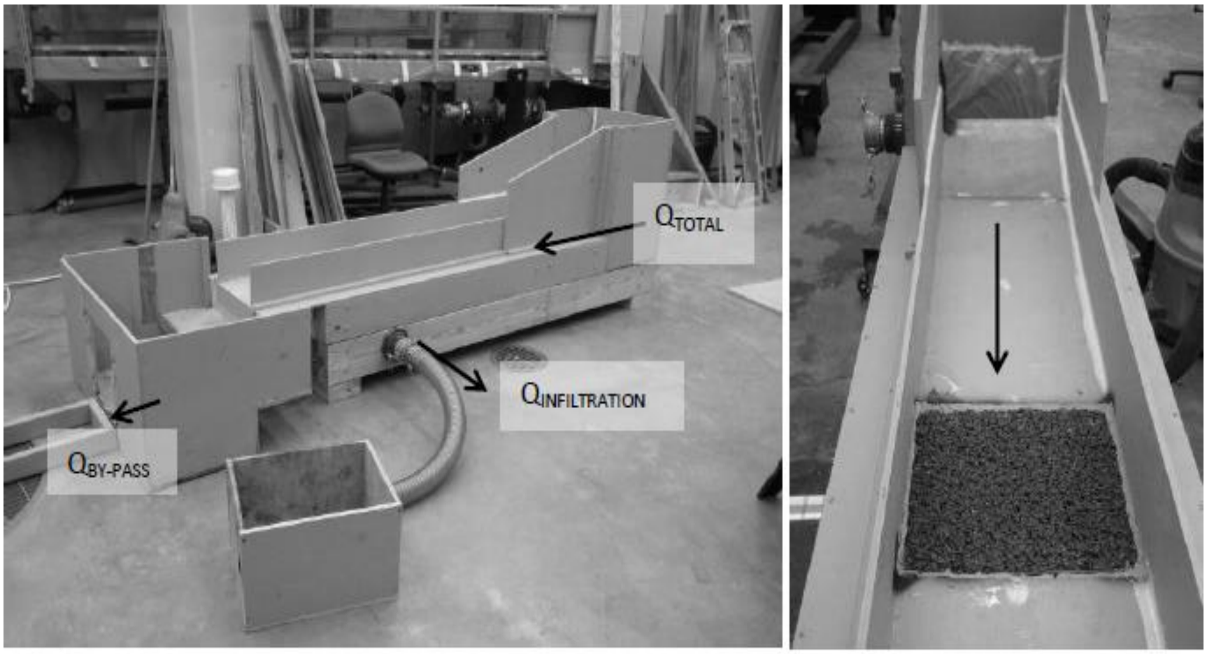

Figure 12. Flume for Pervious Concrete Infiltration Research, (Grahl, 2012)

The hydraulic model for this research focused on the characteristics of surface runoff, also known as overland flow or overflow in hydrologic terms (Richardson, 1989). Conceptually, overflow will occur when the rate of the water source, rainfall or snowmelt exceeds the rate the soil or surface can absorb water. In terms of acting forces, overflow occurs when the gravitational forces overcome the friction forces and surface tension of the fluid, represented in Figure 13 (Richardson, 1989.). The nomenclature used in Figure 13 is as follows: $\hat{\imath}$ represent the rainfall intensity, L represents the length of the plane, h represents the flow depth, τ_0 represents frictional forces, $\bar{u}$ represents the mean velocity, S_0 represents the bed slope, and q represents the unit discharge (Richardson, 1989).

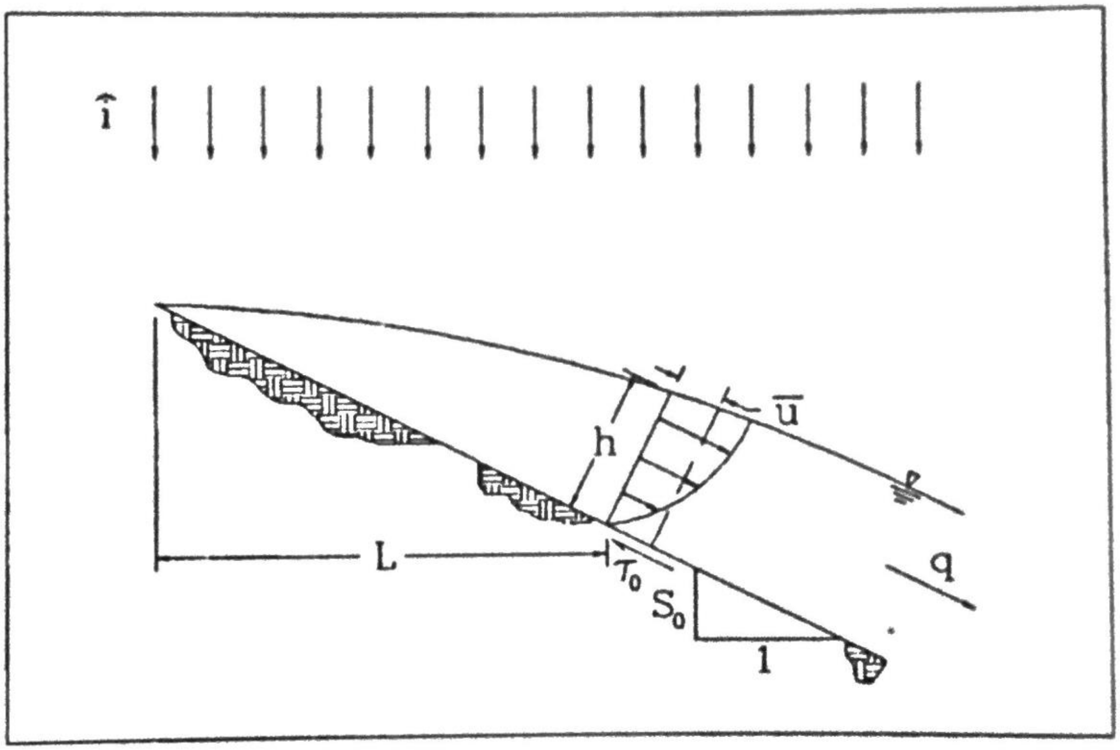

Figure 13. Overland flow Diagram (Richardson, 1989).

Overflow relates to time and a system reaches equilibrium when the discharge no longer varies with time (Richardson, 1989). For the purpose of this research, the design tool later discussed assumes that each site will reach full equilibrium. Full equilibrium assumes that the rate of flow entering and exiting the system are equal. A full equilibrium hydrograph is seen in Figure 14. The vertical axis in Figure 14 represents a dimensionless discharge. The horizontal axis represents time including the time of initial rainfall, T_o, time to equilibrium, T_e, and duration of rainfall, T_r. (Richardson, 1989). Full equilibrium assumes that the duration of rainfall is greater than the time to equilibrium.

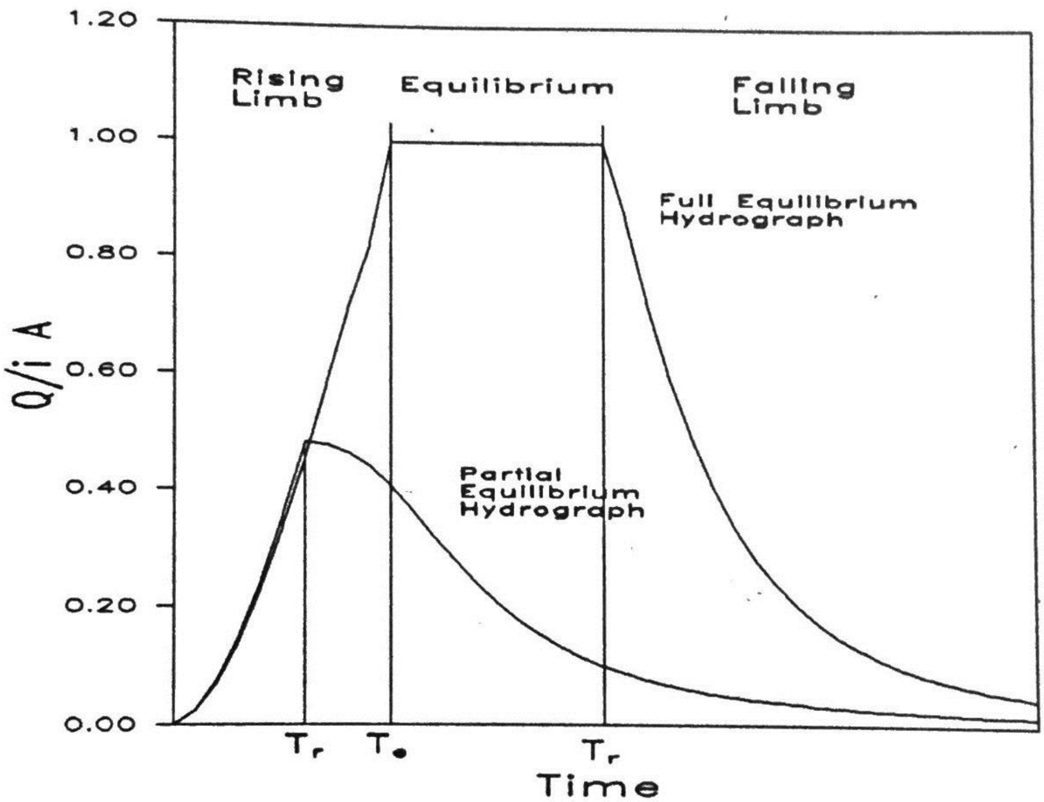

Figure 14. Full and Partial Equilibrium Hydrograph (Richardson, 1989).

This results of this research can be applied to parking lots and sidewalks, the most common use for PICP, although strip parking or highway shoulder applications are similarly designed. Figure 15 shows a typical pavement top view and cross section at insipient overflow. The nomenclature used in Figure 15 is as follows: L represents the length of the impervious overflow plane, L' represent the length of the PICP plane, W represents the width of the section, C_L represents the center line, and q represents the unit discharge. Figure 15 profile is used as the basis of the design throughout this remainder of this research.

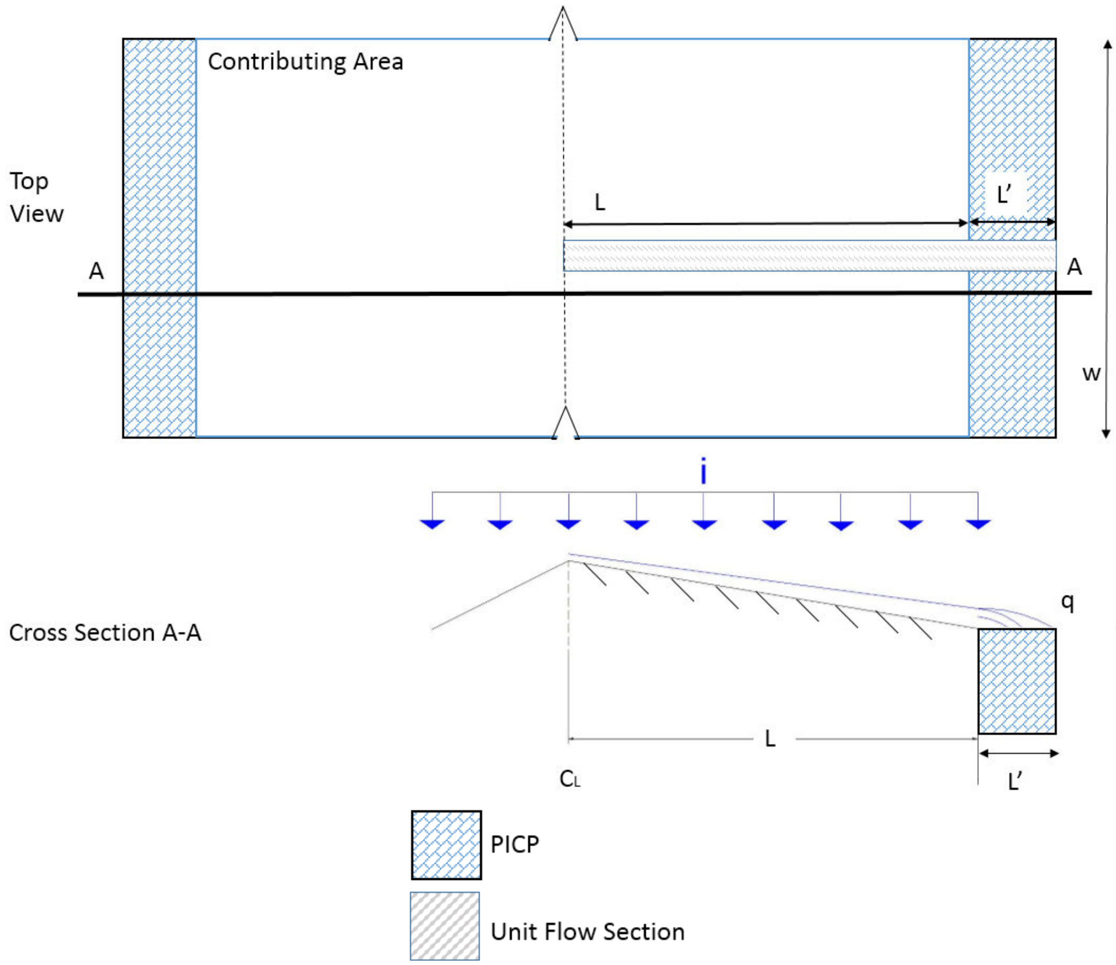

Figure 15. Pavement Top View and Cross Section for Insipient Overflow

2. PICP TESTING

Flume Design

A two layer hydraulic flume was designed to split the flow vertically and horizontally for infiltration experimentation. The flume was manufactured locally with each piece individually drawn in the 3D program of Solidworks prior to construction. Figure 16 through Figure 19 were the produced CAD drawings used in the design. Figure 20 the water flow through the pumping system. As previously mentioned, the initial laboratory deign was based on the thesis research performed from Grahl, (2012).

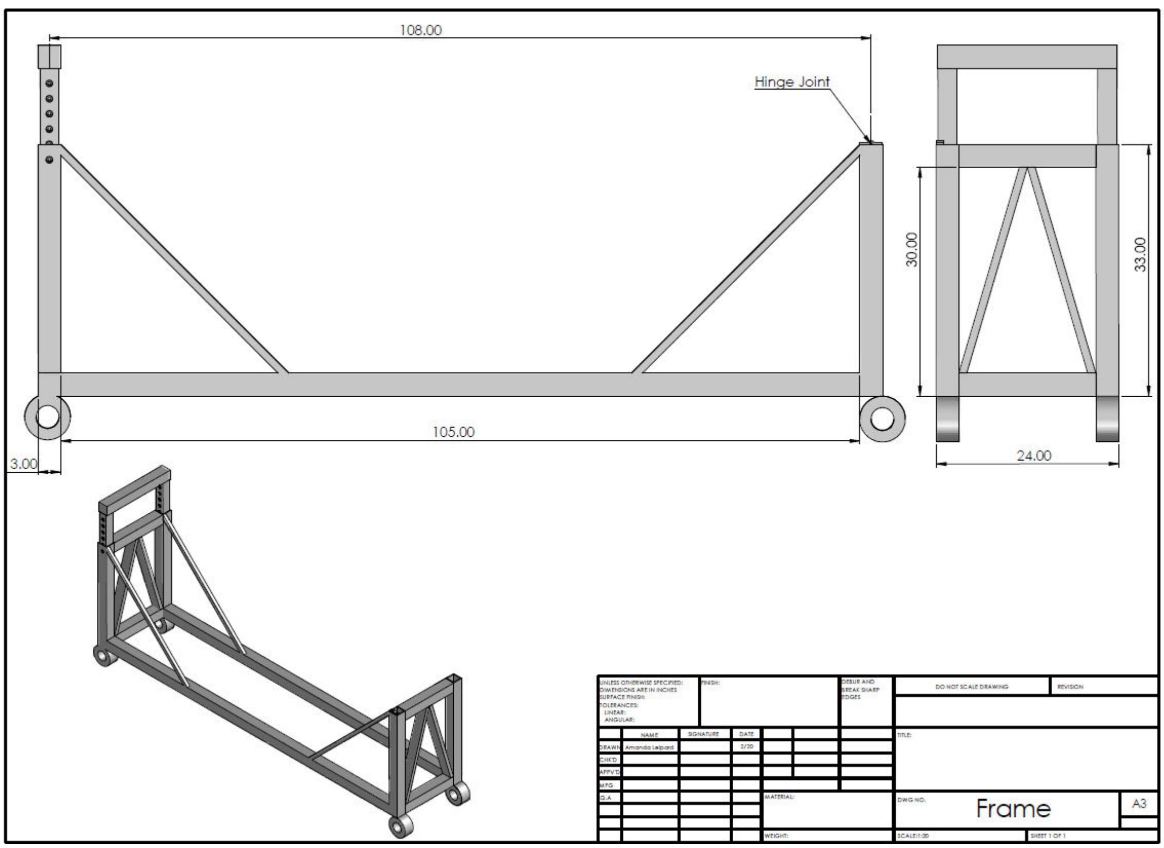

Figure 16. Bottom Support Frame Assembly Drawing

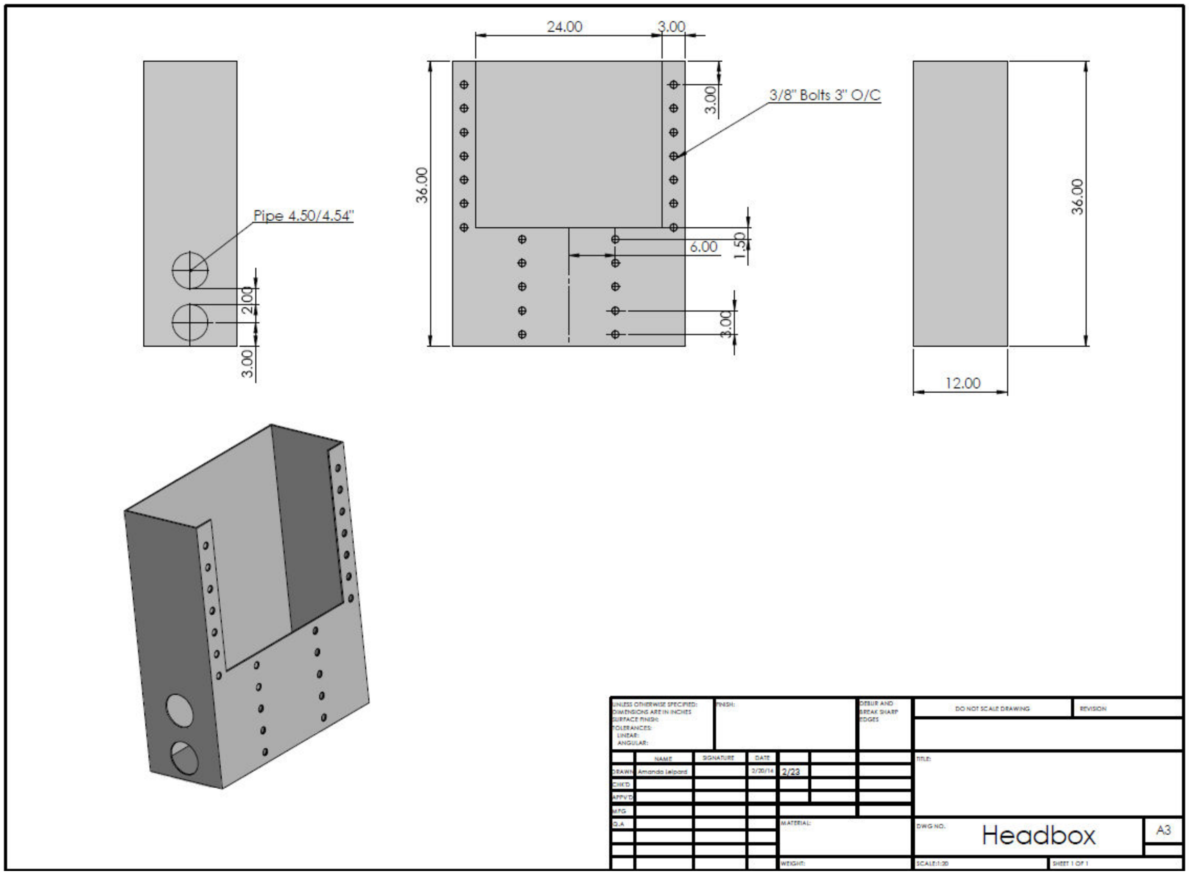

Figure 17. Headbox

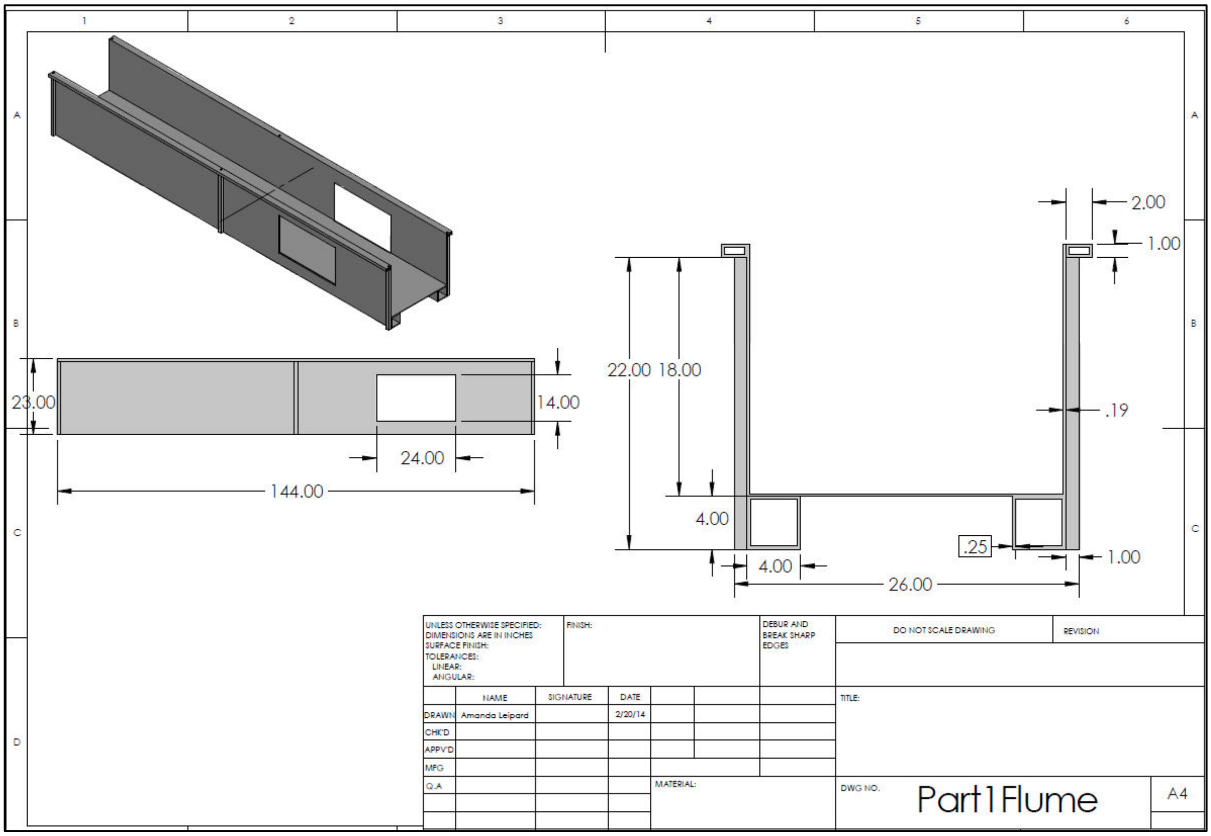

Figure 18. Base Layer Part 1 Drawing

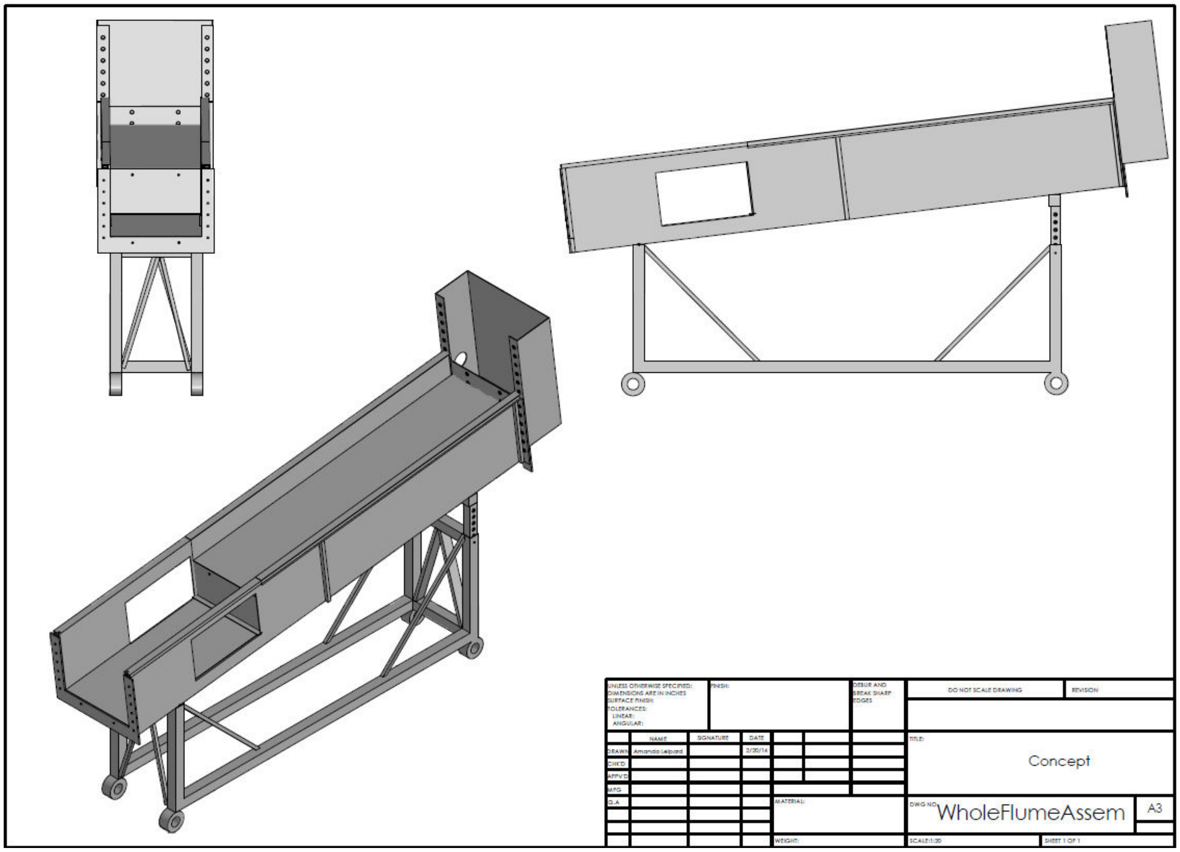

Figure 19. Complete Flume Assembly Drawing

Figure 20 displays the directional flow of water through the pumping circulatory system. The tank was filled and holds an initial amount of water that was pumped through the Venturi meter where the initial total discharge (Qtotal in) was measured. The discharge then flows through the head box of the flume to the upper level of the flume. The discharge flow then moves across the pavement section where the vertical discharge split occurs allowing for the water to either infiltrate or overflow across the test section. The end boxes are retain and split horizontally the discharge flow. V notch weirs were used to measure the infiltration (Q infiltration) and overflow rates (Q overflow). The split discharge is shown in

Figure 21. The infiltration and overflow flow rates when added together calculate the total flow out of the system (Q out) which is compared to the initial venture flow rate for verification of equilibrium.

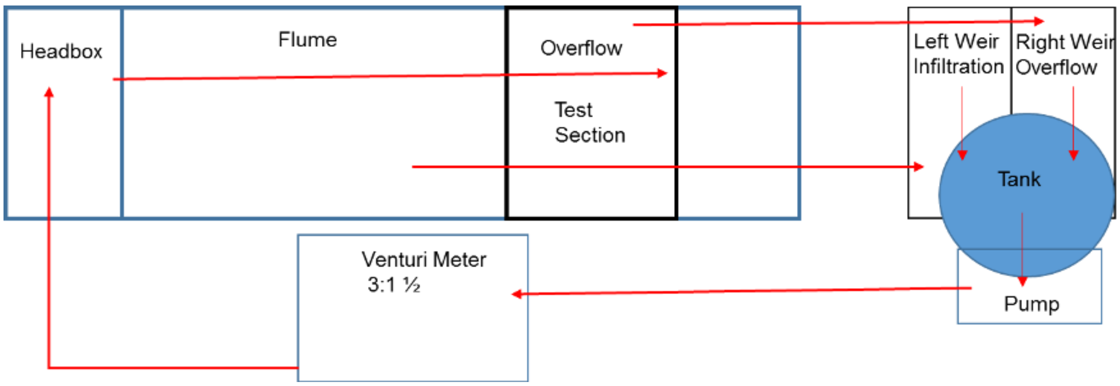

Figure 20. Laboratory Circulation System Schematic

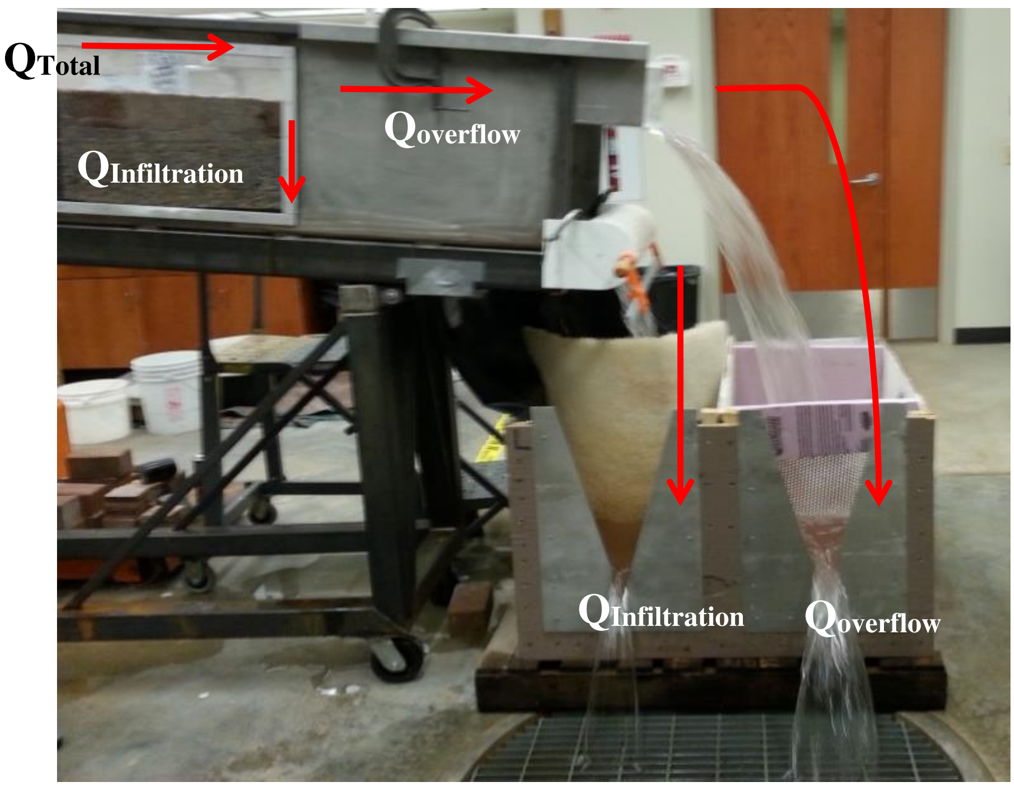

Figure 21. Completed two layer Hydraulic Flume.

The PICP systems were hand placed within the flume. An experimental test section experiencing overflow is shown in Figure 22. Sides were sealed with standard plumbers putty to prevent leakage. For proper hydraulic measurements and horizontal discharge over the test sections upstream supercritical sheet flow was necessary. The flume was designed to have four times the test section length upstream to create stabilized supercritical sheet flow (Figure 23).

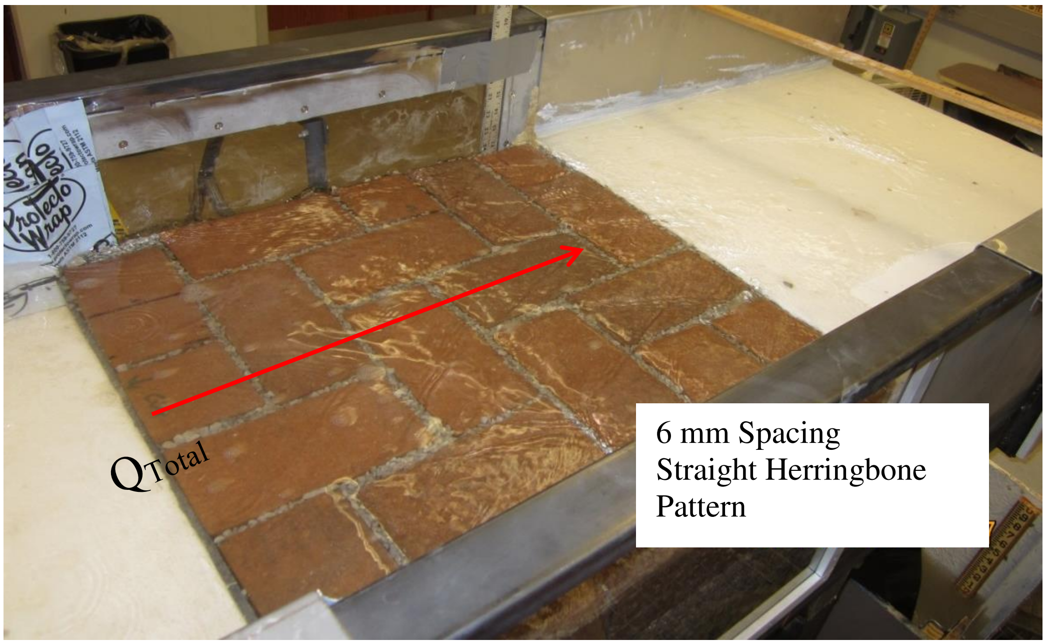

Figure 22. Experiment Testing Section

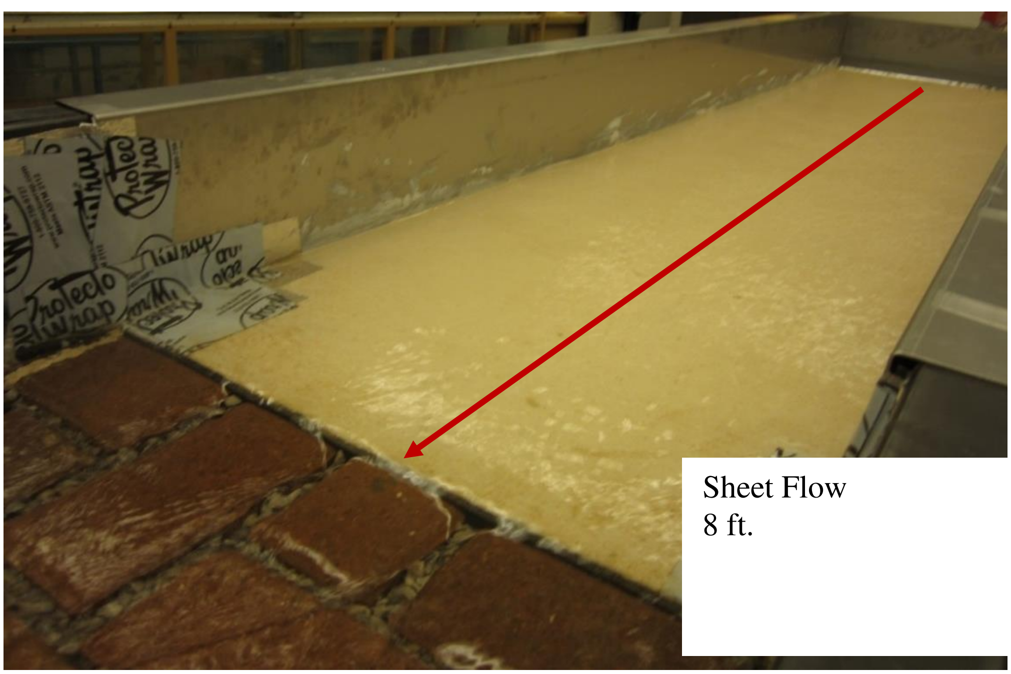

Figure 23. 8 feet of Horizontal Sheet Flow

A hydraulic jack was used to vary the slope of each experimental test. Each set up was tested at five different slopes of 0%, 1%, 2%, 5% and 10%. As previously stated, the flume was designed to maintain 8 feet of horizontal supercritical sheet flow over each of the tests slopes. The jacking system used is shown in Figure 24.

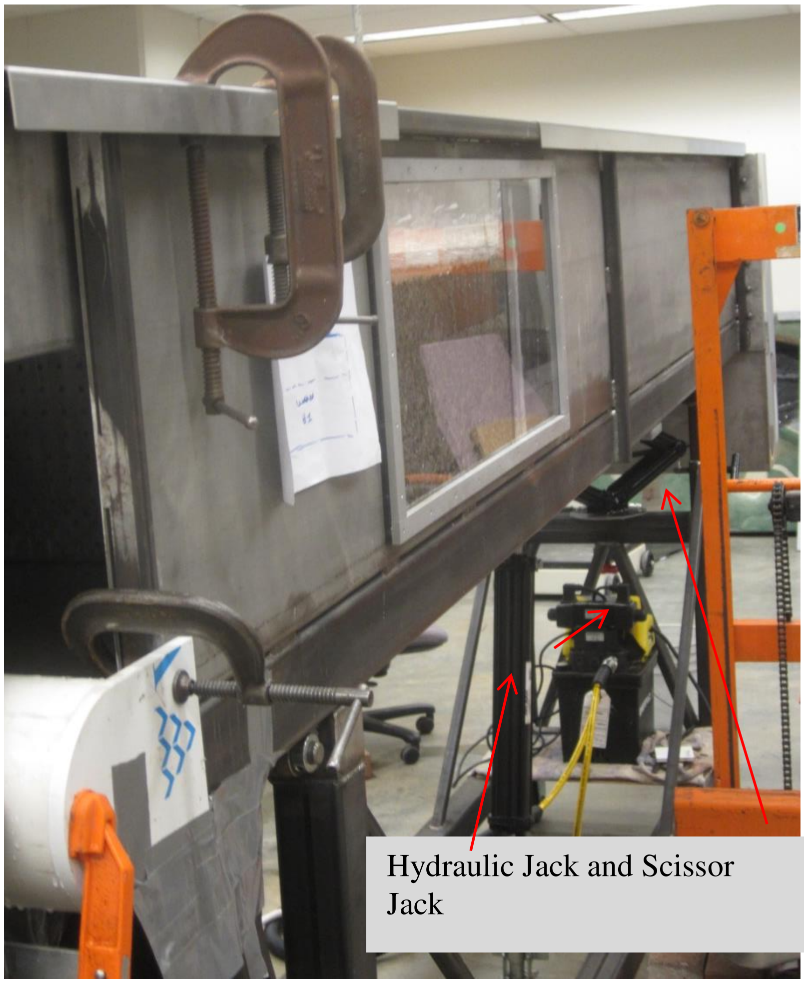

Figure 24. Flume with variable slope and Jacking System

Calibration and Discharge Calculations

The Venturi meter was used to determine the total flow into the system. The manometer for the Venturi meter is shown in Figure 25 and Figure 26. The calculated flow rate through the Venturi was determined by:

Equation 1. Venturi Discharge

$$Q = C_d\sqrt{2gH}$$

Where:

C_d = Calibrated Weir Coefficient

g = gravity, 32.2 ft/s^2

H = Height difference in meter, ft.

H_{in} = HΔ ($SG_{merrium}$ -1) and H_{Δ} is the height difference of dye in Venturi meter.

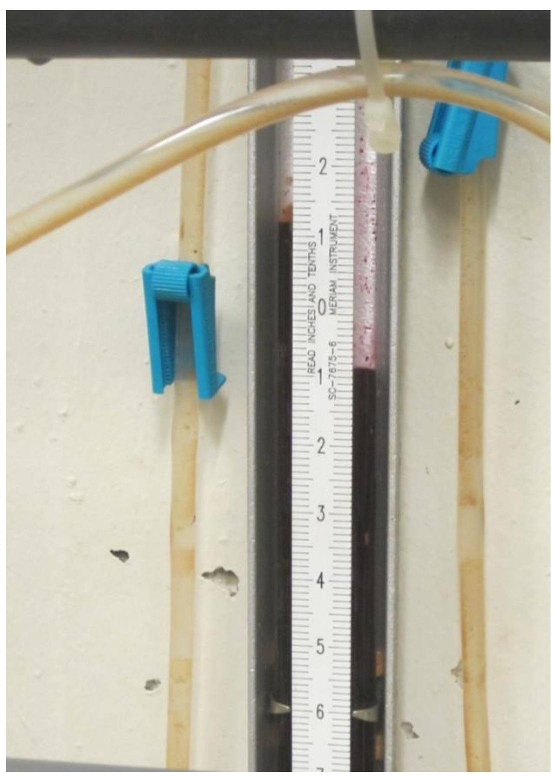

Figure 25. Merrium (SG=2.95) U-Tube Manometer attached to the Venturi Meter for Measurement of Total Flow Rate

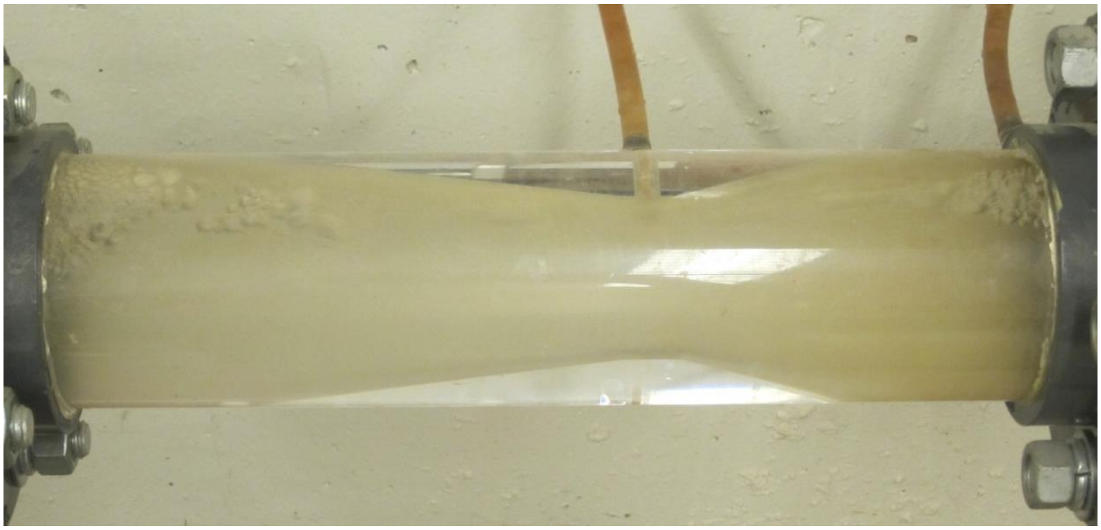

Figure 26. 3in.X1.5in. Venturi Meter

The V-notch weirs were constructed from an eighth inch thick aluminum sheet at 30° degree angle as shown in Figure 27. The use of the V notch weirs were used to determine the infiltration and overflow rate of the experimental sections. Equation 2 was used to determine the required discharge flow rates with a required measured depth of the water upstream of the weirs (H). The individual weir coefficient was a calibrated value for each side of the tail box. The weirs were calibrated against the discharge measured from the Venturi, and verified by volumetrically weighing the weir output for specified time. The coefficient of discharge, Cd, (Equation 2) for each weir was then back calculated with the infiltration weir coefficient found to be 0.844 and Overflow coefficient at 0.799.

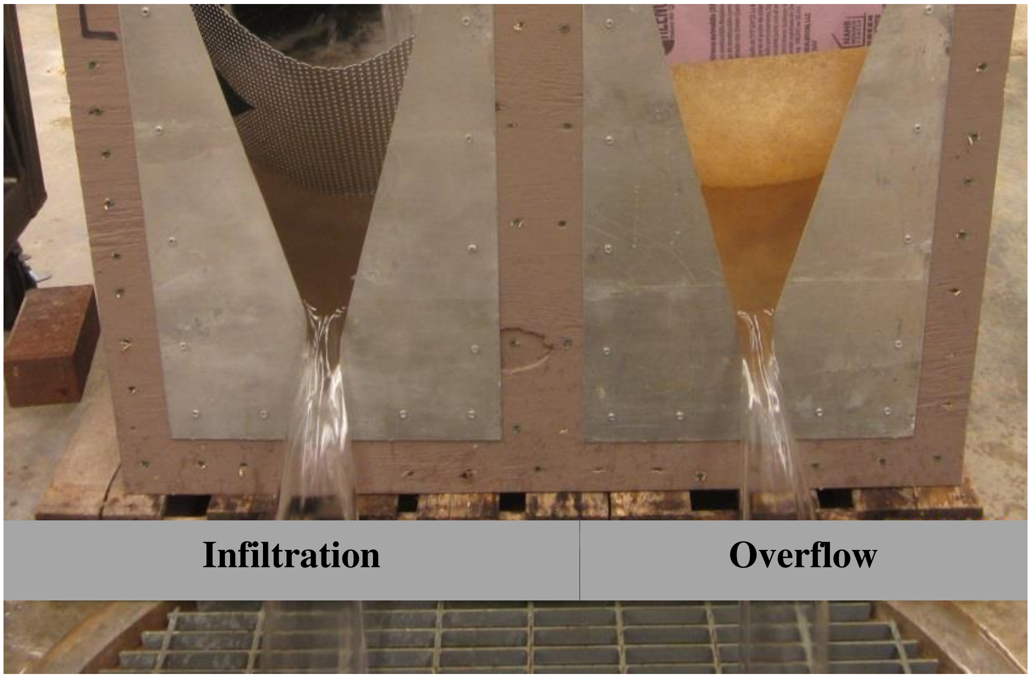

Figure 27. V Notch Weirs in Tail box

Equation 2. Weir Discharge

$$Q = C_d\sqrt{2gH^{5/2}}$$

Where:

C_d = Calibrated Weir Coefficient

g = gravity, 32.2 ft./s^2

H = Head on the weir, ft.

The flume was initially calibrated to determine the coefficients of both the Venturi and v-notch weirs. Using the weir and Venturi meter equations, known area and weir geometry the weirs and meter were calibrated using a known volume. Essentially, as water flowed through the system a known volume was filled and timed providing the measured discharge value, Q in ft^3/s. This value as well as the set known area of the meter and geometry of the weirs the coefficient of discharge was calculated. Thirty tests with readings for each weirs and the venture meter were completed. The resulting coefficients are shown in Table 1.

Table 1. Calibrated Coefficients

Weir	Calibrated Weir Coefficient
Venturi	1.035
Left V-Notch	0.844
Right V-Notch	0.799

Test Section Placement

Various PICP patterns and spacings were installed by hand in the 2 ft. by 12 ft. two layer flume. Each spacing and pattern was cut to fit the 2 foot wide section. The base fill aggregate materials included 7 inches of ASTM #57 limestone, 2 inches of ASTM #8 limestone, followed by the pavers set at different spacing with either #8 or #9 joint filler materials. The finished flume with the system set up and base materials are shown in Figure 28 and Figure 29.

Figure 28. Two Layer Hydraulic Flume

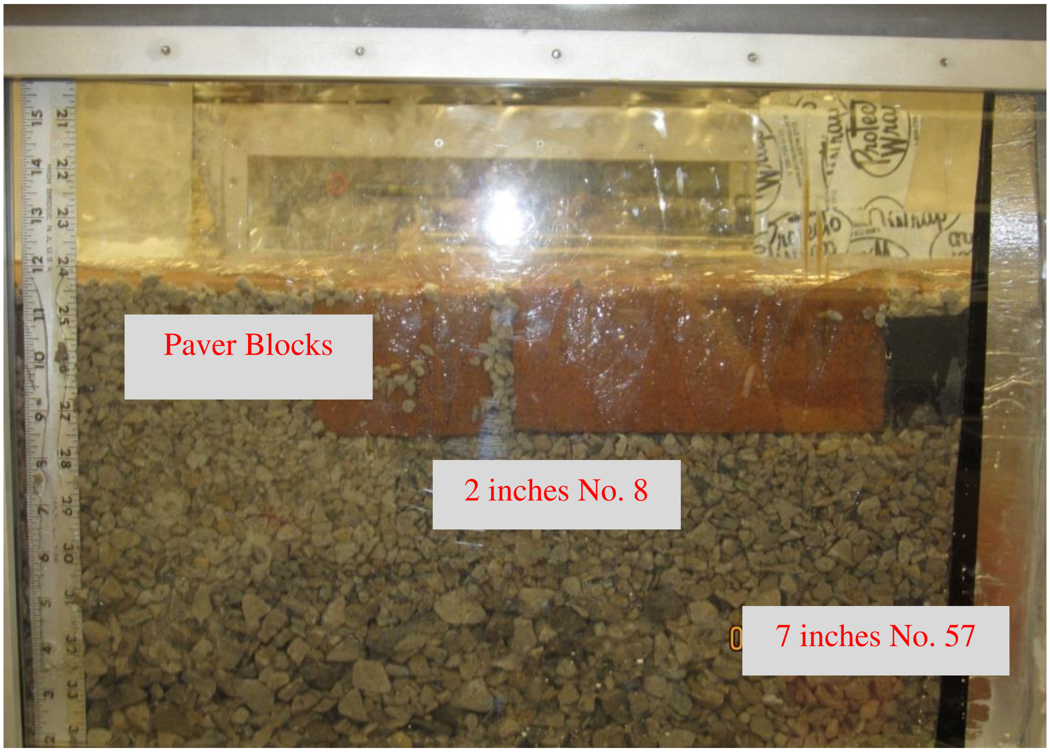

Figure 29. Aggregate Gradation Set in Flume

ASTM #8 gradation limestone was used as the base layer under the PICP pavers as well as the joint filler stone material for the 10 mm and 12.5 mm spacing for the straight herringbone pattern. The ASTM #9 gradation limestone was used as the joint filler material for the 6 mm straight herringbone pattern and the 6 mm 45 degree herringbone pattern. All aggregate used in the study was sieved and graded to ensure conformation to specifications. The actual gradation of the #8 material is shown in Figure 30 with the #9 material shown in Figure 31.

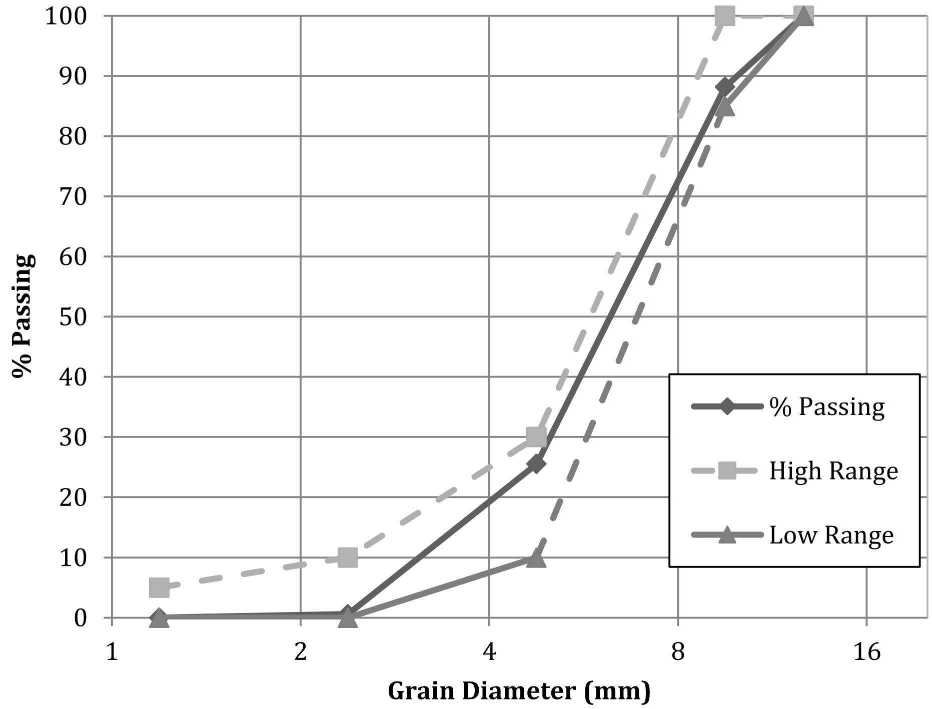

Figure 30. No. 8 Gradation for Base and 10 mm/12.5 mm Spacing Filler Material

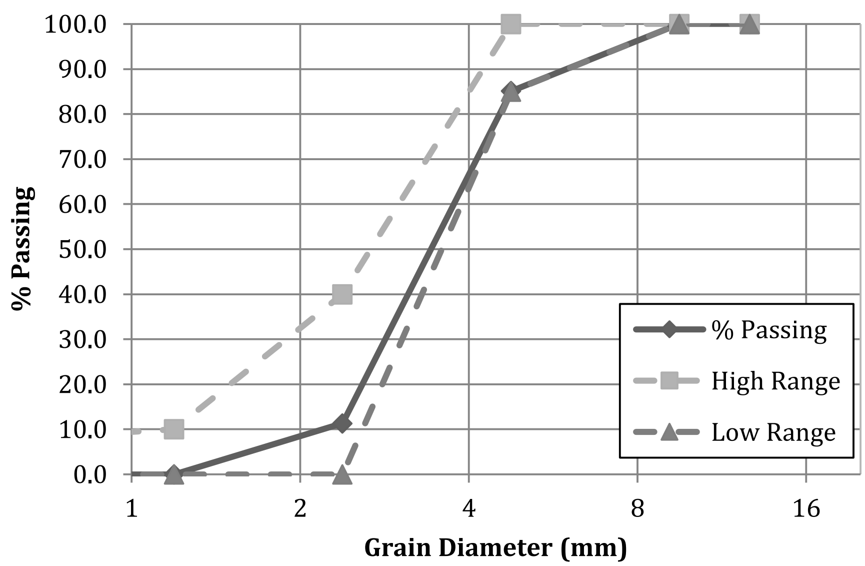

Figure 31. No. 9 Gradation for 6 mm Spacing Filler Material

Two different patterns were used within experimental testing. The majority of the testing was performed on the straight herringbone pattern as shown Figure 32 where water flows either perpendicular or parallel to the joints. Limited testing was also performed on a 45 degree herringbone pattern as shown in Figure 33.

Figure 32. Straight Herringbone Pattern with Horizontal Flow

Figure 33. 45 Degree Herringbone Pattern without Horizontal Flow

The independent variables in the research were the joint spacing and pattern styles between the pavers across various discharge flow measurements. The measured dependent variables were the separated infiltration and over flow rates within the test section at differing degrees of pavement slope. The test section measured dependent variables are shown in Figure 34. Each experiment was allowed to stabilize for 30 minutes before collecting data. All experiments were completed in less than 120 minutes.

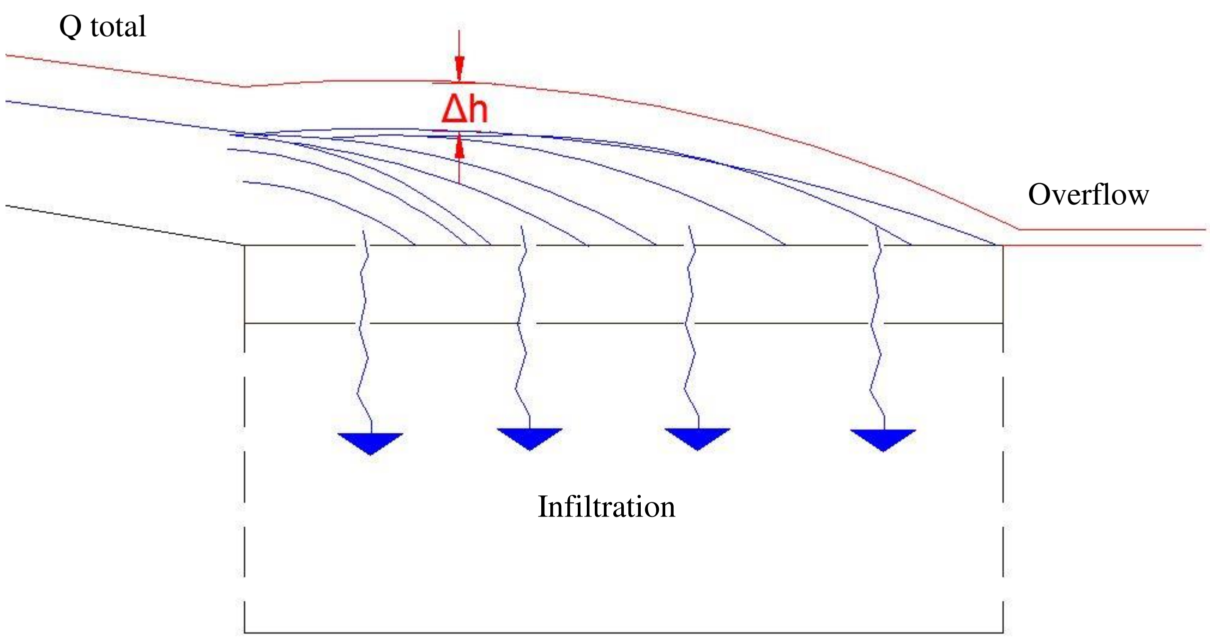

Figure 34. Test Section Infiltration and Overflow Schematic

Infiltration

The current standard to measure pavement infiltration flow rates does not include supercritical horizontal sheet flow. The current standard utilizes the vertical infiltration test defined by the ASTM C 1781 standard (ASTM, 2013). ASTM C 1781 is completed by using a specified amount of water and determining the time the water takes to infiltrate through the section (ASTM, 2013). The procedure utilizes a semi-constant head method where five gallons of water is poured at a constant rate into a specified set area (ring). This infiltration equation per ASTM C1781 was given as follows:

Equation 3. ASTM C1781 Infiltration

$$I = \frac{KM}{D^2 t}$$

Where:

I = infiltration rate in/hr.

K = dimensional constant, in-lbs.

M= mass of water, lbs.

D= diameter of infiltration ring, in.

T= time measured, seconds.

An infiltration testing ring, prior to sealing with putty, is shown in Figure 35. Infiltration was tested for all sets of test conditions before and after hydraulic testing and at all slopes.

Figure 35. Vertical Infiltration C 1781 Test

Test Section Calibration

The initial infiltration results for all joint spacing and slopes are shown in Table 2 and Figure 36. The results indicate that as the PICP block spacing decreases the vertical infiltration increases. For all sections the 2% slope had the highest infiltration capacity.

Table 2. C 1781 Average Vertical Infiltration, in/hr., Before Horizontal Test

Pavement Slope	6 mm, in/hr.	10 mm, in/hr.	12.5 mm, in/hr.
0 %	1077	1505	2012
1%	1088	1558	2345
2%	1226	1628	2532
5%	1140	1514	2505
10%	1115	1495	2439

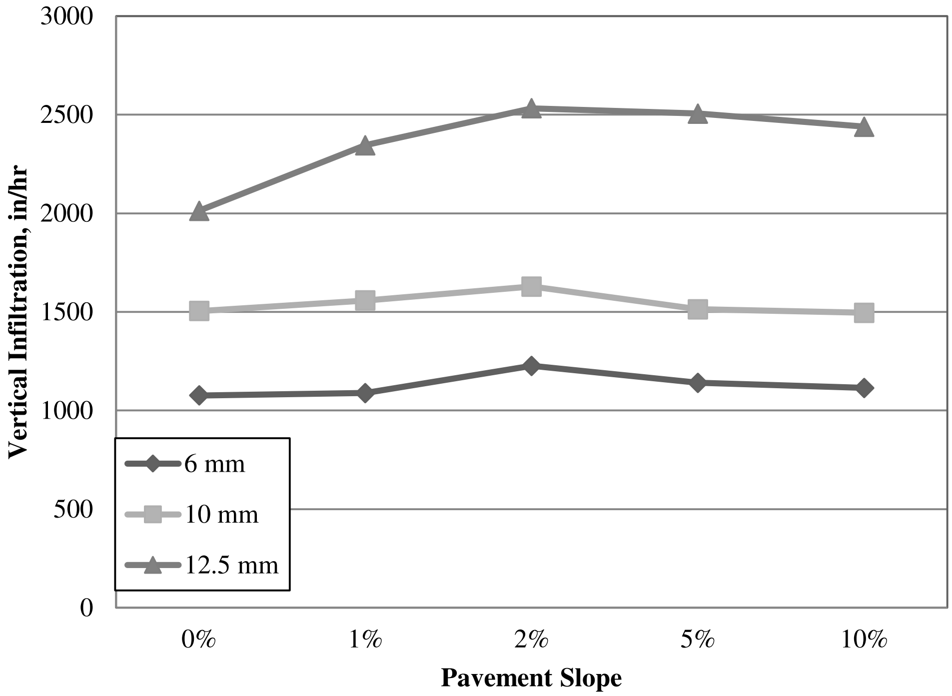

Figure 36. Vertical Infiltration C 1781 vs. Pavement Slope for Each PICP Spacing

The vertical infiltration rates measured in the flume test sections were all much higher than those expected from a variety of field applications. The sections, including all base materials, were removed and reset multiple times. Each time the tested vertical infiltration rate was consistent and higher than expected in the field. In order for the resulting design tool to produce realistic results, a calibration or shift was investigated to better match the laboratory results to those expected in the field. In, "Investigation of Hydraulic Capacity and Water Quality Modification of Stormwater by Permeable Interlocking Concrete Pavement (PICP) System," Kim et al. examined field PICP systems (Kim et. al, 2013). The PICP systems were constructed with base conditions that include mechanical compaction of the base layer aggregate. The study reported infiltration rates for #8 and #9 joint filler materials at 398.5 in/hr. and 271.4 in/hr. with an approximately 9.0% open area.

Since the sections used in the current study had 7%, 11.1%, and 14 % open area for the 6mm, 10mm, and 12.5mm joint spacings, respectively, and the portion of the PICP system controlling infiltration is the permeable void space in the joint; it was assumed that the difference in infiltration rates was due to the inability to compact the filler material using a plate compactor as is typical in the field. Previous research indicates that field installations which include mechanical compaction display a lower hydraulic conductivity compared to permeable pavements tested in the laboratory (McCain and Dewoolkar, 2010).

During the laboratory study the Kansas City Water Services Department was upgrading their Swope Parkway campus with permeable pavements. One of the sections included a straight herringbone pattern PICP with a 6mm joint spacing and #9 filling stone over a similar base to this study which allowed a direct comparison of field activities to laboratory results. The field installation of the No. 57 base stone material is shown in Figure 37 over a non-woven geotextile filter fabric. Two inches of bedding material was then placed over the base as shown in Figure 38. The straight herringbone pattern was then set by hand as shown in Figure 39 with joint filling stone brushed into the surface and compacted before completion (Figure 40).

Figure 37. Water Services Base Installation

Figure 38. Final Grading of the Bedding Layer

Figure 39. Setting the Straight Herringbone Pattern By Hand

Figure 40. The Finished Installation after Compaction and Prior to Opening

Vertical infiltration was measured within 7 days of completion and prior to opening to traffic. The final pattern and infiltration ring orientation are shown in Figure 41. The water services new parking lot infiltration ranged from 350-408 in/hr., which is consistent with the Kim et al. reported results and expected field performance (Kim et al., 2013). Since the average infiltration rate at the Water Services location was 369 in./hr. as determined using the same equipment and by the same researchers as the values shown in Table 2, this value was used to calibrate the laboratory results to field expectations.

Figure 41. Water Services Vertical Test and Pavement 6 mm Straight herringbone

The resulting infiltration shift values are shown in Table 3. Please note the calibrated infiltration values are only used in the design tool and the original data is used through the performance curve development, statistical analysis, and clogging sections.

Table 3. ASTM C1781 Experimental and Calibrated Vertical Infiltration

	Infiltration Values per PICP Spacing, in/hr.					
Pavement Slope	6 mm	6 mm Calibrated	10 mm	10 mm Calibrated	12.5 mm	12.5 mm Calibrated
0 %	1077	369	1505	502	2012	671
1%	1088	363	1558	519	2345	782
2%	1226	409	1628	543	2532	844
5%	1140	380	1514	505	2505	835
10%	1115	372	1495	498	2439	813

3. FLOW RATE PERFORMANCE CURVE DEVELOPMENT

The results presented within this chapter are for the hydraulic response for unclogged permeable interlocking concrete pavements (PICP) for the straight herringbone pattern. Three sections at joint spacings of 6 mm, 10 mm, and 12.5 mm were tested at five different cross slopes. Figure 42 displays a typical performance curve. Results indicate that as the flow rate increased infiltration increased until overflow occurred. As flow rate was increased beyond overflow, the additional water head caused a small additional increase in the infiltration.

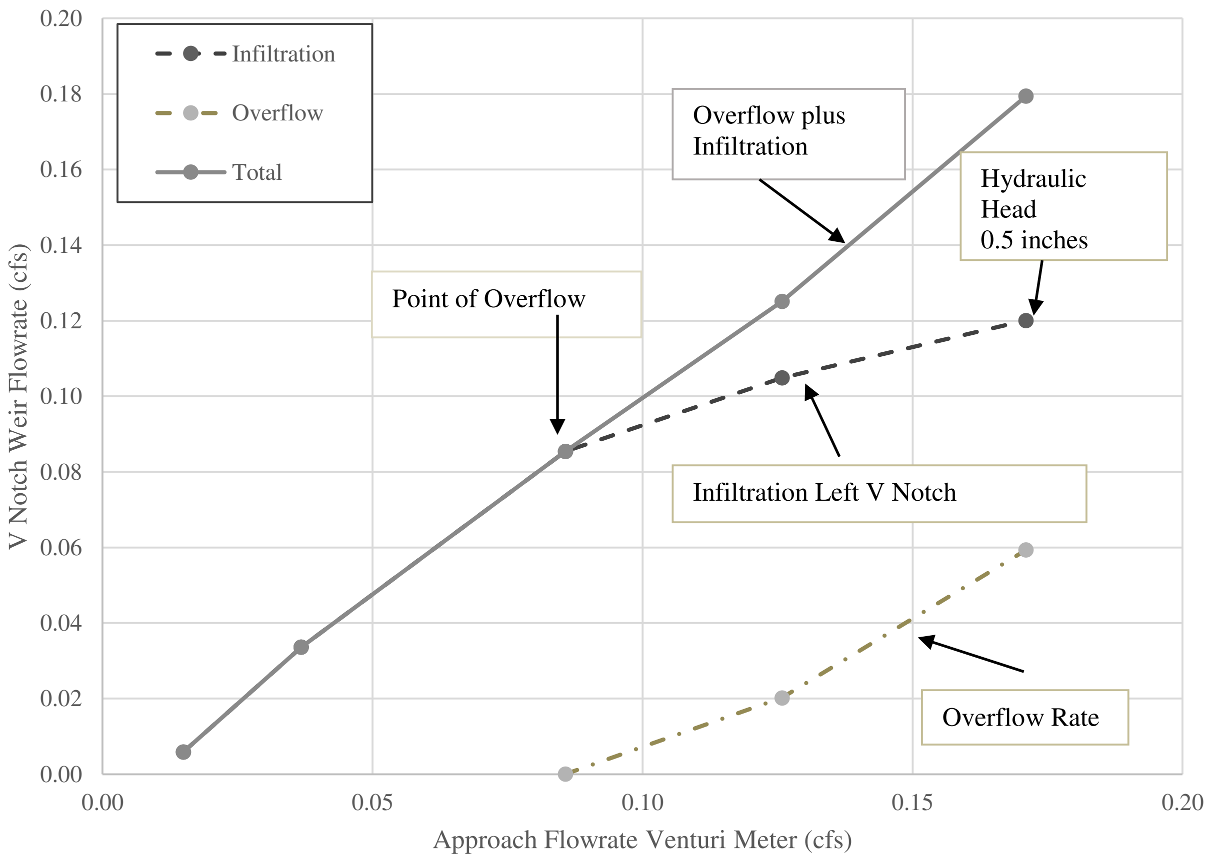

Figure 42. Typical Performance Curve Explanation

A performance curve was developed for each block spacing and slope. Triplicate sections were constructed and tested with an average performance curve also developed for the set. The general shape for performance curves was similar and Figure 43 through Figure 45 represent the average curves for three PICP spacings at the 0 % cross slope. The point of overflow shown in Figure 42 occurs at incipient overflow. The overflow point was defined at the maximum amount of flow that will infiltrate the section prior to water overflowing the test section and back calculated as the horizontal infiltration capacity.

The performance curves shown in Figure 43 to Figure 45 indicate that as the joint spacing was increased (along with void ratio) the infiltration increased, as expected. At the wider joint spacing the point of overflow shifts right on the x-axis.

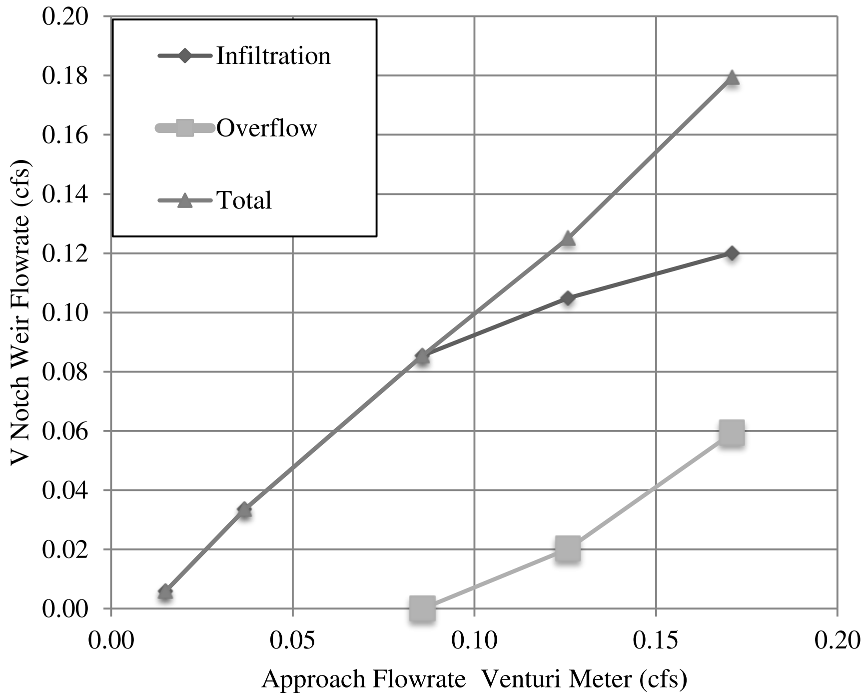

Figure 43. Performance Curve 6 mm Spacing 0 % Slope

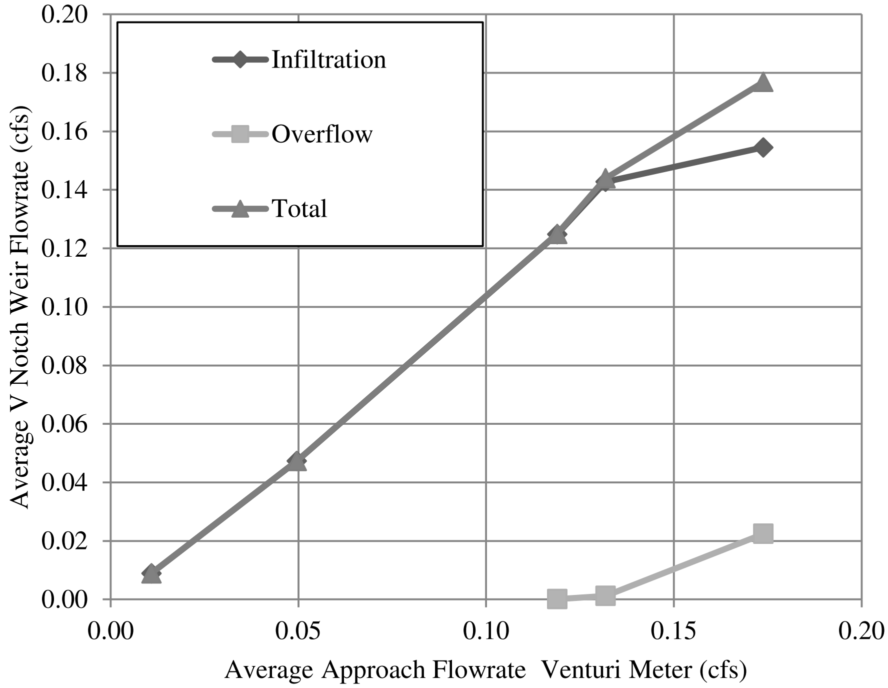

Figure 44. Performance Curve 10 mm Spacing 0 % Slope

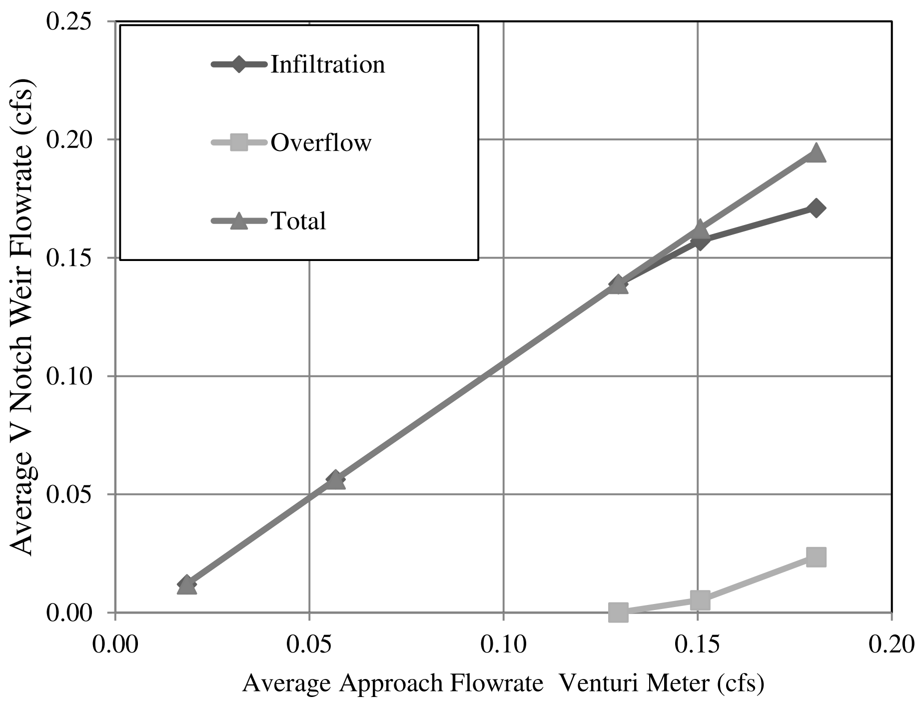

Figure 45. Performance Curve 12.5 mm Spacing 0 % Slope

The average maximum over flow discharge rates per pavement slope for each of the PICP spacing are shown in Table 4 and Figure 46. Infiltration rate decreased with increased slope for the 6mm samples. However, for the 10 mm arrangement the infiltration rate increased slightly from 0% to 1%. Slope did not impact infiltration rate for the 12.5 mm arrangement at maximum discharge.

Table 4. Average Max Overflow Rates per Pavement Cross Slope

	Pavement Cross Slope				
Spacing	0 %	1%	2%	5%	10 %
	Overflow Rates, cfs				
6 mm	0.090	0.079	0.074	0.067	0.061
10 mm	0.125	0.133	0.135	0.135	0.138
12.5 mm	0.139	0.140	0.140	0.139	0.138

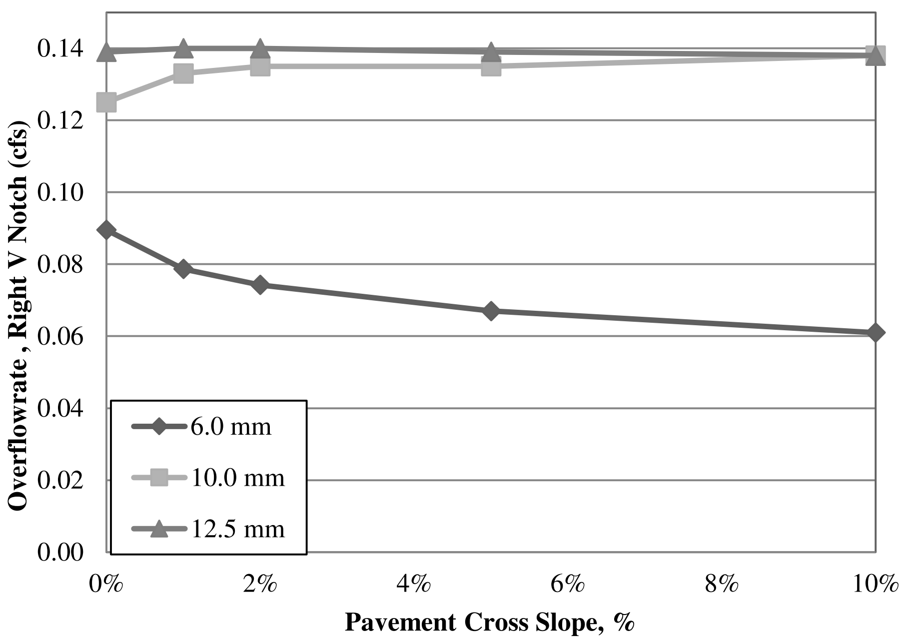

Figure 46. Average Max Overflow Rates per Pavement Slope

Incipient Overflow Rate

Of more importance to normal performance and design is the impact slope and joint spacing has on the horizontal infiltration rate as determined as a linear regression of the overflow data (shown in Figure 47 shown as infiltration). Horizontal infiltration rates were converted from the effective intensity values by a unit transformation by multiplying the intensity values from 43,200 (3600 seconds per 1 hour multiplied by 12 inches per foot). The equation from the overflow trend line was used to calculate the point where overflow initially began (x-axis intercept). The calculated maximum overflow rates are shown in Figure 47 and Table 5. The data indicates that as spacing size was increased the infiltration rate at overflow increased, as expected.

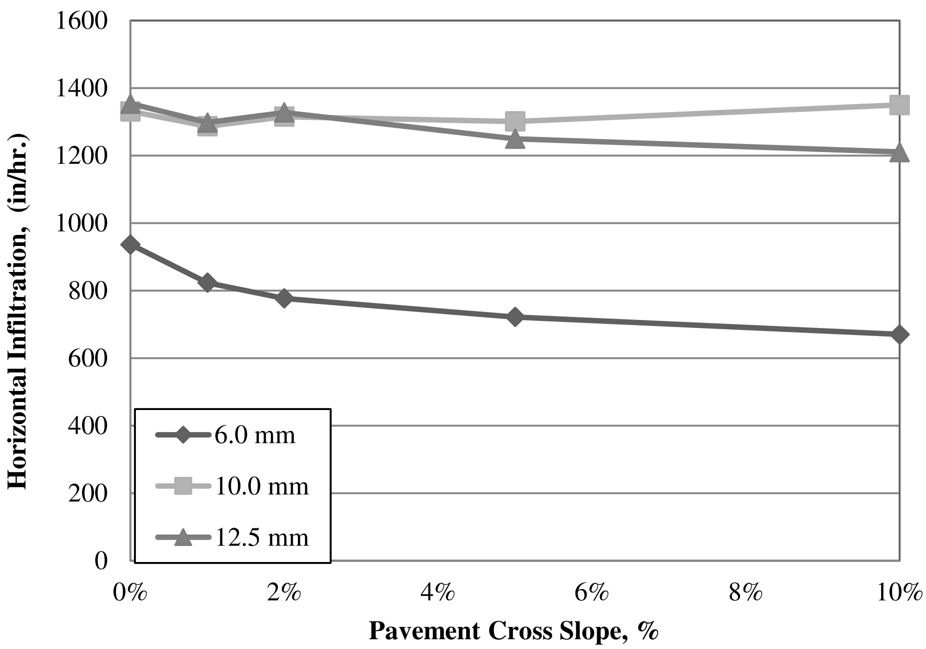

Figure 47. Average Incipient Overflow Rates per Pavement Slope

Table 5. Calculated Maximum Overflow Rates per Pavement Cross Slope

Slope	Block Spacing		
	6 mm	10 mm	12.5 mm
		In/hr.	
0%	937	1331	1353
1%	823	1286	1298
2%	777	1315	1327
5%	722	1301	1250
10%	670	1350	1210

Horizontal infiltration for each of the investigated PICP joint spacing arrangements plotted along with the vertical infiltration C 1781 values for each pavement cross slope are shown in Figure 48. For all tested sections the infiltration rate as determined from ASTM C1781 was greater than the actual flow rate determined at incipient overflow. Figure 48 also indicates that as the spacing sizes increase infiltration both the vertical or horizontal increase. The displacement between the 6 mm and the 12.5 mm spacing was shown to be approximately 1000 in/hr. regardless of pavement slope. The values of the infiltration also slightly decrease and level off as the pavement slope increases suggesting that the PICP system is more efficient at a lower pavement slope and most efficient at a 1-2% pavement slope, in particular for the 6 mm spacing. Less of an affect was observed for the 12.5 mm spacing on the pavement slope and block spacing sizes.

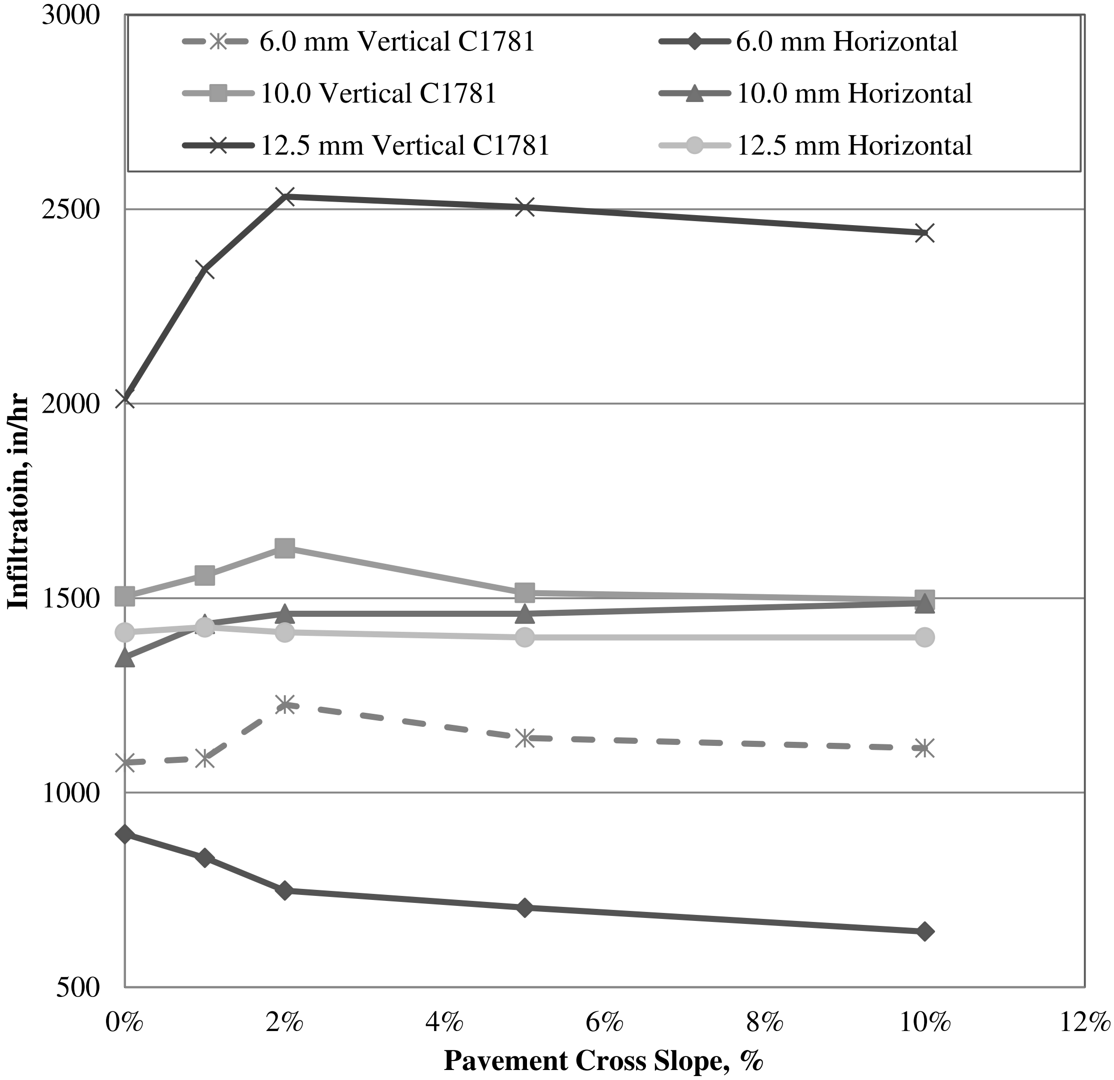

Figure 48. Vertical Infiltration and Horizontal Infiltration across Pavement Slopes

Rotated Pattern Investigation

A series of tests were also performed using the 6mm spacing in a rotated 45 degree herringbone pattern. It was hypothesized that the angle the water impacted the joint sections may influence infiltration capacity. The test was completed on the 6 mm spacing regular pattern as this pattern was the most sensitive within the research experiments. The different patterns are shown in Figure 49.

Figure 49. (Left) Straight herringbone Pattern 6 mm Spacing (right) 45 Degree Herringbone Pattern 6 mm Spacing

Table 6 and Table 7 display the infiltration rates at overflow per section area for each experimental groups. The results above that the 45 degree herringbone pattern had lower infiltration than the straight herringbone pattern. As such, statistical analysis was completed on the values to determine differences between the groups. For such analyses the raw data values as well as the effective intensity values for the experiments were used. Table 6 displays an example of the raw data for the 0 % slope for the 45 degree herringbone pattern. Each slope was included within the statistical analysis shown in Chapter 4.

Table 6. Infiltration Rate at Overflow per Section Area per Group, cfs/section area.

Slope	45° Herringbone Pattern	Average Straight herringbone
	Flow Rate (cfs)	
0.00%	0.016	0.021
1.00%	0.015	0.022
2.00%	0.015	0.017
5.00%	0.014	0.016
10.00%	0.014	0.015

Table 7. Example of Raw Data Values Used in Statistical Analysis

	45 degree Herringbone Pattern			
Slope	Q in Total	Overflow	Infiltration	Q Out Total
		Discharge Rates, cfs		
0%	0.013	0	0.0133	0.013
	0.034	0	0.0334	0.033
	0.064	0.00001	0.0652	0.065
	0.081	0.00558	0.0753	0.081

4. STATISTICAL ANALYSIS OF PERFORMANCE CURVE TESTING

The main objective of the statistical analysis was to determine similarity of the means within the experimental groups. Statistical analysis included a One-Way ANOVA to compare the unknown variance (unknown means) of the five experimental group's capture discharge flow rates. The assumed null hypothesis was that all of the means were equal with the alternative hypothesis assumed to be that at least one group mean was different. The statistical significance level used was 0.05 or 5%. A One-Way ANOVA is based on the assumption that the sample populations are normally distributed and as such a comparison to the normal population was included. Each group contained five values of a calculated effective intensity capture discharge flow rate at each of the five pavement slopes: 0%, 1%, 2%, 5% and 10%.

Analyzed Data and Normality Test

The incipient overflow rates (point at which water just begins to overflow the test section) was used as the most sensitive experimental value and was based upon the linearly regressed equation found from the averages. Table 8 displays the incipient overflow rates per group spacing.

Table 8. Incipient Overflow Rates per Group Spacing, Slope

Spacing	Pavement Cross Slope				
	0 %	1%	2%	5%	10 %
	Overflow Rates, cfs				
6 mm	0.088	0.099	0.074	0.069	0.064
10 mm	0.123	0.119	0.122	0.120	0.123
12.5 mm	0.130	0.129	0.130	0.123	0.118
45 degree Herringbone	0.065	0.061	0.061	0.056	0.061

As the ANOVA and t-tests are based on the assumption of normal distribution an initial normal distribution check was ran on the data sets. Figure 50 displays the results. The data sets appeared to be normally distributed based a p value greater than 0.05 for all groups.

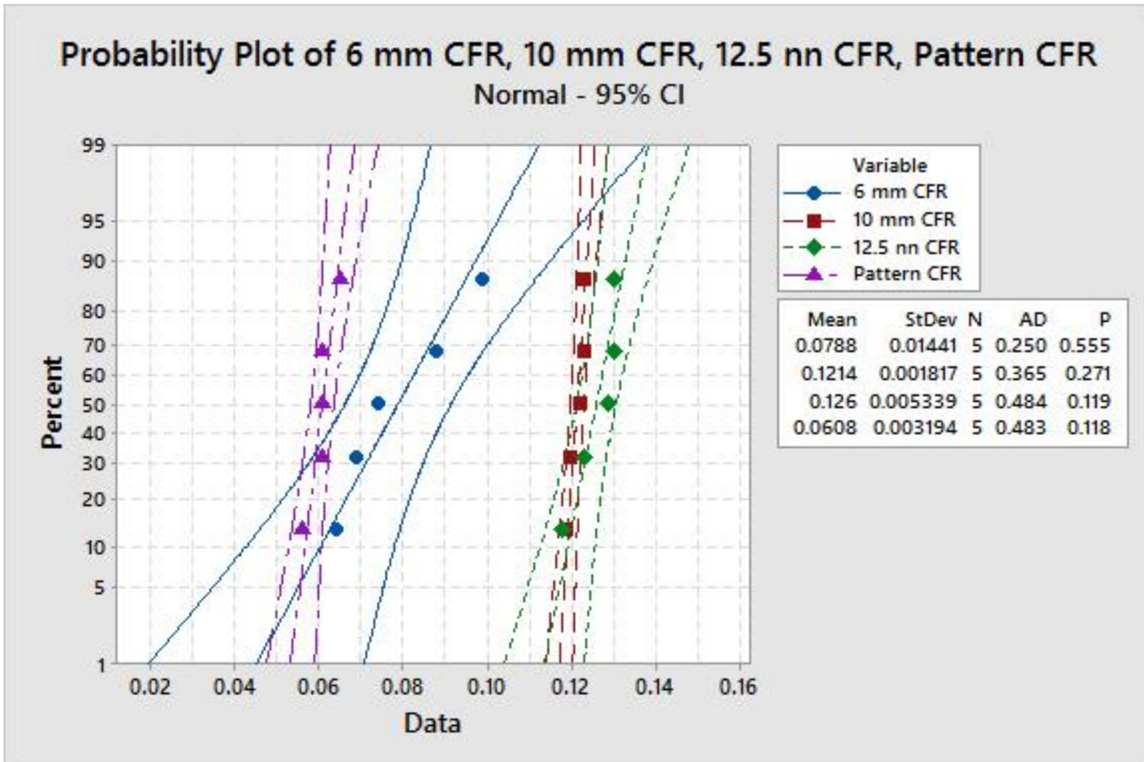

Figure 50. Normal Probability Check

One-Way ANOVA Results

A One-Way ANOVA to compare the unknown variance (unknown means) of the four experimental groups' effective intensity capture discharge flow rates. The null hypothesis was that all of the means were equal with the alternative hypothesis that at least one group mean was different with a significance level of 0.05 or 5%. Each group contained five values of a calculated capture discharge flow rate at each of the five pavement slopes: 0%, 1%, 2%, 5% and 10%. The interval plot appears to display differences in the means of some of the groups, particularly the pattern and 6 mm group with the rates from the 10 mm and 12.5 mm groups.

The p-value of 0.000 indicates that the null hypothesis that the means are equal should be rejected and that at least one mean within the group is not equal but is different. The R^2 value of 93.91%, is defined as the fraction of the overall variance resulting from the differences among the group means. A large value indicates that a large fraction of the variation was due to the treatment that defines the groups, in this case the type of spacing between the paver blocks or pattern. Another way of describing the R value is as a descriptive statistic that quantifies the strength of the relationship between groups (6 mm, 10 mm, 12.5 mm, etc.) and the variable measured (effective intensity capture discharge flow rate at overflow). The One-way ANOVA was also run with and without the assumption of equal variances and produced similar results. Table 9 and Table 10 summarize the results of the ANOVA analysis.

Table 9. One Way ANOVA Summary

Standard Deviation	R^2	F –Value	P-Value
0.654	93.91	82.71	0.000

Table 10. Individual Factor Summary and Confidence Intervals

Group (Factor)	Mean	Standard Deviation	99 % Confidence Interval	
45 degree Herringbone	0.061	0.0039	0.0533	0.06829
6 mm	0.079	0.01441	0.0713	0.08269
10 mm	0.0121	0.00181	0.1139	0.12889
12.5 mm	0.126	0.00543	0.1185	0.13349

Figure 51 displays the box plot of the ANOVA test and indicates that a large difference occurs between the 6 mm spacing and the other spacing sizes. To investigate the differences between the groups individual t tests were conducted.

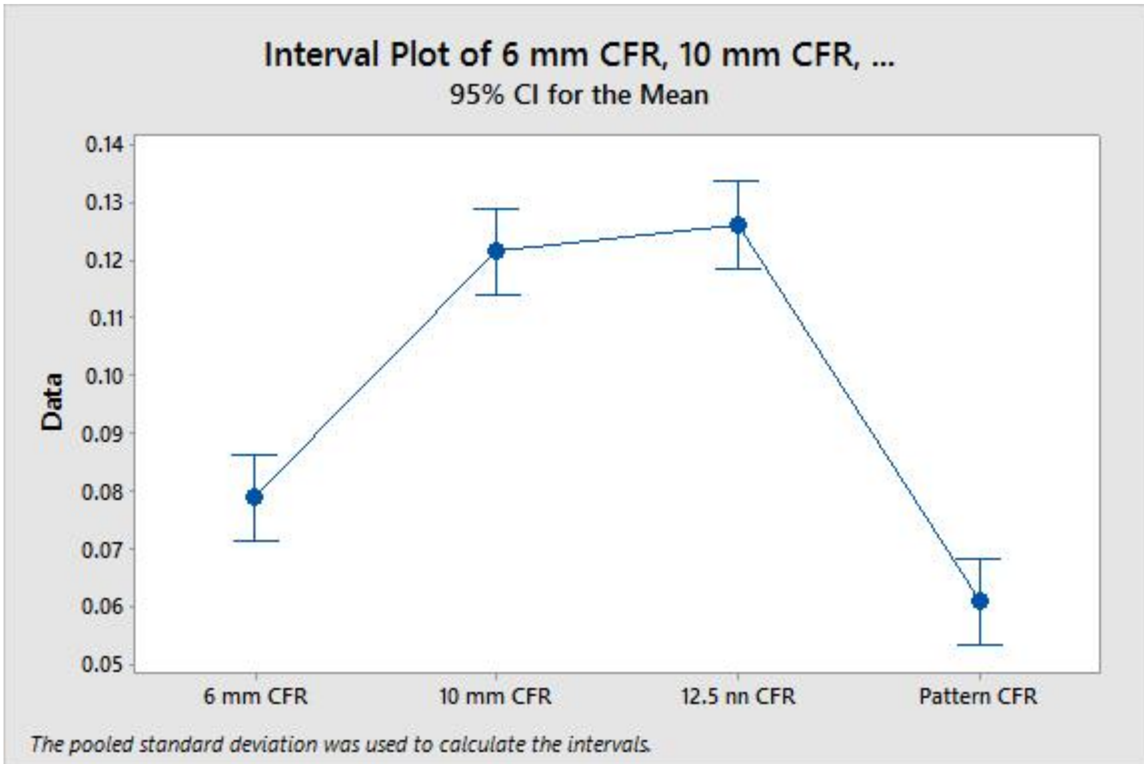

Figure 51. Interval Plot of ANOVA Groups

T-Test Comparisons

An additional analysis included individual two sample t-tests (Table 11) between the 6 mm spacing group and the 10 mm spacing groups. Infiltration, incipient overflow rate, and values at overflow were all compared. The null hypothesis was assumed to be that the means were equal with zero difference with the alternative hypothesis indicated as the means were not equal with a significance level, alpha of 0.05 or 5% (Figure 52).

Table 11. T-test Summary Comparison between 6 mm and 10 mm

Experimental Group Value Test	P-Value	Indication
6 mm and 10 mm Incipient Overflow Rates	0.003	Reject Null Hypothesis
6 mm and 10 mm Infiltration Values	0.049	Reject Null Hypothesis
6 mm and 10 mm Overflow Values	0.042	Reject Null Hypothesis

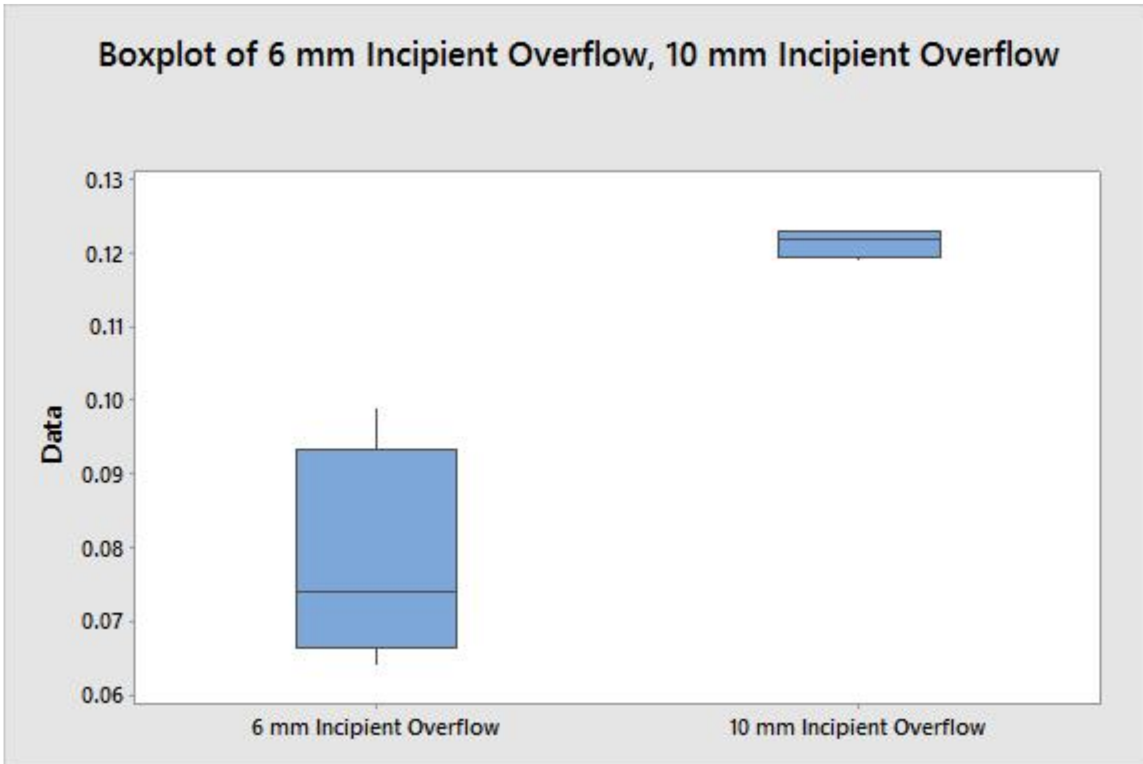

Figure 52. Boxplot Incipient Overflow Rate between 6 mm and 10 mm

The p values of ≤ 0.05 indicate a rejection of the null hypothesis suggesting that there is some indication that the 6 mm spacing separation differs from the 10 mm. An additional analysis included individual two sample t-tests between the 10 mm spacing group and the 12.5 mm spacing groups. Infiltration, Incipient Overflow rate, and values at Overflow were all compared. The null hypothesis was assumed to be that the means were equal with zero difference with the alternative hypothesis indicated as the means were not equal with a significance level, alpha of 0.05 or 5%. Figure 53 and Table 12 display the results. The p values of greater than 0.05 indicate that there is not statistical difference between the means of the 10 and 12.5 mm groups.

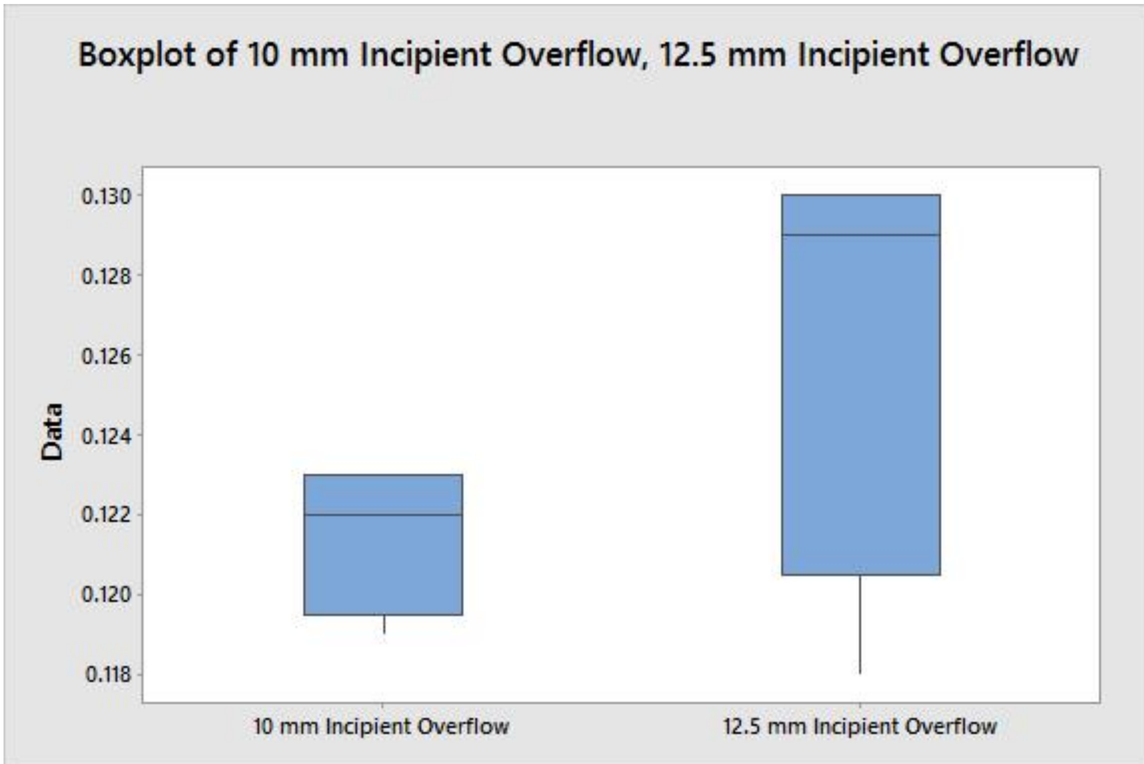

Figure 53. Boxplot Incipient Overflow Rate between 10 mm and 12.5 mm.

Table 12. T-test Summary Comparison between 10 mm and 12.5 mm

Experimental Group Value Test	P-Value	Indication
10 mm and 12.5 mm Incipient Overflow Rate	0.142	Fail Reject Null Hypothesis
10 mm and 12.5 mm Infiltration Values	0.487	Fail Reject Null Hypothesis
10 mm and 12.5 mm Overflow Values	0.455	Fail Reject Null Hypothesis

Additionally, the 45 degree herringbone pattern was compared to the straight herringbone pattern data points. As stated previously, infiltration, infiltration at overflow per section area, and overflow values were all compared. The null hypothesis was that the means were equal with zero difference with the alternative hypothesis indicated as the means were not equal with a significance level, alpha of 0.01 or 1%. The smaller the value of alpha, the less likely it is that a rejection or a true null hypothesis will occur. The variances were not assumed to be equivalent. Figure 54 displays the box plot values for the infiltration at overflow per section.

The t-tests between the 45 degree herringbone pattern and the 6 mm spacing group was completed with both a significant level of 0.05 (5%) and 0.01 or 1 % significance. This analysis was completed upon the infiltration, Infiltration at overflow per section area and values at Overflow. The null hypothesis was assumed to be that the means were equal with zero difference with the alternative hypothesis indicated as the means were not equal. The p value of 0.030 indicates a failure to reject of the null hypothesis value for an alpha of 0.01. However this p value for an alpha of 0.05 indicates a rejection of the null hypothesis indicating that the pattern data differs slightly from the regular 6 mm pattern. Table 13 displays the results. Further experiments and at alternate spacing would be suggested for additional research to explore pattern differences.

Table 13. T-t Summary All 6 mm data values and Pattern Comparison

Experimental Group Value Test	P-Value	Indication
6 mm Average vs. 45 degree pattern: Infiltration at Overflow per section Area	0.030	Reject Null Hypothesis at 5%
6 mm Infiltration vs. Pattern Infiltration Values	0.270	Fail to Reject Null Hypothesis
6 mm vs. Pattern Overflow Values	0.822	Fail to Reject Null Hypothesis

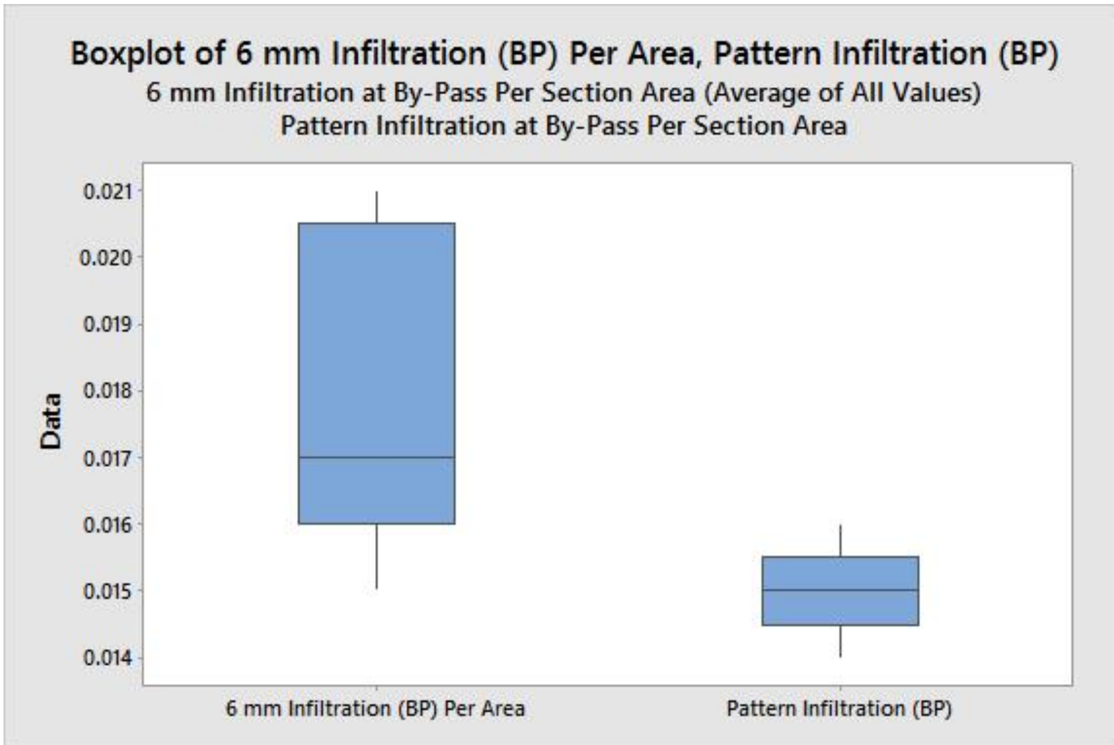

Figure 54. Boxplot Average 6 mm vs. Herringbone Pattern Infiltration per Section Area (cfs/ft^2)

Correlation Analysis was completed between pavement slope and different spacing capture discharge rates. The strength of the correlation was determined if the absolute value was closer to 1. The sign indicates the direction of the relationship. All negative values indicate an inverse relationship meaning that as the slope of the pavement increases the capture flow rate decreases. The Spearman Rho and Pearson correlation tests were used. Pearson is used in a linear relationship while Spearman Rho is used as the tests were not necessarily linearly based. The analysis was performed on the 6 mm spacing as this was the most sensitive experiment to the pavement slope. The results are shown in Table 14 and indicate that a strong inverse correlation between the overflow rates and pavement slope only for the 6mm joint arrangement.

Table 14. Correlation Summary between Pavement Slopes and Overflow Rate

Experiment	Spearman Rho	Pearson
6 mm	-0.901	-0.801

5. HYDRAULIC PERFORMANCE DURING CLOGGING

Infiltration systems such as PICPs are widely used in urban environments as a deterrent to water pollution and to control urban runoff volumes. One aspect that impacts the functionality of infiltration systems is the likelihood of the systems to become clogged. The most common water pollutant within the US is sediment (Ostercamp, 1998) which is a large component to stormwater (Sansalone, 1998).

For PICP arrangements clogged in this study, synthetic storm water was formulated to closely fit the gradation from the New Jersey Corporation for Advanced Technology, NJCAT. This gradation was determined to be a sandy silt soil classification according to the United Soil Classification System (USCS) Standard. The silt and clay fraction was collected from the North Kansas City location shown in Figure 55.

Synthetic Stormwater Properties

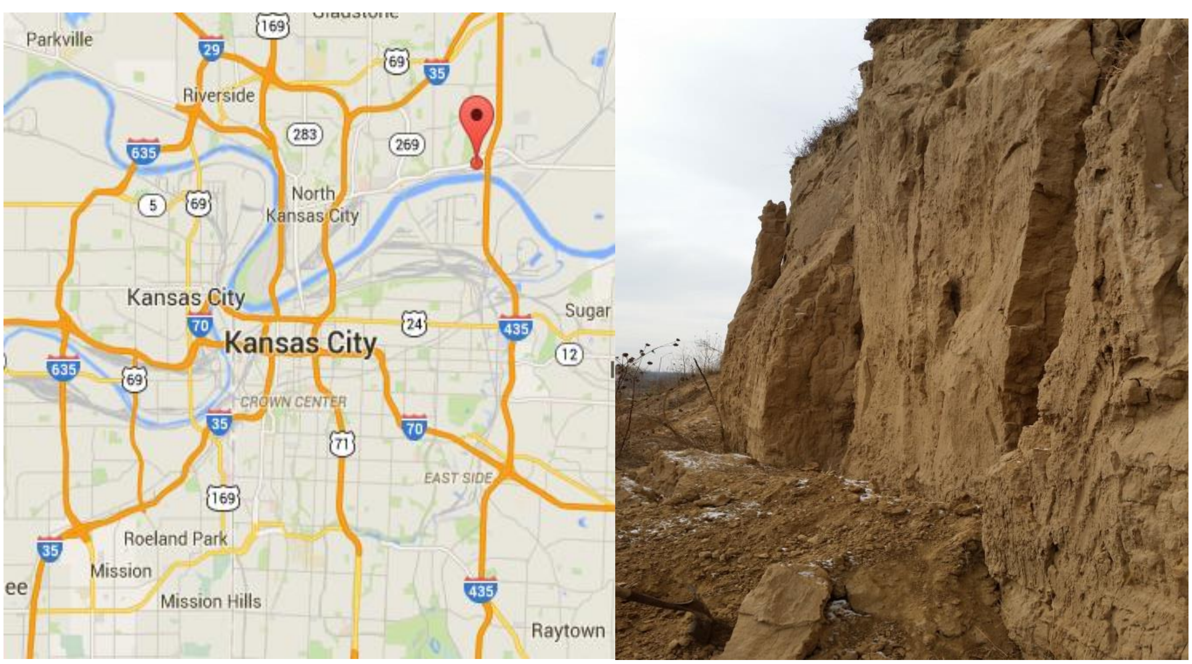

Figure 55. Location and Picture of Synthetic Stormwater Soil Location

A sieve analysis was performed initially on the silt and clay material. The synthetic stormwater contained 45% of finer silt and clay materials blended with river sand. The actual gradation of the created synthetic stormwater is show in Table 15

Table 15. Synthetic Stormwater Soil Particle Size and Percent by Mass

Particle Size (microns, µm)	Percent By Mass
500-1000 (Coarse Sand)	5%
250-500 (Medium Sand)	5%
100-250 (Find Sand)	30%
50-100 (Very Fine Sand)	15%
1-50 (Silt and Clay)	45%

The clogging procedure used in this study was fundamentally different than any previously reported in the literature. Typically the synthetic stormwater solutions are applied within a given area vertically inside a standard ASTM C1781 testing ring. The Kim et al., J. Y. et al. study (2013), "Investigation of Hydraulic Capacity and Water Quality Modification of Stormwater by Permeable Interlocking Concrete Pavement (PICP) System" that used progressive vertical applications at 100, 200, and 300 mg/l to simulate loading reductions with time. Stormwater loading was applied to evaluate performance over an anticipated 20 year lifespan. Since this study was the first to determine infiltration capacity using horizontally moving water and likewise clogging using material moving also horizontally across the pavement, compared to other studies and values reported in the literature the stormwater mass loading needed to be higher for moving water clogging to produce similar rates of clogging.

For each joint spacing arrangement, the flume was adjusted to the point of incipient by-pass. The synthetic stormwater was then applied upstream of the test section as shown in Figure 56 in 500g applications. As seen in Figure 57 the stormwater was uniformly mixed and dispersed when flowing onto the test section. The synthetic stormwater solution was applied upstream of the test section and allowed to be carried onto and through the test sections which is much more representative of how soil particles are actually carried onto PICP. Using assumptions from the previously mentioned research reported by Kim et al. (2013), each application of 500g of soil represented anticipated loading for 3.27 years. When using dry loading assumptions suggested by Sansalone et al. (1998), each application of 500g of soil represented anticipated loading for 2.60 years.

It should be noted at when the test commenced all of the flow was captured by the test areas. As the testing progressed and the infiltration rate decreased a portion of the flow overflowed the section and the sediment was carried over the PICP rather than into the system which helps to explain the higher than expected number of applications to caused clogging.

Figure 56. Synthetic Stormwater Dispensed Upstream of the Test Section

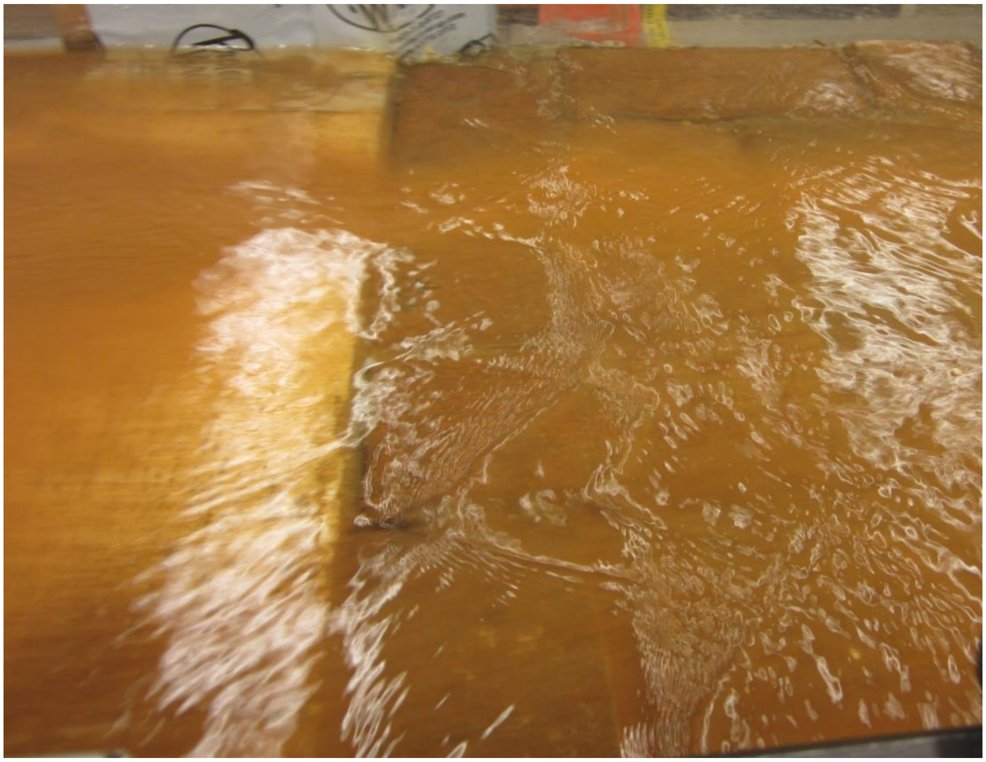
Figure 57. Synthetic Stormwater Passing over the Test Section

Infiltration Flowrate (Left V Notch Weir) vs. Application Results

Clogging tests were performed on the straight herringbone pattern at 6 mm, 10 mm and 12.5 mm spacing. The results show the 6 mm spacing was clogged at a much higher rate (fewer applications) than either the 10 mm or 12.5 mm spacing. The 12.5 mm spacing required the greatest number of applications of synthetic stormwater. Figure 58 to Figure 60 display the results for the clogging testing. Samples were considered clogged once the infiltrated flow reached an asymptote. It should be noted that the 12.5 mm spacing test required nearly 5 times the number of applications that the 6 mm spacing test required. After clogging the sections were vacuumed using a wet/dry shop vacuum and the joint filler stone replaced to determine the amount of recovery which might be expected when sections became clogged using moving water.

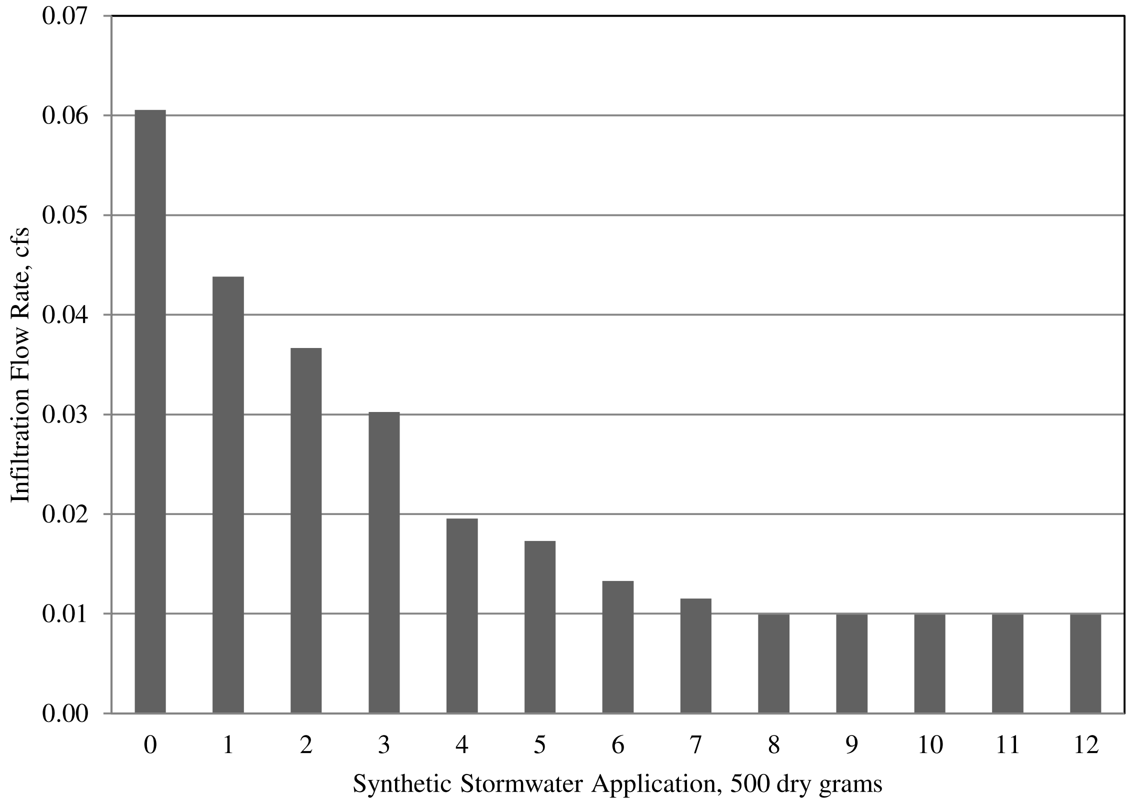

Figure 58. 6 mm Spacing Flow Rate vs. Application Result

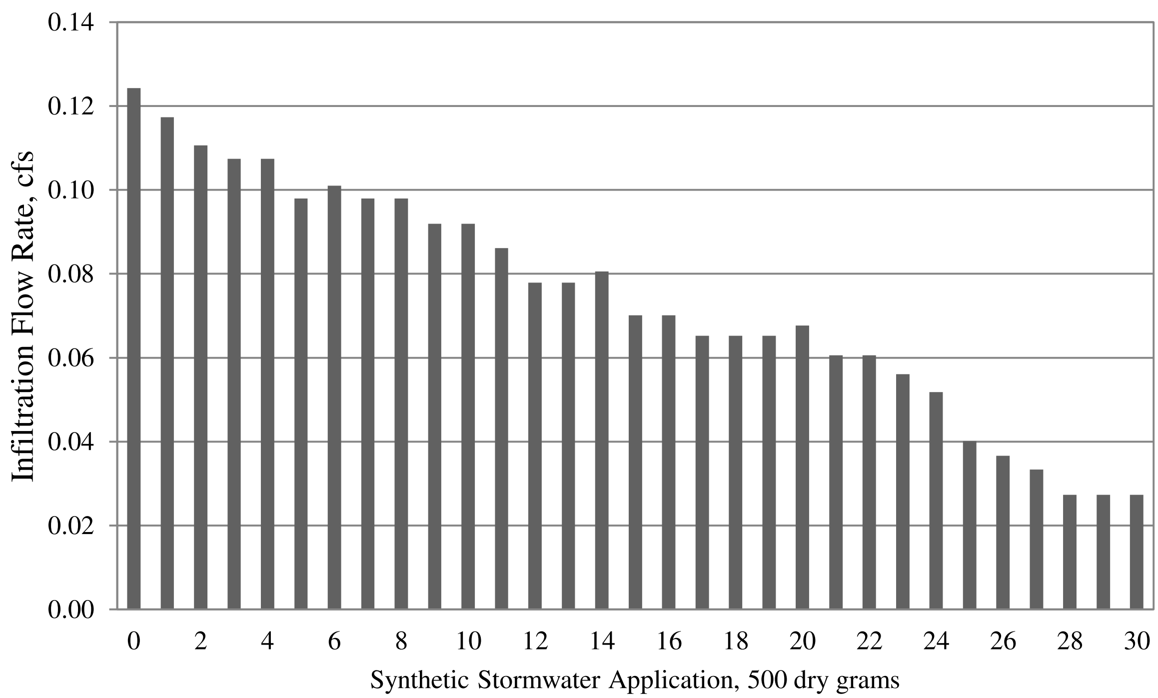

Figure 59. 10 mm Spacing Flow Rate vs. Application Result

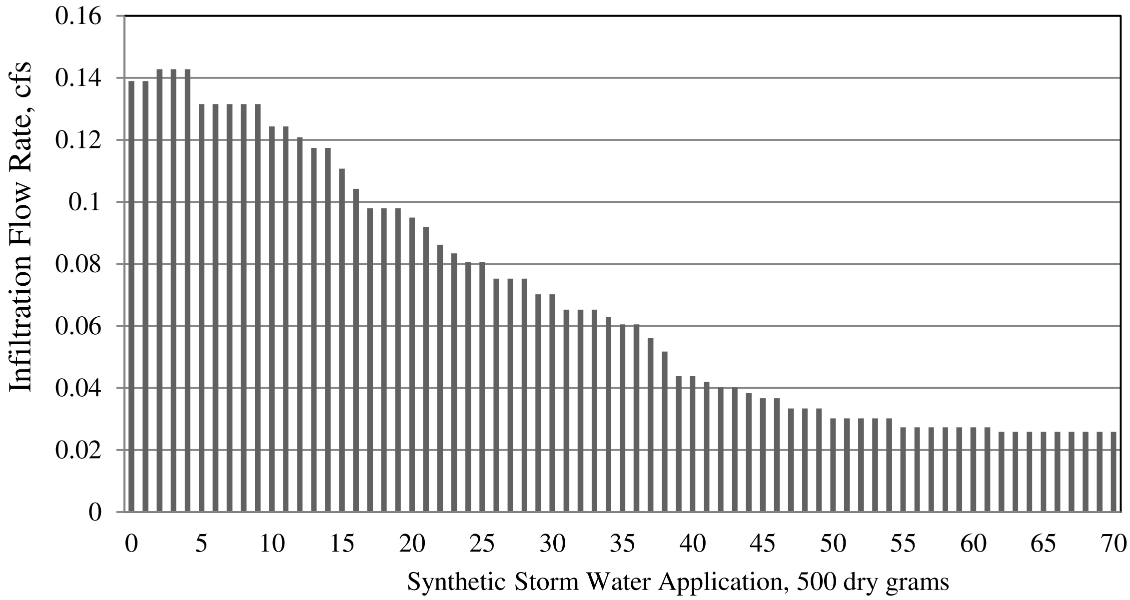

Figure 60. 12.5 mm Spacing Flow Rate vs. Application Result

Each of the three tests was analyzed within Minitab 17.0 for linear best fit equations and plots. The linear equations with the larges R values, a predictor of test strength, were chosen and each of the tests had a cubic equation as the best fit. Figure 61 to Figure 63 display each of the three test fitted line plots.

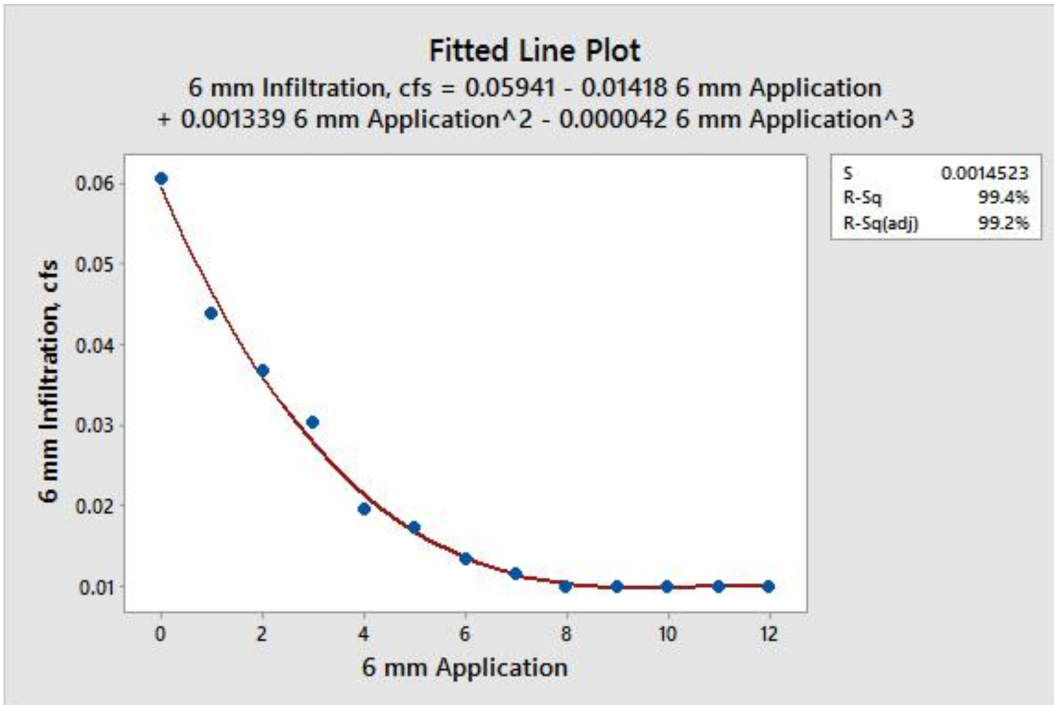

Figure 61. 12.5 mm Spacing Flow Rate vs. Application Result

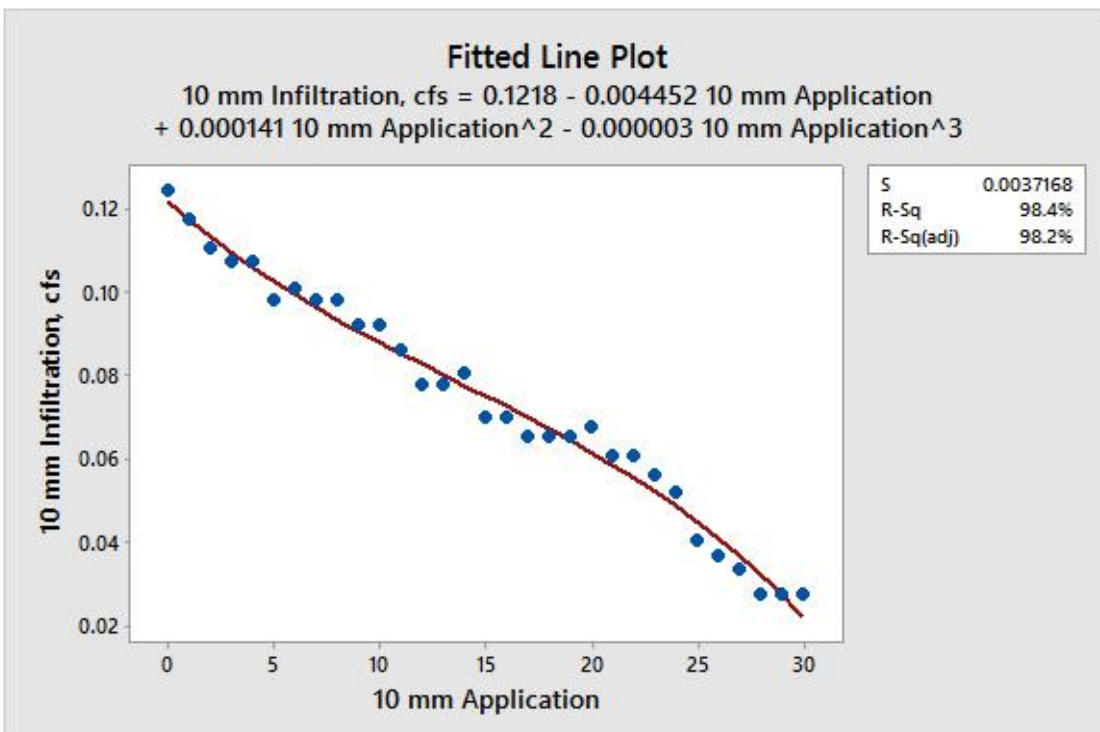

Figure 62. 10 mm Spacing Flow Rate vs. Application Result

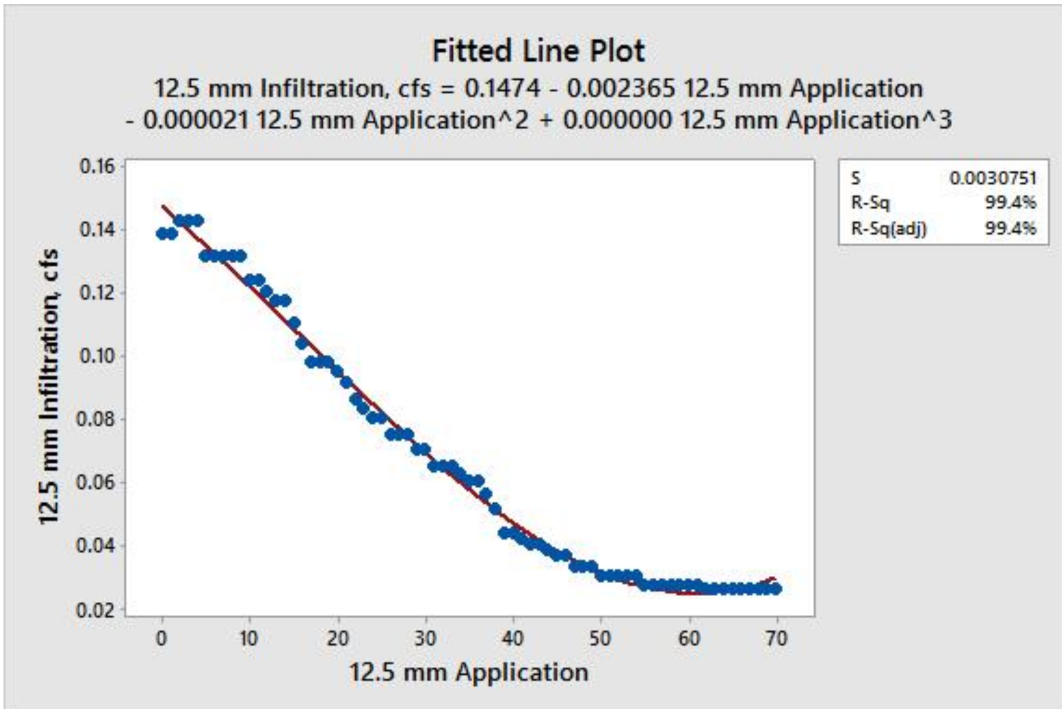

Figure 63. 12.5 mm Spacing Flow Rate vs. Application Result

Infiltration and Overflow Rate Results and Comparisons

The calculated infiltration values before and after sediment application are shown in Table 16 through Table 18. These values display the pretest, after samples were clogged, and posttest after joint filling materials were removed and replaced. Since the 12.5mm specimens had a high clogged infiltration rate, remediation was not performed.

Table 16. 6 mm Clogging Test Infiltration and Application Summary

Test Description	Application	Infiltration, in/hr.
Pretest: No Clogging	0	2511
After Clogging	12	411
Posttest: After Filler Replacement	5	718

Table 17. 10 mm Clogging Test Infiltration and Application Summary

Test Description	Application	Infiltration, in/hr.
Pretest: No Clogging	0	5155
After Clogging	30	1133
Posttest: After Filler Replacement	10	3813

Table 18. 12.5 mm Clogging Test Infiltration and Application Summary

Test Description	Application	Infiltration, in/hr.
Pretest: No Clogging	0	5648
After Clogging	70	1054

Results indicate that the infiltration discharge rate at the overflow point decreased with increased stormwater applications as shown for a 6 mm section in Table 19. Figure 64 displays the set entrance flow rate, the infiltration rate and overflow. During testing the overflow rate increased to the point where the majority of the stormwater would be carried across the top of the test section preventing complete clogging to zero infiltration.

Table 19. 6 mm Summary Incipient Overflow Rate, Infiltration Rate per Section Area

Stormwater Applications	Overflow, cfs	Infiltration Rate, cfs
0	0.0003	0.0438
5	0.0286	0.0173
12	0.0380	0.0099

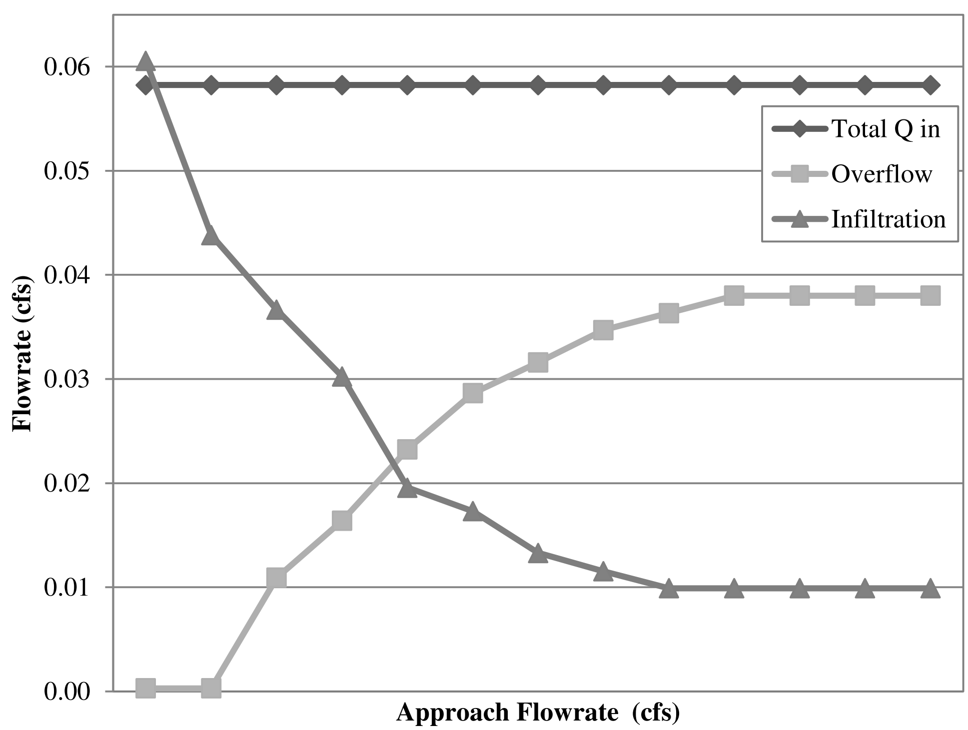

Figure 64. 6 mm Total Discharge, Overflow, Infiltration Rates

The straight line indicates the set flow rate of the clogging experiments. This value is the flowrate at which overflow first occurred and was not changed during the test. The horizontal infiltration values were observed to display a slight increase at the beginning of the experiment. The initial application of stormwater to the flow was observed to increase the viscosity (thickness) of the stormwater which may account for this phenomenon. The 10mm results are shown in Table 20 and Figure 65 and 12.5mm in Table 21 and Figure 66.

Table 20. 10 mm Summary of Infiltration discharge per Stormwater Applications

Stormwater Applications	Infiltration, cfs
0	0.124
5	0.098
10	0.092
20	0.068
30	0.027

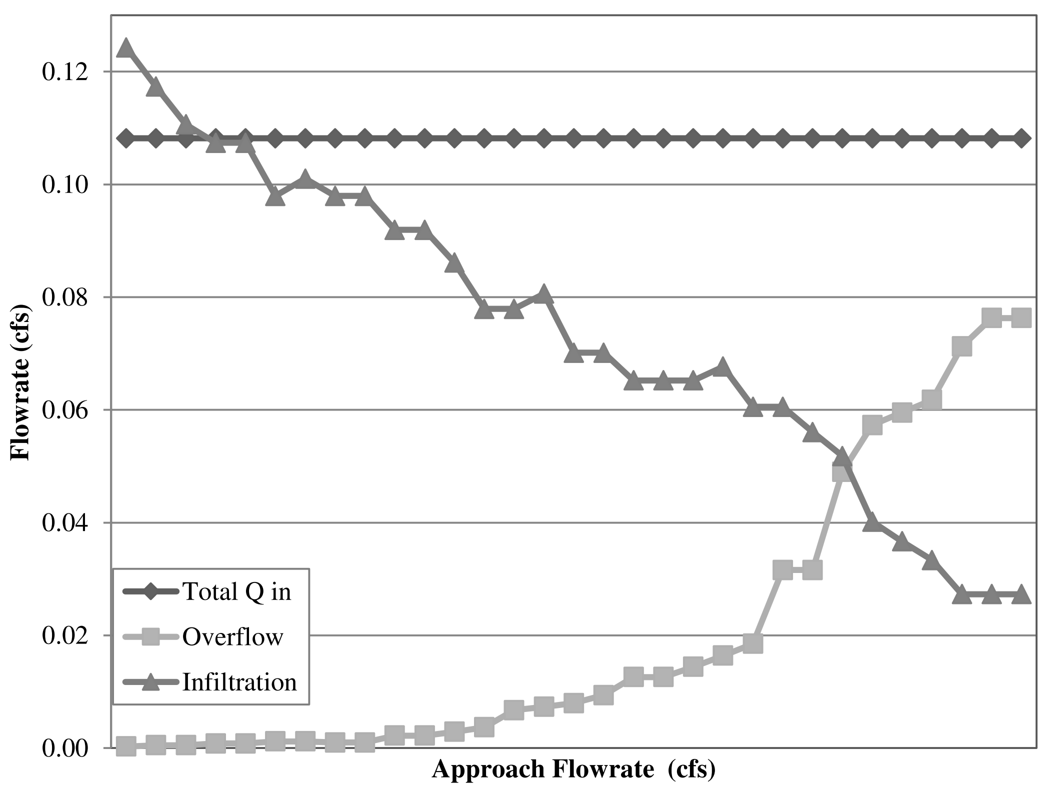

Figure 65. 10 mm Total Discharge, Overflow, Infiltration Rate

Table 21. 12.5 mm Summary of Infiltration discharge per Stormwater Applications

Stormwater Applications	Infiltration, cfs
0	0.139
5	0.131
10	0.124
30	0.070
50	0.030
70	0.026

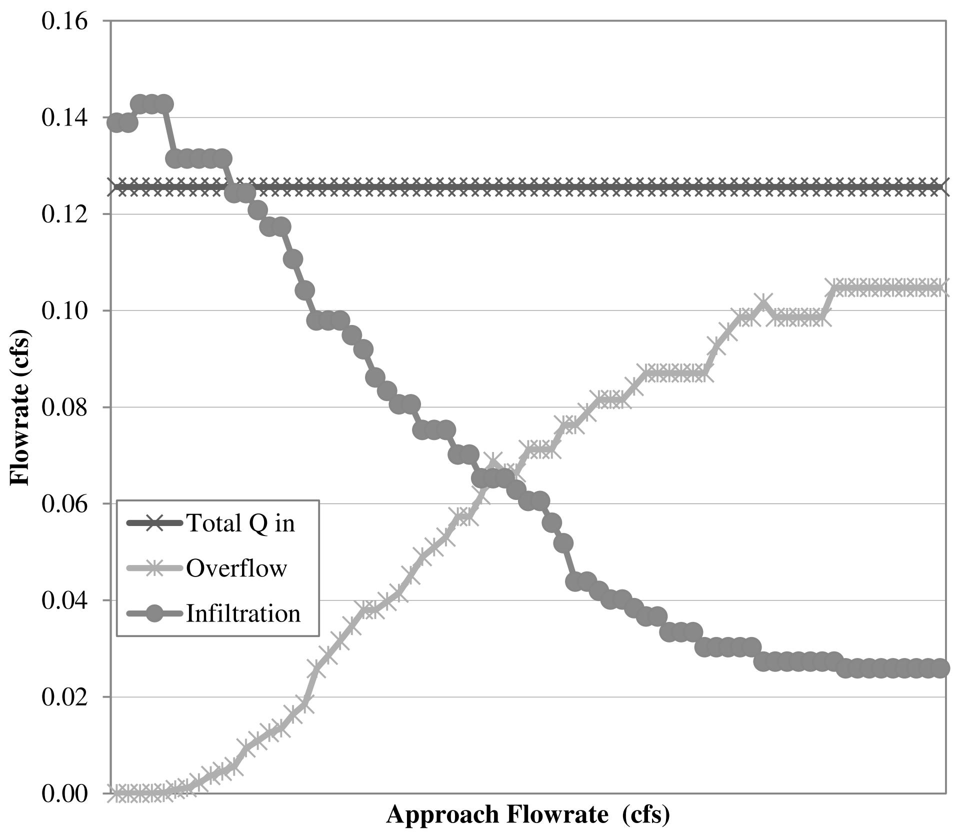

Figure 66. 12.5 mm Total Discharge, Overflow, and Infiltration Rate

After clogging was completed the sections were vacuumed, the filler material was replaced and a five point performance curve developed. The amount of flow rate recovered is shown in Figure 67 through Figure 69.

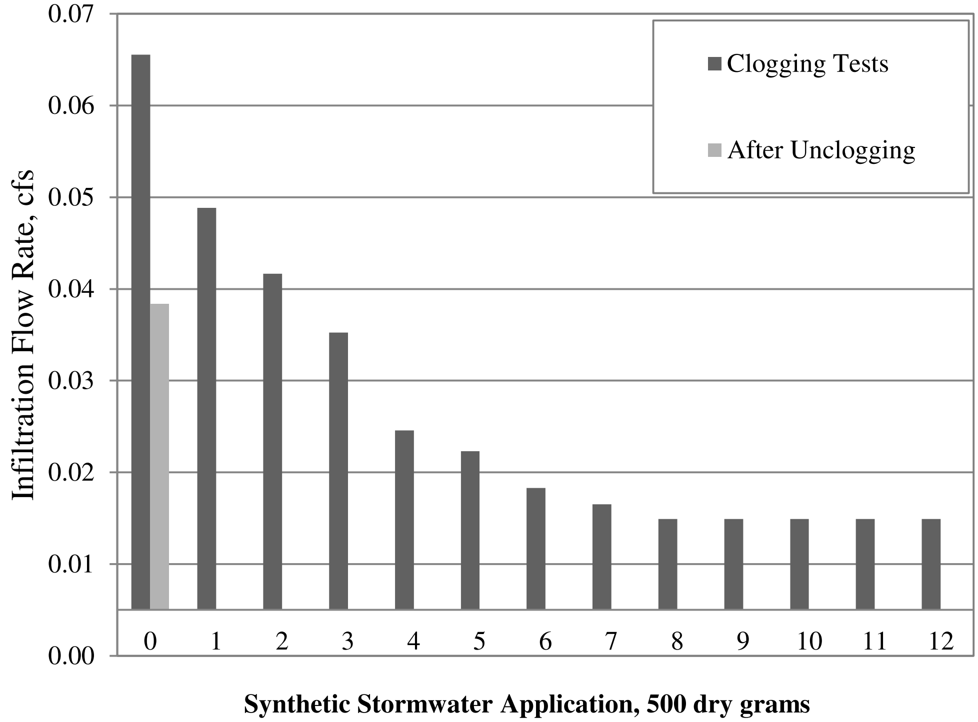

Figure 67. 6 mm after Clogging Recapture Rate vs. Application Result

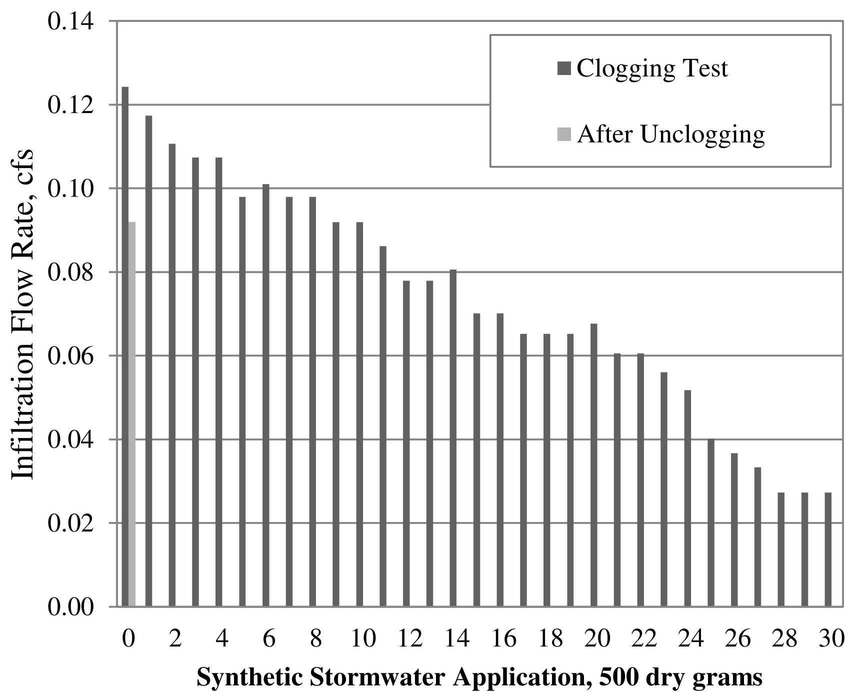

Figure 68. 10 mm after Clogging Recapture Rate vs. Application Result

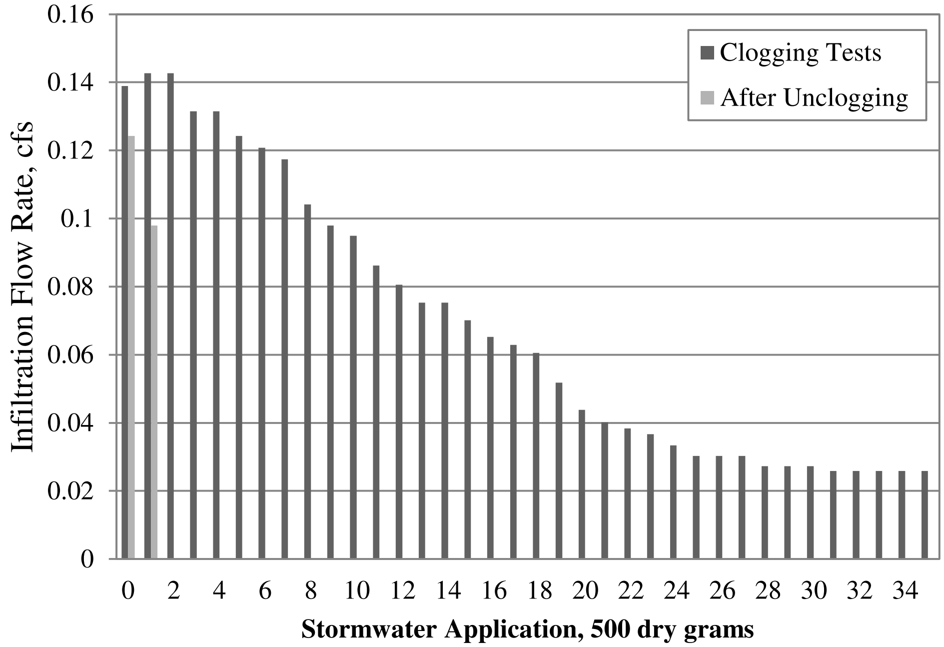

Figure 69. 12.5 mm after Clogging Recapture Rate vs. Application Result

Performance curves pre and post clogging (maintenance) tests were completed for comparison. Figure 70 to Figure 72 display these curves. The overflows rates before are much lower than the maintenance overflow values. Infiltration rates prior to clogging are much greater than the maintenance values.

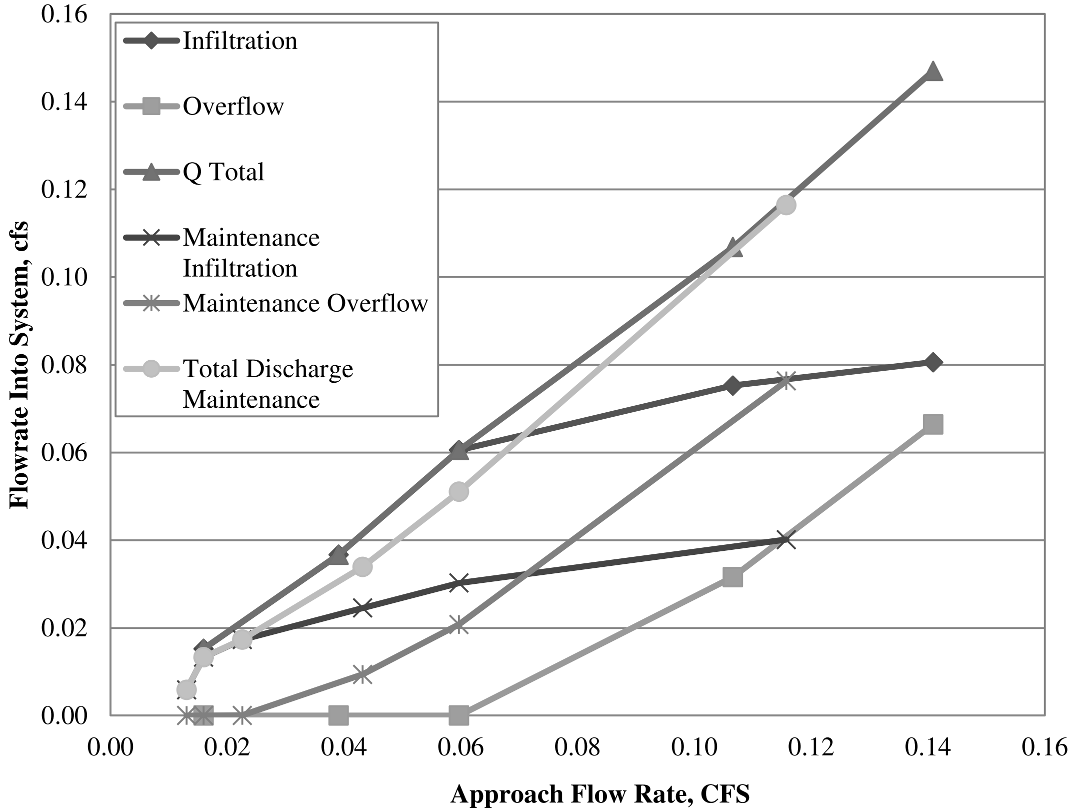

Figure 70. 6 mm Before and After Clogging Performance Curve

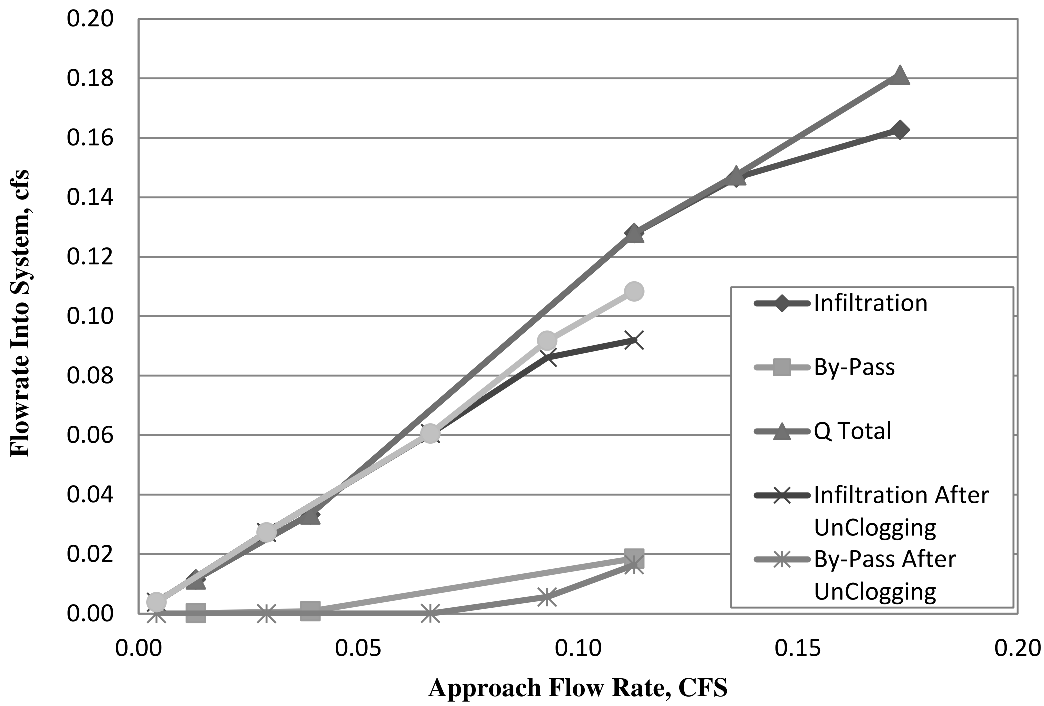

Figure 71. 10 mm Before and After Clogging Performance Curve

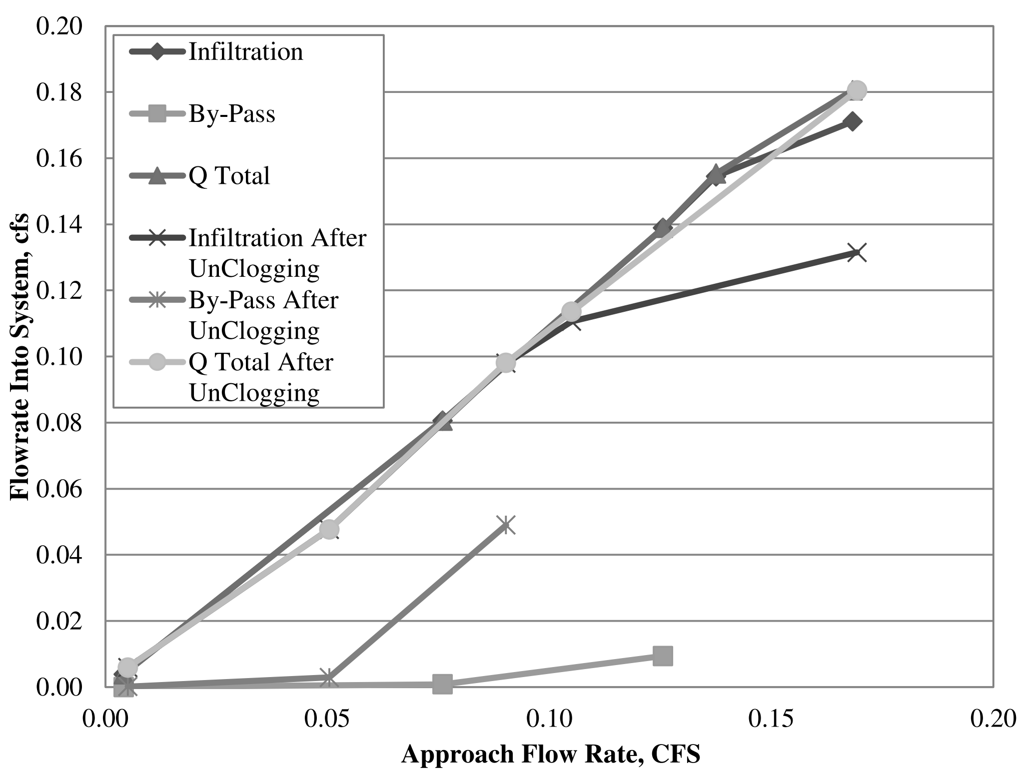

Figure 72. 12.5 mm before and After Clogging Performance Curve

In summary, as the applications of synthetic stormwater increased the infiltration decreased and the overflow rate increased, as expected. The results also indicate a linear relationship between applications and decreased infiltration and that as the spacing size increases the number of required applications of stormwater necessary to clog the system increases. After maintenance was completed the sections were retested and the system recovered anywhere from 55-89 % of the initial infiltration values.

Infiltration per Previous Field Research

As stated earlier, the synthetic stormwater load was greater compared to other experimental studies, but the trends were similar. A greater synthetic loading rate was required for experimental completion to occur in a reasonable amount of time. For comparison purposes the linear regressed equation found from the clogging experiments were used to translate (decrease) to the field data found in the study, "Investigation of Hydraulic Capacity and Water Quality Modification of Stormwater by Permeable Interlocking Concrete Pavement (PICP) System," by Kim et al. (2013). Table 22 states the beginning and ending infiltration values for 300 mg/l loading from the Kim et al. study (2013). These values were used to find a translated lower multiplier to use with the linear regression equations as shown in Figure 73 to Figure 75.

Table 22. Kim et al. Infiltration Values per Aggregate Filler Spacing (Kim et al., 2013)

	Kim et. al. Data 300 mg/l Loading	
Filler Aggregate	Start Infiltration in/hr.	Ending Infiltration in/hr.
No. 9 Gradation	275.5	7.9
No. 8 Gradation	405.5	26.9

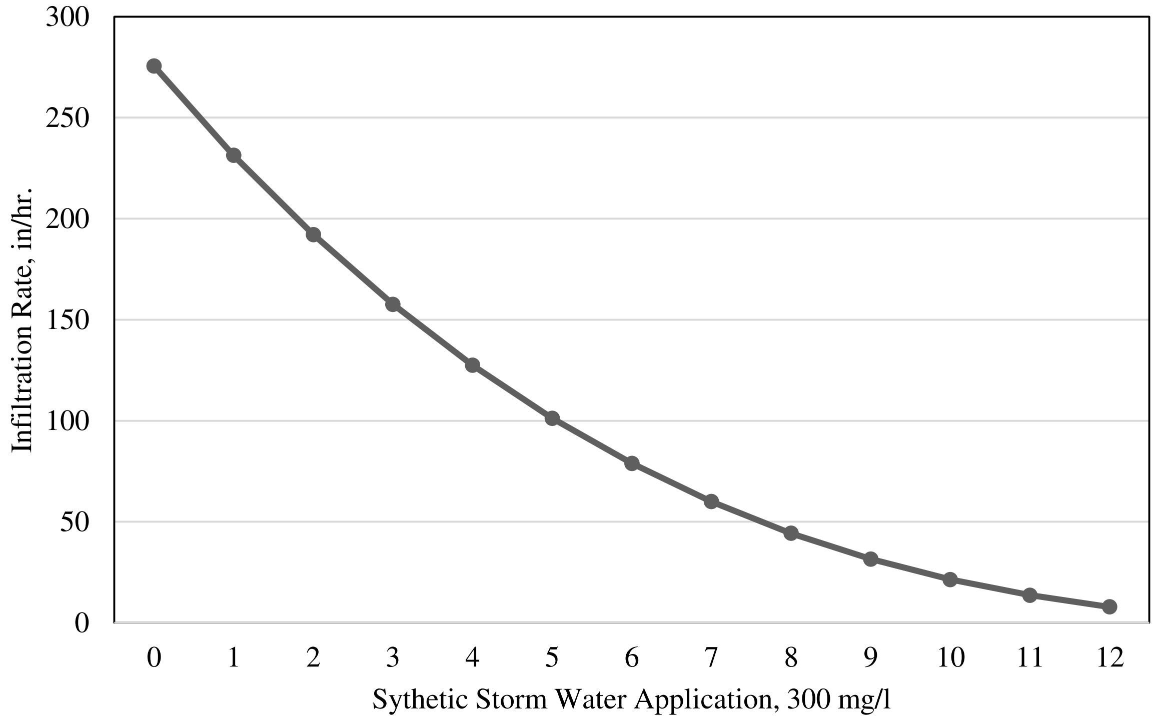

Figure 73. 6 mm Calibrated Infiltration Rate per Stormwater Application Curve

Two assumptions were made for the 12.5 mm and 10 mm clogging calibrated analysis. Figure 74 and Figure 75 display the calibrated 10 mm and 12.5 mm experimental infiltration values per stormwater application with the assumption that the data for the No. 8 aggregate filler material at the 300 mg/l loading would closely match both. In addition to both using the same initial and ending values, both used the linear regression equation found from the 12.5 mm spacing experiment. The 12.5 mm experiment had a greater amount of data to find a fitted equation the calibrated data resembles previous research (Kim et. al., 2013).

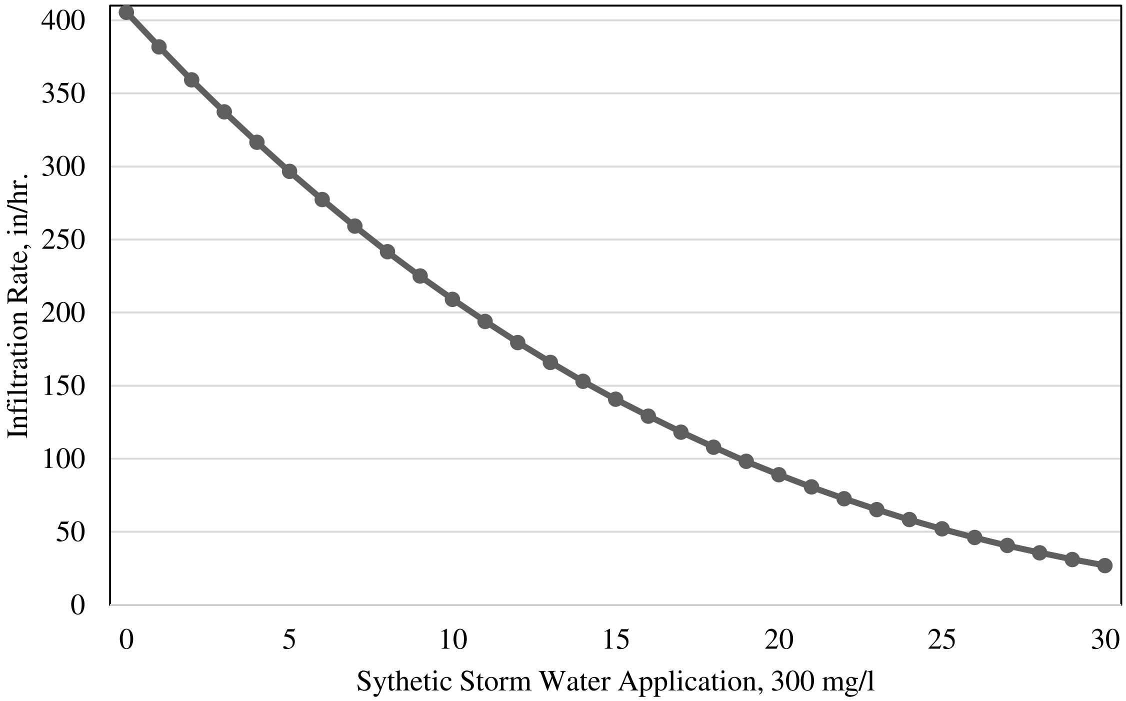

Figure 74. 10 mm Calibrated Infiltration Rate per Stormwater Application Curve

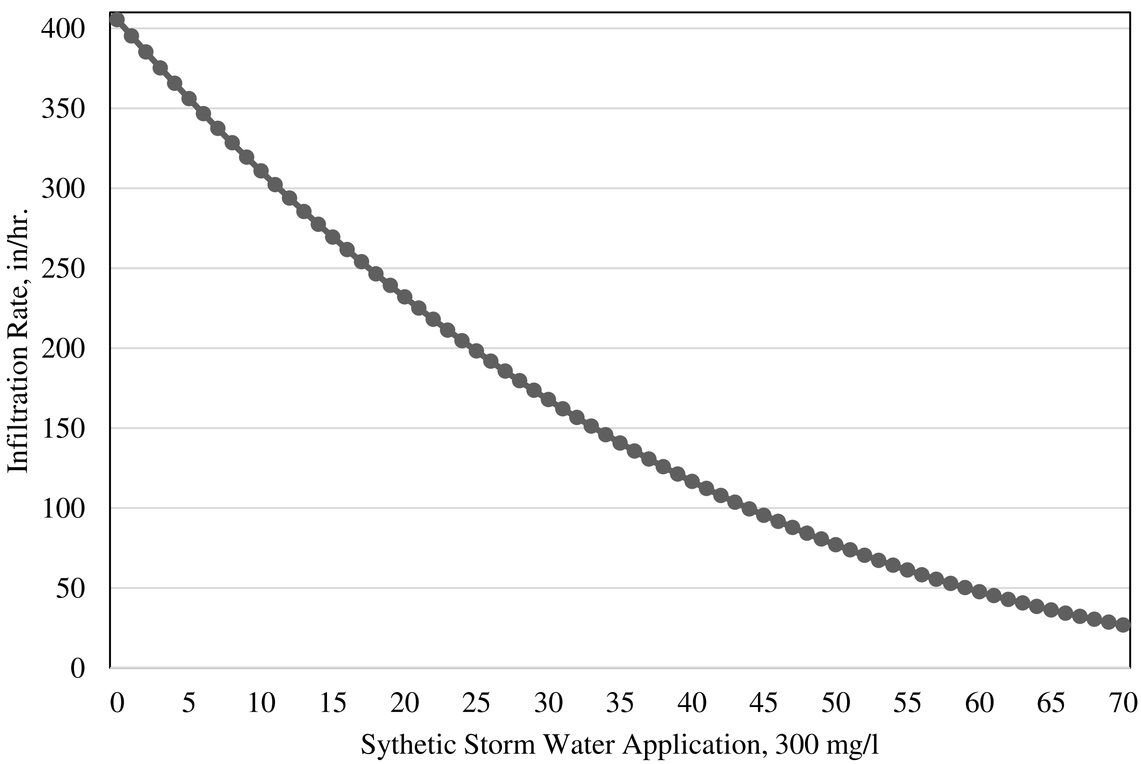

Figure 75. 12.5 mm Calibrated Infiltration Rate per Stormwater Application Curve

6. HYDRAULIC DESIGN

This chapter summarizes the materials and tools used in the hydraulic data collection process. Representative PICP sections were developed with 6mm, 10mm and 12.5 mm spacing between blocks. These sections were tested at 0%, 1%, 2%, 5% and 10% slope.

Analyzing Flume Results

As previously mentioned a series of tests were performed and average values were determined for each measurement point to create an average performance curve. All of the testing results are presented in Appendix A. From the average performance curve, a linear regression of the overflow was utilized to determine the maximum overflow discharge at varying levels. An example of the resulting plots is seen in Figure 76. The resulting linear equations are found in Table 23.

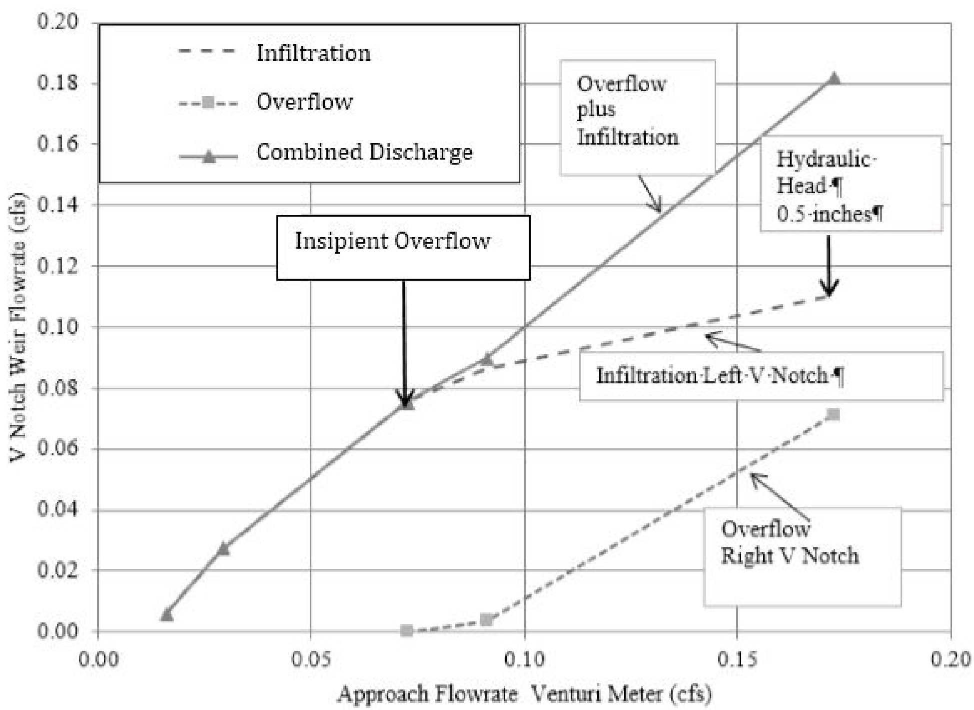

Figure 76. Performance Curve

The performance curves were used to determine linear regression of the "Overflow Right V-Notch" curve. The results were determined in the form of a linear equation, seen in Equation 4.

Equation 4. Linear Regressed Overflow Equation

$$Q_{CASE} = m*Q_{TOTAL} + b.$$

Where:

Q_{CASE} = Overflow across the system at relative case level (cfs)

m = slope

Q_{TOTAL} = Total flow in the system (cfs)

b = y-intercept (cfs)

Table 23. Linear Regressed Overflow Equations

Space (mm)	Slope (%)	m	b	Case Level 1	Case Level 2	Case Level 3
6	0	0.685	-0.060	0.000	0.020	0.059
6	1	0.598	-0.059	0.000	0.014	0.053
6	2	0.644	-0.048	0.000	0.032	0.069
6	5	0.638	-0.044	0.000	0.037	0.075
6	10	0.628	-0.040	0.000	0.047	0.076
10	0	0.430	-0.053	0.000	0.001	0.022
10	1	0.518	-0.062	0.000	0.007	0.033
10	2	0.538	-0.066	0.000	0.020	0.033
10	5	0.558	-0.067	0.000	0.013	0.035
10	10	0.569	-0.071	0.000	0.017	0.034
12.5	0	0.470	-0.063	0.000	0.004	0.018
12.5	1	0.528	-0.067	0.000	0.008	0.022
12.5	2	0.617	-0.081	0.000	0.011	0.025
12.5	5	0.512	-0.063	0.000	0.011	0.024
12.5	10	0.429	-0.051	0.000	0.009	0.020

The *case levels* references the level of overflow across the PICP section. Case I was calculated with the linear regression equation equal to 0 cfs for determining insipient overflow. For the design purpose, Case I will allow the least amount of water across the PICP system and is most conservative. A Case I design would be appropriate if no other BMPs are in-line with the PICP section. Figure 77 will be referred to as case I for the remainder of this document.

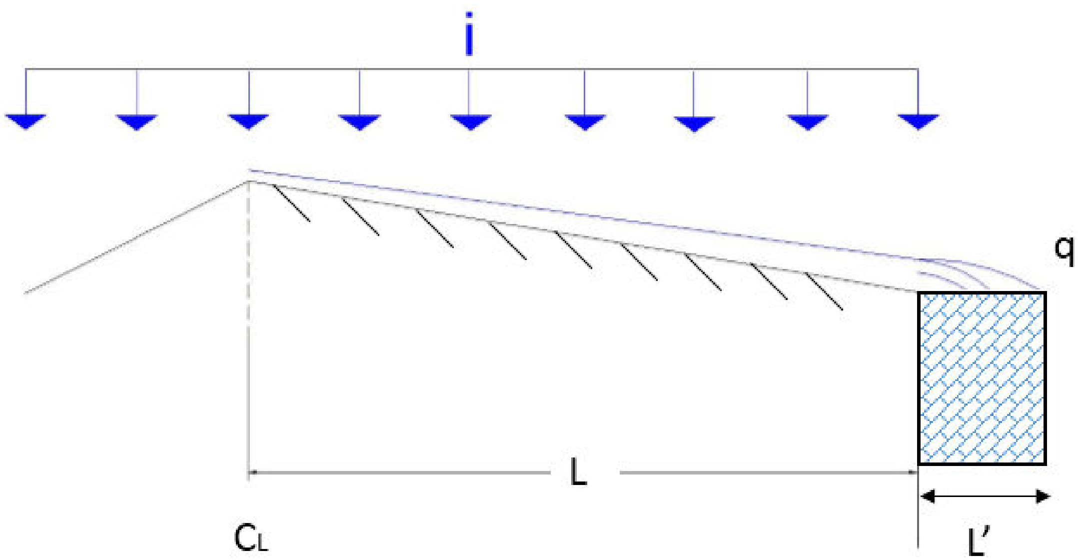

Figure 77. Case I - Pavement Top View and Cross Section for Insipient Overflow

Case II was calculated at the overflow flow value of ¼ in. head for the associated slope and spacing condition. In a perfect system, Case II will allow ¼ in. off head across the PICP section; therefore, in field, Case II will allow an intermediate amount of head across the PICP system and would be appropriate where at least one additional BMP is located downstream, seen in Figure 78.

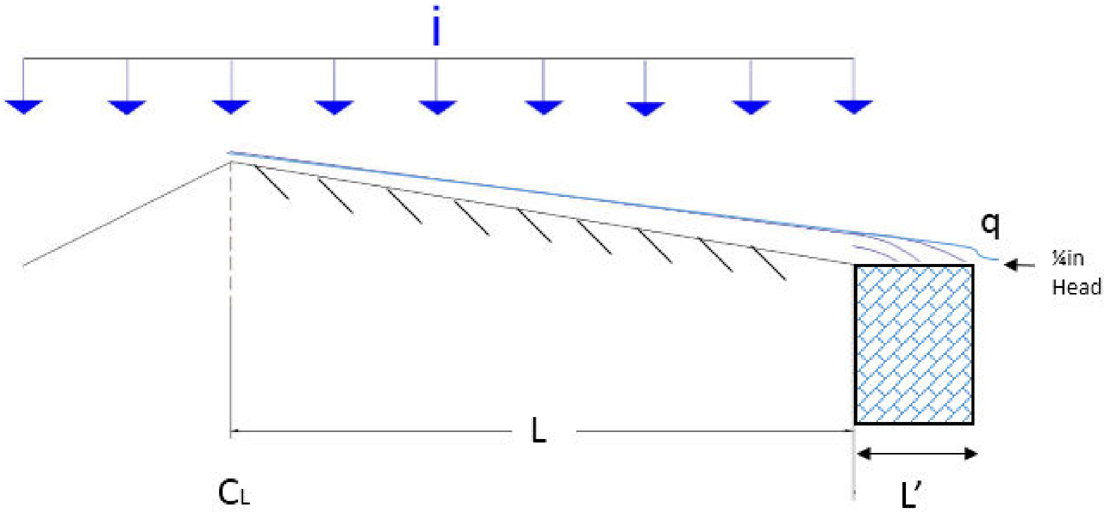

Figure 78. Case II - Pavement Top View and Cross Section for 1/4in Head

Case III was calculated at the overflow flow value of ½ in head for the greatest amount of overflow across the PICP section, seen in Figure 79. Case III is the least conservative would be appropriate when multiple BMPs are installed downstream of the PICP section.

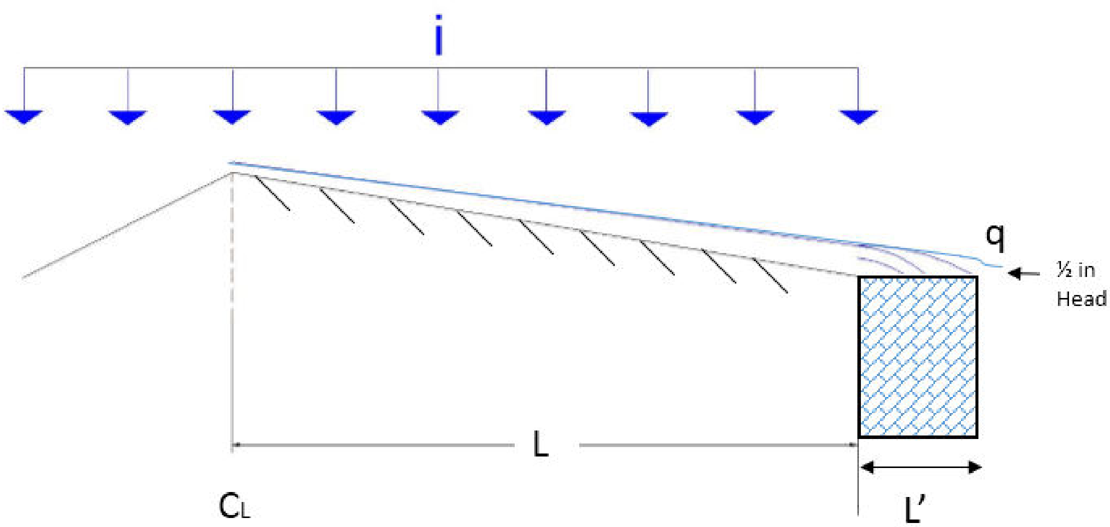

Figure 79. Case III - Pavement Top View and Cross Section for 1/2in Head

The unit overflow rate for each spacing and Case are shown in

Table 24. The general trends are increasing capacity from Case I to III with increased spacing. These are also shown visually in Figure 80 to Figure 82.

Table 24. Average Max Overflow Unit Rates per Pavement Cross Slope (cfs/ft.)

Spacing	Case	Pavement Cross Slope 0 %	1%	2%	5%	10 %
6 mm	I	0.044	0.050	0.037	0.035	0.032
10 mm	I	0.062	0.060	0.061	0.060	0.062
12.5 mm	I	0.065	0.065	0.065	0.062	0.059
6 mm	II	0.059	0.061	0.062	0.064	0.070
10 mm	II	0.063	0.066	0.080	0.072	0.078
12.5 mm	II	0.071	0.072	0.074	0.072	0.070
6 mm	III	0.059	0.061	0.062	0.064	0.070
10 mm	III	0.063	0.066	0.080	0.072	0.078
12.5 mm	III	0.071	0.072	0.074	0.072	0.070

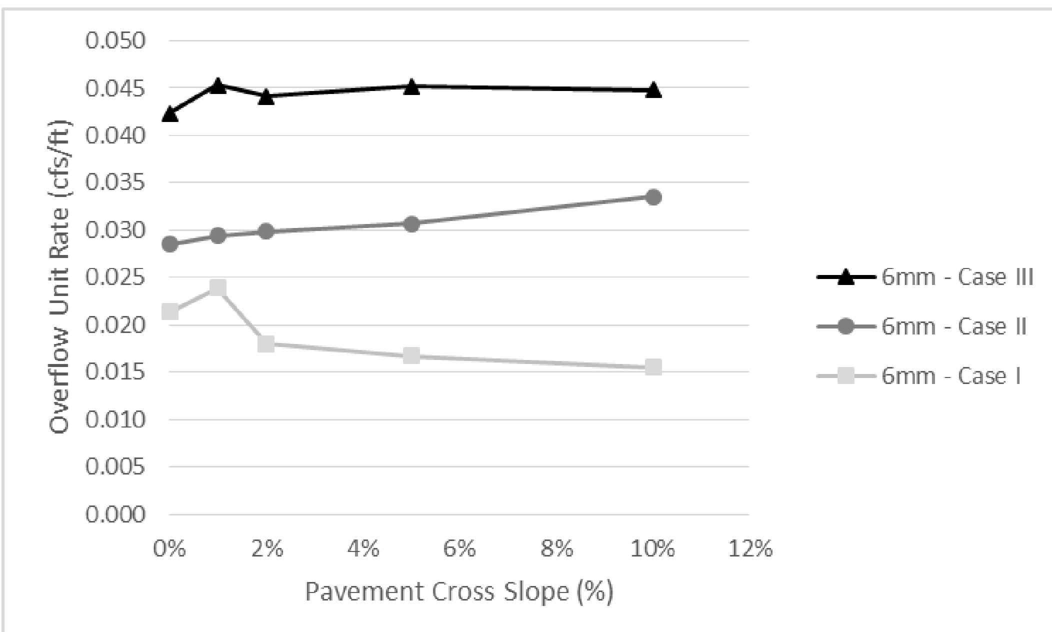

Figure 80. 6 mm Average Max Overflow Unit Rate per Pavement Cross Slope

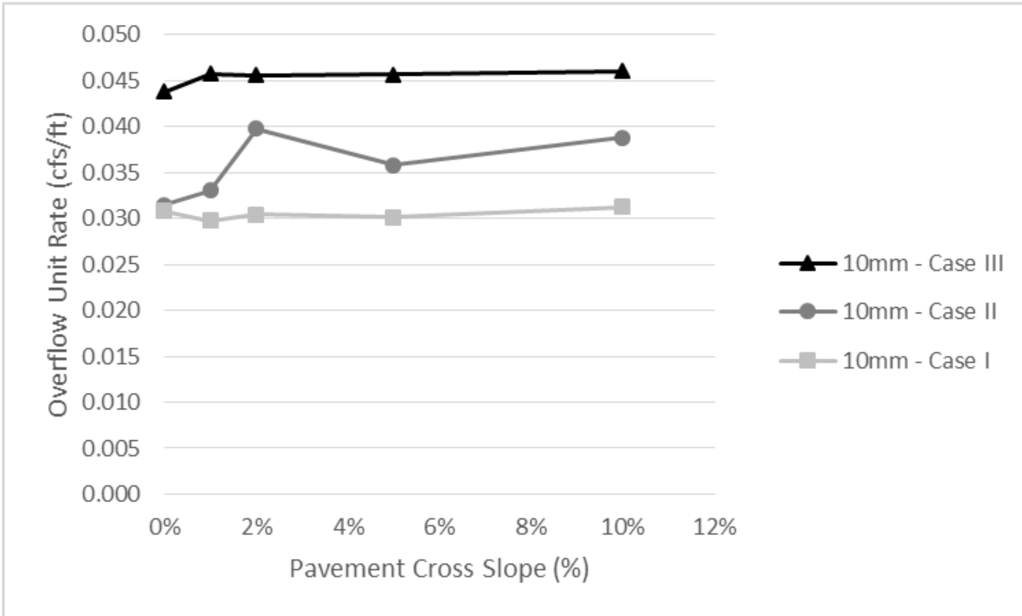

Figure 81. 10mm Average Max Overflow Unit Rate per Pavement Cross Slope

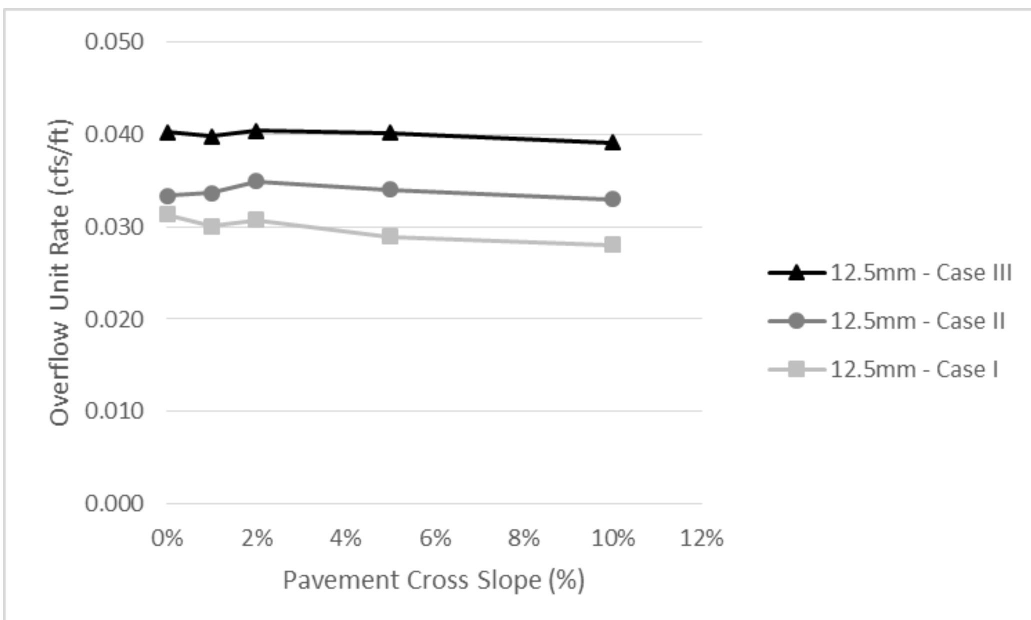

Figure 82. 12.5 Average Max Overflow Unit Rate per Pavement Cross Slope

The horizontal infiltration rates were determined using Equation 5, as converted from overflow. The results are shown in Table 25.

.

Equation 5. Horizontal Infiltration Rate

$$Q_{HORIZONTAL} = \frac{q}{L_m} * 43{,}200$$

Where:

$Q_{HORIZONTAL}$ = Horizontal Infiltration Rate (in/hr.)

q = Maximum capture flow rate before overflow per unit width (cfs)

L_m = Length of the section of the model (ft.)

Conversion Factor = 43,200 (3,600 sec/hr. * 12 in/ft.)

Table 25. Average Horizontal Infiltration Rates (in/hr.)

Spacing	Case	0%	1%	2%	5%	10%
6 mm	I	922	1031	777	721	670
10 mm	I	1331	1286	1315	1301	1350
12.5 mm	I	1353	1298	1327	1250	1210
6 mm	II	4924	5078	5164	5306	5798
10 mm	II	5445	5710	6873	6194	6700
12.5 mm	II	5756	5821	5849	9704	6243
6 mm	III	7314	7837	7620	7804	7741
10 mm	III	7575	7909	7881	7896	7959
12.5 mm	III	7737	7426	7531	7588	7383

Calibrated Values for Design Model

As previously discussed in Chapter 2, infiltration values were calibrated to expected field values. Table 26 shows the original and calibrated ASTM C1781 values and Table 27 the horizontal infiltration rates used within the design tool.

Table 26. C 1781 Experimental and Calibrated ASTM C1781 Vertical Infiltration (in/hr.)

Spacing	0%	1%	2%	5%	10%
6 mm	1077	1088	1226	1140	1114
6 mm Adjusted	359	363	409	380	372
10 mm	1504	1558	1628	1514	1495
10 mm Calibrated	502	519	543	505	498
12.5 mm	2012	2345	2532	2505	2439
12.5mm Calibrated	671	782	844	835	813

Table 27.Experimental and Calibrated Horizontal Infiltration Rates (in/hr.)

Spacing	Case	0%	1%	2%	5%	10%
6 mm	I	922	1031	777	721	670
6 mm Calibrated	I	307	344	259	240	223
10 mm	I	1331	1286	1315	1301	1350
10 mm Calibrated	I	444	429	438	434	450
12.5 mm	I	1353	1298	1327	1250	1210
12.5mm Calibrated	I	451	433	442	417	403
6mm	II	4924	5078	5164	5306	5798
6 mm Calibrated	II	1641	1693	1721	1769	1933
10 mm	II	5445	5710	6873	6194	6700
10 mm Calibrated	II	1815	1903	2291	2065	2233
12.5 mm	II	5756	5821	5849	9704	6243
12.5mm Calibrated	II	1919	1940	1950	3235	2081
6mm	III	7314	7837	7620	7804	7741
6 mm Calibrated	III	2438	2612	2540	2601	2580
10 mm	III	7575	7909	7881	7896	7959
10 mm Calibrated	III	2525	2636	2627	2632	2653
12.5 mm	III	7737	7426	7531	7588	7383
12.5mm Calibrated	III	2579	2475	2510	2529	2461

Incorporation of Clogging Into the Hydraulic Design

A large factor in the performance of PICP is the rate at which the PICP will clog, and therefore, the length of time it will take before maintenance must occur. PCIP is placed in many urban environments in many different types of locations. As discussed previously, one of the largest contributions to pollution is sediment. Placing PICP locations are downstream of sand, dirt, sediment, or other small particles that will restrict flow into the system, the amount of water the system can contain will drastically decrease (Ostercamp, 1998). Therefore, it was necessary for this research to investigate the effects of clogging on PICP section through hydraulic laboratory testing.

The synthetic stormwater was applied upstream to simulate polluted flow, similar to what would be seen in the field. In having this flow combine with water, a greater amount of a sediment is necessary due to some sediment in suspension overflowing the system, instead of being applied directly onto the system. Although the magnitude of the data differed, the results found the same trend. By normalizing the data based on a linear regression compared to field studies, Figure 83, Figure 84, and Figure 85 were represent clogged flow through the system.

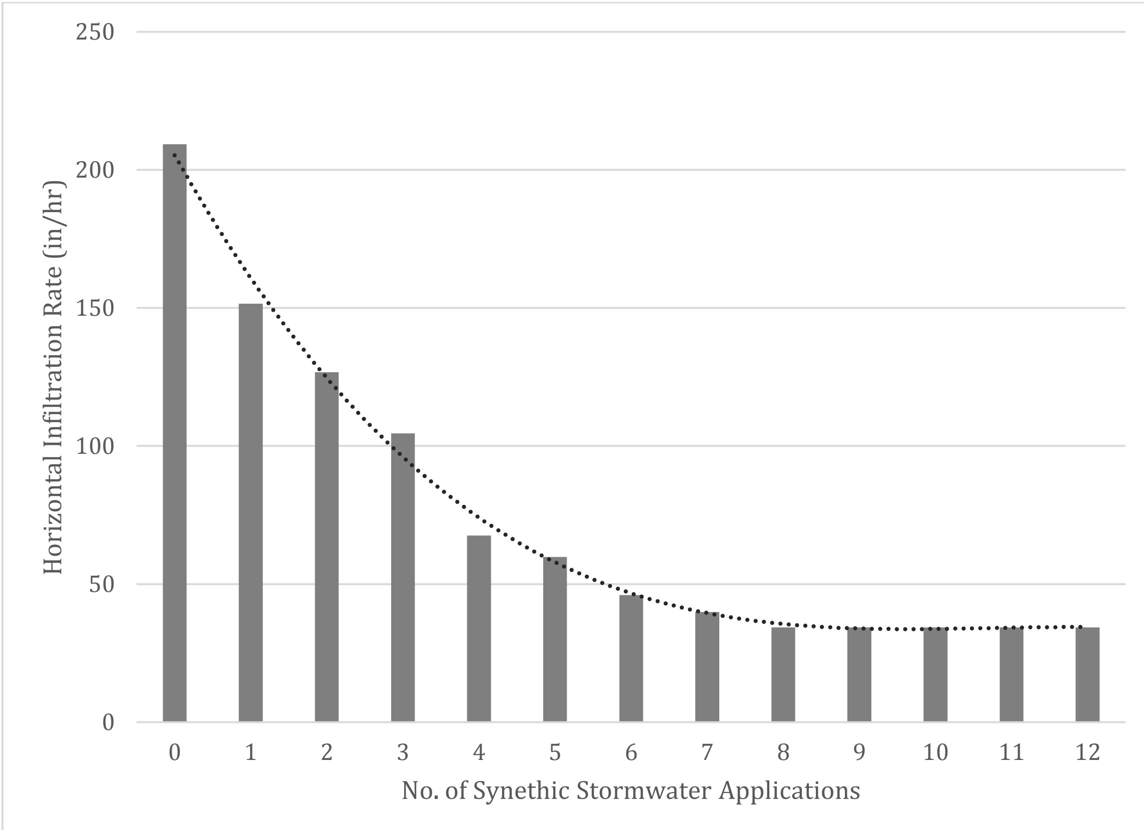

Figure 83. Infiltration vs. Application for the 6mm spacing

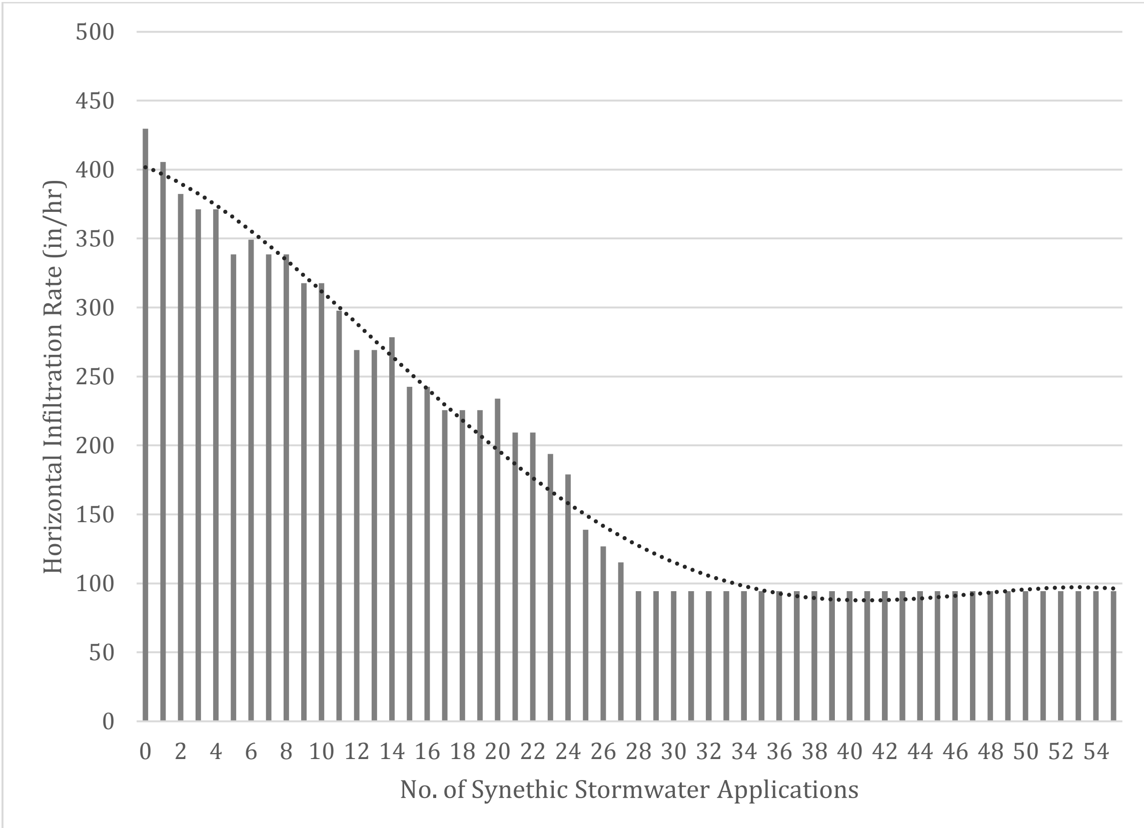

Figure 84. Infiltration vs. Application for the 10mm spacing

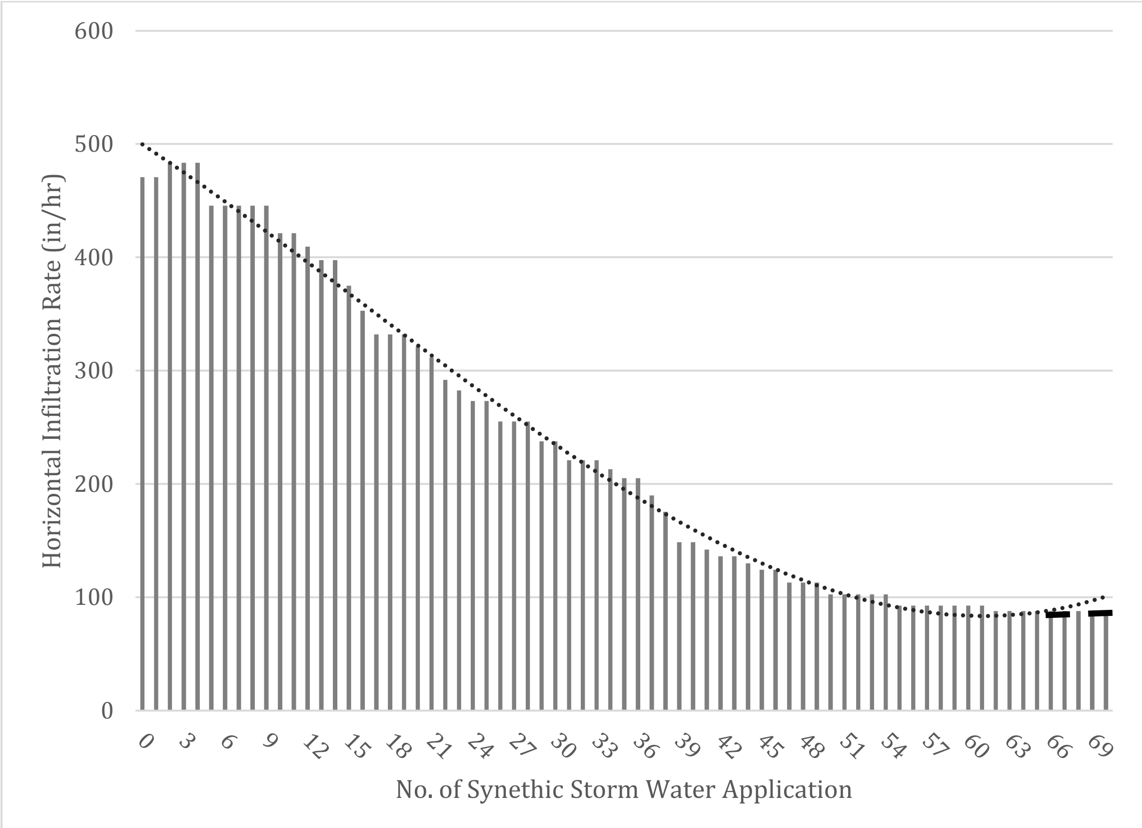

Figure 85. Infiltration vs. Application for the 12.5mm spacing

The infiltration rate decreased with continuous application of synthetic stormwater and clogging occurred faster for the narrower joint spacing. A third order polynomial was fit to the resulting data. The form of the equation can be seen in Equation 6, and all parameters listed in Table 28.

Equation 6. Clogging Regression Fitting

$$Q_{HORIZONTAL}\text{ (in/hr.)} = a * SSA^3 + b * SSA^2 + c * SSA + d.$$

Where:

$Q_{HORIZONTAL}$ = Horizontal infiltration rate (in/hr.)

a, b, c, d = Curve parameters

SSA = No. of synthetic stormwater applications

Table 28. Clogging Equation Parameters

Spacing (mm)	**a**	**b**	**c**	**d**
6	-4.00E-10	1.00E-05	-9.34E-02	2.76E+02
10	-3.00E-11	2.00E-06	-4.63E-02	3.56E+02
12.5	-2.00E-12	4.00E-07	-2.07E-02	4.06E+02

The results verify the conclusion that the point of complete clogging occurred at a much faster rate for smaller spacing and that post clogging maintenance will increase the infiltration rate. Maintenance was performed on the system for the 6mm and 10mm spacing, and the infiltration rates were tested. The results found that after are summarized in Table 29. These results show an average percent reduction in the infiltration rate of the PICP after maintenance occurs is approximately 50%.

Table 29. 6mm Clogging Test Summary

Spacing	Test Description	Calibrated Infiltration Rate* (in/hr.)
6 mm	Pre-Test	837
6 mm	Post Maintenance	239
6 mm	Percent Reduction	71.4%
10 mm	Pre-Test	1718
10 mm	Post Maintenance	1217
10 mm	Percent Reduction	29.1%
Average		50.3%

7. PERVIOUS CONCRETE AS A BASE MATERIAL

Portland Cement Pervious Concrete (PCPC), like PICP, is a permeable structure that are used to infiltrate urban runoff and increase water quality. PCPC are generally set in place sections that have been shown to infiltrate at a higher rate than PICP and exhibit higher loading strength. As such a system that would include PCPC under a paver block system would be attractive to increase pavement strength while not jeopardizing infiltration rates.

Material Properties

For the purpose of this experimentation a light-weight PCPC platform was constructed. For a light-weight concrete, coarse aggregate was replaced with a light-weight aggregate mixture. The fine aggregate was also replaced with a medium absorption material from Hydraulic Press Brick Company from Brooklyn, Indiana. The sample was mixed according to ASTM C192. Table 30 displays the summary of the concrete mixture including the water to cement ratio (w/c). Figure 86 displays the PCPC platform set in place within the flume. Table 31 and Table 32 provide the concrete testing results.

Table 30. Summary of Concrete Mixture

Cement (PCY)	Coarse Aggregate SSD (pcy)	Fine Aggregate SSD (pcy)	Water (pcy)	W/C
573	1127 (WSD)	145 (WSD)	195	0.34

*Mass of coarse aggregate is provided as wetted surface dry (WSD)

Figure 86. PCPC Lightweight Platform

Table 31. Hardened Concrete Results

Fresh Unit Weight ASTM C1688	Hardened Unit Weight ASTM C1754		Voids ASTM C1754		Permeability ASTM C1754	
Avg. (pcy)	Avg. (pcf)	COV (%)	Avg. (%)	COV (%)	Avg.(in/hr.)	COV (%)
76.4	63.3	0.3	42.8	0.9	4600	5.5

Table 32. Strength Testing Results

Compressive Strength 7 Day ASTM C39		Compressive Strength 28-day C39		Tensile Strength 28-day ASTM C497	
Avg. (psi)	COV (%)	Avg. (psi)	COV (%)	Avg. (psi)	COV (%)
817	39.2	897	4.0	213	4.7

Platform Infiltration

A regular five point experiment, with the same testing procedure was completed on the lightweight PCPC platform to develop a performance curve, as shown in Figure 87. The PCPC platform was also tested for vertical infiltration according to the C1701 standard (ASTM, 2007). The average infiltration was found to be 2201.9 in/hr. for the section which was considerably higher than the PICP vertical infiltration test.

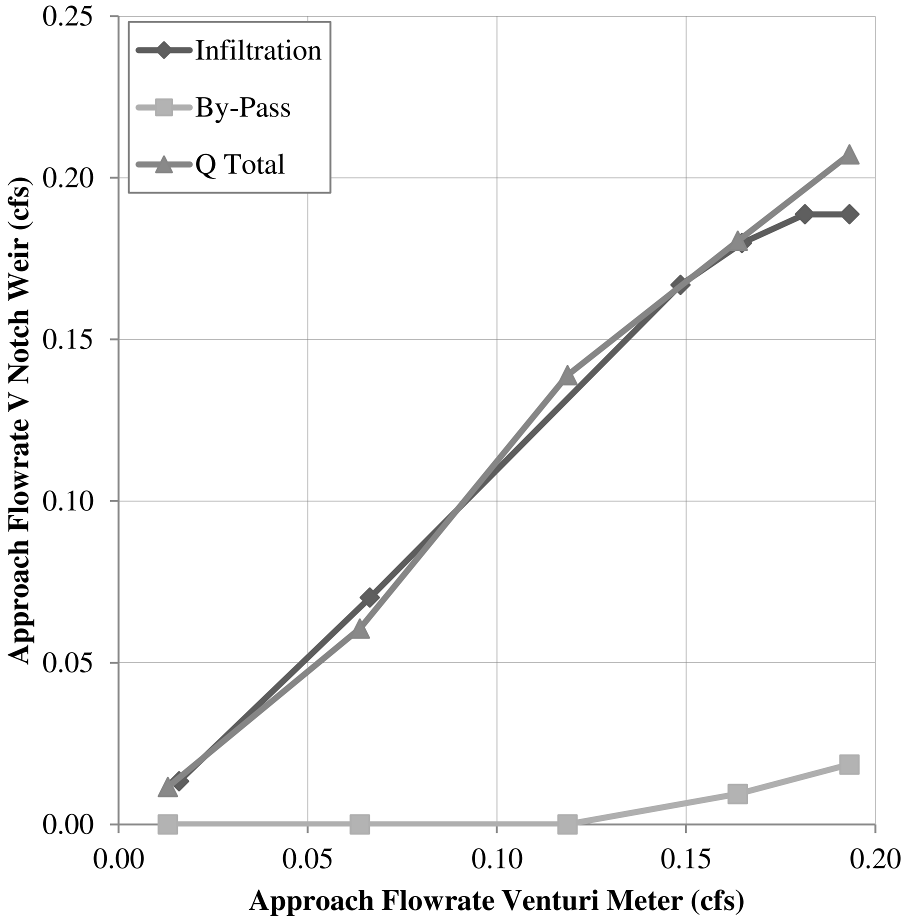

Figure 87. PCPC Platform Performance Curve

Horizontal infiltration was calculated for the PCPC platform without the PICP system to assess the functionality of the platform as a base layer to the PICP system. The platform was expected to have a higher horizontal infiltration than the greatest space sizing in the PICP system (12.5 mm). Table 33 displays the comparison between the platform and the average horizontal infiltration values per pavement slope for each type of spacing set on a conventional aggregate base.

Table 33. Horizontal Infiltration Averages per Pavement Slope

Slope	Platform	12.5 mm	10 mm	6 mm
		Infiltration, in/hr.		
0%	1827.50	1411.97	1348.25	893.37
1%	1739.23	1424.87	1433.71	992.80
2%	1696.07	1411.97	1460.01	748.15
5%	1411.97	1399.29	1460.01	704.15
10%	1489.96	1399.29	1486.74	642.75

PICP and Platform System

PICP blocks were then placed on top of the PCPC platform for an additional test. The 12.5 mm with the number 8 gradation joint filler material was used because it had the highest infiltration and would be most susceptible to influences of the supporting material. The observed infiltration was similar to the infiltration found without the lower PCPC platform base. This finding indicates that the infiltration rate for the experimental test sections is governed by the filler spacing and the top layer of the system. Figure 88 displays an example of the performance curve for the system. Figure 89 displays the horizontal infiltration at the overflow point comparison for the platform PCPC, PICP and PCPC system, and the average 12.5 mm spacing tests. This is the first time the effect of slope on infiltration rate has been compared for PCPC and PICP. Figure 89 indicates that PCPC is much more sensitive to slope by PICP systems.

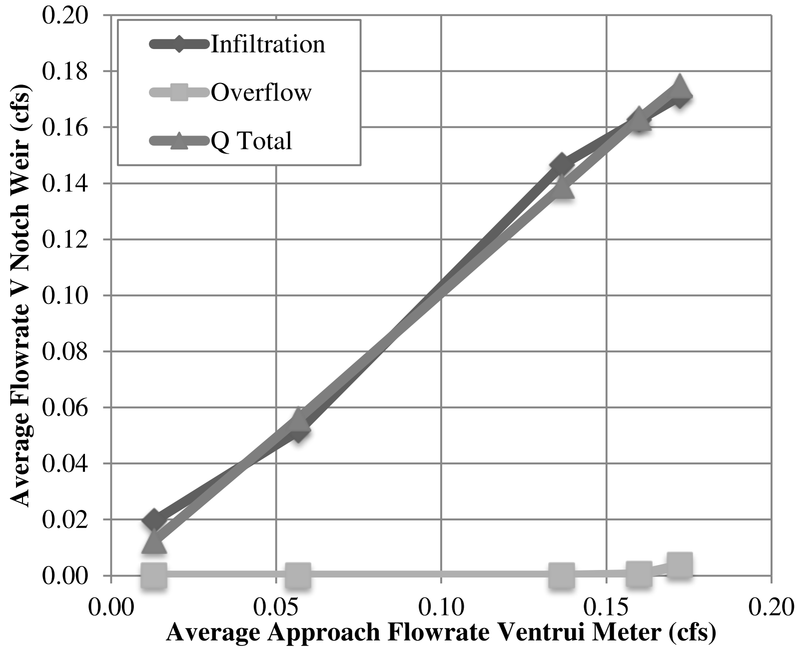

Figure 88. PICP and PCPC Platform System Performance Curve

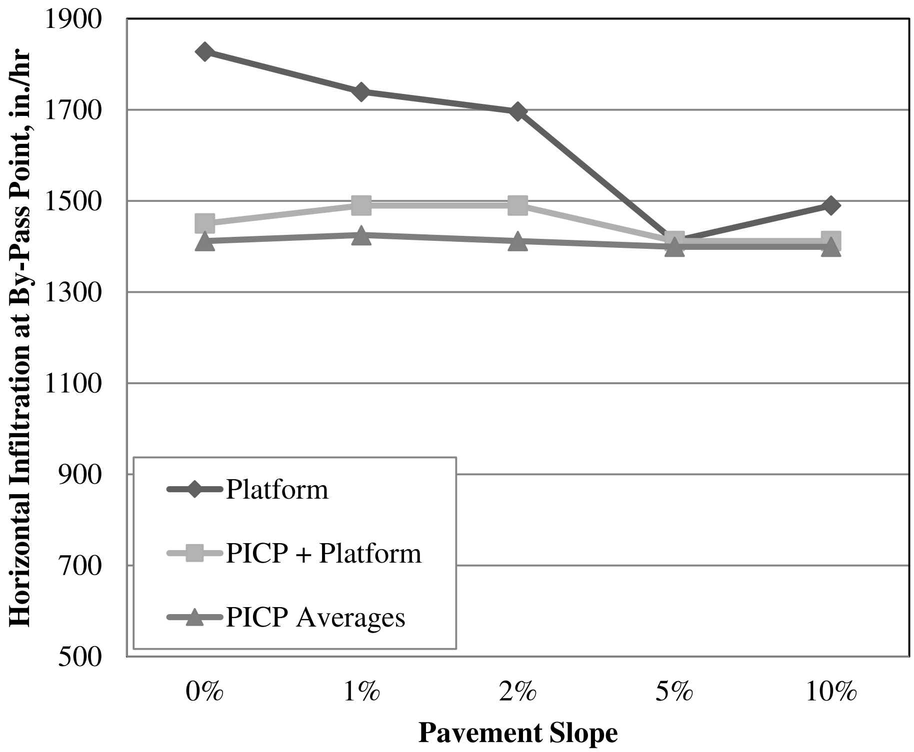

Figure 89. PICP, PCPC Platform, and 12.5 mm Averages per Payment Slope

The results of the horizontal combined system experiment displays that the infiltration was controlled by the top layer within the experiment. However, as noted in Chapter 5 this may not be the case within the field. It should also be noted that the platform and the pavers and platform system at the higher slopes, 10-5%, displayed cavitation during experimentation as shown in Figure 75. Cavitation across a pavement will display a lower infiltration as indicated in the results. Table 32 displays the horizontal infiltration comparison values.

Table 34. Horizontal Infiltration at Overflow Point per Pavement Slope

Slope	Platform	Pavers +Platform System Infiltration, in/hr.	Average 12.5 mm Pavers
0%	1827.50	1450.65	1411.97
1%	1739.23	1489.96	1424.87
2%	1696.07	1489.96	1411.97
5%	1411.97	1411.97	1399.29
10%	1489.96	1411.97	1399.29

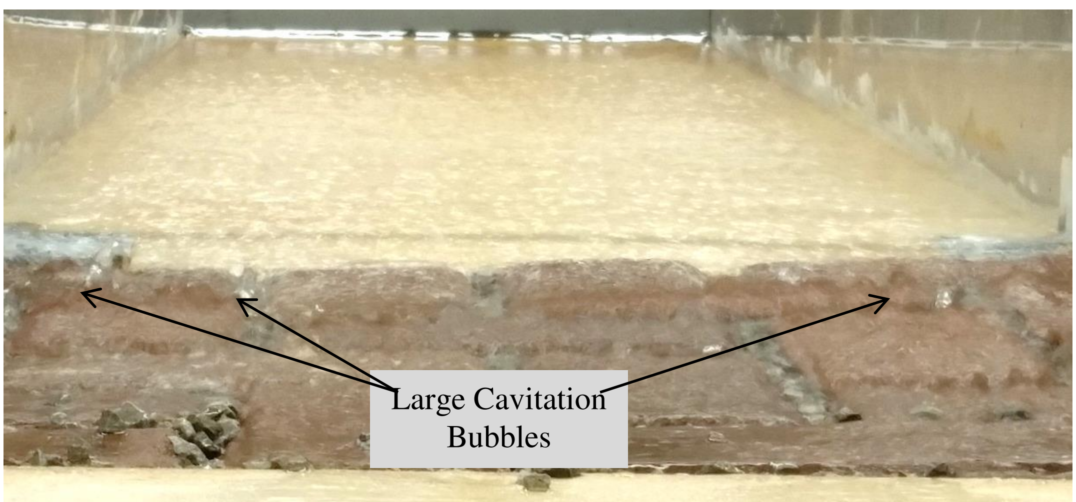

Figure 90. Cavitation Example 10 % Slope

8. Design tool for Specifying PICP

The PICP testing results have been described in the previous chapters. This research lead to the creation of the Hydraulic Design Tool. Due to an increase in urbanization resulting in an increase in surface runoff to nearby water bodies and ecosystems, green stormwater management practices and technologies are fundamental to addressing stormwater volume reductions. Installing PICP as a BMP provides stormwater management by reducing the overall quantity of stormwater through infiltration, attenuating water within the conveyance system, and improving water quality through filtering and promotion of natural degradation processes. PICP has recently been realized as a highly effective BMP, therefore, supporting further refinement of the design process. Both the structural and hydrologic factors have been thoroughly assessed, while this research address the hydraulic component.

The previous chapters describe in detail the equipment, testing protocol, materials specifications, and testing methodology for establishing the hydraulic performance of PICP systems. The previous chapters also present a method to test PICP systems for clogging which leads to a method for assessing the long-term performance of these systems. These protocols, established at the hydraulics laboratory at the University of Missouri Kansas City, are well documented in Ms. Amanda Leipard's thesis (Leipard, 2015).

Leipard's research establishes a testing standard for PICP, where the performance of any PICP system can evaluated. Leipard's research results also allowed for the development of a spreadsheet based PICP hydraulic design tool Stochl (2015). This hydraulic design tool is documented in Appendix B. To further support the design tool, specific examples and case studies are provided in Appendix C. Appendices B and C are presented as stand-alone documents to support the PICP design tool. As such only a brief summary of the features are discussed herein.

The goal for the development of the design tool was to provide users to determine the applicability of and/or size the extents of a PICP system given a design hydrologic event. It also assess the long-term performance and/or expected frequency of maintenance required due to potential clogging. Finally, the design of the tool was open-ended so that the hydraulic performance of different PICP block types/configurations could be evaluated (provided they had been hydraulically tested consistent with the methods of Leipard, 2015).

The design tool assumes full-equilibrium, overland flow over a unit width of contributing area. This is consistent with the Hortonian concept over overland flow over impervious surfaces (Richardson, 1989). Rainfall intensities and durations differ significantly depending on location. As such, the PICP design tool adapted the rainfall estimation methods SCS-TR55 methodology (USDA 1986). Based on storm information, relative to the geographic site of the PICP location, and site attributes including areas and development type, the vertical infiltration, horizontal infiltration, and overflow rate for a variation of slope and block spacing arrangements the adequacy of a particular PICP system can be assessed as seen as adequate or inadequate. The tool also predicts the time necessary to maintenance based on the stormwater pollutant concentration.

9. Project Summary and Conclusions

This report summarizes the research effort of Leipard (2015) and Stochl (2015). Leipard's thesis lays out a detailed testing methodology for which any PICP system can be hydraulically tested in a consistent reputable manner. Stochl's thesis uses the result obtained from Leipard (2015), and presents a scalable, adaptable Hydraulic design tool for PICP. Both documents contain significantly more detail than can be incorporated into this report. Consequently the reader is referred to these documents to provide a more in-depth treatment of the means, methods, statistics and methods assess the hydraulic performance of PICP systems in a consistent manner. As this is a report of the performance of one PICP system.

The ability of water to infiltrate a PICP system is significantly less when the water runs horizontally over the PICP as opposed to flowing vertically. The research and design tool documented in this report present a method for testing and designing PICP systems to adequately absorb overland flow. The testing protocol and methodologies are documented in detail in the supporting thesis by Leipard (2015). The supporting analysis for the design tool is documented in Stochl (2015).

The environmental benefits of permeable pavements are significant and include stormwater quantity reduction, stormwater quality improvement, urban heat island mitigation, and groundwater recharge, among others. Permeable Interlocking Concrete Pavements explicitly infiltrate water, a new concept to engineering practice for pavements. This technology as a load-carrying surface has not yet been fully characterized nor has the decades of design and performance experience of conventional pavements. This research project developed a hydraulic design methodology for PICPs. Test sections were evaluated in a two layer hydraulic flume to determine infiltration rates, and overflow rates for various block spacing, patterns, and across a broad range of pavement cross slopes. The research results included the following:

- Comparison of vertical to horizontal infiltration.
- Development of horizontal infiltration at different hydraulic heads.
- Incipient overflow infiltration identification per gap spacing.
- Infiltration capacity related to cross slope.
- Infiltration reduction with synthetic stormwater application.
- Maintenance to recapture infiltration.
- Evaluation of hydraulic performance when pervious concrete was used as a base material.
- Development of a usable hydraulic Design Tool.

Results showed the infiltration rate of the PICPs exposed to horizontal sheet flow is lower than the measured vertical infiltration rate by 35%-11% which is currently used in field verification. The results also demonstrate that the infiltration discharge rates are inversely related to the cross slope of the pavement with a Spearman Rho of -0.91. The horizontal and vertical infiltration rates were higher than field observations by a factor of three, the data was translated and compared to vertical field observation tests completed in the local Water Services Department of Kansas City Missouri's newly constructed parking lot.

Clogging tests which included the creation of synthetic stormwater for PICP was completed and analyzed. The experimental tests included setting the initial testing discharge to a set flowrate, the rate at which overflow occurs for each of the PICP spacings. The synthetic stormwater was applied at a fixed dry mass amount that was dissipated as the flow was running across each of the three test sections; 6 mm, 10 mm, 12.5 mm straight herringbone pattern. The results indicate an inverse relationship between the amount of stormwater applications and infiltration as expected. Results also indicate that as the applications of stormwater increase the overflow rate increases. Similar to the vertical infiltration tests the clogging loading rates were higher than previous research (300 mg/l) which is used field data. However, the overall trend of the clogging research matched previous research and as such linear trend line regressions were created and can be used to predict system clogging patterns. After maintenance the PICP system recaptured approximately 45% of initial infiltration for the 6 mm filler spacing pattern.

Additional research included permeable concrete pavement as an alternative sub-base which displayed infiltration and overflow rates similar to previous 12.5 mm straight herringbone patter data. This result indicates that for the experimental set up the infiltration and overflow rates are controlled by the surface aggregate and open area. Since Infiltration and overflow rates of the permeable concrete pavement are greater than the controlling PICP, a system which includes the pavement as a sub base layer would be a viable option and would provide greater strength. Experimental results indicated a possible cavitation at the higher pavements slopes indicating that infiltration may possibly be reduced. Future research to further examine these affects and a combination PCPC and PICP system would perhaps expand the use of PICP providing broader applications including perhaps where greater pavement loading is required.

10. References

Adler, R., Landman, J., and Cameron, D. (1993). *The Clean Water Act 20 Years Later*. Library Of Congress Cataloging-in-publication Data. Island Press, Washington, DC. 1993.

American Public Works Association (APWA) (2006). "Standard Specification Criteria: Section 600 Storm Drainage Systems and Facilities." Kansas City Metropolitan Chapter, APWA.

American Public Works Association. (2011). The Clean Water Team Guidance Compendium for Watershed Monitoring and Assessment State Water Resources Control Board 5.1.3 FS-(RC)

American Society for Testing and Materials (ASTM). (2007). "Standard Test Method for Infiltration Rate of In Place Concrete." C1701/C1701M-09, West Conshohocken, Pa.

American Society for Testing and Materials (ASTM). (2013). "Standard Test Method for Infiltration Rate of Permeable Unit Pavement." C1781-13, West Conshohocken, Pa, 1-3.

American Society for Testing and Materials (ASTM). (2013). "Standard Test Method for Infiltration Rate of Permeable Unit Pavement." C1781-13, West Conshohocken, Pa.

Barnard, T. (2002). "Compliance with Phase II Stormwater Regulations." Pollution Engineering. 34,5. 20.

Booth, D., and Brattebo, B. (2003). "Long-Term Stormwater Quantity and Quality Performance of Permeable Pavement Systems." Journal of Water Research. Vol 37. No. 18. 4369-4376.

Brown, R. A., and Borst, M. (2014). "Evaluation of Surface Infiltration Testing Procedures in Permeable Pavement Systems." Journal of Environmental Engineering, Vol. 140. No. 3.

Cass County Government. (2014). "6 Minimum Control Measures." Stormwater Management. https://www.casscountynd.gov/county/depts/planning/Pages/StormwaterManagement.aspx

Collins, K., Hunt, W., and Hathaway, J. (2008). "Hydrologic Comparison of Four Types of Permeable Pavement and Standard Asphalt in Eastern North Carolina." Journal of Hydrologic Engineering. 13,12. 1146–1157.

Environmental Protection Agency (2000). "Storm Water Phase II Compliance Guide." United States Protection Agency: EPA-833-R-00-002. Office of Water. Washington D.C.

Environmental Protection Agency (2004 a). "National Management Measures to Control Non-point Source Pollution from Urban Areas." United States Protection Agency: EPA-941-B-05-004. Office of Water. Washington D.C.

Environmental Protection Agency (2004 b). "Stormwater Best Management Practice Design Guide: Volume 1 – General Considerations." United States Protection Agency: EPA-600-R-04-185552. Office of Water. Washington D.C.

Environmental Protection Agency (2010). "Introduction to the Clean Water Act." United States Protection Agency: EPA-Office of Water. Washington D.C.

Environmental Protection Agency (2011), Office of Water. Washington D.C. Environmental Protection Agency. (2011). "Point Source." EPA 40 CFR 122.2.

Environmental Protection Agency (2014), Office of Water. Washington D.C. Environmental Protection Agency. (2014). “Best Management Practices.”

Environmental Protection Agency, (2014), Office of Water. Washington D.C. Environmental Protection Agency. (2014). “Water: Polluted Runoff.”

Environmental Protection Agency, (2015), Office of Water. Washington D.C. Environmental Protection Agency. (2015). “Water: Stormwater.”

Environmental Protection Agency. (2005). “National Management Measures to Control Nonpoint Source Pollution from Urban Areas.” EPA-841-B-05-004.

Environmental Protection Agency. (August 1999). “Preliminary Data Summary of Urban Stormwater Best Management Practices.” EPA-821-R-99-012. United States Protection Agency: EPA-Office of Water. Washington D.C.

Fassman, E.A. and Blackbourn, S. (2010). “Permeable Pavement Performance over 3 Years of Monitoring.” American Society of Civil Engineers Low Impact Development 2010: Redefining Water in the City. 152-165.

Grahl, N. A. (2012). “Hydraulic Design of Pervious Concrete Highway Shoulders.” http://gradworks.umi.com/15/40/1540649.html.

Hunt, III, W. (2010). “Working with Regulators to Change Permeable Pavements Acceptance.” American Society of Civil Engineers Low Impact Development 2010: Redefining Water in the City. 1270-1280.

Interlocking Concrete Pavement Institute (2014). “Design: Permeable Interlocking Concrete Pavers (PICP).” Retrieved from http://www.icpi.org/design.

Interlocking Concrete Pavement Institute. (2014). “Design.” Chantilly, VA. http://www.icpi.org/

Interlocking Concrete Pavement Institute. (2014). “Permeable Pavement Cross Section.” Chantilly, VA. http://www.icpi.org/node/2960

Interlocking Concrete Pavement Institute. (2014). “Tech Spec 18: Construction of Permeable Interlocking Concrete Pavement Systems.” Chantilly, VA.

Kevern, J., Haselbach, L., and Schaefer, V. (2012). “Hot Weather Comparative Heat Balances in Pervious Concrete and Impervious Concrete Pavement Systems." *Journal of Heat Island Institute International.* Vol 7. No. 2. 231-237.

Kim, J. Y., Slater, C., and Gil, G (2013).   “Investigation of Hydraulic Capacity and Water Quality Modification of Stormwater by Permeable Interlocking Concrete Pavement (PICP) System,” Florida Gulf Coast University, for Oldcastle Architectural, Inc. Atlanta GA.

Leipard, A.R., 2015, “Hydraulic Characterization of Permeable Interlocking Concrete Pavements”, Master’s Thesis, University of Missouri Kansas City, IMI# 1591071, 2015.

Li, H ; Harvey, J T ; Holland, T J ; and Kayhanian, M., (2013). "The Use of Reflective and Permeable Pavements as a Potential Practice for Heat Island Mitigation and Stormwater Management." *Environmental Research Letters*. Vol 8. No. 1. 1-14.

Lucke, T., and Beecham, S. (2011). “Field Investigation of Clogging in a Permeable Pavement System.” *Building Research and Information*, Vo. 39. No. 6. 603-615.

McCain, G. and Dewoolkar, M. (2010). “Porous Concrete Pavements: Mechanical and Hydraulic Properties.” Transportation Research Record: Journal of the Transportation Research Board, Vol 2164. No. 1. 66-75.

McCall III, D.K., (2014). “Clean Water Act”. Environmental Law Handbook. 22nd Edition, 329-394.

Mullaney, J. and Lucke, T. (December 2013). “Practical Review of Pervious Pavement Designs.” CLEAN- Soil, Air, and Water. 42,2. 111—124.

National Oceanic and Atmospheric Association’s National Weather Service. (2014). “Hydrometerological Design Studies Center Precipitation Frequency Data Server PFDAS)” Silver Spring, MD. http://hdsc.nws.noaa.gov/hdsc/pfds/

Ostercamp, W.R., Heilman, P., and LaneI.J., (1998). “Economic Considerations of Continental Sediment-Monitoring Program.” International Journal of Sediment Research, Vol 13. No 4. 12-24.

Richardson, J. (1989). "The Effects of Moving Precipitation Fields on Overland Flow Using One-Dimensional Finite Elements.” Dissertation, Colorado State University.

Roseen, R., Ballestero, T., Houle, J., Briggs, J., and Houle, K. (2012). "Water Quality and Hydrologic Performance of a Porous Asphalt Pavement as a Storm-Water Treatment Strategy in a Cold Climate." J. Environ. Eng., 10.1061/(ASCE)EE.1943-7870.0000459, 81-89.

Rutgers, the State University of New Jersey. (2015). “Rain Barrels.” http://water.rutgers.edu/Stormwater_Management/rainbarrels.html

Schotzl, M. Grabowiecki, P. (2007). “Review of Permeable Pavement Systems.” Science Direct: Building and Environment. Vol 42. No. 11. 3830-3836.

Smith, D.R. and Hunt, III, W. (2010). “Structural/Hydrologic Design and Maintenance of Permeable Interlocking Concrete Pavers.” American Society of Civil Engineers Low Impact Development 2010: Redefining Water in the City. 360-377.

State University of New York College of Environmental Science and Forestry. (SUNY-ESF). (2015). “Rain Gardens.” http://www.esf.edu/ere/endreny/GICalculator/RainGardenIntro.html

Stochl, M.R.,2015, “Hydraulic Design of Interlocking Permeable Concrete Pavers”, Master’s Thesis, University of Missouri Kansas City, IMI# 1598478, 2015.

United States Department of Agriculture’s Natural Resource Conservations, (1986). Urban Hydrology for Small Watershed Technical Release-55. Washington, DC. ftp://ftp.wcc.nrcs.usda.gov/downloads/hydrology_hydraulics/tr55/tr55.pdf (1986).

Virginia DCR Stormwater Design Specification No. 7: Permeable Pavement Version 1.7. 2010.

White, S. S., and Boswell, M. R. (2007.) “Stormwater Quality and Local Government Innovation.” Journal of the American Planning Association 73, 2: 185-193.

APPENDIX A – TESTING RESULTS

1. Results of Hydraulic testing-All Tests

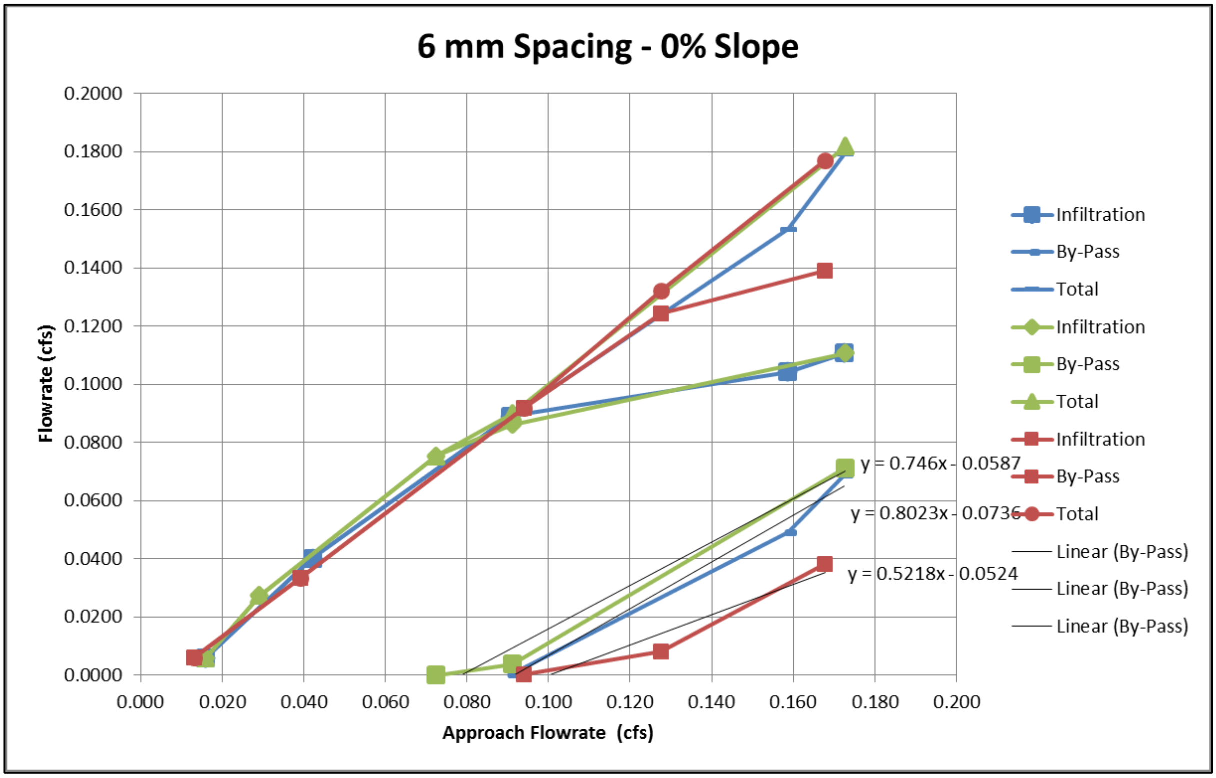

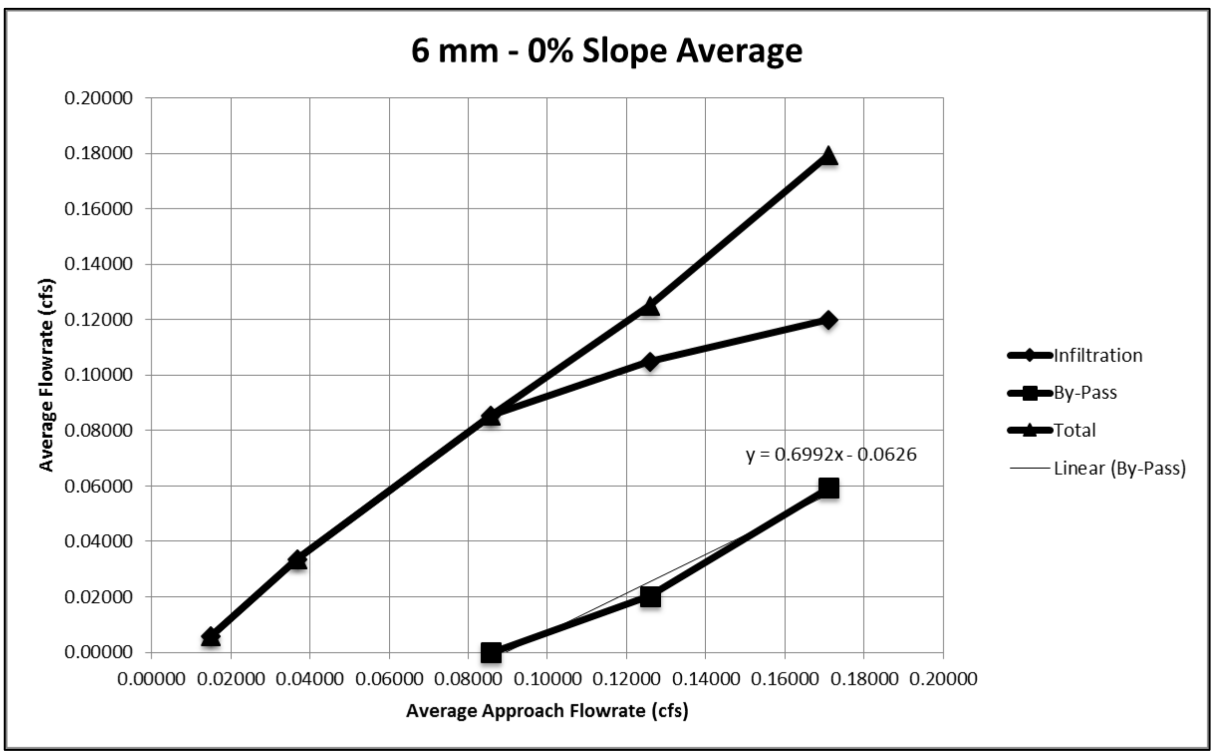

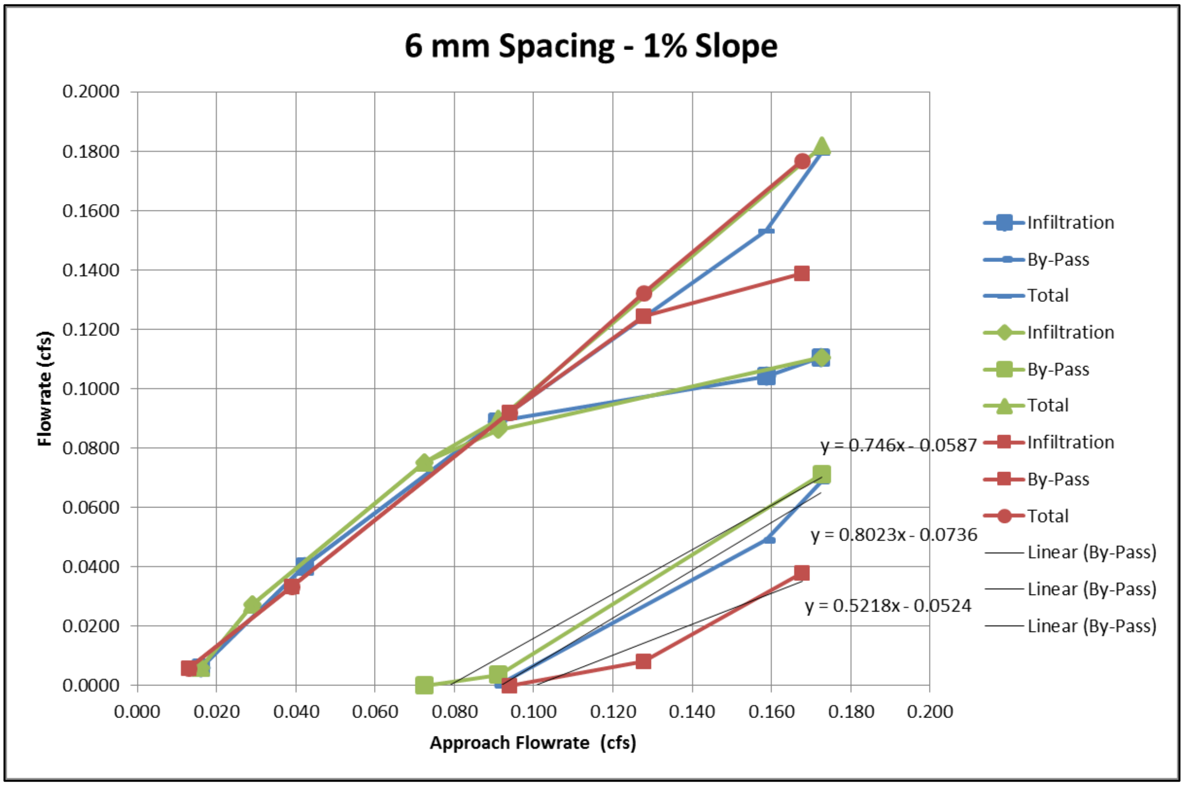
6 mm Spacing - 1% Slope
Flowrate (cfs)
Approach Flowrate (cfs)
y = 0.746x - 0.0587
y = 0.8023x - 0.0736
y = 0.5218x - 0.0524
Infiltration
By-Pass
Total
Infiltration
By-Pass
Total
Infiltration
By-Pass
Total
Linear (By-Pass)
Linear (By-Pass)
Linear (By-Pass)

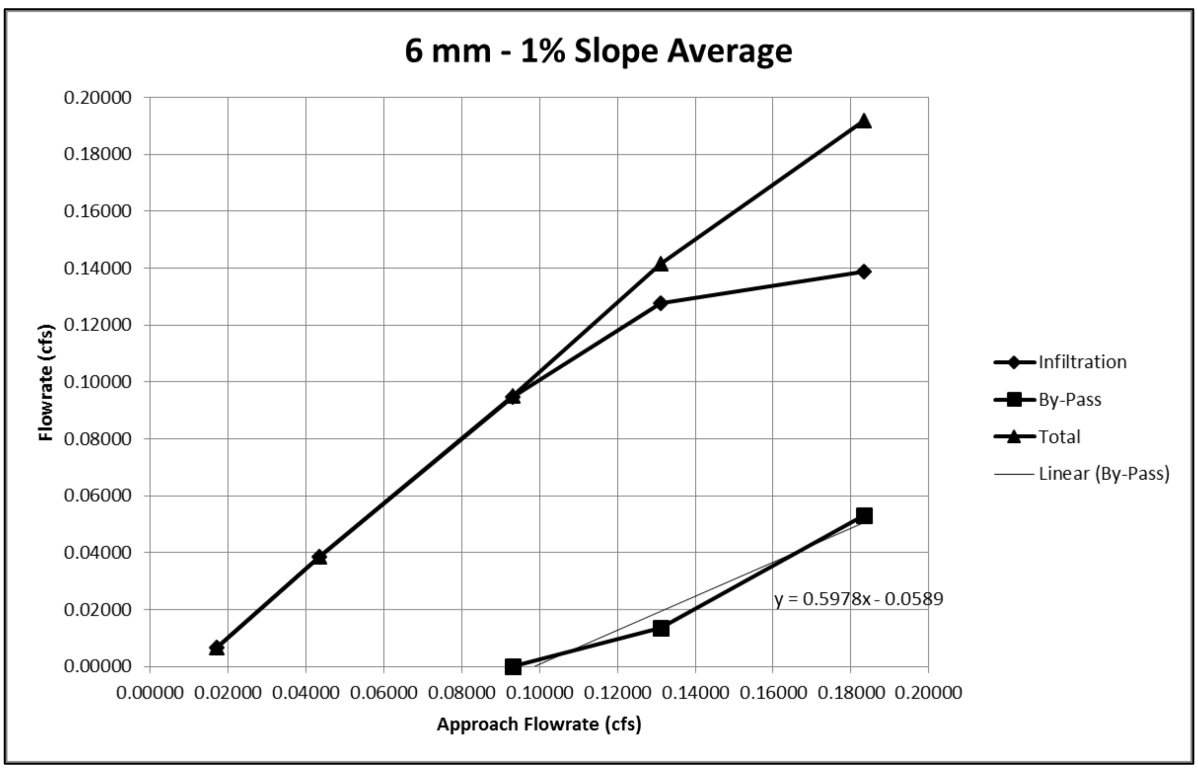
6 mm - 1% Slope Average
Flowrate (cfs)
Approach Flowrate (cfs)
y = 0.5978x - 0.0589
Infiltration
By-Pass
Total
Linear (By-Pass)

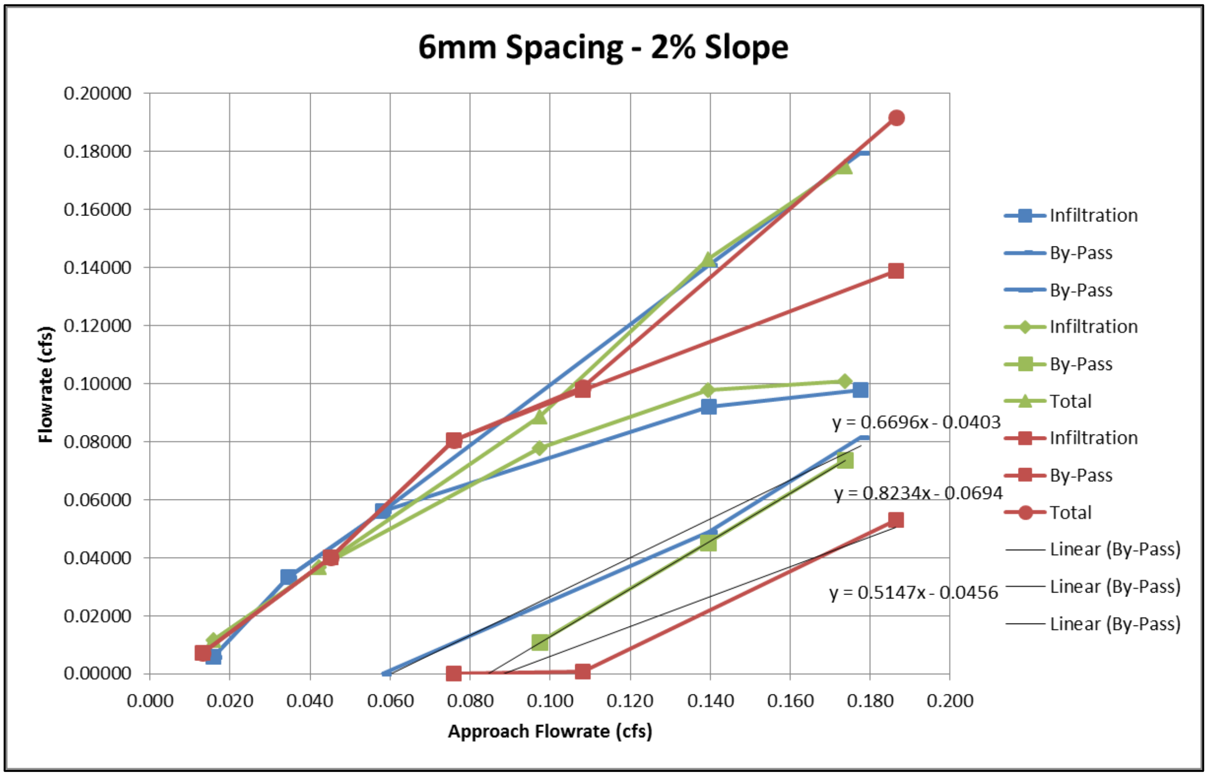

6mm Spacing - 2% Slope
Flowrate (cfs)
Approach Flowrate (cfs)
0.20000
0.18000
0.16000
0.14000
0.12000
0.10000
0.08000
0.06000
0.04000
0.02000
0.00000
0.000
0.020
0.040
0.060
0.080
0.100
0.120
0.140
0.160
0.180
0.200
y = 0.6696x - 0.0403
y = 0.8234x - 0.0694
y = 0.5147x - 0.0456
Infiltration
By-Pass
By-Pass
Infiltration
By-Pass
Total
Infiltration
By-Pass
Total
Linear (By-Pass)
Linear (By-Pass)
Linear (By-Pass)

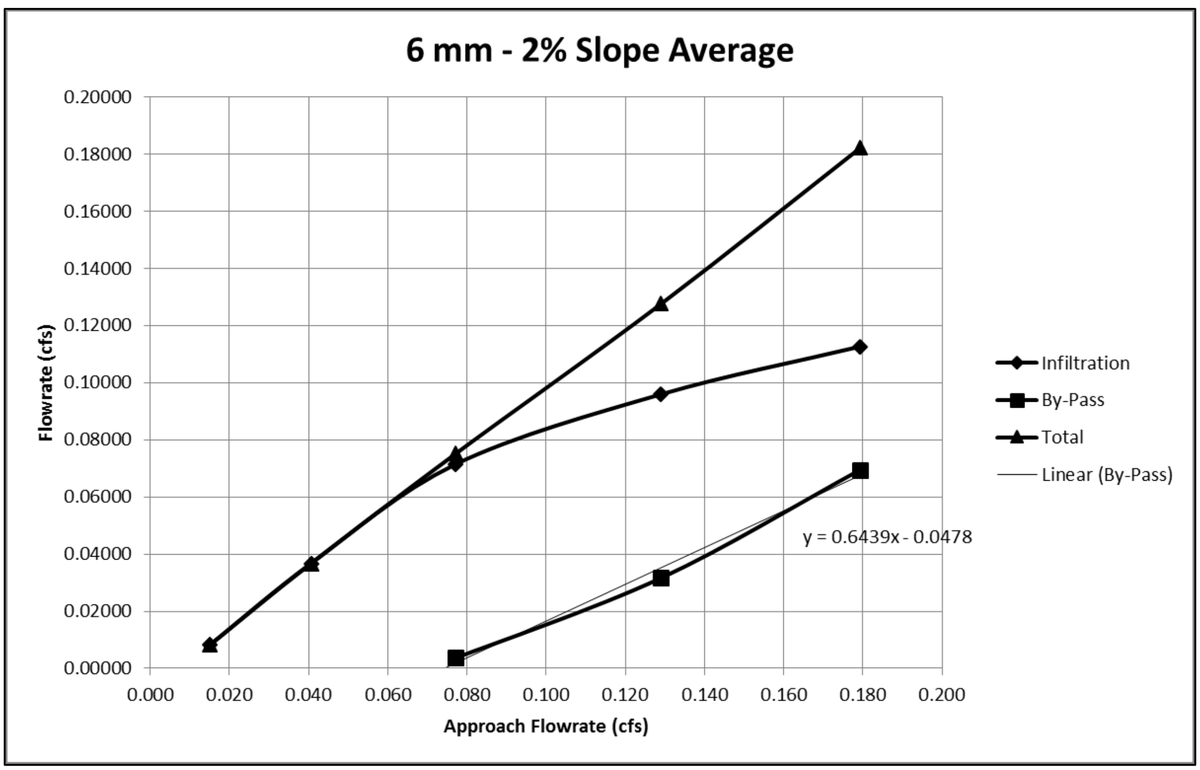

6 mm - 2% Slope Average
Flowrate (cfs)
Approach Flowrate (cfs)
0.20000
0.18000
0.16000
0.14000
0.12000
0.10000
0.08000
0.06000
0.04000
0.02000
0.00000
0.000
0.020
0.040
0.060
0.080
0.100
0.120
0.140
0.160
0.180
0.200
y = 0.6439x - 0.0478
Infiltration
By-Pass
Total
Linear (By-Pass)

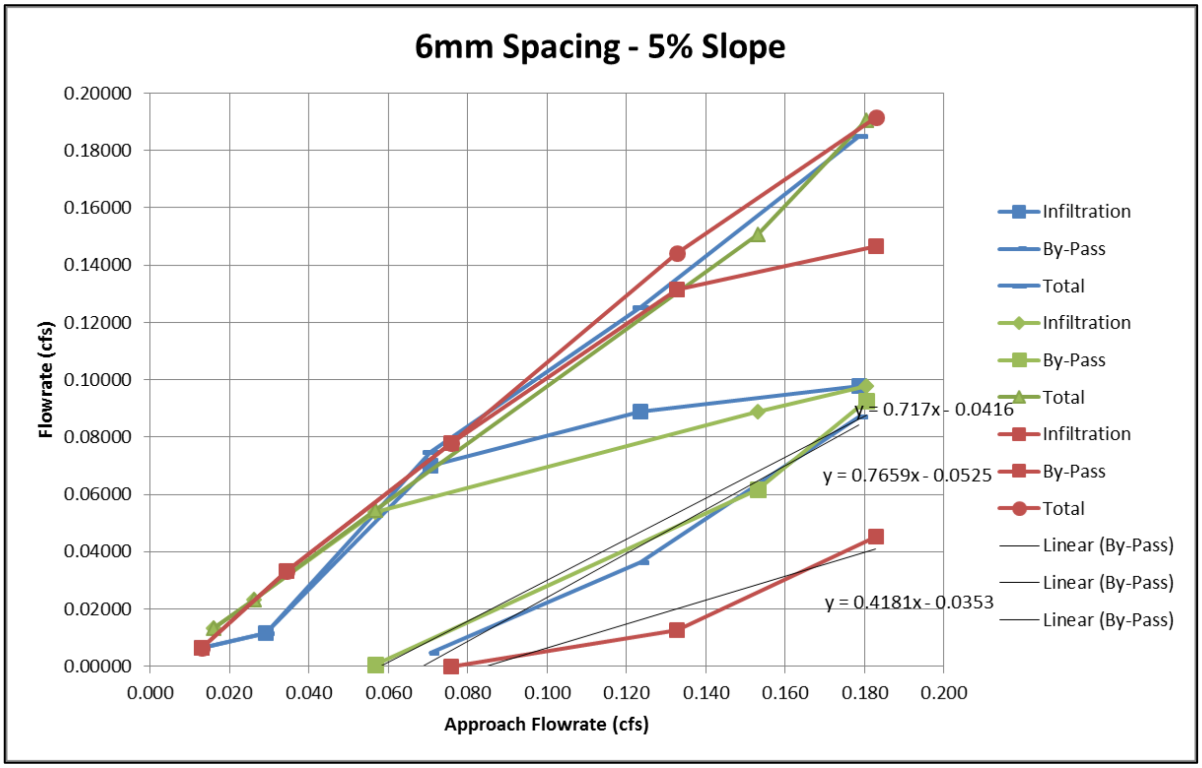
6mm Spacing - 5% Slope
Flowrate (cfs)
Approach Flowrate (cfs)
0.20000
0.18000
0.16000
0.14000
0.12000
0.10000
0.08000
0.06000
0.04000
0.02000
0.00000
0.000
0.020
0.040
0.060
0.080
0.100
0.120
0.140
0.160
0.180
0.200
Infiltration
By-Pass
Total
Infiltration
By-Pass
Total
Infiltration
By-Pass
Total
Linear (By-Pass)
Linear (By-Pass)
Linear (By-Pass)
y = 0.717x - 0.0416
y = 0.7659x - 0.0525
y = 0.4181x - 0.0353

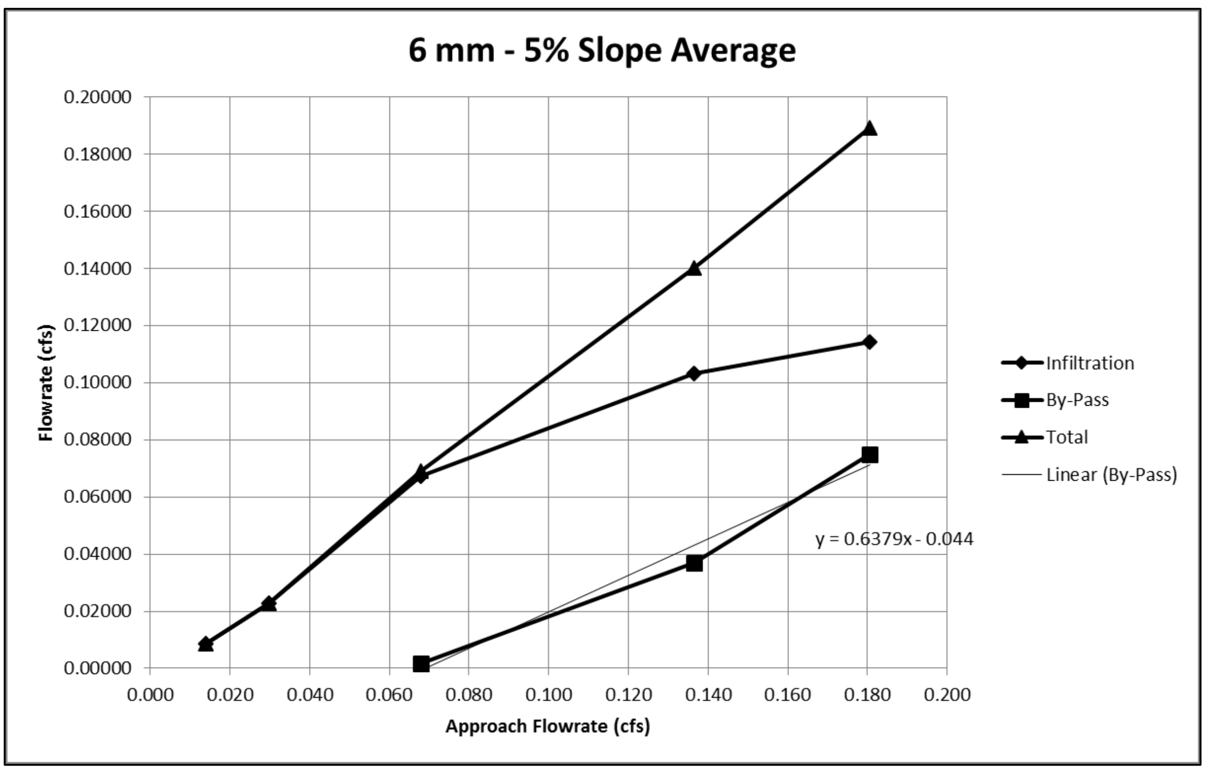
6 mm - 5% Slope Average
Flowrate (cfs)
Approach Flowrate (cfs)
0.20000
0.18000
0.16000
0.14000
0.12000
0.10000
0.08000
0.06000
0.04000
0.02000
0.00000
0.000
0.020
0.040
0.060
0.080
0.100
0.120
0.140
0.160
0.180
0.200
Infiltration
By-Pass
Total
Linear (By-Pass)
y = 0.6379x - 0.044

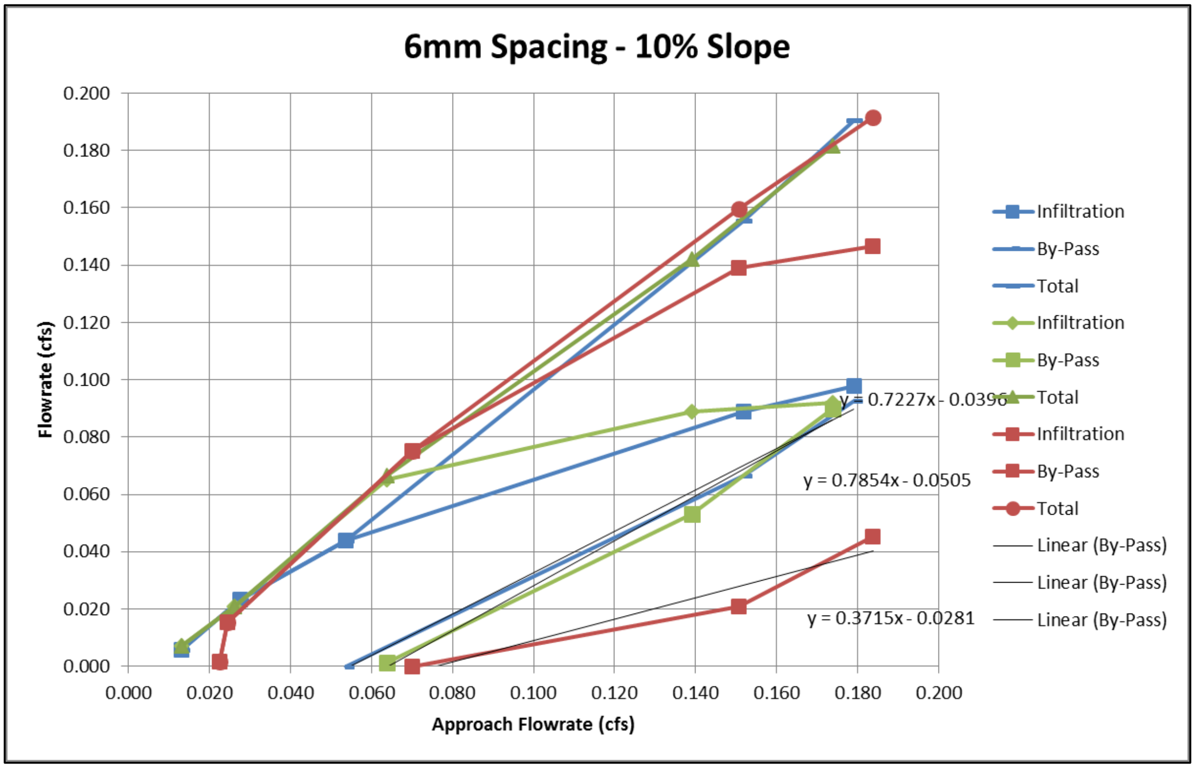
6mm Spacing - 10% Slope
Flowrate (cfs)
Approach Flowrate (cfs)
0.200
0.180
0.160
0.140
0.120
0.100
0.080
0.060
0.040
0.020
0.000
0.000
0.020
0.040
0.060
0.080
0.100
0.120
0.140
0.160
0.180
0.200
y = 0.7227x - 0.0396
y = 0.7854x - 0.0505
y = 0.3715x - 0.0281
Infiltration
By-Pass
Total
Infiltration
By-Pass
Total
Infiltration
By-Pass
Total
Linear (By-Pass)
Linear (By-Pass)
Linear (By-Pass)

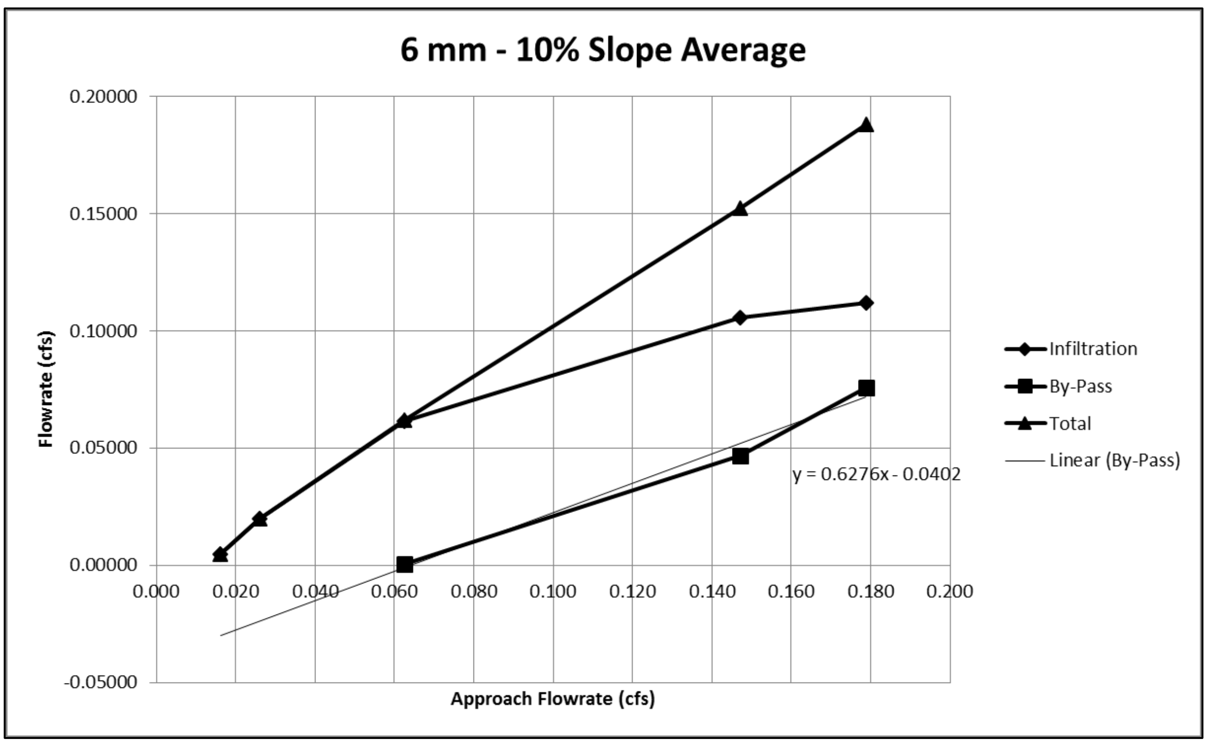
6 mm - 10% Slope Average
Flowrate (cfs)
Approach Flowrate (cfs)
0.20000
0.15000
0.10000
0.05000
0.00000
-0.05000
0.000
0.020
0.040
0.060
0.080
0.100
0.120
0.140
0.160
0.180
0.200
y = 0.6276x - 0.0402
Infiltration
By-Pass
Total
Linear (By-Pass)

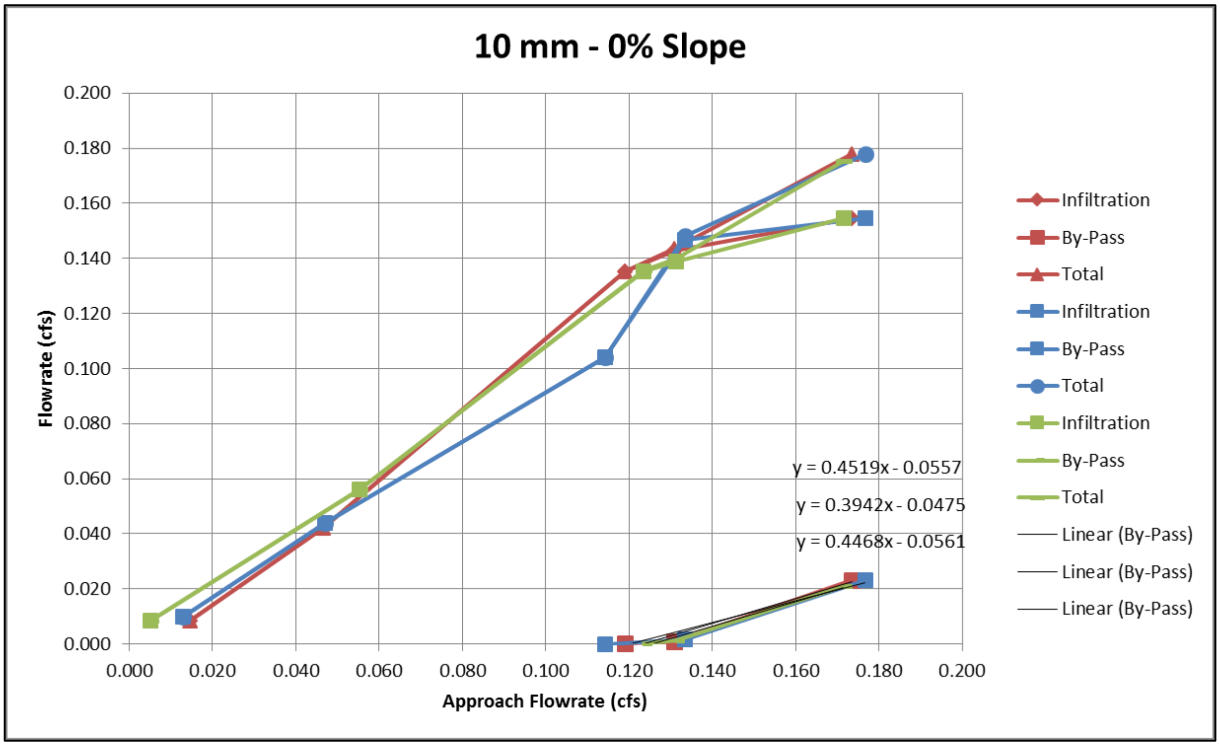

10 mm - 0% Slope
Flowrate (cfs)
Approach Flowrate (cfs)
0.000
0.020
0.040
0.060
0.080
0.100
0.120
0.140
0.160
0.180
0.200
y = 0.4519x - 0.0557
y = 0.3942x - 0.0475
y = 0.4468x - 0.0561
Infiltration
By-Pass
Total
Infiltration
By-Pass
Total
Infiltration
By-Pass
Total
Linear (By-Pass)
Linear (By-Pass)
Linear (By-Pass)

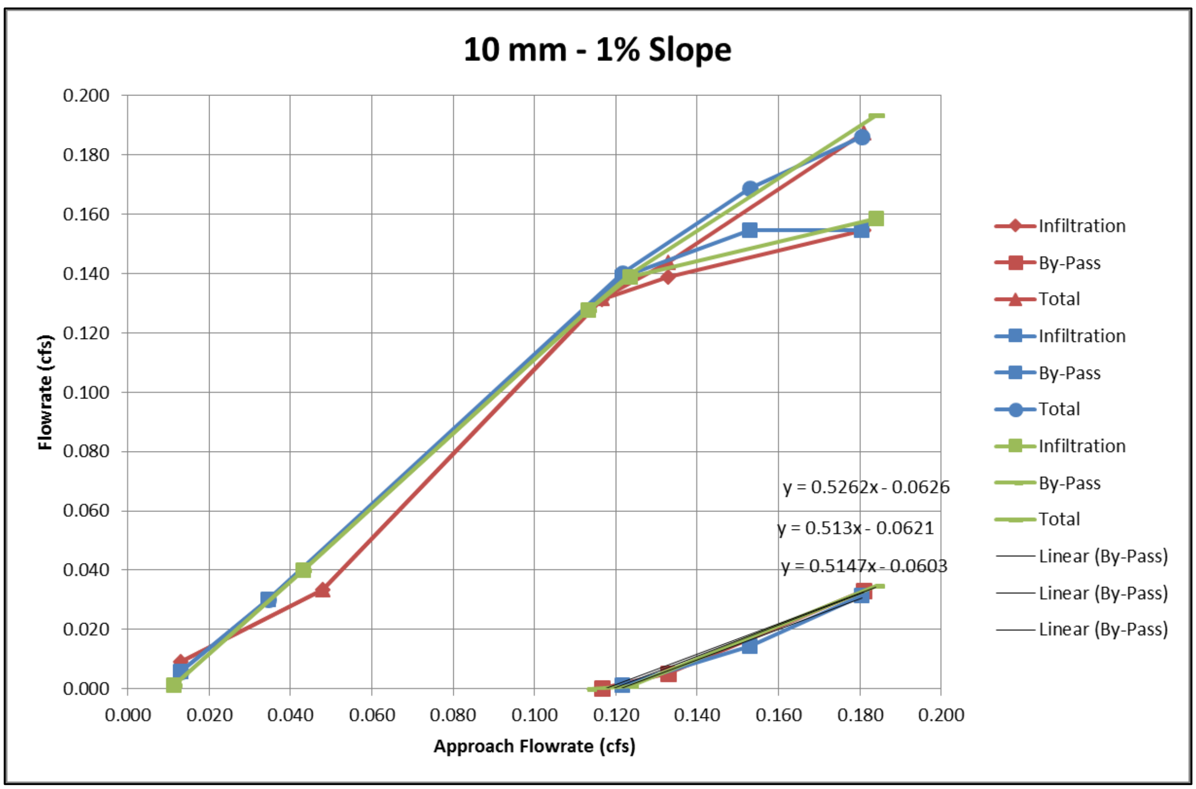

10 mm - 1% Slope
Flowrate (cfs)
Approach Flowrate (cfs)
0.000
0.020
0.040
0.060
0.080
0.100
0.120
0.140
0.160
0.180
0.200
y = 0.5262x - 0.0626
y = 0.513x - 0.0621
y = 0.5147x - 0.0603
Infiltration
By-Pass
Total
Infiltration
By-Pass
Total
Infiltration
By-Pass
Total
Linear (By-Pass)
Linear (By-Pass)
Linear (By-Pass)

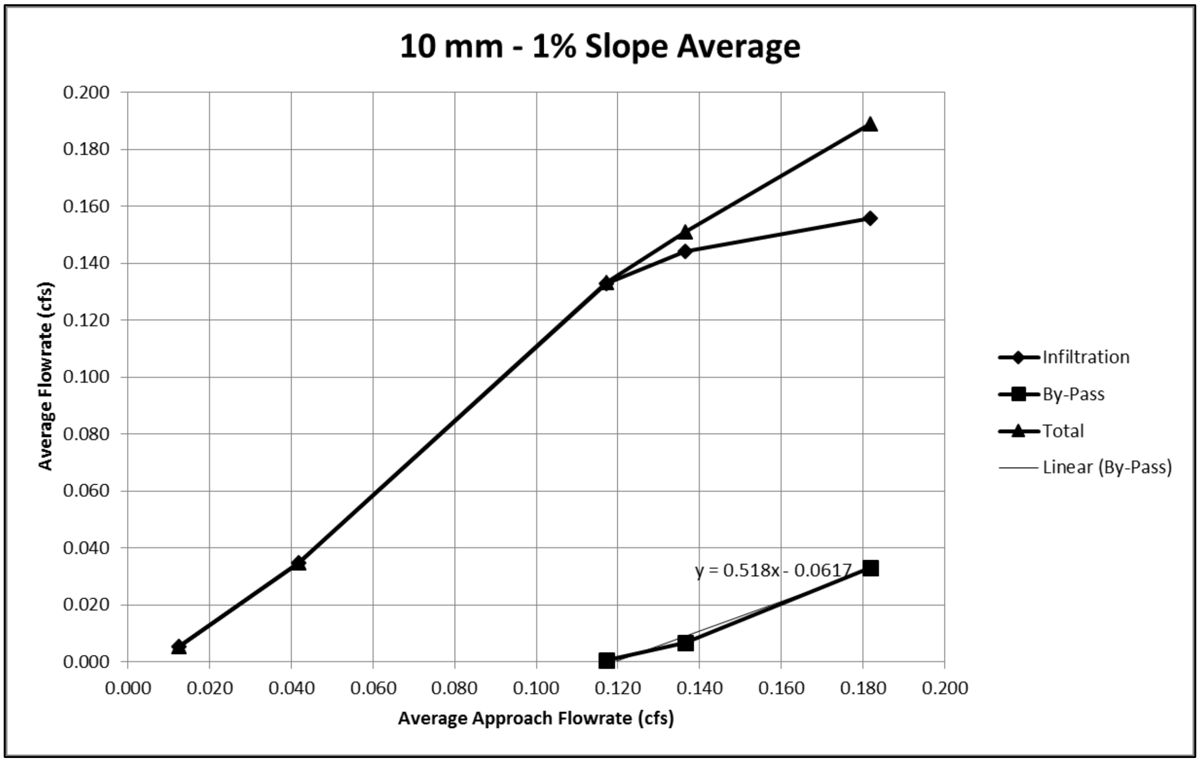

10 mm - 1% Slope Average
Average Flowrate (cfs)
Average Approach Flowrate (cfs)
0.000
0.020
0.040
0.060
0.080
0.100
0.120
0.140
0.160
0.180
0.200
Infiltration
By-Pass
Total
Linear (By-Pass)
y = 0.518x - 0.0617

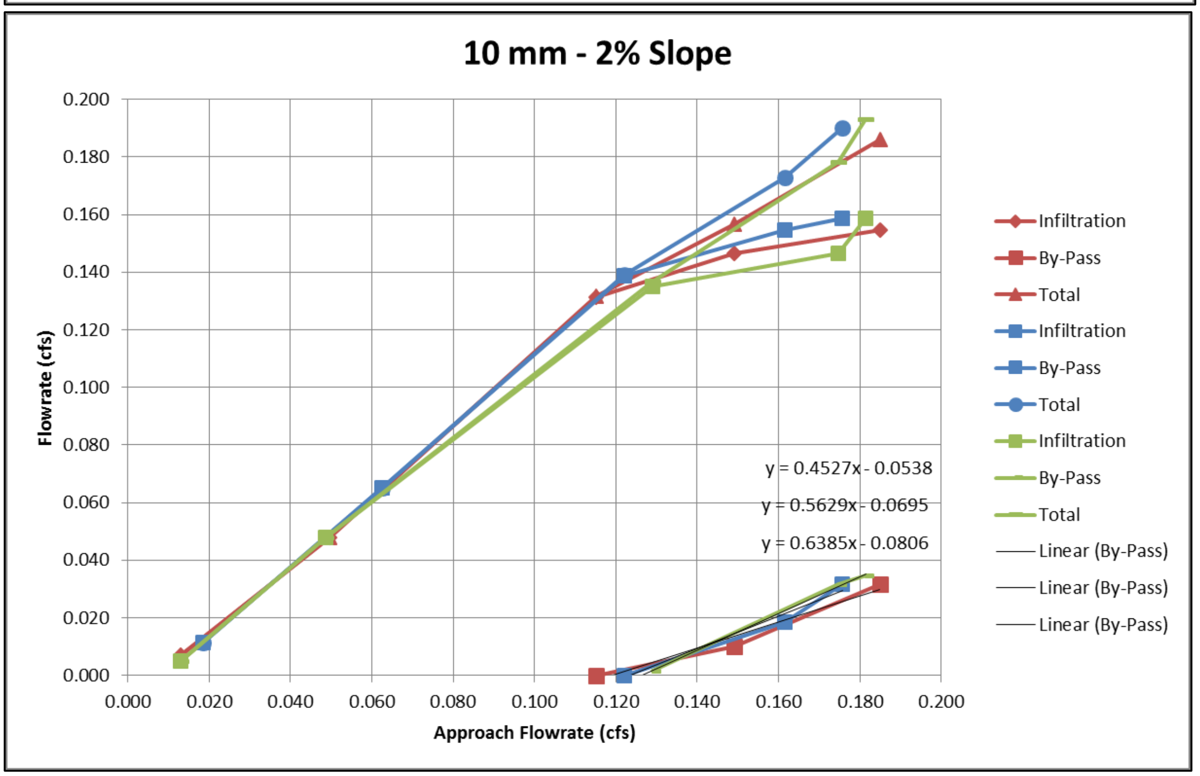

10 mm - 2% Slope
Flowrate (cfs)
Approach Flowrate (cfs)
0.000
0.020
0.040
0.060
0.080
0.100
0.120
0.140
0.160
0.180
0.200
Infiltration
By-Pass
Total
Infiltration
By-Pass
Total
Infiltration
By-Pass
Total
Linear (By-Pass)
Linear (By-Pass)
Linear (By-Pass)
y = 0.4527x - 0.0538
y = 0.5629x - 0.0695
y = 0.6385x - 0.0806

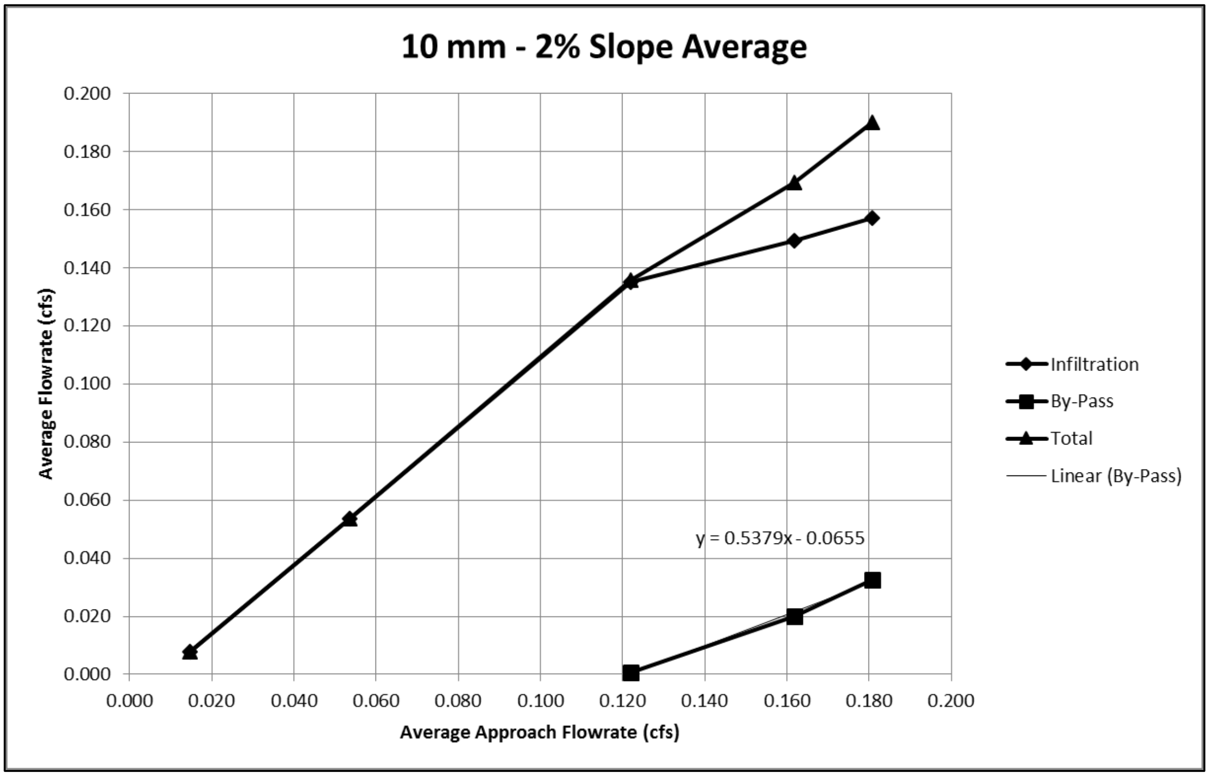
10 mm - 2% Slope Average
Average Flowrate (cfs)
0.200
0.180
0.160
0.140
0.120
0.100
0.080
0.060
0.040
0.020
0.000
0.000 0.020 0.040 0.060 0.080 0.100 0.120 0.140 0.160 0.180 0.200
Average Approach Flowrate (cfs)
y = 0.5379x - 0.0655
Infiltration
By-Pass
Total
Linear (By-Pass)

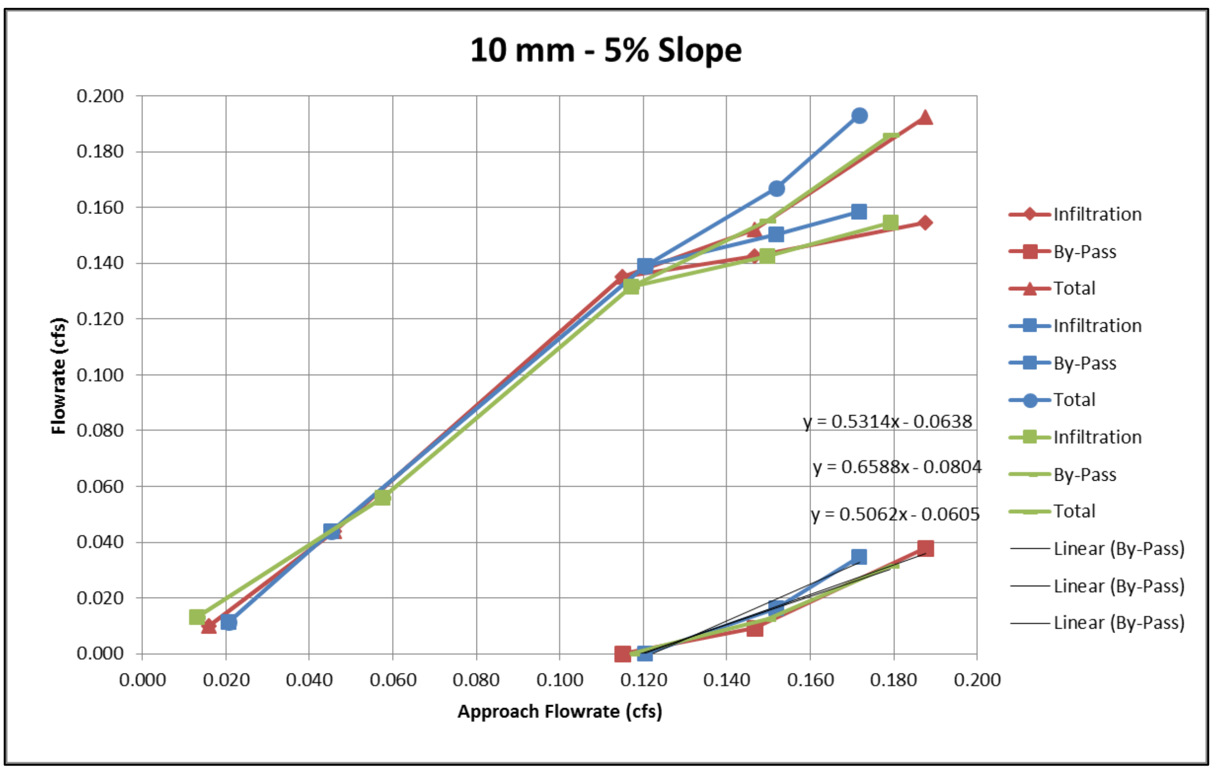
10 mm - 5% Slope
Flowrate (cfs)
0.200
0.180
0.160
0.140
0.120
0.100
0.080
0.060
0.040
0.020
0.000
0.000 0.020 0.040 0.060 0.080 0.100 0.120 0.140 0.160 0.180 0.200
Approach Flowrate (cfs)
y = 0.5314x - 0.0638
y = 0.6588x - 0.0804
y = 0.5062x - 0.0605
Infiltration
By-Pass
Total
Infiltration
By-Pass
Total
Infiltration
By-Pass
Total
Linear (By-Pass)
Linear (By-Pass)
Linear (By-Pass)

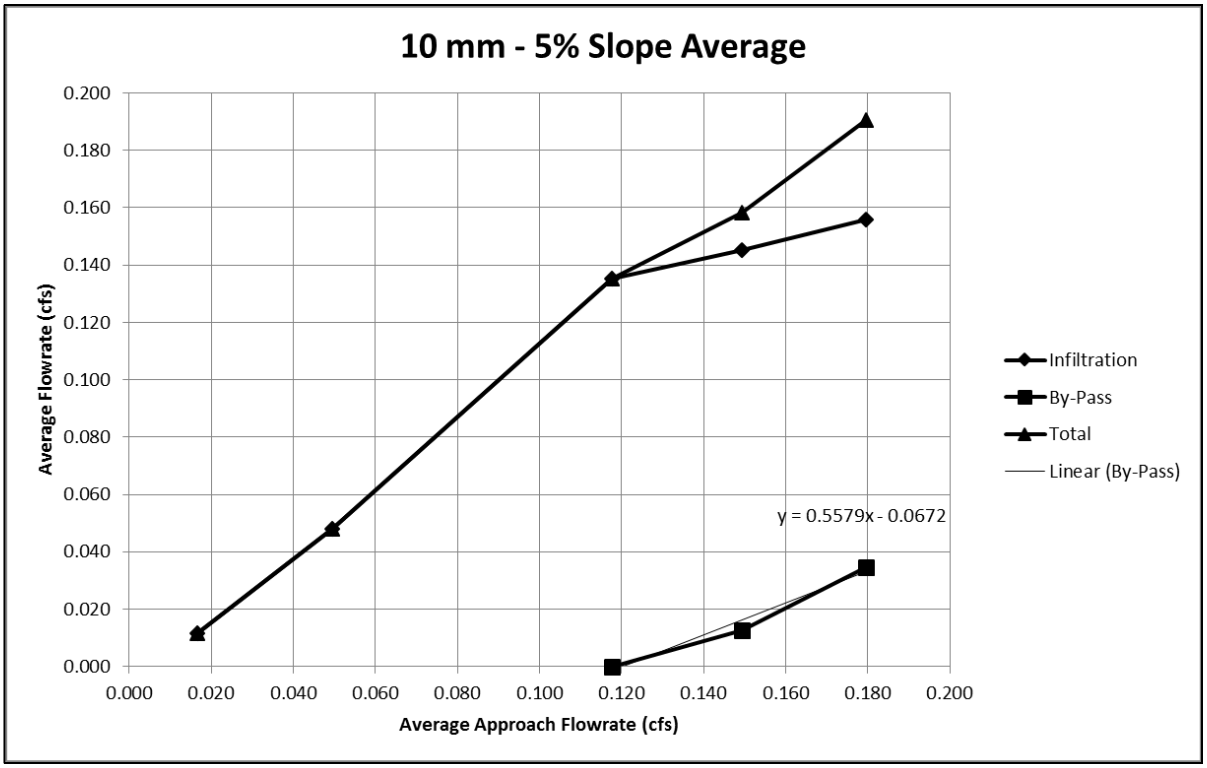
10 mm - 5% Slope Average
Average Flowrate (cfs)
Average Approach Flowrate (cfs)
0.000
0.020
0.040
0.060
0.080
0.100
0.120
0.140
0.160
0.180
0.200
Infiltration
By-Pass
Total
Linear (By-Pass)
y = 0.5579x - 0.0672

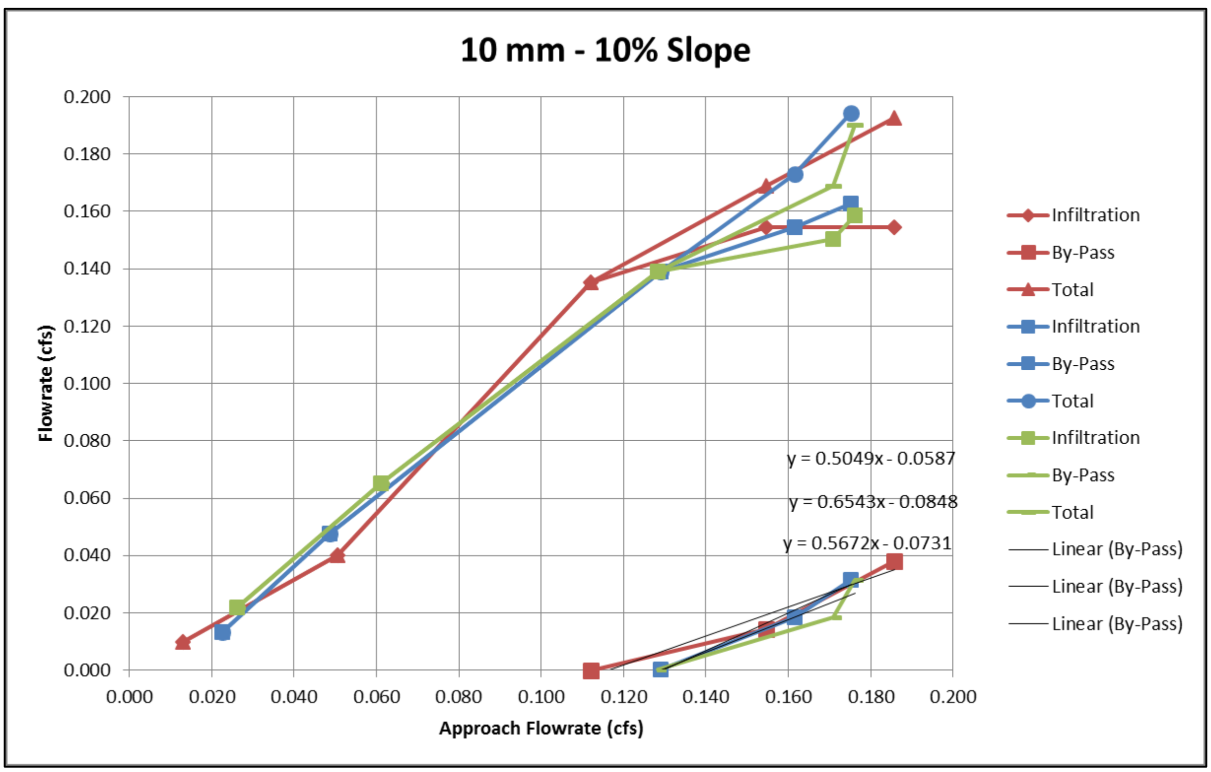
10 mm - 10% Slope
Flowrate (cfs)
Approach Flowrate (cfs)
0.000
0.020
0.040
0.060
0.080
0.100
0.120
0.140
0.160
0.180
0.200
Infiltration
By-Pass
Total
Infiltration
By-Pass
Total
Infiltration
By-Pass
Total
Linear (By-Pass)
Linear (By-Pass)
Linear (By-Pass)
y = 0.5049x - 0.0587
y = 0.6543x - 0.0848
y = 0.5672x - 0.0731

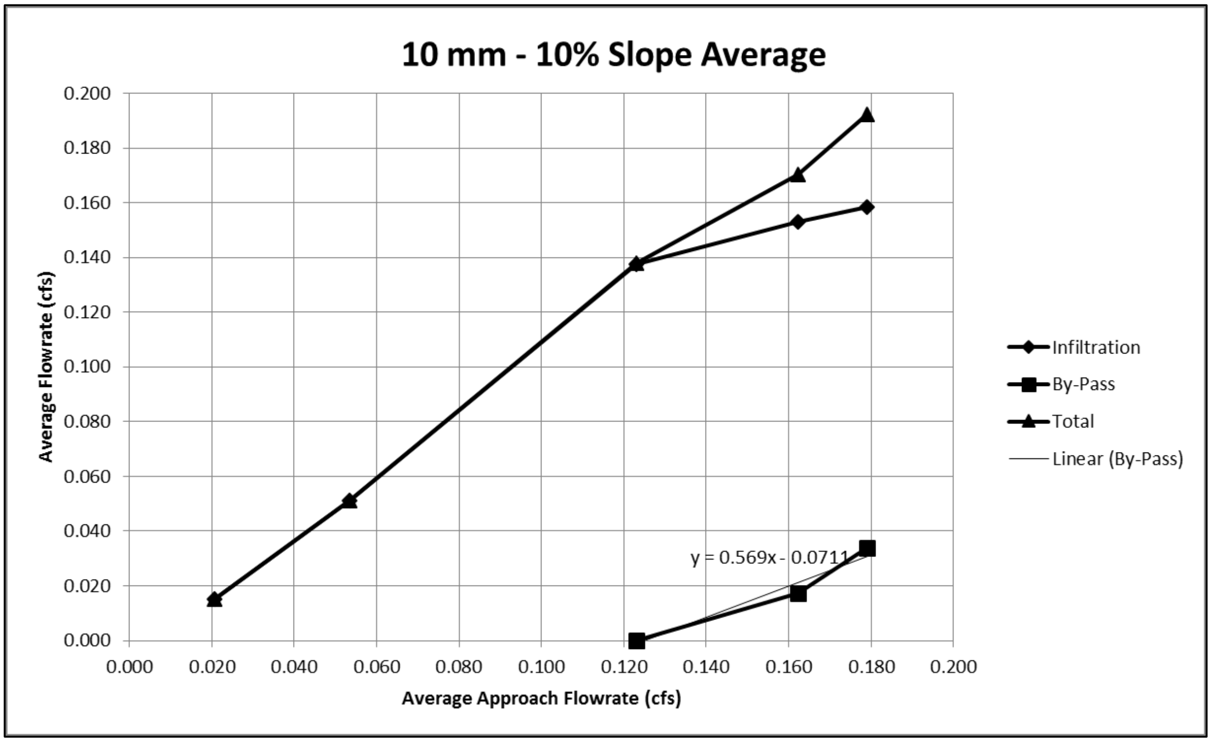
10 mm - 10% Slope Average
Average Flowrate (cfs)
Average Approach Flowrate (cfs)
0.000
0.020
0.040
0.060
0.080
0.100
0.120
0.140
0.160
0.180
0.200
y = 0.569x - 0.0711
Infiltration
By-Pass
Total
Linear (By-Pass)

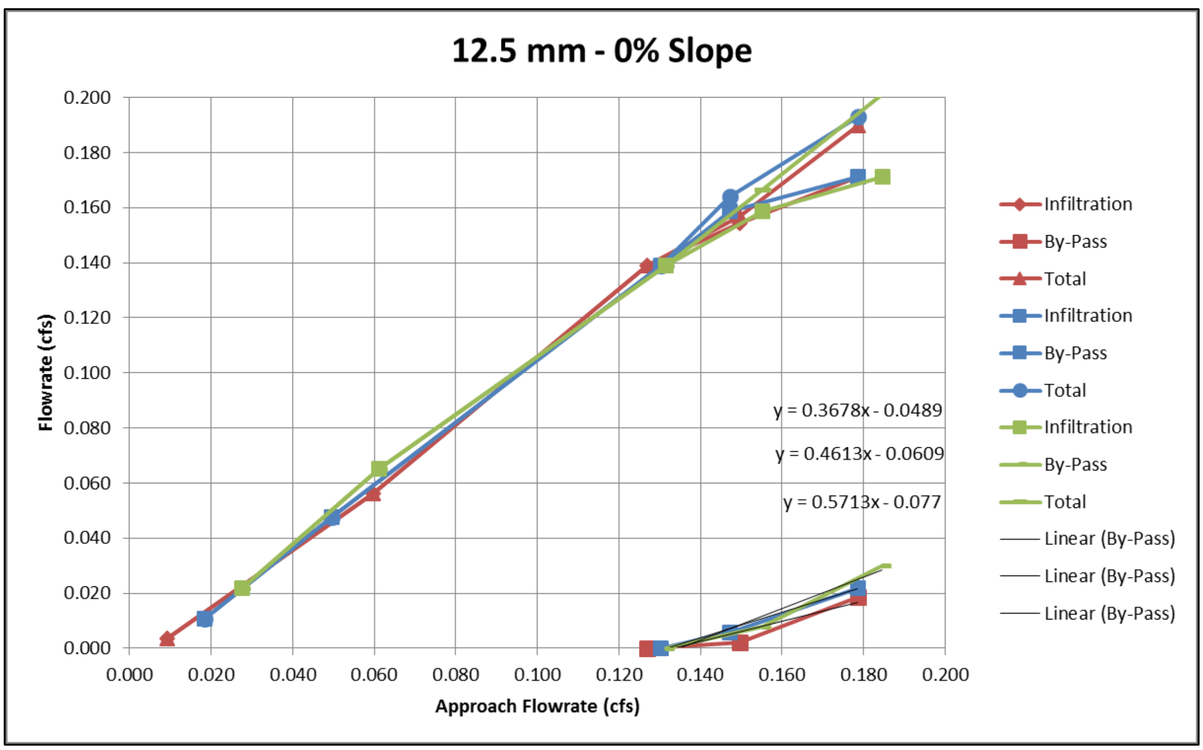
12.5 mm - 0% Slope
Flowrate (cfs)
Approach Flowrate (cfs)
0.000
0.020
0.040
0.060
0.080
0.100
0.120
0.140
0.160
0.180
0.200
y = 0.3678x - 0.0489
y = 0.4613x - 0.0609
y = 0.5713x - 0.077
Infiltration
By-Pass
Total
Infiltration
By-Pass
Total
Infiltration
By-Pass
Total
Linear (By-Pass)
Linear (By-Pass)
Linear (By-Pass)

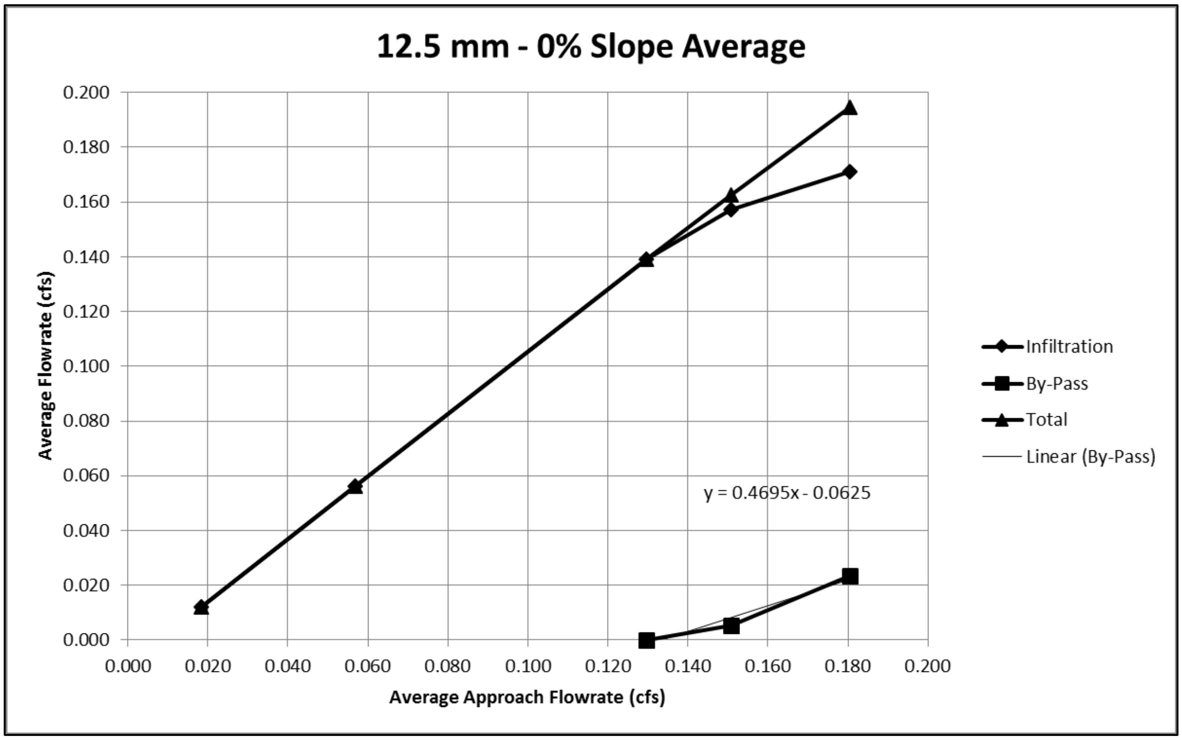
12.5 mm - 0% Slope Average
Average Flowrate (cfs)
0.200
0.180
0.160
0.140
0.120
0.100
0.080
0.060
0.040
0.020
0.000
0.000
0.020
0.040
0.060
0.080
0.100
0.120
0.140
0.160
0.180
0.200
Average Approach Flowrate (cfs)
y = 0.4695x - 0.0625
Infiltration
By-Pass
Total
Linear (By-Pass)

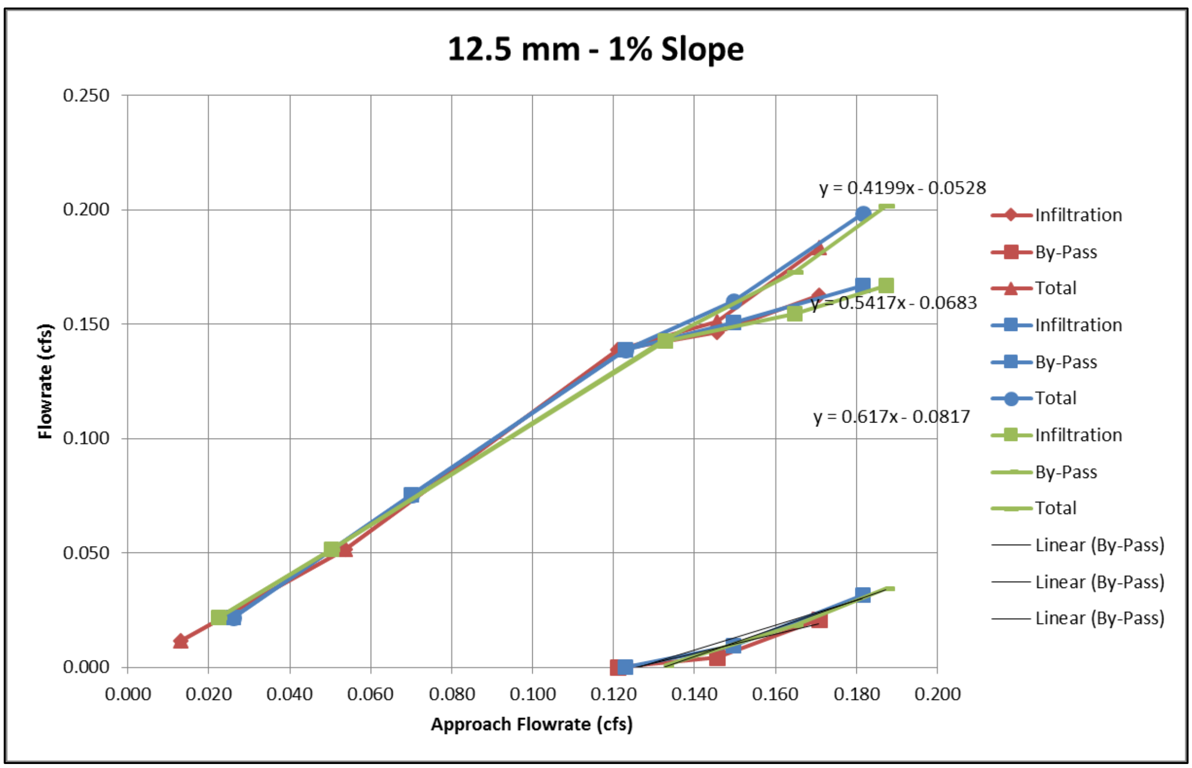
12.5 mm - 1% Slope
Flowrate (cfs)
0.250
0.200
0.150
0.100
0.050
0.000
0.000
0.020
0.040
0.060
0.080
0.100
0.120
0.140
0.160
0.180
0.200
Approach Flowrate (cfs)
y = 0.4199x - 0.0528
y = 0.5417x - 0.0683
y = 0.617x - 0.0817
Infiltration
By-Pass
Total
Infiltration
By-Pass
Total
Infiltration
By-Pass
Total
Linear (By-Pass)
Linear (By-Pass)
Linear (By-Pass)

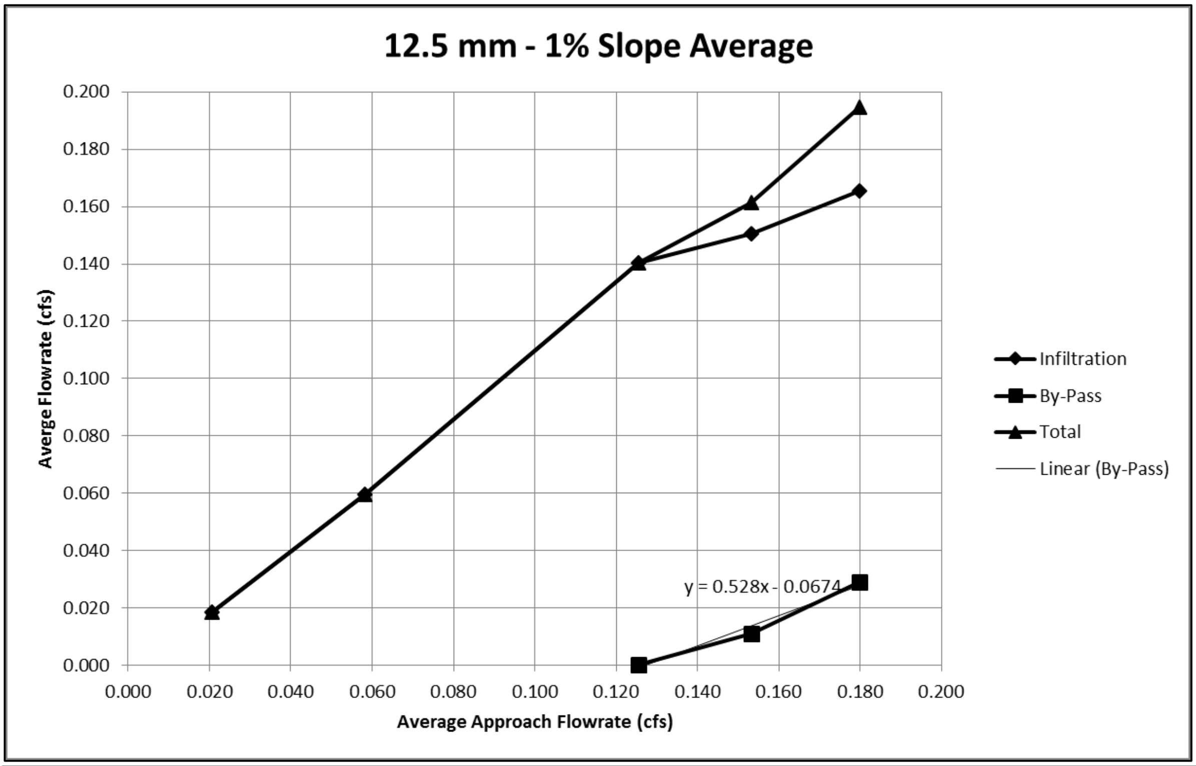
12.5 mm - 1% Slope Average
Averge Flowrate (cfs)
Average Approach Flowrate (cfs)
0.000
0.020
0.040
0.060
0.080
0.100
0.120
0.140
0.160
0.180
0.200
y = 0.528x - 0.0674
Infiltration
By-Pass
Total
Linear (By-Pass)

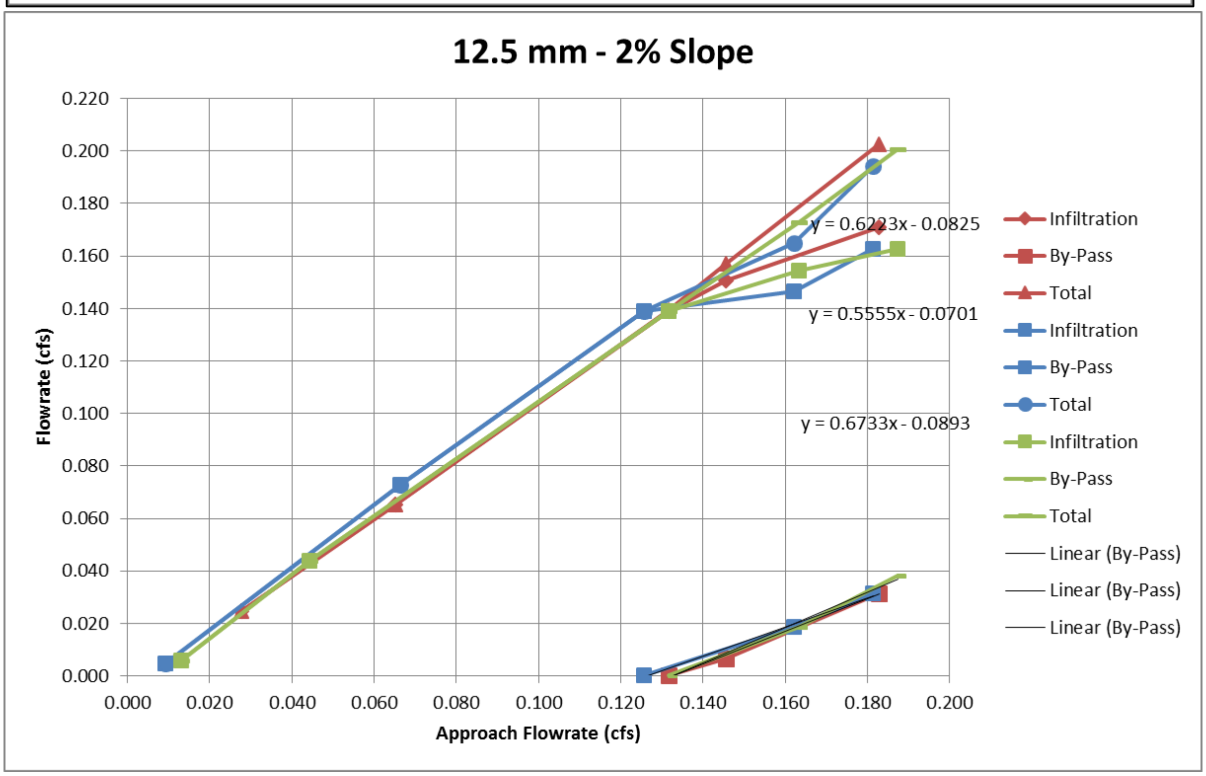
12.5 mm - 2% Slope
Flowrate (cfs)
Approach Flowrate (cfs)
0.000
0.020
0.040
0.060
0.080
0.100
0.120
0.140
0.160
0.180
0.200
0.220
y = 0.6223x - 0.0825
y = 0.5555x - 0.0701
y = 0.6733x - 0.0893
Infiltration
By-Pass
Total
Infiltration
By-Pass
Total
Infiltration
By-Pass
Total
Linear (By-Pass)
Linear (By-Pass)
Linear (By-Pass)

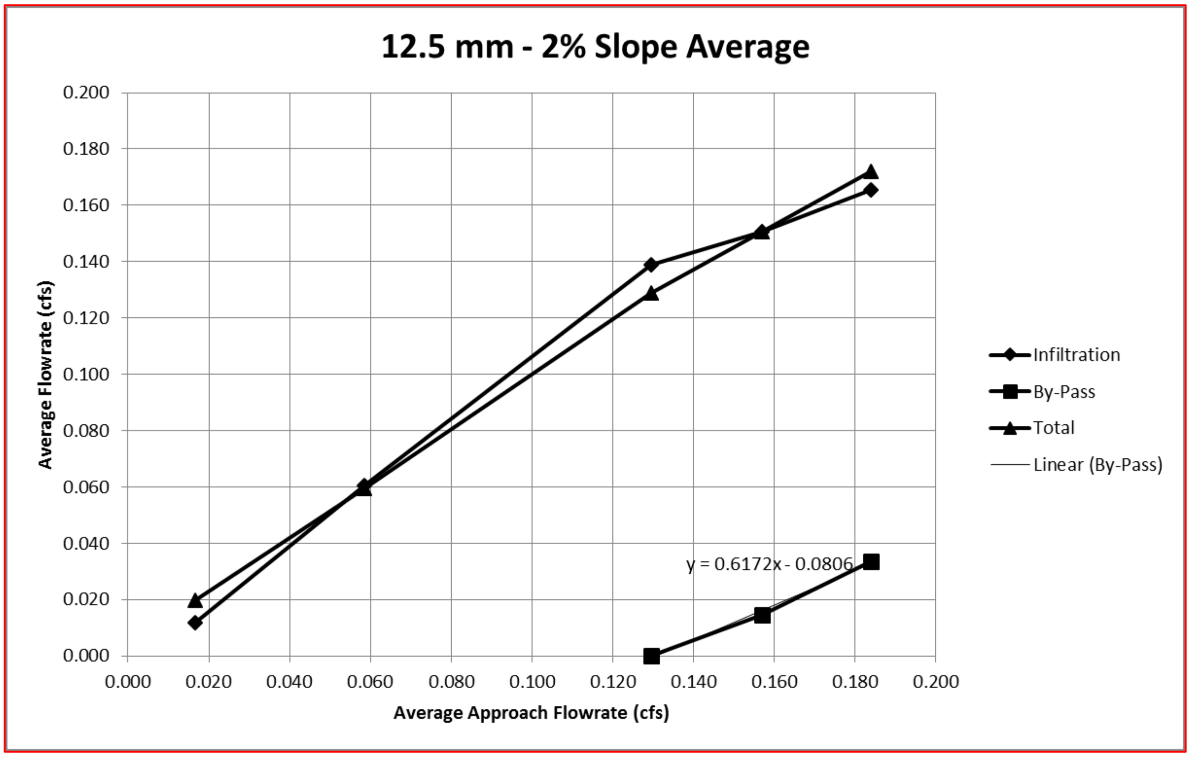

12.5 mm - 2% Slope Average
Average Flowrate (cfs)
Average Approach Flowrate (cfs)
0.000
0.020
0.040
0.060
0.080
0.100
0.120
0.140
0.160
0.180
0.200
y = 0.6172x - 0.0806
Infiltration
By-Pass
Total
Linear (By-Pass)

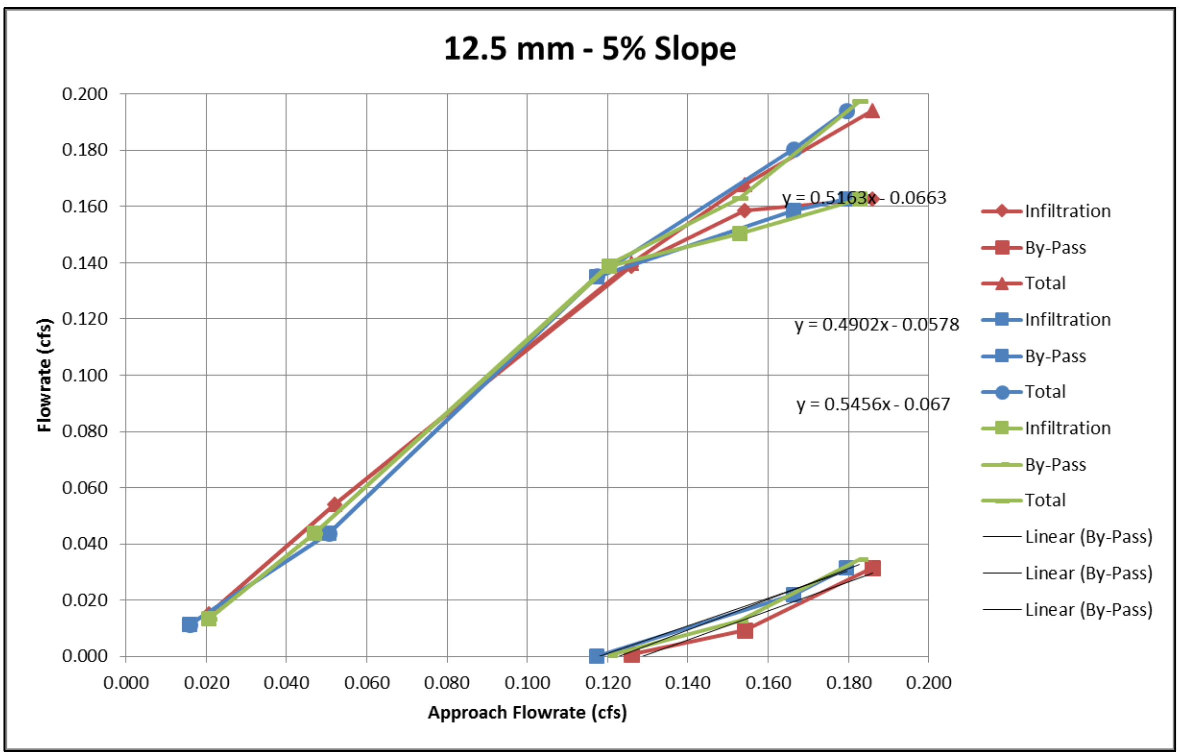

12.5 mm - 5% Slope
Flowrate (cfs)
Approach Flowrate (cfs)
0.000
0.020
0.040
0.060
0.080
0.100
0.120
0.140
0.160
0.180
0.200
y = 0.5163x - 0.0663
y = 0.4902x - 0.0578
y = 0.5456x - 0.067
Infiltration
By-Pass
Total
Infiltration
By-Pass
Total
Infiltration
By-Pass
Total
Linear (By-Pass)
Linear (By-Pass)
Linear (By-Pass)

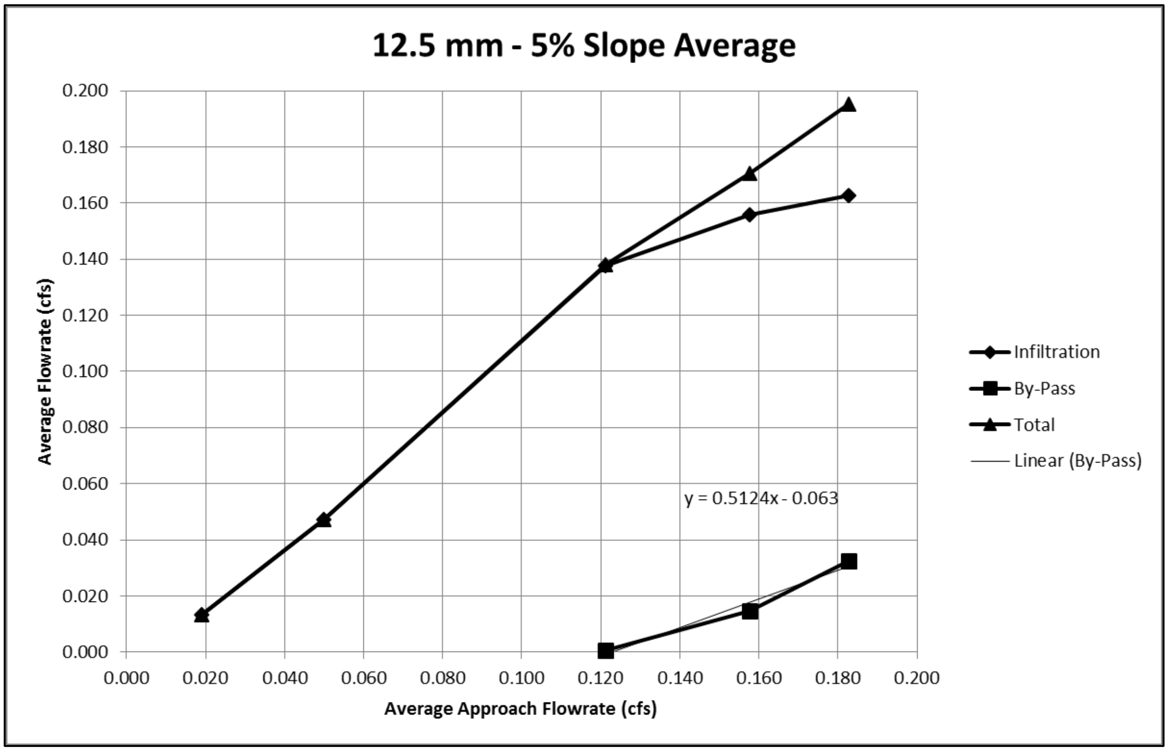

12.5 mm - 5% Slope Average
Average Flowrate (cfs)
0.200
0.180
0.160
0.140
0.120
0.100
0.080
0.060
0.040
0.020
0.000
0.000
0.020
0.040
0.060
0.080
0.100
0.120
0.140
0.160
0.180
0.200
Average Approach Flowrate (cfs)
y = 0.5124x - 0.063
Infiltration
By-Pass
Total
Linear (By-Pass)

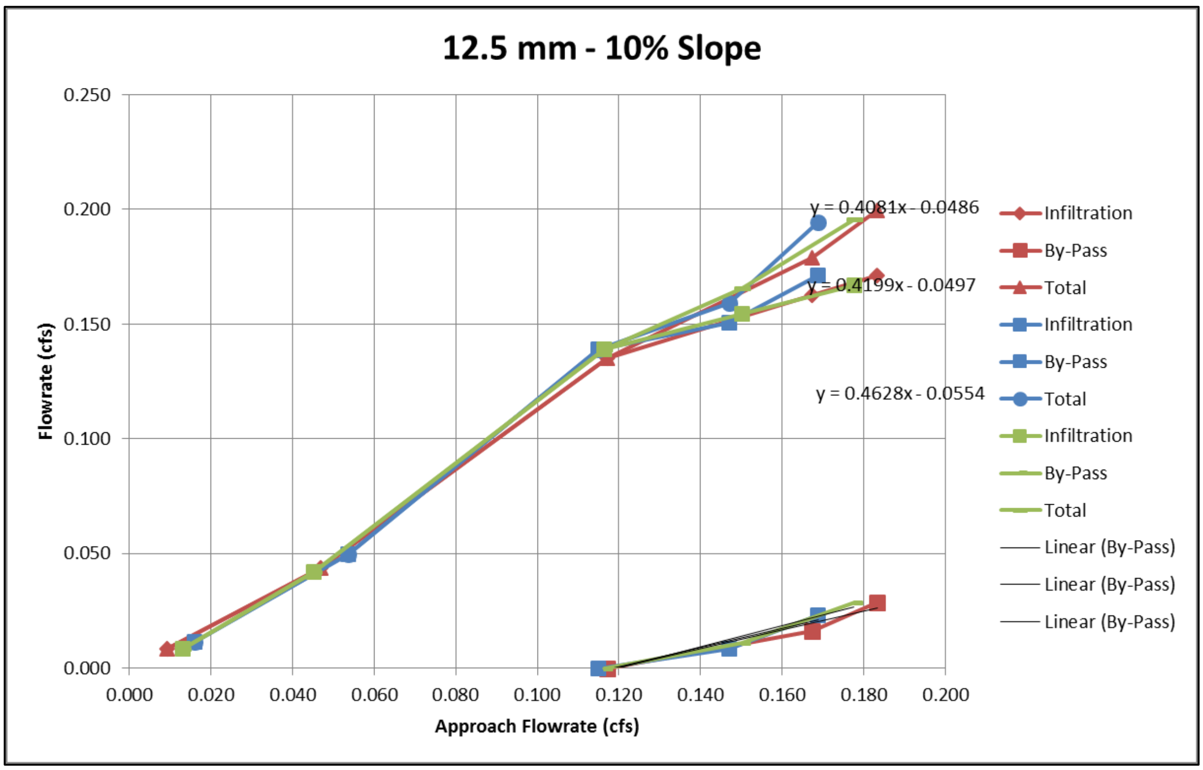

12.5 mm - 10% Slope
Flowrate (cfs)
0.250
0.200
0.150
0.100
0.050
0.000
0.000
0.020
0.040
0.060
0.080
0.100
0.120
0.140
0.160
0.180
0.200
Approach Flowrate (cfs)
y = 0.4081x - 0.0486
y = 0.4199x - 0.0497
y = 0.4628x - 0.0554
Infiltration
By-Pass
Total
Infiltration
By-Pass
Total
Infiltration
By-Pass
Total
Linear (By-Pass)
Linear (By-Pass)
Linear (By-Pass)

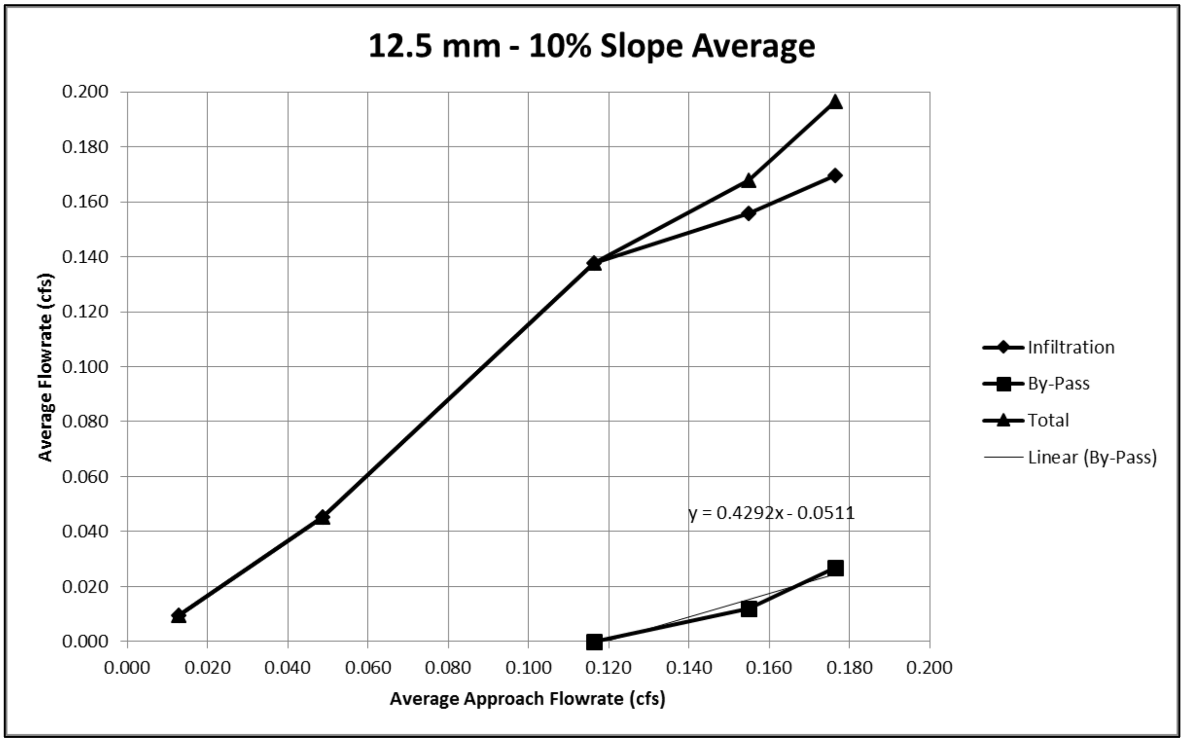
12.5 mm - 10% Slope Average
Average Flowrate (cfs)
0.200
0.180
0.160
0.140
0.120
0.100
0.080
0.060
0.040
0.020
0.000
0.000
0.020
0.040
0.060
0.080
0.100
0.120
0.140
0.160
0.180
0.200
Average Approach Flowrate (cfs)
y = 0.4292x - 0.0511
Infiltration
By-Pass
Total
Linear (By-Pass)

2. Statistical Analysis of Hydraulic Testing

Data:

C64	C65
6 mm Infiltration (BP) Per Area	Pattern Infiltration (BP)
0.020	0.016
0.021	0.015
0.017	0.015
0.017	0.014
0.015	0.015

Result:

Two-Sample T-Test and CI: 6 mm Infiltration (BP) Per Area, Pattern Infiltration (BP)

```
Two-sample T for 6 mm Infiltration (BP) Per Area vs Pattern Infiltration (BP)

                          N      Mean     StDev  SE Mean
6 mm Infiltration (BP) P  5   0.01800   0.00245   0.0011
Pattern Infiltration (BP  5  0.015000  0.000707  0.00032


Difference = μ (6 mm Infiltration (BP) Per Area) - μ (Pattern Infiltration (BP))
Estimate for difference:  0.00300
99% CI for difference:  (-0.00083, 0.00683)
T-Test of difference = 0 (vs ≠): T-Value = 2.63  P-Value = 0.030  DF = 8
Both use Pooled StDev = 0.0018
```

Data:

In Minitab Worksheet. Average of all 6 mm test compared to pattern (1 test) data

Two-Sample T-Test and CI: 6 mm Overflow (all), Pattern Bypass

```
Two-sample T for 6 mm Overflow (all) vs Pattern Bypass

                      N    Mean   StDev  SE Mean
6 mm Overflow (all)  15  0.0316  0.0293   0.0076
Pattern Bypass       15  0.0290  0.0321   0.0083


Difference = μ (6 mm Overflow (all)) - μ (Pattern Bypass)
Estimate for difference:  0.0026
99% CI for difference:  (-0.0285, 0.0337)
T-Test of difference = 0 (vs ≠): T-Value = 0.23  P-Value = 0.822  DF = 27
```

Two-Sample T-Test and CI: 6 mm Infiltration (all), Pattern Infiltration (Q1)

```
Two-sample T for 6 mm Infiltration (all) vs Pattern Infiltration (Q1)

                          N    Mean   StDev  SE Mean
6 mm Infiltration (all)   25  0.0637  0.0425   0.0085
Pattern Infiltration (Q1  25  0.0526  0.0252   0.0050


Difference = μ (6 mm Infiltration (all)) - μ (Pattern Infiltration (Q1))
Estimate for difference:  0.01105
99% CI for difference:  (-0.01572, 0.03782)
T-Test of difference = 0 (vs ≠): T-Value = 1.12  P-Value = 0.270  DF = 38
```

Two-Sample T-Test and CI: Average Running Bond, Validation

```
Two-sample T for Average Running Bond vs Validation

                     N     Mean    StDev  SE Mean
Average Running Bond  5  0.01834  0.00324   0.0014
Validation            5  0.01589  0.00124  0.00055


Difference = μ (Average Running Bond) - μ (Validation)
Estimate for difference:  0.00245
99% CI for difference:  (-0.00275, 0.00765)
T-Test of difference = 0 (vs ≠): T-Value = 1.58  P-Value = 0.153  DF = 8
Both use Pooled StDev = 0.0025
```

Two-Sample T-Test and CI: Validation Average Infiltration, Average 6 mm Infiltration

```
Two-sample T for Validation Average Infiltration vs Average 6 mm Infiltration

                         N    Mean   StDev  SE Mean
Validation Average Infil  25  0.0569  0.0303   0.0061
Average 6 mm Infiltratio  25  0.0681  0.0454   0.0091


Difference = μ (Validation Average Infiltration) - μ (Average 6 mm Infiltration)
Estimate for difference:  -0.0112
99% CI for difference:  (-0.0405, 0.0181)
T-Test of difference = 0 (vs ≠): T-Value = -1.03  P-Value = 0.310  DF = 48
Both use Pooled StDev = 0.0386
```

Two-Sample T-Test and CI: Validation Bypass, Average 6 mm Overflow

```
Two-sample T for Validation Bypass vs Average 6 mm Overflow

                      N    Mean   StDev  SE Mean
Validation Bypass     15  0.0288  0.0329   0.0085
Average 6 mm Overflow  15  0.0325  0.0291   0.0075


Difference = μ (Validation Bypass) - μ (Average 6 mm Overflow)
Estimate for difference:  -0.0037
99% CI for difference:  (-0.0350, 0.0276)
T-Test of difference = 0 (vs ≠): T-Value = -0.33  P-Value = 0.747  DF = 28
Both use Pooled StDev = 0.0310
```

Two-Sample T-Test and CI: 6 mm CFR, 10 mm CFR

```
Two-sample T for 6 mm CFR vs 10 mm CFR

          N     Mean    StDev  SE Mean
6 mm CFR   5   0.0788   0.0144   0.0064
10 mm CFR  5  0.12140  0.00182  0.00081


Difference = μ (6 mm CFR) - μ (10 mm CFR)
Estimate for difference:  -0.04260
99% CI for difference:  (-0.07251, -0.01269)
T-Test of difference = 0 (vs ≠): T-Value = -6.56  P-Value = 0.003  DF = 4
```

Two-Sample T-Test and CI: Summer Average Infiltation, Summer Average Infiltation_10mm

```
Two-sample T for Summer Average Infiltation vs Summer Average Infiltation_10mm

                          N    Mean   StDev  SE Mean
Summer Average Infiltati  25  0.0681  0.0454   0.0091
Summer Average Infiltati  25  0.0986  0.0604    0.012


Difference = μ (Summer Average Infiltation) - μ (Summer Average Infiltation_10mm)
Estimate for difference:  -0.0305
99% CI for difference:  (-0.0712, 0.0101)
T-Test of difference = 0 (vs ≠): T-Value = -2.02  P-Value = 0.049  DF = 44
```

Two-Sample T-Test and CI: Summer Average Bypass, Summer Average Bypass_10 mm

```
Two-sample T for Summer Average Bypass vs Summer Average Bypass_10 mm

                          N    Mean   StDev  SE Mean
Summer Average Bypass     15  0.0325  0.0291   0.0075
Summer Average Bypass_10  15  0.0144  0.0142   0.0037


Difference = μ (Summer Average Bypass) - μ (Summer Average Bypass_10 mm)
Estimate for difference:  0.01811
99% CI for difference:  (-0.00565, 0.04188)
T-Test of difference = 0 (vs ≠): T-Value = 2.17  P-Value = 0.042  DF = 20
```

One-way ANOVA: 6 mm CFR, 10 mm CFR, 12.5 nn CFR, Pattern CFR

Method

Null hypothesis	All means are equal
Alternative hypothesis	At least one mean is different
Significance level	$\alpha = 0.05$

Equal variances were assumed for the analysis.

Factor Information

Factor	Levels	Values
Factor	4	6 mm CFR, 10 mm CFR, 12.5 mm CFR, Pattern CFR

Analysis of Variance

Source	DF	Adj SS	Adj MS	F-Value	P-Value
Factor	3	0.015389	0.005130	82.17	0.000
Error	16	0.000999	0.000062		
Total	19	0.016388			

Model Summary

S	R-sq	R-sq(adj)	R-sq(pred)
0.0079009	93.91%	92.76%	90.48%

Means

Factor	N	Mean	StDev	95% CI
6 mm CFR	5	0.07880	0.01441	(0.07131, 0.08629)
10 mm CFR	5	0.121400	0.001817	(0.113910, 0.128890)
12.5 mm CFR	5	0.12600	0.00534	(0.11851, 0.13349)
Pattern CFR	5	0.06080	0.00319	(0.05331, 0.06829)

Pooled StDev = 0.00790095

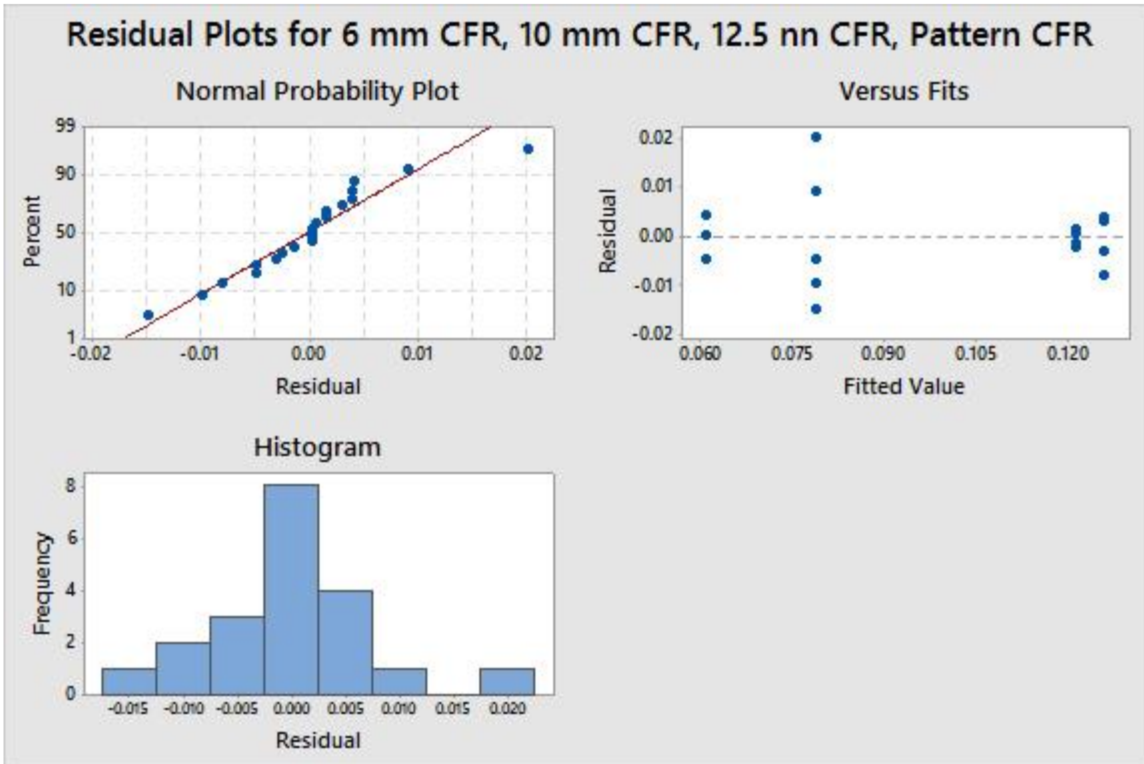
Residual Plots for 6 mm CFR, 10 mm CFR, 12.5 nn CFR, Pattern CFR
Normal Probability Plot
Percent
99
90
50
10
1
-0.02
-0.01
0.00
0.01
0.02
Residual
Versus Fits
Residual
0.02
0.01
0.00
-0.01
-0.02
0.060
0.075
0.090
0.105
0.120
Fitted Value
Histogram
Frequency
8
6
4
2
0
-0.015
-0.010
-0.005
0.000
0.005
0.010
0.015
0.020
Residual

Two-Sample T-Test and CI: 12.5 mm CFR, 10 mm CFR

```
Two-sample T for 12.5 nn CFR vs 10 mm CFR

             N     Mean    StDev  SE Mean
12.5 nn CFR  5  0.12600  0.00534   0.0024
10 mm CFR    5  0.12140  0.00182  0.00081


Difference = μ (12.5 nn CFR) - μ (10 mm CFR)
Estimate for difference:  0.00460
99% CI for difference:  (-0.00701, 0.01621)
T-Test of difference = 0 (vs ≠): T-Value = 1.82  P-Value = 0.142  DF = 4
```

Two-Sample T-Test and CI: Summer Average Bypass_10 mm, Summer Average Bypass_12.5mm

Two-sample T for Summer Average Bypass_10 mm vs Summer Average Bypass_12.5mm

	N	Mean	StDev	SE Mean
Summer Average Bypass_10	15	0.0144	0.0142	0.0037
Summer Average Bypass_12	15	0.0112	0.0104	0.0027

Difference = μ (Summer Average Bypass_10 mm) - μ (Summer Average Bypass_12.5mm)
Estimate for difference: 0.00320
95% CI for difference: (-0.00614, 0.01255)
T-Test of difference = 0 (vs ≠): T-Value = 0.71 P-Value = 0.487 DF = 25

Two-Sample T-Test and CI: Summer Average Infiltation_10mm, Summer Average Infiltation_12.5

Two-sample T for Summer Average Infiltation_10mm vs Summer Average Infiltation_12.5

	N	Mean	StDev	SE Mean
Summer Average Infiltati	25	0.0986	0.0604	0.012
Summer Average Infiltati	25	0.1122	0.0671	0.013

Difference = μ (Summer Average Infiltation_10mm) - μ (Summer Average Infiltation_12.5)
Estimate for difference: -0.0136
95% CI for difference: (-0.0499, 0.0227)
T-Test of difference = 0 (vs ≠): T-Value = -0.75 P-Value = 0.455 DF = 47

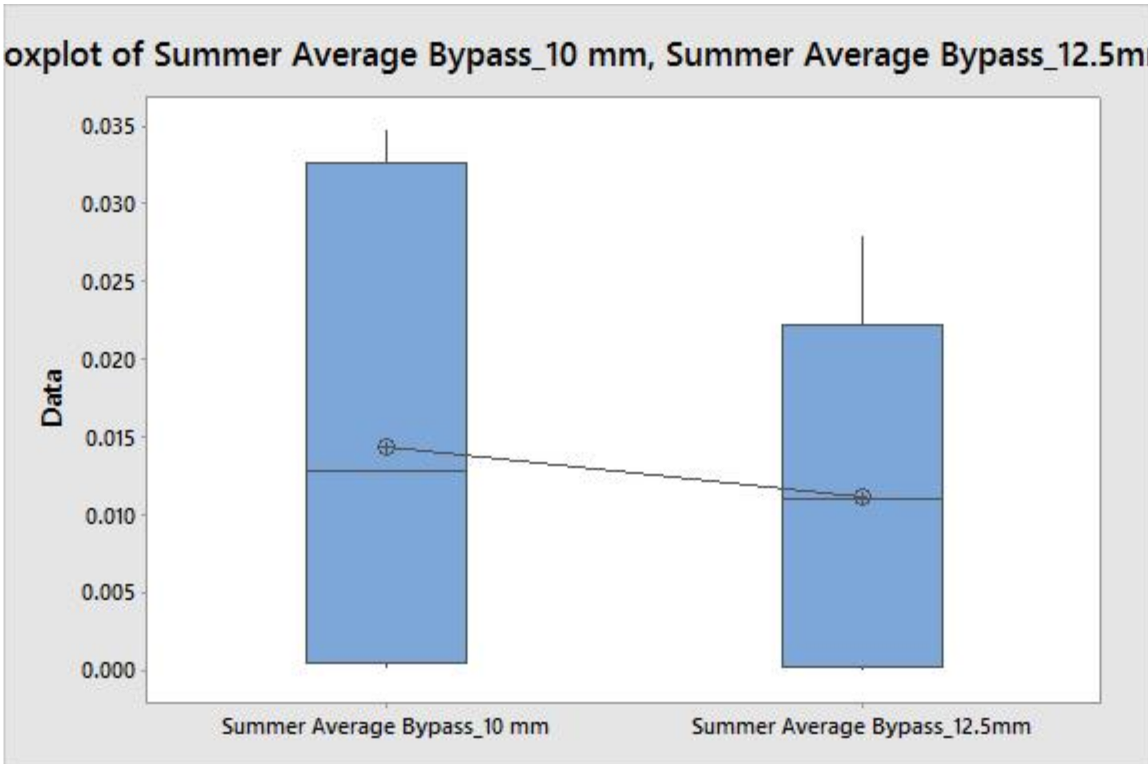
oxplot of Summer Average Bypass_10 mm, Summer Average Bypass_12.5mr
0.035
0.030
0.025
0.020
0.015
0.010
0.005
0.000
Data
Summer Average Bypass_10 mm
Summer Average Bypass_12.5mm

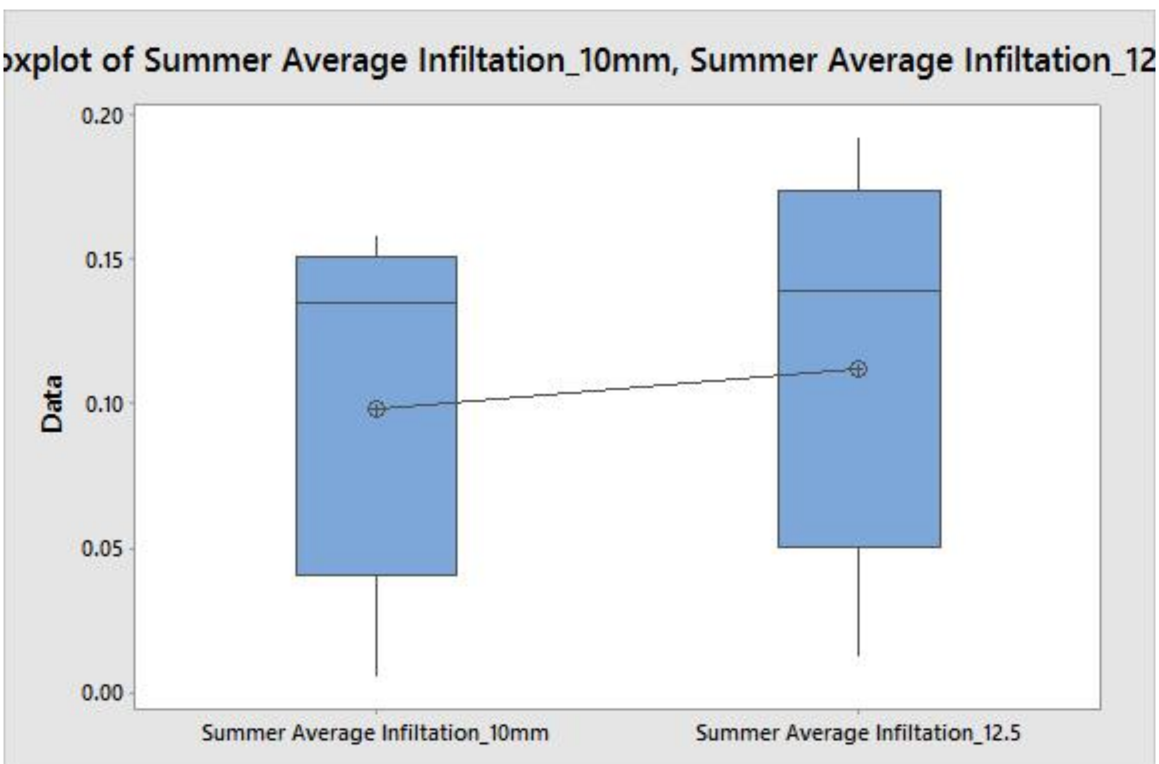
oxplot of Summer Average Infiltation_10mm, Summer Average Infiltation_12
0.20
0.15
0.10
0.05
0.00
Data
Summer Average Infiltation_10mm
Summer Average Infiltation_12.5

3. Hydraulic performance PICP with Pervious Platform

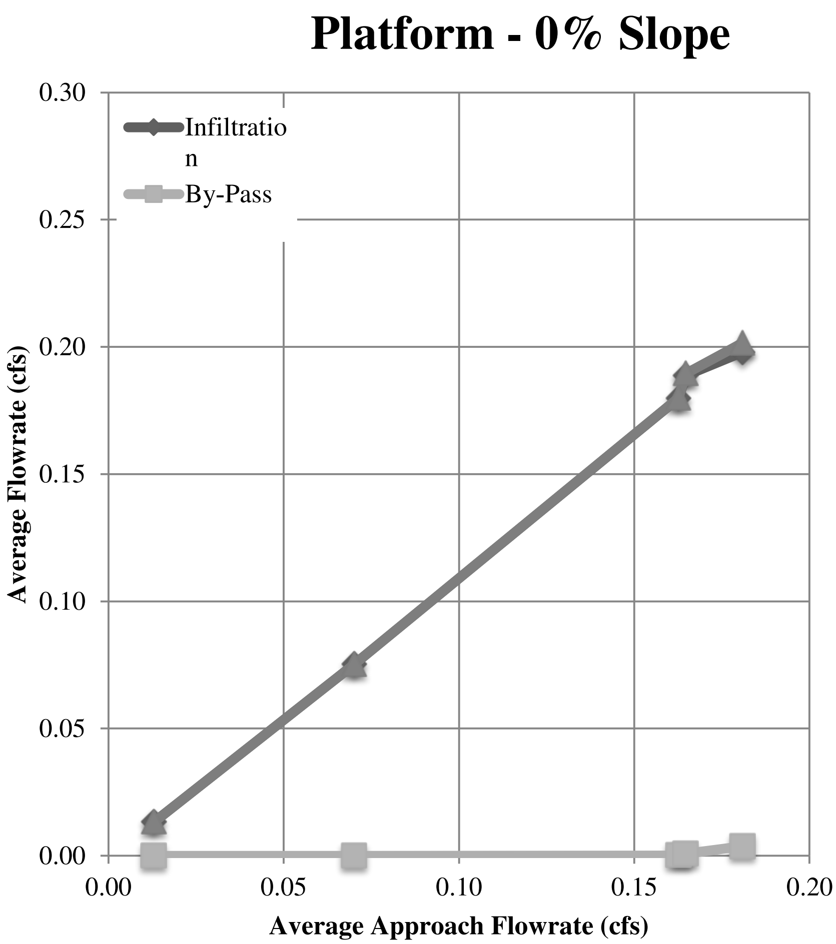

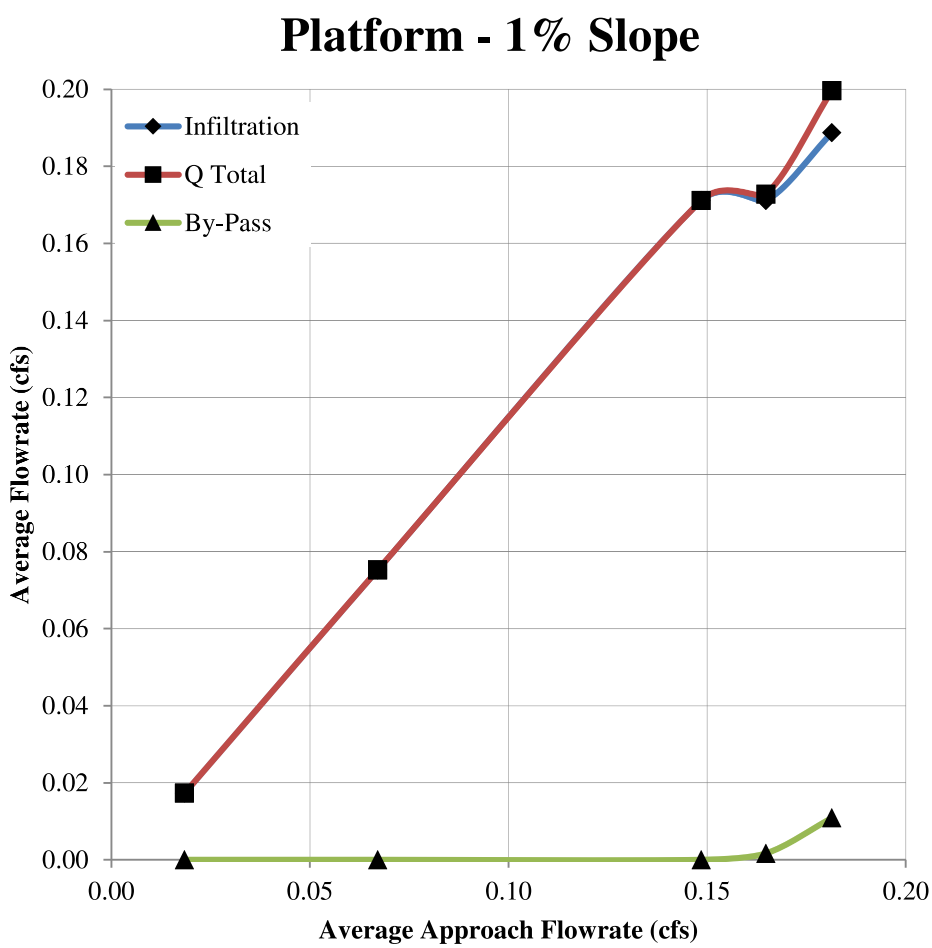

Platform - 1% Slope
Infiltration
Q Total
By-Pass
Average Flowrate (cfs)
Average Approach Flowrate (cfs)
0.00
0.02
0.04
0.06
0.08
0.10
0.12
0.14
0.16
0.18
0.20
0.00
0.05
0.10
0.15
0.20

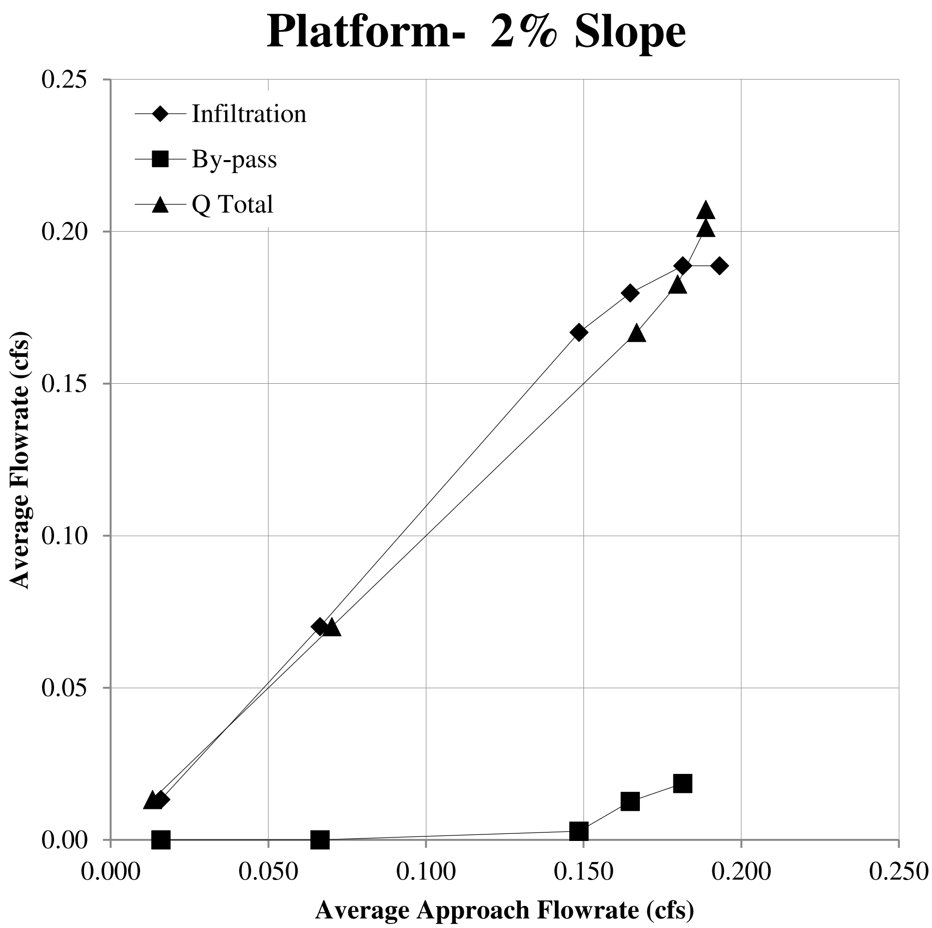
Platform- 2% Slope
Infiltration
By-pass
Q Total
Average Flowrate (cfs)
0.25
0.20
0.15
0.10
0.05
0.00
0.000
0.050
0.100
0.150
0.200
0.250
Average Approach Flowrate (cfs)

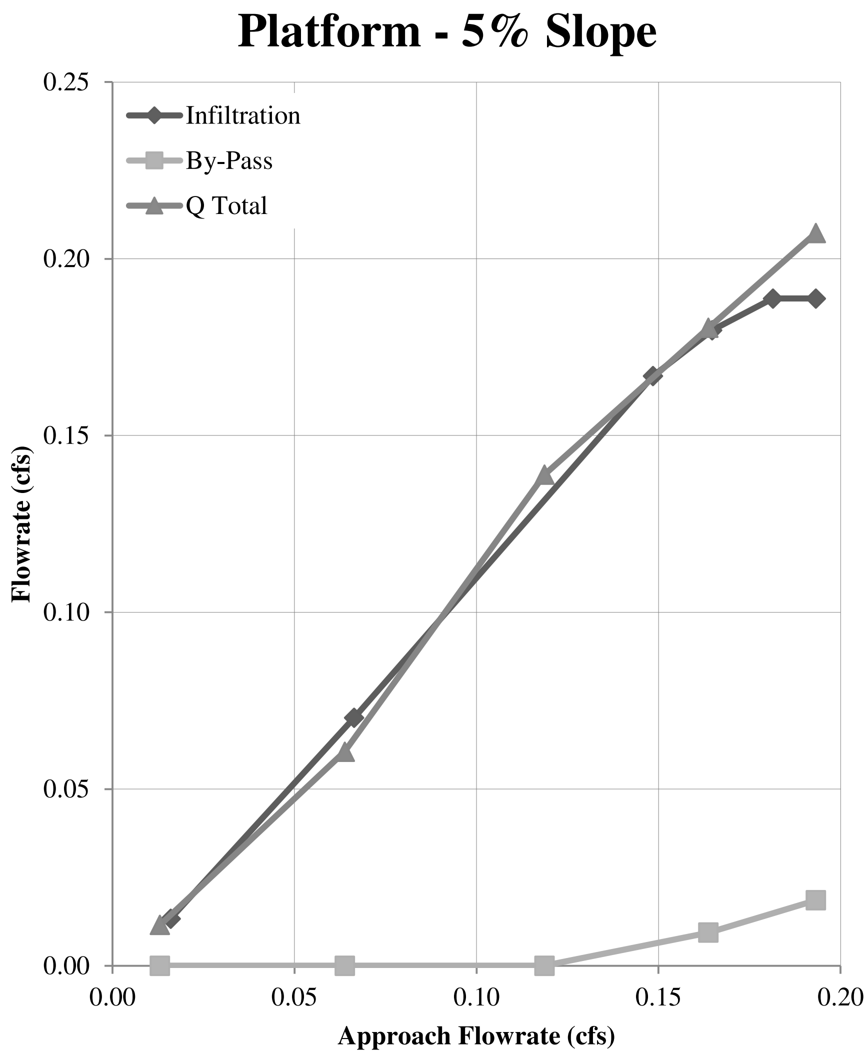

Platform - 5% Slope
0.25
0.20
0.15
0.10
0.05
0.00
Flowrate (cfs)
0.00
0.05
0.10
0.15
0.20
Approach Flowrate (cfs)
Infiltration
By-Pass
Q Total

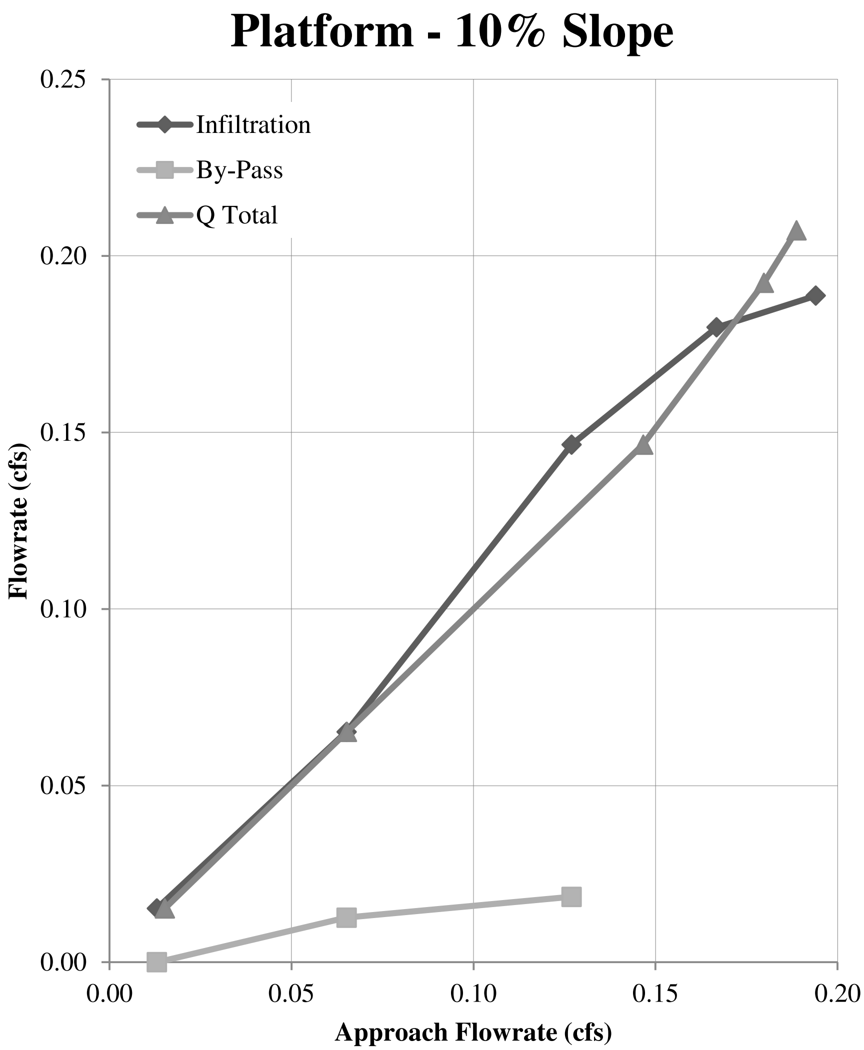

Platform - 10% Slope
0.25
0.20
0.15
0.10
0.05
0.00
Flowrate (cfs)
0.00
0.05
0.10
0.15
0.20
Approach Flowrate (cfs)
Infiltration
By-Pass
Q Total

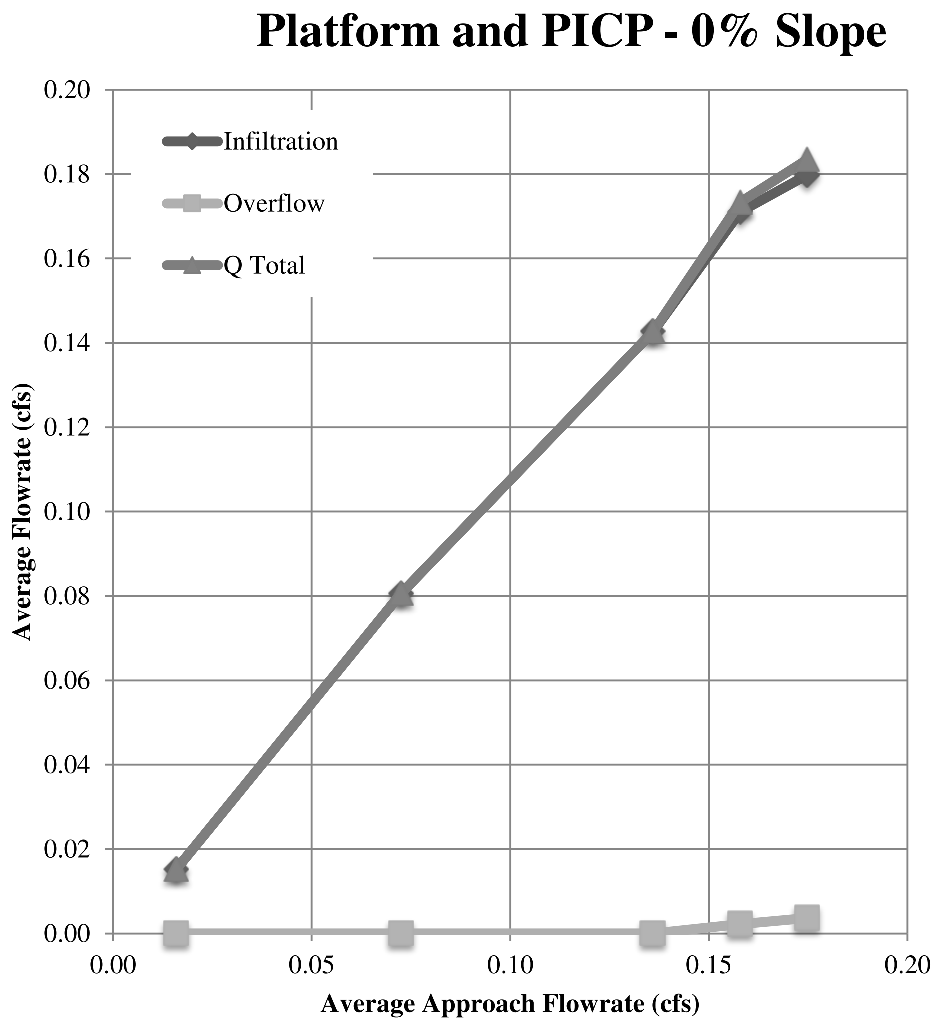
Platform and PICP - 0% Slope
Infiltration
Overflow
Q Total
Average Flowrate (cfs)
Average Approach Flowrate (cfs)
0.00
0.02
0.04
0.06
0.08
0.10
0.12
0.14
0.16
0.18
0.20
0.00
0.05
0.10
0.15
0.20

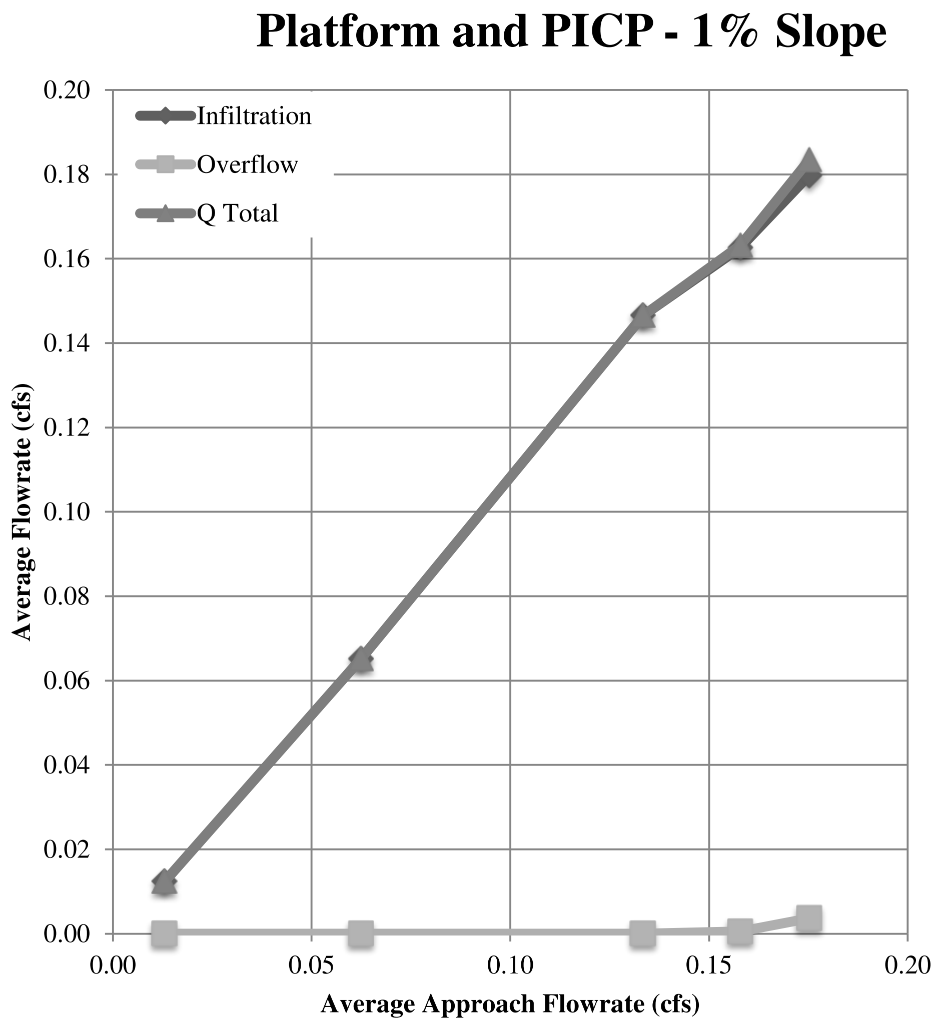
Platform and PICP - 1% Slope
Infiltration
Overflow
Q Total
0.20
0.18
0.16
0.14
0.12
0.10
0.08
0.06
0.04
0.02
0.00
Average Flowrate (cfs)
0.00
0.05
0.10
0.15
0.20
Average Approach Flowrate (cfs)

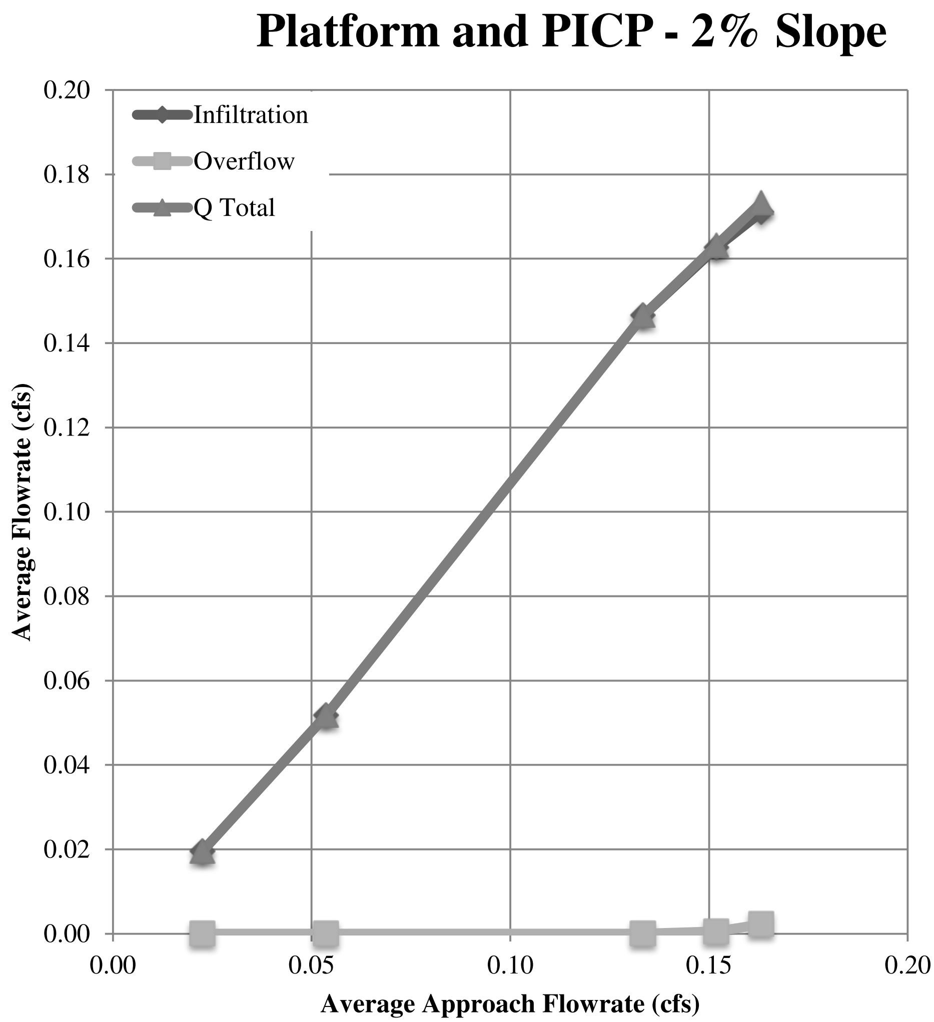

Platform and PICP - 2% Slope
Infiltration
Overflow
Q Total
Average Flowrate (cfs)
0.20
0.18
0.16
0.14
0.12
0.10
0.08
0.06
0.04
0.02
0.00
0.00
0.05
0.10
0.15
0.20
Average Approach Flowrate (cfs)

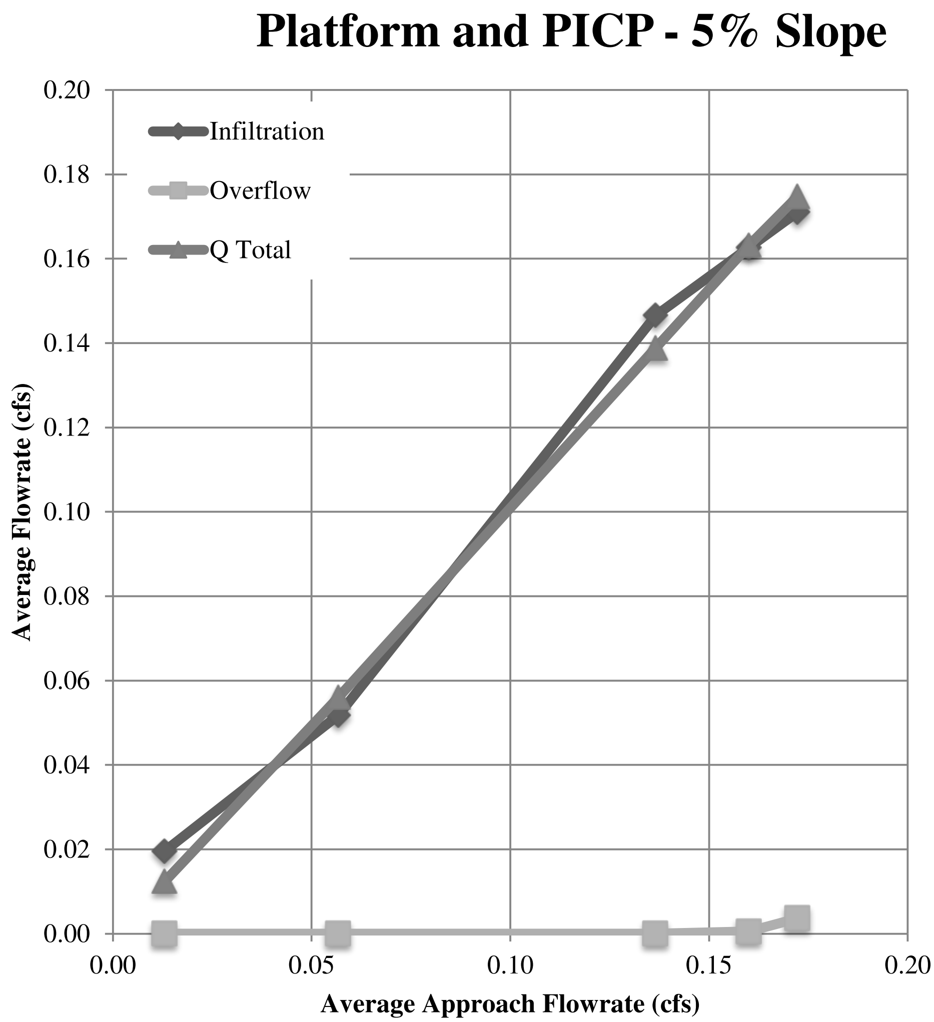

Platform and PICP - 5% Slope
Infiltration
Overflow
Q Total
Average Flowrate (cfs)
Average Approach Flowrate (cfs)
0.00
0.02
0.04
0.06
0.08
0.10
0.12
0.14
0.16
0.18
0.20
0.00
0.05
0.10
0.15
0.20

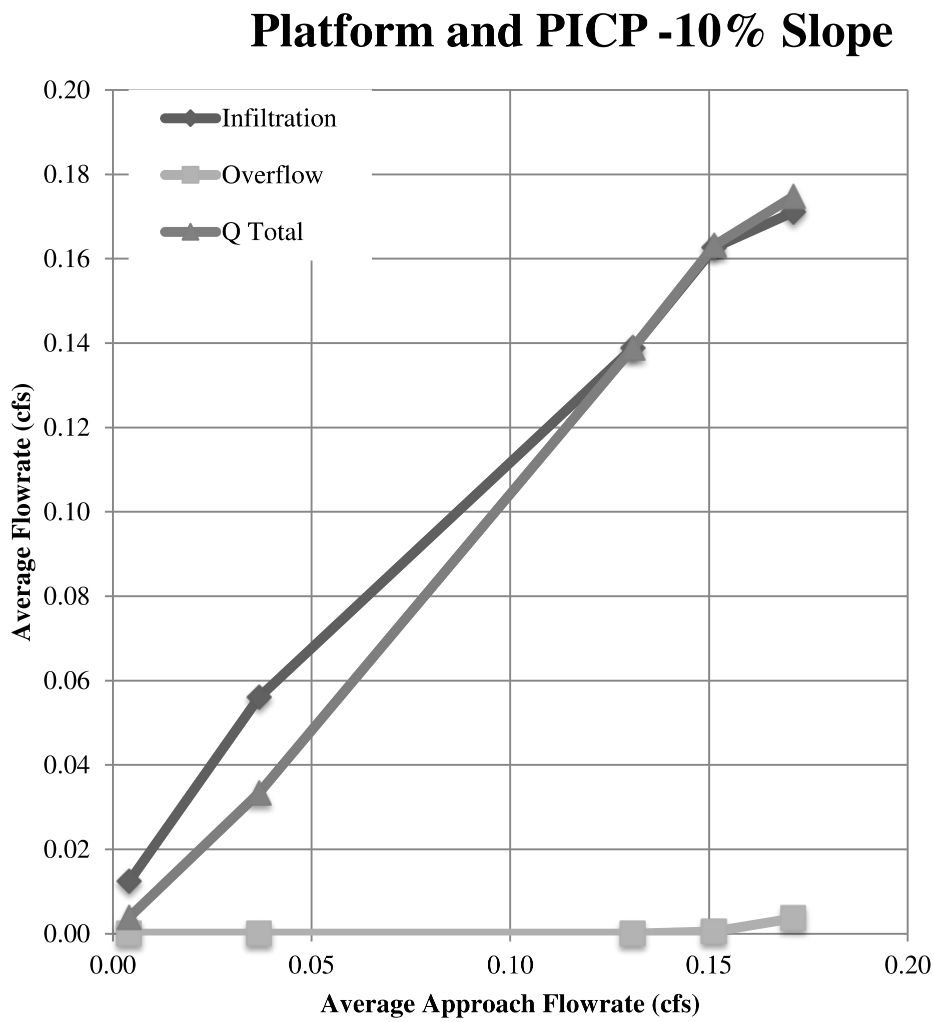
Platform and PICP -10% Slope
Infiltration
Overflow
Q Total
Average Flowrate (cfs)
Average Approach Flowrate (cfs)
0.00
0.02
0.04
0.06
0.08
0.10
0.12
0.14
0.16
0.18
0.20
0.00
0.05
0.10
0.15
0.20

APPENDIX B- DESIGN TOOL

Owner's Manual

Inputs

This PICP design tool is used to determine design criteria necessary based specific site input information. This manual is created to assist the engineer in the design phase to conclude proper hydraulic parameters for the site.

Each input for the design tool has been given an identification number for the user's reference. The input interface is seen in Figure 91 with the identification reference numbers listed to the right. Each input will be further explained in throughout this manual under corresponding identification reference.

Input		
Storm Information		
Storm Region	Missouri	**1**
Duration	10-min	**2**
Recurrence Interval	100	**3**
Project ID	Example 1B	**4**
Site Information		
Site Width, w (ft)	800	**5**
Pervious Length, L' (ft)	20	**6**
Contributing Length, L (ft)	10	**7**
Contributing Area Land Category	Streets	**8**
Contributing Area Land Type	Asphaltic	**9**
Contributing Area C-Value Range	Max	**10**
Slope (%)	2	**11**
Case Level	Case I	**12**
Gap Size	6	**13**

Figure 91. Input Interface

Project ID

The project ID is a reference used for the design engineer to better identify their project. This box is a direct input, and it will not impact the design.

Storm Information

1) <u>Storm Region</u>

The storm region is based upon the site location state. The storm region will be used to determine intensity and was found from the National Oceanic and Atmospheric Administration (NOAA)'s National Weather Service Precipitation Frequency Data Server (NOAA, 2014). Not all states are updated with accurate rainfall intensities. All 50 states are included in the design tool with accurate rainfall intensities with the exception of Connecticut, Idaho, Maine, Massachusetts, Montana, New Hampshire, New York, Oregon, Rhode Island, Texas, Vermont, Washington, and Wyoming.

For the states that data was not provided, the storm region is categorized by SCS Storm Type for a simple reference, seen in the map in Figure 92. There are four SCS storm types throughout the United States: Type I, Type IA, Type II, and Type III. The SCS method was not used as the calculation basis for design, only as a location reference in determining the region the rainfall will occur.

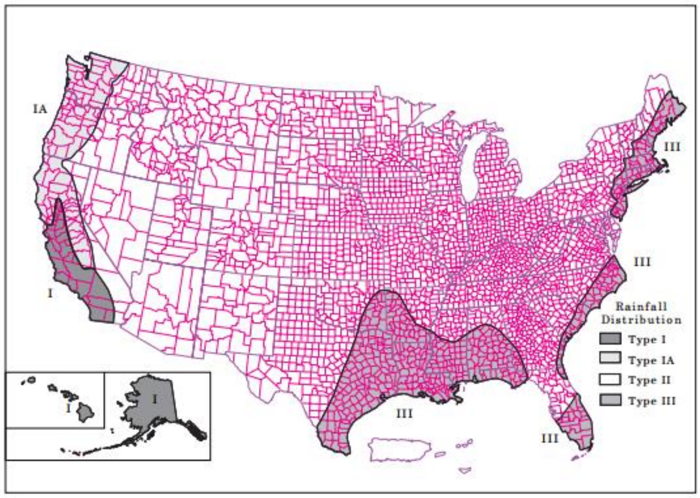

Figure 92. (USDA-NRCS, 1986) SCS TR-55 Storm Map

2) <u>Duration</u>

For each storm type, a duration will be chosen to determine the length time rainfall will be impacting the system. The duration is proportional to rainfall intensity and will be used in calculating the runoff. The analysis for this design tool, discussed further in this Chapter, is based on unit discharge rate. For a site of unit width, it can be assumed that the intensity of the storm will not exceed a 10-min time of concentration. Therefore, tool can calculate 5-min and 10-min duration.

3) <u>Recurrence Interval</u>

After the duration is chosen to properly anticipate recurrence interval are chosen. Recurrence intervals give the probability of a storm event occurring. A 10 year storm does not mean that a storm will occur every 10 years, but that the probability that a storm of that depth will occur at the chosen location of the site. The following list gives all the possible options included in the design tool: 2 yr., 5 yr., 10 yr., 25 yr., 50 yr., 100 yr., 200 yr., 500 yr. and 1000 yr.

Site Area Information

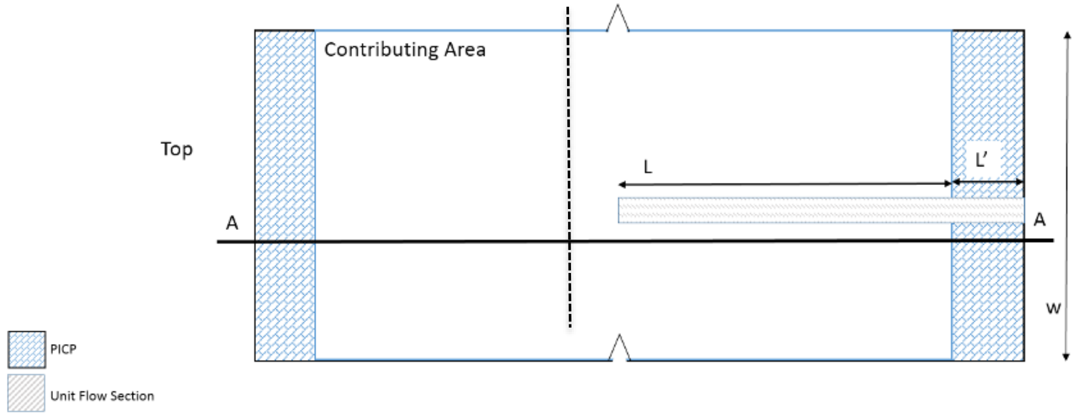

Figure 93. Total Proposed Site Area

4) Site Width, w (ft.)

The site width is determined in feet and is in reference to the width in Figure 93.

5) Pervious Length, L (sqft)

The pervious length represent the length of the unit strip of the pervious area in the site area, seen in Figure 93.

6) Contributing Area, L' (sqft)

The contributing length represents the length of the unit strip of the contributing area in the site area, seen in Figure 93. For the purpose of this design tool, the contributing area to pervious area ratio cannot exceed a 5:1 ratio.

7) Contributing Area Land Category

The contributing land category defines where the contributing runoff is descending from. The contributing area is considered completely impervious unless specified otherwise. The possible category options included are Business, Residential, Suburban, Apartment Dwelling Areas, Industrial, Parks, Cemeteries, Playgrounds, Railroad Yard Areas, Unimproved Areas, Lawns, Streets, and Roof.

8) Contributing Land sub-Type

After choosing the contributing land category, a contributing land type will then be available. The possible land sub-types are listed relative land category in Table 35. Certain land categories can be described fully by category, and therefore, do not need a sub-type to accurately estimate flow that would reach the PICP section.

Table 35. Land Category and Sub-type Relation

Land Category	Land Sub-type
Business	Downtown
	Neighborhood
Residential	Single family
	Multi units, detached
	Multi units, attached
Suburban	-
Apartment Dwelling Areas	-
Industrial:	Light
	Heavy
Parks, Cemeteries	-
Playgrounds	-
Railroad Yard Areas	-
Unimproved Areas	-
Lawns	Sandy soil (Flat 2%)
	Sandy soil (Average 2-7%)
	Sandy soil (Steep 7%)
	Heavy soil (Flat 2%)
	Heavy soil (Average 2-7%)
	Heavy soil (Steep 7%)
Streets	Asphaltic
	Concrete
	Brick
Roof	-

9) Contributing Area Runoff coefficient Range

A Runoff coefficient is chosen from a range of "Max" or "Min". A lower Runoff coefficient will results in a lower runoff rate. The "Max" runoff coefficients will increase the amount of runoff, and therefore require a higher infiltration.

10) Slope (%)

The slope of the site area can be chosen from the slopes tested in a laboratory. The possible slope options included in the design tool are 0%, 1%, 2%, 5%, and 10%.

11) Case Level

The designing engineer must consider the level of conservation to be applied to the proposed site area. The decision will be made by considering the attributes of the surrounding and contributing area. There are three possible cases that can be applied to the design, which correspond to the level of overflow allowed over the PICP section. Case I being the least amount, and Case III being the greatest amount. The amount of water flowing across the system is defined by case level, which are described in Table 36.

Table 36. Case Level Characteristics

Case Level	I	II	III
Head Stage	Insipient overflow	¼ in head	½ in head
BMP Treatment Train Characteristics	-Need additional treatment -Need additional flow attenuation	-PICP used along with another BMP, such as rain garden or another permeable pavement	-PICP used along in large treatment train -Very little need for treatment in system -Very little need for flow attenuation in system
Infiltration Level	Minimum	Medium	Maximum

Case I will be applied to a site with no additional treatment or possible flow attenuation, seen in Figure 94. An example would be a PCIP section at the end of a parking lot.

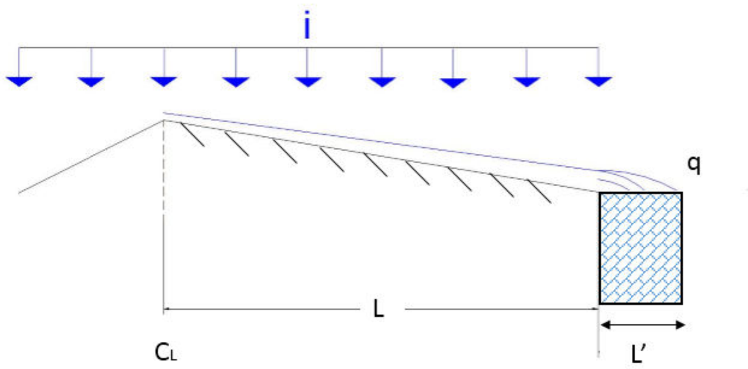

Figure 94. Case I Profile and Cross Section

Case II will be applied when PICP was used along with another BMP. Profile seen in Figure 95. For example, another permeable pavement or a rain barrel added to the site. This addition of a BMP that is not meant for very large amounts of flow attenuation or treatment, but will reduce the flow to the PICP section and decrease necessary amounts of treatment within the system.

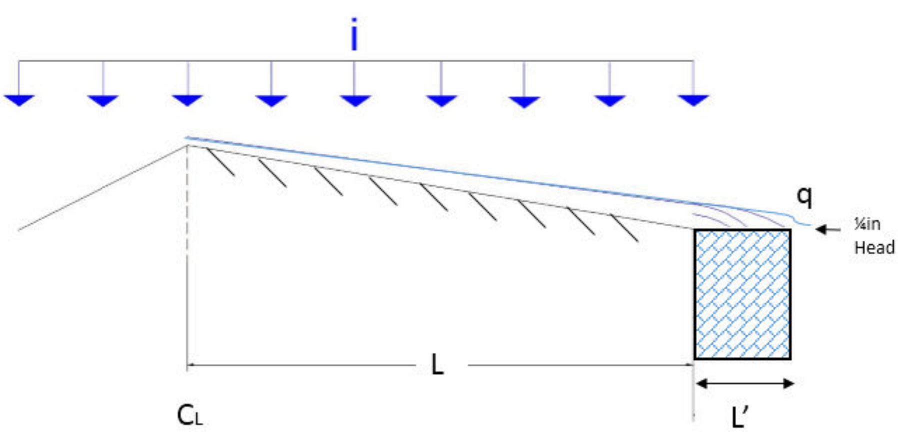

Figure 95. Case II Profile and Cross Section

Case III will be applied when the PICP section would be used at the end of the treatment train of BMPs, such as a rain garden with rain barrels and PICP at the end of the flow path. The flow ultimately reaching the PICP would be very low.

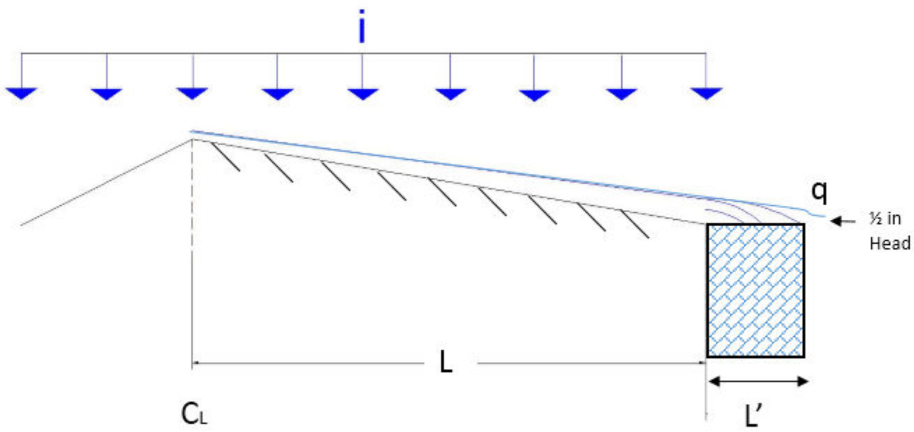

Figure 96. Case III Profile and Cross Section

12) Gap Size (mm)

The gap size of the PICP section area can be chosen from the PICP sections tested in a laboratory. This gap size is in reference to the length of the space between each of the blocks that will be filled with pervious material. The following list gives all the possible options included in the design tool: 6mm, 7mm, 8mm, 9mm, 10mm, and 12.5mm.

Outputs

The output interface is seen in Figure 97 with the identification reference numbers listed to the right. Each output will be further explained in throughout this section of the manual under corresponding identification reference.

Output		
Site Analysis		
Total Site Area (sqft)	24000	**14**
Pervious Area (sqft)	16000	**15**
Contributing Area (sqft)	8000	**16**
Storm Analysis		
Contributing Runoff Coefficient	0.95	**17**
Composite Runoff Coefficient	0.52	**18**
Intensity (in/hr)	8.22	**19**
Unit Discharge Rate (cfs/ft)	0.006	**20**
System Horizontal Infiltration (in/hr)	259	**21**
Design Considerations		
Runoff Rate (cfs)	0.079	**22**
Unit Overflow Rate (cfs/ft)	0.370	**23**
ASTM C 1781 Vertical Infiltration (in/hr)	409	**24**
Gap Size	**Within Range**	**25**

Figure 97. Output Interface

Site Analysis

13) Total Site Area (sqft)

The total site area includes the square footage of the entire proposed area, seen in Figure 93. The site area represents the entire proposed site, including the contributing and pervious area.

14) Pervious Area (sqft)

The pervious area is determined in square feet and is in reference to the width in Figure 93.

15) Contributing Area (sqft)

The pervious area is determined in square feet and is in reference to the width in Figure 93.

Storm Analysis

16) Contributing Runoff Coefficient

Using the results of inputs Contributing Land Category, Contributing Land Sub-type, and Contributing Runoff coefficient range, a contributing runoff coefficient is found Table 37.

Table 37. Runoff Coefficients (American Public Works Association)

Type of Drainage Area	Runoff Coefficient Min - Max
Business:	
Downtown areas	0.7 - 0.95
Neighborhood areas	0.5 - 0.7
Residential:	
Single Family	0.3 - 0.5
Multi Units (Detached)	0.4 - 0.6
Multi Units (Attached)	0.6 - 0.75
Suburban	0.25 - 0.4
Apartment Dwelling Areas	0.5 - 0.7
Industrial:	
Light	0.5 - 0.8
Heavy	0.6 - 0.9
Parks, Cemeteries	0.1 - 0.25
Playgrounds	0.2 - 0.4
Railroad Yard Areas	0.2 - 0.4
Unimproved Areas	0.1 - 0.3
Lawns:	
Sandy soil (Flat 2%)	0.05 - 0.1
Sandy soil (Average 2-7%)	0.1 - 0.15
Sandy soil (Steep 7%)	0.15 - 0.2
Heavy soil (Flat 2%)	0.13 - 0.17
Heavy soil (Average 2-7%)	0.18 - 0.25
Heavy soil (Steep 7%)	0.25 - 0.35
Streets:	
Asphaltic	0.7 - 0.95
Concrete	0.8 - 0.95
Brick	0.7 - 0.85
Drives and Walks	0.75 - 0.85
Roof	0.75 - 0.95

17) <u>Composite Runoff Coefficient</u>

A composite Runoff coefficient is calculated as a weighted average based on area. For this analysis, it is appropriate to weight the runoff coefficient to determine an accurate value. The runoff coefficient of the PICP section is represented at 0.3 in the design. Pervious area yields significantly lower Runoff coefficients. (ICPI, 2008) The composite runoff coefficient equation is seen in Equation 7.

Equation 7. Composite Runoff Coefficient

$$C = \frac{A_C C_C + A_P C_P}{A_T}$$

Where:

C = Composite Runoff Coefficient

A_C = Contributing Area (acres)

C_C = Contributing Runoff Coefficient

AP = Pervious Area (acres)

C_P = Pervious Runoff Coefficient

A_T = Total Site Area (acres)

18) Intensity (in/hr.)

Using the results of 1) SCS storm type, 2) Duration, and 3) Recurrence Interval, and intensity is determined using an intensity-duration-frequency curve for each design site from the National Oceanic and Atmospheric Administration's National Weather Service Precipitation Frequency Data Server. Tables found in Appendix B.

19) Unit Discharge Rate (cfs/ft.)

The unit discharge rate is identified as q in Figure 93. The unit discharge is calculated assuming that each system reaches full equilibrium and the concepts of conservation of mass.

20) System Horizontal Infiltration (in/hr.)

Horizontal infiltration is calculated using the results of laboratory testing. The horizontal infiltration represents the rate at which the rate at which water will flow across the system.

Design Considerations

21) Runoff Rate (cfs)

The flow rate at each site was determined using the rational method, seen in Equation 8. The rational method uses the results of the input section, including the intensity, composite runoff coefficient, and area.

Equation 8. Rational Method

$$Q = 1.008CiA$$

Where:

Q = Flow rate (cfs)

C = Composite runoff coefficient

i = Intensity (in/hr.)

A = Area (acres)

22) Unit Overflow Rate (cfs/ft.)

Overflow rate is calculated using the results of laboratory testing. The overflow rate is converted to a unit rate by using the relative laboratory results per area of the PICP section in the laboratory flume, 4 feet, multiplied by the length of the pervious length, L'. This resulting unit overflow rate is compared to the unit discharge rates calculated for the site.

23) ASTM C1781Vertical Infiltration (in/hr.)

Vertical infiltration is calculated using the results of laboratory testing ASTM C1781 (ASTM, 2013) testing procedure. The vertical infiltration represents the rate at which the rate at which water will flow directly into the system.

24) Gap Size - Check

The check of the gap size will give the designing engineer a proclamation of "Within Range" or "Out of Range". This will conclude whether or not the chosen 13) Gap Size is adequate for the PICP section to properly contain and handle the flow onto and through the section. The hydraulic characteristics used as results are seen in Table 38 through Table 43.

Table 38. 6mm Hydraulic Characteristics Summary.

Case Level	Hydraulic Characteristic	Units	0%	1%	2%	5%	10%
	Overflow Discharge	cfs	0.088	0.099	0.074	0.069	0.064
I	Horizontal Infiltration	in/hr.	307	344	259	240	223
	Vertical Infiltration	in/hr.	359	363	409	380	371
	Overflow Discharge	cfs	0.118	0.121	0.123	0.127	0.139
II	Horizontal Infiltration	in/hr.	410	423	430	442	483
	Vertical Infiltration	in/hr.	359	363	409	380	371
	Overflow Discharge	cfs	0.175	0.187	0.182	0.187	0.185
III	Horizontal Infiltration	in/hr.	609	653	635	650	645
	Vertical Infiltration	in/hr.	359	363	409	380	371

Table 39. 7mm Hydraulic Characteristics Summary

Case Level	Hydraulic Characteristic	Units	0%	1%	2%	5%	10%
	Overflow Discharge	cfs	0.100	0.103	0.083	0.086	0.086
I	Horizontal Infiltration	in/hr.	356	374	324	314	315
	Vertical Infiltration	in/hr.	380	372	402	365	360
	Overflow Discharge	cfs	0.117	0.126	0.140	0.131	0.146
II	Horizontal Infiltration	in/hr.	421	441	495	474	753
	Vertical Infiltration	in/hr.	380	372	402	365	360
	Overflow Discharge	cfs	0.176	0.189	0.184	0.187	0.188
III	Horizontal Infiltration	in/hr.	627	671	657	668	671
	Vertical Infiltration	in/hr.	380	372	402	365	360

Table 40. 8 mm Hydraulic Characteristics Summary

Case Level	Hydraulic Characteristic	Units	0%	1%	2%	5%	10%
	Overflow Discharge	cfs	0.110	0.107	0.095	0.100	0.103
I	Horizontal Infiltration	in/hr.	395	398	375	371	383
	Vertical Infiltration	in/hr.	410	401	422	380	377
	Overflow Discharge	cfs	0.118	0.129	0.152	0.136	0.151
II	Horizontal Infiltration	in/hr.	432	455	541	497	780
	Vertical Infiltration	in/hr.	410	401	422	380	377
	Overflow Discharge	cfs	0.177	0.189	0.184	0.187	0.189
III	Horizontal Infiltration	in/hr.	637	678	668	675	682
	Vertical Infiltration	in/hr.	410	401	422	380	377

Table 41. 9 mm Hydraulic Characteristics Summary

Case Level	Hydraulic Characteristic	Units	0%	1%	2%	5%	10%
	Overflow Discharge	cfs	0.118	0.111	0.104	0.111	0.114
I	Horizontal Infiltration	in/hr.	424	417	413	411	428
	Vertical Infiltration	in/hr.	451	450	469	427	423
	Overflow Discharge	cfs	0.120	0.133	0.159	0.139	0.153
II	Horizontal Infiltration	in/hr.	443	467	567	511	790
	Vertical Infiltration	in/hr.	451	450	469	427	423
	Overflow Discharge	cfs	0.176	0.187	0.183	0.185	0.187
III	Horizontal Infiltration	in/hr.	638	674	668	672	680
	Vertical Infiltration	in/hr.	451	450	469	427	423

Table 42. 10mm Hydraulic Characteristics Summary

Case Level	Hydraulic Characteristic	Units	0%	1%	2%	5%	10%
	Overflow Discharge	cfs	0.123	0.119	0.122	0.120	0.123
I	Horizontal Infiltration	in/hr.	444	429	438	434	450
	Vertical Infiltration	in/hr.	501	519	543	505	498
	Overflow Discharge	cfs	0.126	0.132	0.159	0.143	0.155
II	Horizontal Infiltration	in/hr.	454	476	573	516	558
	Vertical Infiltration	in/hr.	501	519	543	505	498
	Overflow Discharge	cfs	0.175	0.183	0.182	0.183	0.184
III	Horizontal Infiltration	in/hr.	631	659	657	658	663
	Vertical Infiltration	in/hr.	501	519	543	505	498

Table 43. 12.5 mm Hydraulic Characteristics Summary

Case Level	Hydraulic Characteristic	Units	0%	1%	2%	5%	10%
	Overflow Discharge	cfs	0.130	0.129	0.130	0.123	0.118
I	Horizontal Infiltration	in/hr.	451	433	442	417	403
	Vertical Infiltration	in/hr.	671	782	844	835	813
	Overflow Discharge	cfs	0.142	0.143	0.148	0.144	0.140
II	Horizontal Infiltration	in/hr.	480	485	503	489	474
	Vertical Infiltration	in/hr.	671	782	844	835	813
	Overflow Discharge	cfs	0.171	0.169	0.172	0.171	0.166
III	Horizontal Infiltration	in/hr.	578	572	581	578	562
	Vertical Infiltration	in/hr.	671	782	844	835	813

Clogging Considerations

Clogging		
Stormwater Pollutant Concentration (mg/l)	300	**26**
Annual Rainfall (in)	38.2	**27**
Time to Maintenance (Years)	17	**28**

Figure 98. Clogging Interface

25) Stormwater Pollutant Concentration (mg/l)

The solid sediment pollutant is the total amount of sediment that will be applied to the sediment loading rate. Figure 99 presents a table in lb. /acre-yr. of the typical pollutant loading based on urban land use. TSS represents total suspended solids, which can be analyzed using this design tool (EPA, 2006).

Land Use	TSS	TP	TKN	NH_3-N	NO_2+NO_3-N	BOD	COD	Pb	Zn	Cu
Commercial	1000	1.5	6.7	1.9	3.1	62	420	2.7	2.1	0.4
Parking Lot	400	0.7	5.1	2	2.9	47	270	0.8	0.8	0.04
HDR	420	1	4.2	0.8	2	27	170	0.8	0.7	0.03
MDR	190	0.5	2.5	0.5	1.4	13	72	0.2	0.2	0.14
LDR	10	0.04	0.03	0.02	0.1	NA	NA	0.01	0.04	0.01
Freeway	880	0.9	7.9	1.5	4.2	NA	NA	4.5	2.1	0.37
Industrial	860	1.3	3.8	0.2	1.3	NA	NA	2.4	7.3	0.5
Park	3	0.03	1.5	NA	0.3	NA	2	0	NA	NA
Construction	6000	80	NA	NA	NA	NA	NA	NA	NA	NA

HDR: High Density Residential, MDR: Medium Density Residential, LDR: Low Density Residential
NA: Not available; insufficient data to characterize loadings
Source: Horner et al, 1994

Figure 99. Typical Pollutant Loadings from Runoff by Urban Land Use (lb. /acre-yr.) (EPA, 2006)

26) Annual Rainfall (in)

The annual rainfall is the total amount of rainfall that is common to the geographic region in inches. This information can be easily accessed through the National Weather Service results.

27) Time to Maintenance (years)

The time to maintenance in the results years it will take for the system to become clogged based on the loading rate applied by the solid sediment in the flow. This time is based on the results of the clogging analysis, which show that full infiltration can be reclaimed up to approximately 50% infiltration in the system.

APPENDIX C - DESIGN TOOL EXAMPLES

This chapter details the results of examples set by PICP to assess functionality of the design tool.

Example 1

Assume a PICP parking lane along an entire block that's 800 feet long. The PICP parking lane against the curb is 10 feet wide. The (impervious) adjacent travel lane is 12 feet wide and slopes from the middle by 2% to the PICP parking lane. In other words, there is a crown in the road centerline that divides the runoff flow to each side of the road. A schematic is depicted in Figure 100.

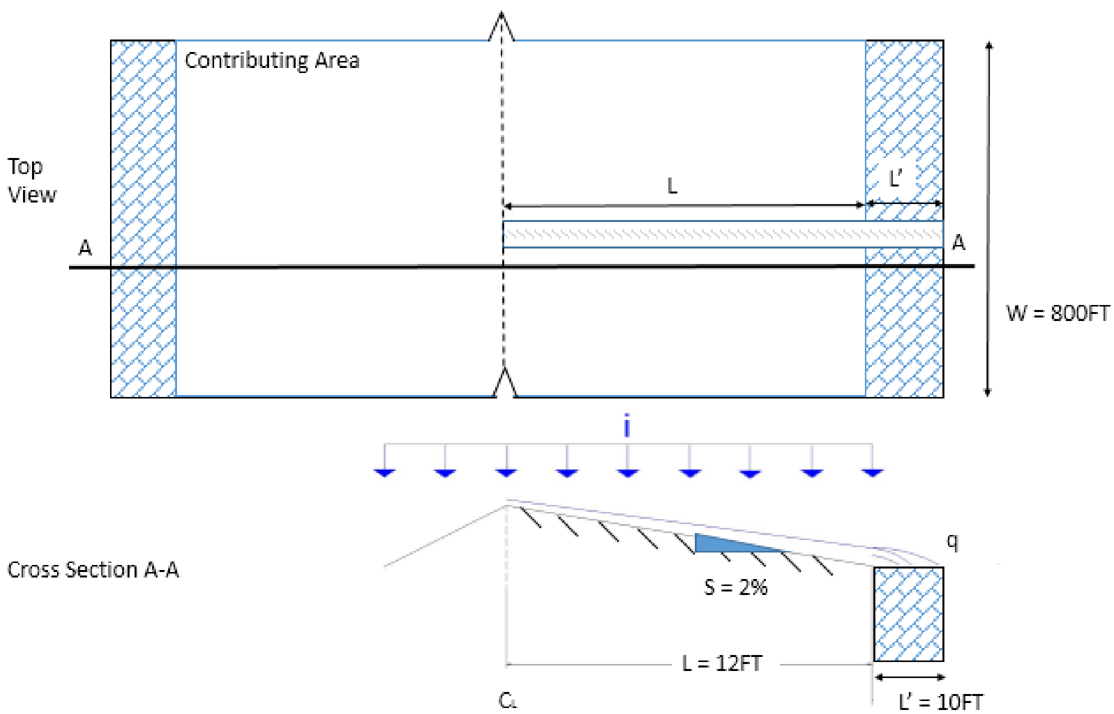

Figure 100. Example 1 Schematic and Cross Section

At what point in time will it clog assuming an average runoff concentration of 300 mg/m3? Assume Kansas City, MO rainfall. Assume 10 mm wide joints with No. 8 stone in them.

Input		
Storm Information		
Storm Region	Missouri	**1**
Duration	10-min	**2**
Recurrence Interval	50	**3**
Project ID	Example 1	**4**
Site Information		
Site Width, w (ft)	800	**5**
Pervious Length, L' (ft)	10	**6**
Contributing Length, L (ft)	12	**7**
Contributing Area Land Category	Streets	**8**
Contributing Area Land Type	Concrete	**9**
Contributing Area C-Value Range	Max	**10**
Slope (%)	2	**11**
Case Level	Case I	**12**
Gap Size	10	**13**

Figure 101. Example 1 Input Interface

Output		
Site Analysis		
Total Site Area (sqft)	17600	**14**
Pervious Area (sqft)	8000	**15**
Contributing Area (sqft)	9600	**16**
Storm Analysis		
Contributing Runoff Coefficient	0.95	**17**
Composite Runoff Coefficient	0.65	**18**
Intensity (in/hr)	7.39	**19**
Unit Discharge Rate (cfs/ft)	0.004	**20**
System Horizontal Infiltration (in/hr)	259	**21**
Design Considerations		
Runoff Rate (cfs)	0.090	**22**
Unit Overflow Rate (cfs/ft)	0.185	**23**
ASTM C 1781 Vertical Infiltration (in/hr)	409	**24**
Gap Size	**Within Range**	**25**
Clogging		
Stormwater Pollutant Concentration (mg/l)	300	**26**
Annual Rainfall (in)	38.2	**27**
Time to Maintenance (Years)	15	**28**

Figure 102. Example 1 Output Interface

Example 1A

Run the same problem above except make the travel lane 24 feet wide, in other words, double the runoff from this impervious area into the PICP parking lane. A schematic is seen in Figure 103.

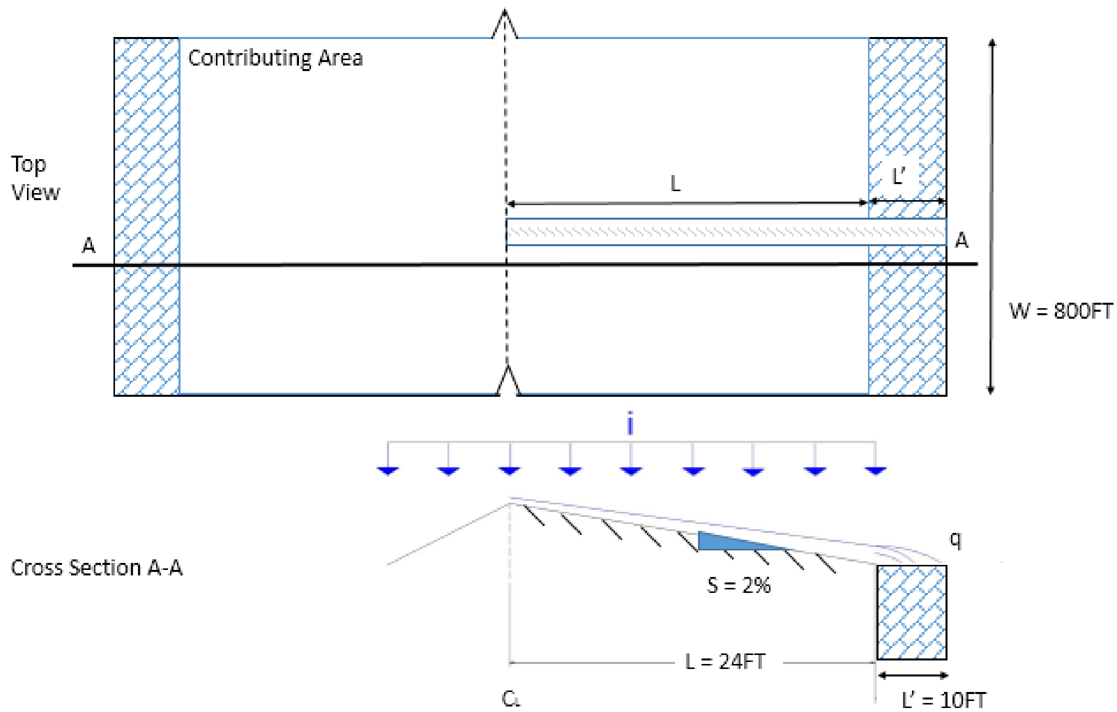

Figure 103. Example IA and IB Schematic and Cross Section

Input		
Storm Information		
Storm Region	Missouri	**1**
Duration	10-min	**2**
Recurrence Interval	50	**3**
Project ID	Example 1A	**4**
Site Information		
Site Width, w (ft)	800	**5**
Pervious Length, L' (ft)	10	**6**
Contributing Length, L (ft)	24	**7**
Contributing Area Land Category	Streets	**8**
Contributing Area Land Type	Concrete	**9**
Contributing Area C-Value Range	Max	**10**
Slope (%)	2	**11**
Case Level	Case I	**12**
Gap Size	10	**13**

Figure 104. Example 1A Input Interface

Output		
Site Analysis		
Total Site Area (sqft)	27200	**14**
Pervious Area (sqft)	8000	**15**
Contributing Area (sqft)	19200	**16**
Storm Analysis		
Contributing Runoff Coefficient	0.95	**17**
Composite Runoff Coefficient	0.76	**18**
Intensity (in/hr)	7.39	**19**
Unit Discharge Rate (cfs/ft)	0.006	**20**
System Horizontal Infiltration (in/hr)	259	**21**
Design Considerations		
Runoff Rate (cfs)	0.104	**22**
Unit Overflow Rate (cfs/ft)	0.185	**23**
ASTM C 1781 Vertical Infiltration (in/hr)	409	**24**
Gap Size	**Within Range**	**25**
Clogging		
Stormwater Pollutant Concentration (mg/l)	300	**26**
Annual Rainfall (in)	38.2	**27**
Time to Maintenance (Years)	15	**28**

Figure 105. Example 1A Output Interface

Example 1B

Change the pavers to 6 mm joints with No. 9 stone in them. A schematic can be referenced in Figure 103.

Input		
Storm Information		
Storm Region	Missouri	**1**
Duration	10-min	**2**
Recurrence Interval	50	**3**
Project ID	Example 1B	**4**
Site Information		
Site Width, w (ft)	800	**5**
Pervious Length, L' (ft)	10	**6**
Contributing Length, L (ft)	24	**7**
Contributing Area Land Category	Streets	**8**
Contributing Area Land Type	Concrete	**9**
Contributing Area C-Value Range	Max	**10**
Slope (%)	2	**11**
Case Level	Case I	**12**
Gap Size	6	**13**

Figure 106. Example 1B Input Interface

Output		
Site Analysis		
Total Site Area (sqft)	27200	**14**
Pervious Area (sqft)	8000	**15**
Contributing Area (sqft)	19200	**16**
Storm Analysis		
Contributing Runoff Coefficient	0.95	**17**
Composite Runoff Coefficient	0.76	**18**
Intensity (in/hr)	7.39	**19**
Unit Discharge Rate (cfs/ft)	0.006	**20**
System Horizontal Infiltration (in/hr)	259	**21**
Design Considerations		
Runoff Rate (cfs)	0.104	**22**
Unit Overflow Rate (cfs/ft)	0.185	**23**
ASTM C 1781 Vertical Infiltration (in/hr)	409	**24**
Gap Size	**Within Range**	**25**
Clogging		
Stormwater Pollutant Concentration (mg/l)	300	**26**
Annual Rainfall (in)	38.2	**27**
Time to Maintenance (Years)	9	**28**

Figure 107. Example 1B Output Interface

Example 2

This is an existing PICP parking lot project in La Jolla, CA right on the beach, seen in Figure 108.

Figure 108. Photo of Example 2 PICP Parking Lot in La Jolla, CA (ICPI, 2015)

The small hexagonal hatch patterns on each end of the parking lot represents PICP and the remainder of the parking lot is asphalt. See attached photo. While there are no grades indicated on the plan, please assume that half the parking lot slopes from the middle to each of the two PICP areas on the ends. The top of the drawing faces the beach and the Pacific Ocean. The bottom PICP receives car traffic and maybe runoff from the adjacent impervious cover. Let’s assume that does not exist in order to simplify this calculation where runoff is only coming from inside the impervious parking lot.

Use La Jolla, CA rainfall. At what point in time will it clog assuming an average runoff concentration of 300 mg/l? Assume the PICP has a 1% slope toward the beach (the top of the drawing). Assume 6 mm wide joints with No. 9 stone in them. The following example portrays the site represented in with a large amount of impervious area contributing to the PICP area. See the attached site in Figure 110 .A schematic of the site is seen in Figure 109.

The results of this analysis show that a 5:1 ratio can be exceeded for PICP to function adequately.

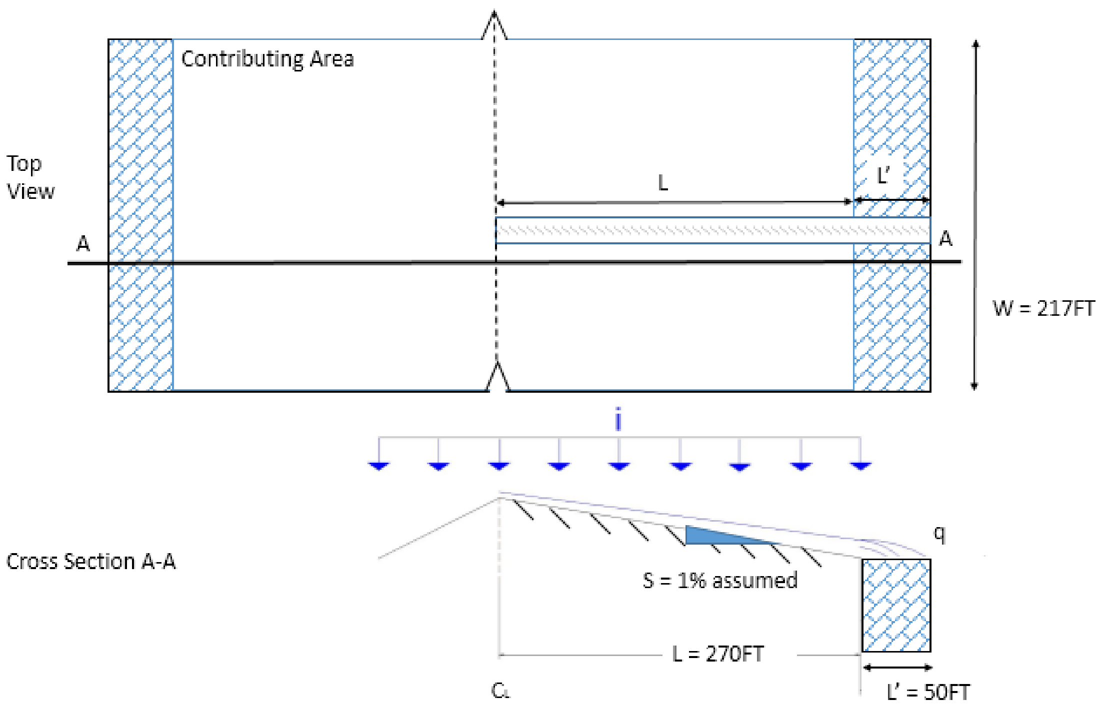

Figure 109. Example 2 Schematic and Cross Section

Figure 110. Example 2 Plans for Construction

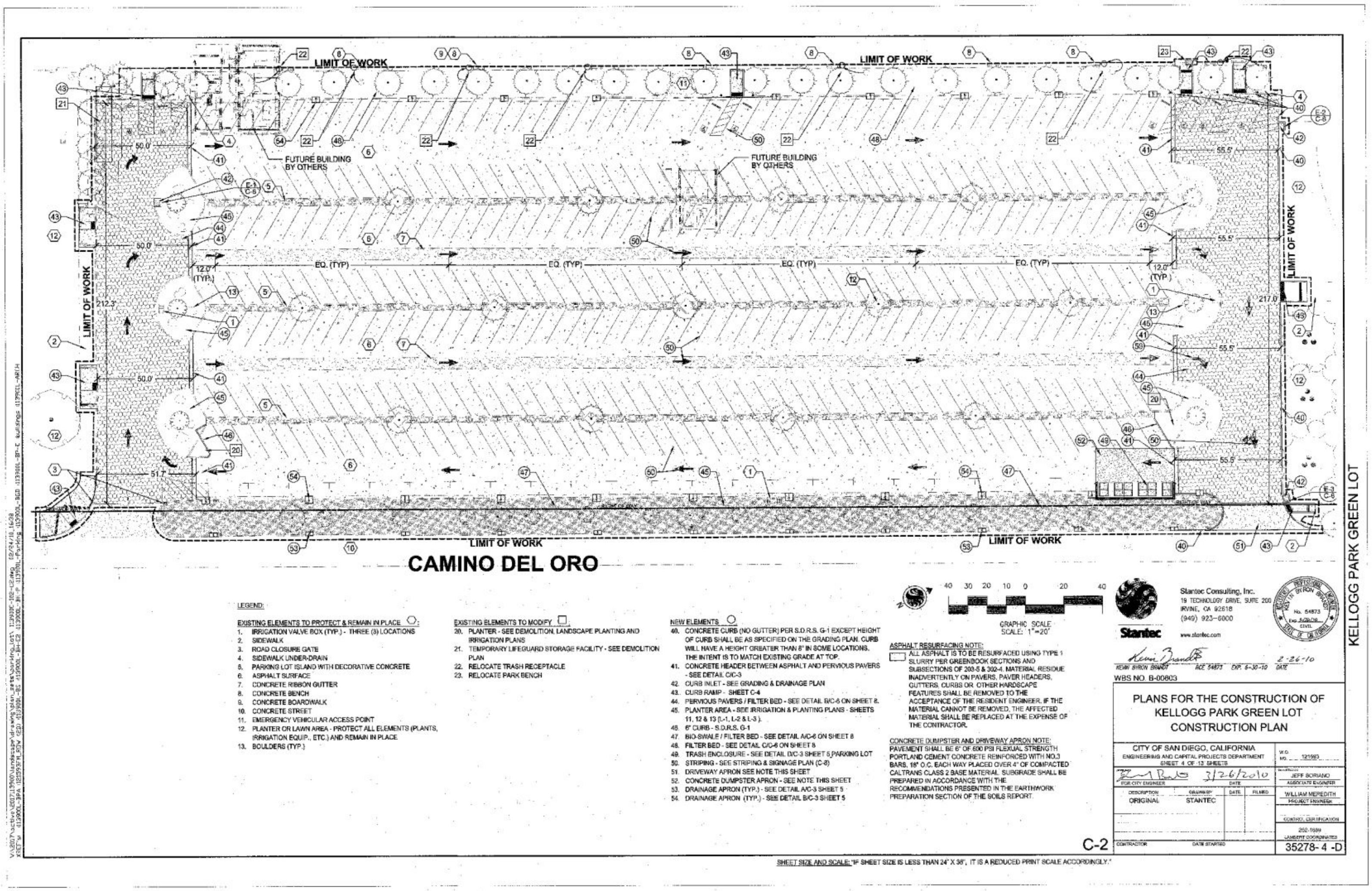

Input		
Storm Information		
Storm Region	California	**1**
Duration	10-min	**2**
Recurrence Interval	50	**3**
Project ID	Example 2	**4**
Site Information		
Site Width, w (ft)	217	**5**
Pervious Length, L' (ft)	50	**6**
Contributing Length, L (ft)	270	**7**
Contributing Area Land Category	Streets	**8**
Contributing Area Land Type	Concrete	**9**
Contributing Area C-Value Range	Max	**10**
Slope (%)	2	**11**
Case Level	Case I	**12**
Gap Size	6	**13**

Figure 111. Example 2 Input Interface

Output		
Site Analysis		
Total Site Area (sqft)	69440	**14**
Pervious Area (sqft)	10850	**15**
Contributing Area (sqft)	58590	**16**
Storm Analysis		
Contributing Runoff Coefficient	0.95	**17**
Composite Runoff Coefficient	0.85	**18**
Intensity (in/hr)	4.19	**19**
Unit Discharge Rate (cfs/ft)	Check Length Ratio	**20**
System Horizontal Infiltration (in/hr)	Not in Range	**21**
Design Considerations		
Runoff Rate (cfs)	0.018	**22**
Unit Overflow Rate (cfs/ft)	Not in Range	**23**
ASTM C 1781 Vertical Infiltration (in/hr)	Not in Range	**24**
Gap Size	**Unacceptable**	**25**
Clogging		
Stormwater Pollutant Concentration (mg/l)	300	**26**
Annual Rainfall (in)	38.2	**27**
Time to Maintenance (Years)		**28**

Figure 112. Example 2 Output Interface